Liquefaction of Soils During Earthquakes

Committee on Earthquake Engineering
Commission on Engineering and Technical Systems
National Research Council

NATIONAL ACADEMY PRESS
Washington, D.C. 1985

NOTICE: The project that is the subject of this report was approved by the Governing Board of the National Research Council, whose members are drawn from the councils of the National Academy of Sciences, the National Academy of Engineering, and the Institute of Medicine. The members of the committee responsible for the report were chosen for their special competences and with regard for appropriate balance.

This report has been reviewed by a group other than the authors according to procedures approved by a Report Review Committee consisting of members of the National Academy of Sciences, the National Academy of Engineering, and the Institute of Medicine.

The National Research Council was established by the National Academy of Sciences in 1916 to associate the broad community of science and technology with the Academy's purposes of furthering knowledge and of advising the federal government. The Council operates in accordance with general policies determined by the Academy under the authority of its congressional charter of 1863, which establishes the Academy as a private, nonprofit, self-governing membership corporation. The Council has become the principal operating agency of both the National Academy of Sciences and the National Academy of Engineering in the conduct of their services to the government, the public, and the scientific and engineering communities. It is administered jointly by both Academies and the Institute of Medicine. The National Academy of Engineering and the Institute of Medicine were established in 1964 and 1970, respectively, under the charter of the National Academy of Sciences.

This study was supported by the National Science Foundation under Contract No. CEE 8418379 to the National Academy of Sciences. Any opinions, findings, and conclusions or recommendations expressed in this report are those of the committee and do not necessarily reflect the views of the National Science Foundation.

A limited number of copies of this report are available from:

Committee on Earthquake Engineering
National Academy of Sciences
2101 Constitution Avenue, N.W.
Washington, D.C. 20418

Also available from:

National Technical Information Service
Attention: Document Sales
5285 Port Royal Road
Springfield, Virginia 22161

Printed in the United States of America

50272-101

REPORT DOCUMENTATION PAGE	1. REPORT NO.	2.	3. Recipient's Accession No. PB86 163110/AS
4. Title and Subtitle: Liquefaction of Soils During Earthquakes			5. Report Date: November 1985
			6.
7. Author(s)			8. Performing Organization Rept. No. CETS-EE-001
9. Performing Organization Name and Address: National Research Council, Commission on Engineering and Technical Systems, 2101 Constitution Avenue, NW, Washington DC 20418			10. Project/Task/Work Unit No.
			11. Contract(C) or Grant(G) No. (C) CEE-8418379 (G)
12. Sponsoring Organization Name and Address: National Science Foundation, 1850 G Street NW, Washington DC 20550			13. Type of Report & Period Covered: Final Report
			14.

15. Supplementary Notes

16. Abstract (Limit: 200 words)

This report reviews the state of knowledge of the causes and effects of liquefaction of soils during earthquakes, documents the state of the art of analysis for safety from liquefaction, and recommends future directions for liquefaction research. It is based on a workshop held in Dedham, Massachusetts, on March 28-30, 1985, at which liquefaction specialists from the United States, Japan, Canada, and the United Kingdom came together to discuss present knowledge and agree on directions for the future. The work was conducted in response to requests from the National Science Foundation and the Nuclear Regulatory Commission.

17. Document Analysis a. Descriptors

Liquefaction of soil, soil mechanics, ground failure.

b. Identifiers/Open-Ended Terms

c. COSATI Field/Group

18. Availability Statement: Distribution unlimited.	19. Security Class (This Report): Unclassified	21. No. of Pages: 250
	20. Security Class (This Page): Unclassified	22. Price

(See ANSI-Z39.18) See Instructions on Reverse OPTIONAL FORM 272 (4-77) (Formerly NTIS-35) Department of Commerce

Preceding

COMMITTEE ON EARTHQUAKE ENGINEERING (1984-85)

Chairman

George W. Housner, California Institute of Technology, Pasadena

Members

Robert G. Bea, P.M.B. Systems Engineering, Inc., San Francisco
Ricardo Dobry, Department of Civil Engineering, Rensselaer Polytechnic Institute, Troy, New York
William J. Hall, Department of Civil Engineering, University of Illinois, Urbana-Champaign
John Loss, School of Architecture, University of Maryland, College Park
Frank E. McClure, Lawrence Berkeley Laboratory, University of California, Berkeley
Joanne Nigg, Center for Public Affairs, Arizona State University, Tempe
Otto W. Nuttli, Earth and Atmospheric Sciences Department, St. Louis University, Missouri

Staff

O. Allen Israelsen, Executive Secretary
Steve Olson, Consultant Editor
Barbara J. Rice, Consultant Editor
Lally Anne Anderson, Administrative Secretary

Liaison Representatives

William A. Anderson, Program Director, Societal Response Research, Division of Civil and Environmental Engineering, National Science Foundation, Washington, D.C.
Ugo Morelli, Office of Natural and Technological Hazards, Federal Emergency Management Agency, Washington, D.C.
Edgar V. Leyendecker, Center for Building Technology, National Bureau of Standards, U.S. Department of Commerce, Washington, D.C.
James Cooper, Strategic Structures Branch, Defense Nuclear Agency, Washington, D.C.
Walter W. Hays, Office of Earthquakes, Volcanoes and Engineering, U.S. Geological Survey, Reston, Virginia

James F. Costello, Division of Engineering Technology, Office of Nuclear Regulatory Research, U.S. Nuclear Regulatory Commission, Washington, D.C.

Richard F. Davidson, Geotechnical Branch, U.S. Army Corps of Engineers, U.S. Department of the Army, Washington, D.C.

Joseph Tyrell, Naval Facilities Engineering Command, U.S. Department of the Navy, Alexandria, Virginia

Lawrence D. Hokanson, Air Force Office of Scientific Research, U.S. Department of the Air Force, Washington, D.C.

J. Lawrence Von Thun, Bureau of Reclamation, Department of the Interior, Denver

G. Robert Fuller, Structural Engineering Division, Office of Architecture and Engineering Standards, Department of Housing and Urban Development, Washington, D.C.

Glen A. Newby, U.S. Department of Energy, Washington, D.C.

Paul Krumpe, Office of U.S. Foreign Disaster Assistance, Agency for International Development, Washington, D.C.

Charles F. Scheffey, Federal Highway Administration, Washington, D.C.

Richard D. McConnell, Veterans Administration, Washington, D.C.

Preface

This report reviews the state of knowledge of the causes and effects of liquefaction of soils during earthquakes, documents the state of the art of analysis for safety from liquefaction, and recommends future directions for liquefaction research. It is based on a workshop held in Dedham, Massachusetts, on March 28-30, 1985, at which liquefaction specialists from the United States, Japan, Canada, and the United Kingdom came together to discuss present knowledge and agree on directions for the future. The work was conducted in response to requests from the National Science Foundation and the Nuclear Regulatory Commission.

A three-member panel of the Committee on Earthquake Engineering organized the workshop. The members of the panel were Ricardo Dobry (Chairman), Robert G. Bea, and Frank E. McClure. Under a subcontract from the National Research Council to the Massachusetts Institute of Technology, Robert V. Whitman, as principal investigator, completed detailed plans for the workshop and prepared the draft report, with the assistance of Samson Liao. Portions of the draft were rewritten at the workshop, and comments from participants submitted following the workshop were incorporated based on the best judgment of the chairman of the panel and the principal investigator. While disagreements among the participants regarding details of this document may still remain, we believe the report reflects the consensus of the workshop on the main aspects of the liquefaction problem.

The Committee on Earthquake Engineering has also held three one-day public seminars to provide the opportunity for interested engineers, researchers, public officials, and educators to learn and discuss the findings of the workshop. These seminars were held between September and November 1985 in Washington, D.C.; Denver, Colorado; and San Francisco, California.

George W. Housner, *Chairman*
Committee on Earthquake
Engineering

PARTICIPANTS AND OBSERVERS AT THE WORKSHOP ON LIQUEFACTION

Dedham, Massachusetts, March 28-30, 1985

Participants

*Robert G. Bea, P.M.B. Systems Engineering, Inc., San Francisco
Gonzalo Castro, Geotechnical Engineers, Inc., Winchester, Massachusetts
John T. Christian, Stone and Webster Engineering Corporation, Boston
Ricardo Dobry, Rensselaer Polytechnic Institute, Troy, New York
Neville C. Donovan, Dames and Moore, San Francisco
Richard Eisner, Bay Area Region Earthquake Preparedness Project, Oakland
John M. Ferritto, Naval Civil Engineering Laboratory, Port Hueneme, California
W. D. Liam Finn, University of British Columbia, Vancouver
Richard Fragaszy, Department of Civil Engineering, Washington State University, Pullman
Lyman W. Heller, Geotechnical Section, U.S. Nuclear Regulatory Commission, Washington, D.C.
Alfred J. Hendron, Civil Engineering Department, University of Illinois, Urbana
George Housner, California Institute of Technology, Pasadena
I. M. Idriss, Woodward-Clyde Consultants, Santa Ana, California
Kenji Ishihara, Department of Civil Engineering, University of Tokyo
William D. Kovacs, Department of Civil Engineering, University of Rhode Island, Kingston
William F. Marcuson, U.S. Army Corps of Engineers, Waterways Experiment Station, Vicksburg, Mississippi
*Geoffrey R. Martin, The Earth Technology Corporation, Long Beach, California
Frank E. McClure, Lawrence Berkeley Laboratory, University of California, Berkeley
Andrew N. Schofield, Department of Engineering, University of Cambridge, Cambridge, England
Ronald F. Scott, Civil Engineering Department, California Institute of Technology, Pasadena
H. Bolton Seed, Department of Civil Engineering, University of California, Berkeley
Marshall L. Silver, Department of Civil Engineering, University of Illinois, Chicago

*Provided input but unable to attend workshop.

Kenneth H. Stokoe, Civil Engineering Department, University of Texas, Austin
John Tinsley, U.S. Geological Survey, Menlo Park, California
John L. Von Thun, U.S. Bureau of Reclamation, Denver
Robert V. Whitman, Department of Civil Engineering, Massachusetts Institute of Technology, Cambridge
T. Leslie Youd, Department of Civil Engineering, Brigham Young University, Provo, Utah
Yoshiaki Yoshimi, Tokyo Institute of Technology, Yokahama

Observers

Leon L. Beratan, Office of Nuclear Regulatory Research, Nuclear Regulatory Commission, Washington, D.C.
Riley Chung, Center for Building Technology, National Bureau of Standards, U.S. Department of Commerce, Washington, D.C.
Richard F. Davidson, Geotechnical Branch, U.S. Army Corps of Engineers, U.S. Department of the Army, Washington, D.C.
Lawrence D. Hokanson, Air Force Office of Scientific Research, U.S. Department of the Air Force, Bolling Air Force Base, Washington, D.C.
Thomas L. Holzer, U.S. Geological Survey, Menlo Park, California
O. Allen Israelsen, National Academy of Sciences, Washington, D.C.
K. Thirumalai, Earthquake Hazard Mitigation, Division of Emerging and Critical Engineering Systems, National Science Foundation, Washington, D.C.
Joseph Tyrell, Naval Facilities Engineering Command, U.S. Department of the Navy, Alexandria, Virginia

Contents

Liquefaction of Soils During Earthquakes

Overview

During earthquakes the shaking of ground may cause a loss of strength or stiffness that results in the settlement of buildings, landslides, the failure of earth dams, or other hazards. The process leading to such loss of strength or stiffness is called *soil liquefaction*. It is a phenomenon associated primarily, but not exclusively, with saturated cohesionless soils.

Soil liquefaction has been observed in almost all large earthquakes, and in some cases it has caused much damage. The destructive effects of soil liquefaction were forcibly brought to the attention of engineers by the disastrous 1964 earthquake in Niigata, Japan. This earthquake caused more than $1 billion in damages, due mostly to widespread soil liquefaction. For critical structures, such as nuclear power plants and large earth dams, the possibility of liquefaction presents serious engineering problems.

In the two decades since 1964, impressive progress has been made in recognizing liquefaction hazards, understanding liquefaction phenomena, analyzing and evaluating the potential for liquefaction at a site, and developing the technology for mitigating earthquake hazards. However, significant questions concerning protection against liquefaction still arise, especially when critical facilities are involved.

State of Knowledge

Knowledge concerning liquefaction and its effects has come mainly from three distinct efforts. These are (1) field observations during and following earthquakes, (2) experiments in the laboratory on saturated soil samples and models of foundations and earth structures, and (3) theoretical studies.

The most commonly observed manifestation of liquefaction is the occurrence of "sand boils" on the ground surface. These small volcanolike features indicate that earthquake shaking has generated excess fluid pressure within the soil, causing pore water to make a channel and carry soil particles to the surface. Indeed, this indication has been confirmed by actual measurements of elevated pore water pressures at depth during earthquakes.

The adverse effects of liquefaction take many forms. Some are

catastrophic, such as flow failures of slopes or earth dams, settling and tipping of buildings and piers of bridges, and total or partial collapse of retaining walls. Others are less dramatic, such as lateral spreading of slightly inclined ground, large deformations of the ground surface, and settlement and consequent flooding of large areas. Even these latter effects have in many earthquakes caused extensive damage to highways, railroads, pipelines, and buildings.

Detailed field studies have identified recent geologic deposits and sandy soils to be most susceptible to liquefaction. They have also provided a data base from which correlations of great value to engineering practice have been developed. They have shown, for example, that deposits that liquefy during one earthquake can again liquefy in subsequent earthquakes.

Laboratory tests on soil samples have demonstrated that oscillatory straining can cause pore water pressure to build up in a saturated soil as a result of soil particles being rearranged with a tendency toward closer packing. If the water cannot drain from the soil during the straining, gravity loading is transferred from the mineral skeleton to the pore water, with consequent reduction in the capacity of the soil to resist loading.

These tests have also pinpointed those factors that have a major influence on the susceptibility of soils to liquefaction. Saturated granular soils without cohesive fines (i.e., some silts, sands, and even gravels) are most susceptible to the buildup of pore pressure. However, the greater the content of clays and other fine particles contributing plasticity, the less the susceptibility to pore pressure buildup. The density of a cohesionless soil also is a very important factor, because pore pressures build up rapidly in a loose sand, and a point may be reached where the sand loses much of its initial resistance to shear. Pore pressure buildup occurs even in a dense sand, but at a slower rate; although significant cyclic and permanent strains may develop, the soil can retain its shear resistance. Other factors affecting the degree of pore pressure buildup include the amplitude of the oscillatory straining (there is a threshold cyclic shear strain that must be exceeded before buildup of pore pressure can begin); the past history of stressing; the size, shape, and gradation of particles; the confining pressure acting on the soil; the age of the deposit; the fabric of the soil; and the overconsolidation ratio of the soil.

Laboratory tests have also shown that a soil has a value of undrained steady-state strength that is only a function of its void ratio and is independent of its stress history, including any pore pressure buildup that may have occurred under earthquake loading. Thus, for a soil to be capable of losing strength and flowing, it must be subjected in the field to shear stresses that exceed its steady-state shear strength.

Model tests of foundations and earth structures, especially tests using special centrifuges, have been useful for studying the complex distributions of pore pressure and deformation that can develop. For example, such tests have confirmed that even if a localized portion of an earth mass reaches a condition of liquefaction, a building foundation or an earth structure as a whole may remain stable. Conversely, model tests have also shown that pore pressures can decrease in some localized parts of a shaken mass of denser soil as large permanent strains begin to develop. Such reduced pore pressures tend to stabilize the foundation or earth structure temporarily, but gradual dissipation may lead to delayed failures such as those observed as a result of several earthquakes.

Theoretical analyses of the behavior of assemblages of particles have explained and confirmed the concept of a threshold strain and have offered understanding into the processes of particle rearrangement by oscillatory straining. Progress has also been made in formulating constitutive relations that describe the physical behavior of soil as a continuum.

A Framework of Understanding

From this body of knowledge a framework of understanding has emerged that helps put some controversial aspects of the liquefaction phenomenon into a common perspective.

The word *liquefaction*, as generally used, includes all phenomena involving excessive deformations or movements as a result of transient or repeated disturbance of saturated cohesionless soils.* Thus, both flow failures and deformation failures are said to be liquefaction failures.

Flow failures describe the condition where a soil mass can deform continuously under a shear stress less than or equal to the static shear stress applied to it. Such a condition will cause slope instability or bearing capacity failure. Equilibrium is restored only after enormous displacements or settlements. The failures of the tailings dams in Chile in 1965 and 1985, the failure of the Lower San Fernando Dam in 1971, and the bearing capacity failures in Niigata in 1964 are examples of flow failures.

Deformation failures involve unacceptably large permanent displacements or settlements during (and/or immediately after) shaking, but the earth mass remains stable following shaking without great changes in geometry. Examples are settlements of oil tanks and the slumping and cracking of earth dams (such movements can, if sufficiently large,

*This broad usage of the word *liquefaction* is endorsed by the great majority of engineers, although some would restrict use of the word to flow failures.

be the cause of damaged tanks or excessive dam seepage) and the destruction of roadways and pipelines by large ground oscillations.

If large increases in pore pressure occur within an earth mass as a result of an earthquake, significant cyclic or permanent deformations can occur. In some cases, these deformations may be large enough to constitute a failure. In other cases, a flow failure of the earth mass may develop. Of particular concern is a situation where the pore pressures rise to equal (or nearly equal) the total overburden stress; this is named the $\sigma' \simeq 0$ condition (also sometimes called initial liquefaction).

There are several mechanisms that can account for flow failures of slopes and foundations. If soil remains at constant volume throughout its mass, failure can occur only if the soil is sufficiently loose that its steady-state undrained strength is less than the stress required to hold the applied forces in equilibrium (mechanism A). However, loss of strength can also result from localized internal movement of pore water, allowing some zones to decrease in density (mechanism B). In addition, more widespread movement of pore water can cause overlying or adjacent soils, whose shear resistance is essential for stability but that are not originally degraded by earthquake shaking, to decrease in strength (mechanism C). In any case, for failure to occur there must be both a prior susceptibility to loss of strength in the soil mass and a triggering mechanism (such as an increase in pore pressure). The two combine to initiate the progressive loss of strength within the soil.

Although this framework of understanding is generally accepted, there are differences in viewpoint about some of its aspects. Some experts place more emphasis on flow failure than on deformation failure and believe that one of the mechanisms by which flow failure can occur is much more important than the others. Some experts focus first on the potential for loss of strength, while others emphasize the triggering mechanism. The relative merits of these different approaches can be resolved only through observations of the actual effects of earthquake shaking on dams, foundations, etc. Given the infrequent opportunities to obtain such data, small-scale tests conducted on centrifuges may play an important role in increasing understanding of the liquefaction problem.

State of the Art in Analysis and Evaluation

From a practical point of view, it must be recognized that almost any saturated granular soil can develop increased pore water pressures when shaken, and that these pore pressures can become significant if the intensity and duration of earthquake shaking are great enough. The question that must be answered in a specific case is: What intensity

and duration of shaking will cause liquefaction, or, conversely, can the soil survive the anticipated earthquake shaking without liquefaction? A wide variety of methods have evolved for assessing the likelihood of liquefaction at a specific site or within a small region. These techniques and their limitations are summarized below.

In considering these techniques, it should be remembered that evaluation of liquefaction hazard is an engineering art requiring judgment and experience in addition to testing and analysis. Important advances have been made during the past two decades in understanding liquefaction and in developing tools to help assess safety against liquefaction, but some aspects of the problem remain uncertain.

Level Ground

Level ground is characterized by a horizontal surface of very large extent and the absence of any superimposed or buried structure that imposes significant stresses in the ground. In evaluating this problem the primary goal is to identify the conditions for reaching the $\sigma' \simeq 0$ condition in the soil profile, which triggers the development of liquefaction effects at the ground surface. The case of level ground is of direct interest with regard to the safety of pavements, pipelines, building slabs on grade, and other objects. There are many situations in which evaluation of the level ground adjacent to a building or embankment appears to provide a conservative assessment of the potential of a foundation for failure. In such cases, however, it is difficult to assess the margin of safety in quantitative terms.

For level ground and sandy soils with little gravel, use of charts based on observed field performance together with a standard penetration test (SPT) or, with a lesser degree of certainty, a cone penetration test (CPT) can provide a practical evaluation of the degree of safety. In using this procedure the increased cyclic loading resistance associated with a larger content of silt and clay particles should be taken into account. It is desirable to adopt proposed procedures for standardizing the results of SPT tests for the purpose of evaluating liquefaction resistance. At a minimum, measured blowcount should be corrected to a common basis of energy delivered to the drill rod. The CPT is not as useful as the SPT for assessing safety against liquefaction, but it can be very valuable for locating loose pockets within a sand and for controlling efforts to improve the liquefaction resistance of a sand.

Flow Failures of Slopes and Embankments

The technology for analyzing the safety of slopes and embankments

against a flow failure is not as well developed and agreed upon as in the case of level ground. Two general approaches are in use:

- Method 1 focuses first on the buildup of pore pressures that may trigger liquefaction. The susceptibility of the soil to such buildups is inferred from in-situ penetration resistance or from cyclic load tests on high-quality and disturbed samples. Various computational methods, from very simple and approximate to very sophisticated and complex, are available for predicting the buildup caused by a specific earthquake shaking. Zones where the $\sigma' \simeq 0$ condition occurs are identified, and a residual strength is assigned to those zones using correlations of observed residual strengths with in-situ penetration resistance. A static stability analysis is then performed. This method involves some uncertainties in the prediction of pore pressure buildup, but it has been shown to provide results in good accord with some features of observed field performance in a number of cases.
- Method 2 focuses first on the potential for a flow failure. The evaluation involves the following: (1) determination of the in-situ steady-state strength of the soils by means of laboratory tests complemented with correlations between the measured steady-state strength and field index tests such as SPT or cone penetration; (2) if a potential for flow failure exists, an investigation of the conditions required to trigger the failure using results of laboratory cyclic tests and/or empirical correlations. Some uncertainties exist because determination of the in-situ steady-state strength is sensitive to changes in void ratio during sampling and testing. Thus it is necessary to correct results for these changes.

Both of these methods usually assume that constant volume conditions are maintained within the soil during the earthquake shaking. It has been hypothesized that flow failures can also occur if certain zones of the soil mass become weaker during and after an earthquake owing to redistribution of water content and spreading of pore pressures. The methods currently available to quantify the pore water migration and the associated volume changes are in a crude stage of development. These possible effects are included to some degree in the approach used in Method 1 and might in principle be incorporated into Method 2 as more case histories are used to calibrate the method.

Permanent Deformations

The prediction of deformation in soils not subject to flow failures is a very difficult and complex nonlinear problem that is still far from being resolved. Hence, various approximate methods exist:

- A procedure for computing permanent ground displacements in

the form of translatory landslides is based on the approach of Newmark (1965). The mass above a failure surface is assumed to move only when the shear strength of the soil is exceeded and only during the time in which the strength is exceeded.

- The permanent deformations of soil elements are estimated from laboratory tests, assuming no constraint from adjacent elements. These are referred to as strain potentials. These strain potentials are then interpreted to produce a compatible set of deformations. Several techniques have been proposed for the laboratory testing as well as for producing compatible deformations.
- Dynamic computer models for nonlinear analysis and for plasticity theory produce estimates of permanent deformations. However, the proper modeling of soil properties for the analysis remains a formidable problem.

General Comments on Methods of Investigation

The following comments apply to cases of both level and sloping ground:

- Use of threshold strain provides a conservative assessment of the safety of foundations and earth structures to both triggering of flow failures and development of excessive deformations. The method is based on the values of shear modulus that can be measured in situ using wave propagation techniques. There is also evidence suggesting that this same approach, extended to larger strains by cyclic-strain-controlled laboratory tests, can be used to predict the development of pore water pressures in the field.
- For soils with a significant content of gravel, there is currently no satisfactory procedure for evaluating the safety against liquefaction. There is a great need to develop predictive procedures for these types of soils.
- Use of undisturbed sampling and laboratory cyclic load testing is not recommended as the sole means of assessing liquefaction resistance, except for some soils (e.g., silty or clayey soils, calcareous soils, etc.) for which there is either no or a limited amount of experience. (Obtaining samples for visual inspection and routine classification is, of course, always essential.) When the gathering and testing of soil samples are to be done, it is important to use extreme care and special techniques.
- Problems in which analysis of pore pressure buildup is essential must be approached with great care. These include, for example, cases where reliance is placed on partial dissipation of pore pressure to provide safety against flow failures or excessive deformation. While great advances have been made in the development of suitable

techniques of analysis, more verification is required before they can be considered reliable tools for use in design. Special problems to be resolved include evaluating parameters required for analysis in ways that are not influenced greatly by sample disturbance, and accounting for dilation as significant permanent strains begin to develop.

- Centrifuge tests (and sometimes other small-scale tests) can provide valuable insights in understanding the behavior of foundations and earth structures and in formulating and testing mathematical models to predict performance. However, it is seldom possible to construct a truly scaled model for a specific prototype situation.
- Probabilistic analyses can provide approximate quantitative estimates for the probability of liquefaction, indicating the relative importance of uncertainty in the frequency and intensity of ground shaking and of uncertainty in the occurrence of liquefaction as a result of ground shaking.

Measures to Improve Seismic Stability and Resist Liquefaction

If the soil at a site is determined not to have the requisite resistance to liquefaction, either the site must be abandoned or measures must be undertaken to improve performance. Experience has shown that improving a site may be very costly. Therefore, from an economical point of view, it is extremely important that (1) the method of assessing the potential for liquefaction is reliable and (2) the mitigation method is sound and efficient. The same problems are faced either when planning new facilities or when assessing the safety of existing facilities and trying to decrease the potential for liquefaction at such facilities.

Four general classes of mitigation measures are available to ensure the desired functionality and safety of engineering projects subject to possible liquefaction:

1. Nonstructural solutions—changing operational procedures for the project. This includes relocating or abandoning a structure, accepting the risk and maintaining use but with warnings to potentially affected parties, and in some cases instituting reduced occupany or utilization.
2. Site solutions—improving the soil in situ. A number of techniques can be considered: removal and replacement of unsatisfactory material, in-situ densification and increase of the lateral stress within the soil, and alteration of in-situ material by grouting, chemical stabilization, or other means. The technical and economic feasibility of the various treatments is related to the grain sizes of the soil to be treated.
3. Structural solutions—changing the project structure. This includes such steps as the addition of berms or freeboard to a dam, the use of

end-bearing piles beneath buildings, and the choice of a structural system that is less susceptible to damage as a result of settlement or other movements associated with liquefaction of the foundation.

4. Drainage solutions—controlling undesirable pore water pressures. This includes relief wells, dewatering systems, air injection into the pore water, drains, and groundwater controls.

Of these solutions, improvement of soil in situ and control of undesirable pore water pressures are the most commonly used measures. The methods differ widely with regard to cost, the permanency of the treatment, the danger of adverse secondary effects, and the certainty that the desired improvement will be achieved. Careful evaluation of alternatives is always essential. Under the heading of improvement of in-situ soil, a list of 17 different techniques—together with a critique of applicability and relative cost—has been developed (Table 5-2 in Chapter 5). The cost and efficacy of the various measures need to be evaluated. Whenever an improved site is shaken by an earthquake, the performance of the soil should be documented.

Research Needs

Despite the important progress that has been made in understanding and coping with liquefaction, more research and development are required to achieve economy and confidence in dealing with potential problems. Areas that still require research are:

- The instrumentation of a limited number of selected locations in highly seismic regions in the United States or abroad where there is a high probability that liquefaction will soon occur. The possibility should be explored of developing one of these locations into a major experimental site, with an operating organization to develop, operate, and manage the site.
- Study of soils other than clean sands, including gravels and soils with a content of cohesive fines.
- The development of methods for evaluating the permanent soil deformations that can be induced by prescribed earthquake shaking.
- Validation of the improved behavior of foundations and earth structures that have been treated to increase dynamic stability.
- In-situ study of the effect of the state of stress in soil before an earthquake on resistance to liquefaction.
- Centrifuge model tests on idealized soil structures to provide insights into mechanisms of failure and to provide data for checking the applicability of analytical methods.
- The use of explosion-generated stress waves to study liquefaction.

- Continued investigations of recent earthquake sites where liquefaction has, or unexpectedly has not, occurred.
- Continued development of new methods for measuring in-situ properties that reflect the liquefaction characteristics of soils.
- Continued attention to the development of laboratory test procedures that will provide improved methods for characterizing the liquefaction properties of soils.
- At a basic level, imaginative development of constitutive relations for soils applicable to the special circumstances of liquefaction.
- International cooperation on liquefaction research. Both Japan and China have frequently experienced liquefaction during earthquakes and have active research programs under way. In some ways, research on liquefaction in these two countries is more advanced than is liquefaction research in the United States, particularly in the area of field studies. International cooperation with these and other countries thus offers the possibility of significant benefits.

1
Introduction

This report focuses on important aspects of the liquefaction of soils during earthquakes, places different viewpoints into perspective, and identifies areas of agreement and disagreement. No attempt is made at a thorough, detailed presentation of the many and varied results found in the extensive literature. This report should instead be viewed as a guide to that literature. Its primary emphasis is on earthquake engineering problems, but its conclusions and recommendations have a broader applicability.

In the context of this study, the word *liquefaction* is used to include all phenomena giving rise to a loss of shearing resistance or to the development of excessive strains as a result of transient or repeated disturbance of saturated cohesionless soils. This use of the term *liquefaction* is general and covers a range of phenomena that are not necessarily of the same nature (e.g., problems of strength as well as problems of deformation). As will be noted, more restrictive definitions of liquefaction have also been proposed.

Twenty-One Years Later

It has been two decades since major failures during the Niigata and Alaskan earthquakes of 1964 identified liquefaction as a major problem in earthquake engineering (Seed and Lee, 1966; Seed and Idriss, 1967), although the problem has existed for as long as earthquakes have affected civilization. Considerable effort has been devoted to the study of liquefaction during these 20 years, yet the problem remains very controversial in some respects. Major questions concerning safety against liquefaction still arise, and strong disagreements sometimes occur when assessing the safety of existing structures and facilities. To the nonexpert it often appears that the experts differ in their basic understanding and assessment of the liquefaction problem, although perhaps they disagree only on the certainty with which a claim of safety against liquefaction can be made.

There are a variety of reasons why controversies concerning liquefaction still exist:

1. Soil is a complex material. It is particulate and multiphase and as a consequence is also very nonlinear. The patterns of layering and lensing in an actual soil profile can be extremely complex and have a great effect on geotechnical engineering problems at a site. Engineers are able to view only a very tiny fraction of the soil at a site, and then only by sampling that almost certainly disturbs the samples from their in-situ condition. Finally, the behavior of a site can change with time because of construction that changes the stresses within the soil, fluctuations or permanent changes in the groundwater regime, or other reasons.

2. The word liquefaction, as used by engineers and nonexperts, does not refer to a single well-defined phenomenon, but rather to a complex set of interrelated phenomena that can contribute to the occurrence of unacceptable damage to a building or other facility during an earthquake.

3. There have been very few case studies of the behavior of sites that have experienced major slides and instabilities during earthquakes where both the characteristics of the shaking and the condition of the soil at the site before the earthquake were well known.

4. In addition to uncertainties as to how a specific site behaves during a specified earthquake ground shaking, there are even greater uncertainties as to the intensity and nature of earthquake shakings that may occur in the future.

5. The range of consequences arising from the possible behavior of a site is large, depending on the characteristics of the ground shaking and the structures affected, and the price of adopting a conservative approach that ensures safety can be enormous. Thus, there is a great incentive to seek new methods of evaluation that are less conservative than existing methodologies.

In spite of the apparently controversial nature of some aspects of the problem, much progress has indeed been made in understanding the liquefaction problem, in developing tools for evaluating the safety of a site or facility against a liquefaction-related failure, and in producing methods of mitigating the liquefaction hazard. Researchers agree on many key aspects of liquefaction phenomena, and it is essential to identify and document these areas of agreement. Today competent and experienced engineers can reach sound conclusions concerning the safety of most existing structures or new project designs, although not always with the scientific precision attainable in other areas of engineering practice.

This report documents the understandings that have been reached about liquefaction and the tools of evaluation that have become accepted. It also identifies basic concepts and evaluative techniques that must be clarified or developed through further research.

Scope of the Report

The rest of this report is divided into four chapters followed by a final chapter that presents recommendations concerning future research needs.

Chapter 2 treats the state of knowledge about liquefaction, summarizing briefly what is known concerning the phenomena and emphasizing key points of agreement and disagreement.

Chapter 3 presents a framework for understanding the liquefaction problem. This framework serves to tie together various views of the problem.

Chapter 4 summarizes and critiques various methods—ranging from empirical to theoretical—that have been or are being developed for analyzing and evaluating the safety of a site, building, facility, earth structure, etc., against a liquefaction-related failure. This chapter defines the state of the art in analysis and evaluation.

Chapter 5 provides general guidance to owners and managers of sites or facilities that have been judged susceptible to liquefaction-caused failure or damage. These guidelines indicate the types of steps that may be taken in dealing with the situation.

There is an enormous literature concerning liquefaction, and it would be impossible to cite and review all of it. The diversity and expertise of the participants and observers at the workshop on which this report is based have ensured that attention is given to important ideas, results, and methods, whatever their source. The bibliography at the end of this report, though by no means complete, documents the various points discussed in the report.

There have, of course, been excellent state-of-the-art summaries in the past, and others will appear contemporaneously with this report. Maximum use has been made of these past reviews, including Yoshimi et al. (1977), Seed (1979a,b), and Ishihara (1985). The report *Earthquake Engineering Research—1982* by the Committee on Earthquake Engineering of the National Research Council also contains a discussion of liquefaction.

2
The State of Knowledge

This chapter summarizes what is actually known about the occurrence and nature of liquefaction from observations in the field, from laboratory tests on elements of soil, and from tests on small-scale models. It also offers some insights into liquefaction provided by theory.

Knowledge from Field Observations

Introduction

The earthquake that affected Niigata, Japan, in 1964, produced several classic examples of failures attributable to shaking of saturated cohesionless soils. Figures 2-1 and 2-2 show buildings, otherwise structurally undamaged, that experienced bearing failure. Liquefaction during the Niigata earthquake also led to failures of quay walls that resulted when the sandy backfill between walls lost its strength and to bearing failure beneath bridge piers and spreading of the approach embankments (Figure 2-3). In addition, lateral spreads tore apart buildings, ruptured several pipelines, and thrust bridge abutments toward river channels.

In that same year the Great Alaskan Earthquake caused a massive subaqueous slide that destroyed some of the waterfront in Seward, Whittier, and Valdez. In addition, loss of strength within lenses of sand contributed to damaging landslides in Anchorage. Failure generated by liquefaction also disrupted roads and railroads and compressed or buckled more than 250 bridges.

Within the mainland United States the prime example of a liquefaction-induced failure has been the large slide at the Lower Van Norman Dam that occurred during the San Fernando earthquake of 1971 (Figure 2-4), which nearly led to flooding of a heavily populated area. During the same earthquake a shallow, spreading slide within a sand layer on a very flat slope (less than 1 degree) caused collapse or fracture of several buildings (Figure 2-5).

The events of 1964 and 1971 forcefully drew attention to the problem of earthquake-induced failures involving saturated cohesionless soil. A review of past earthquakes, however, clearly reveals that such

FIGURE 2-1 Tilting and settlement of apartment buildings in Niigata, Japan, because of liquefaction of the underlying soil during the 1964 Niigata earthquake. Photograph: Courtesy of G. W. Housner.

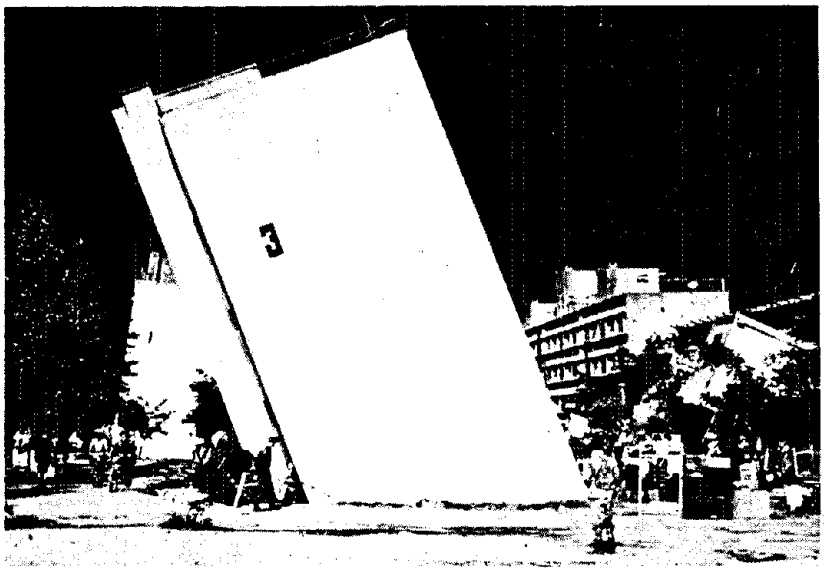

FIGURE 2-2 Close-up view of one of the apartment buildings affected by liquefaction during the Niigata earthquake. Photograph: Courtesy of G. W. Housner.

FIGURE 2-3 Failure of the Showa Bridge during the 1964 Niigata earthquake. Source: Seed and Idriss (1967).

failures are rather common consequences of seismic shaking (Seed, 1968). There was clear evidence of failures of this type in San Francisco in 1906 (Youd and Hoose, 1976). Going further back, there were widespread failures in sands during the New Madrid, Missouri, earthquakes of 1811-12 (Fuller, 1912). Similar failures have occurred in most other major earthquakes around the world.

Failures attributable to shaking of sands continue to take place. A number of such failures occurred during the recent earthquakes in the Imperial Valley of California (Bennett et al., 1981, 1984; Youd and Bennett, 1983; Youd and Wieczorek, 1984). An earthquake in May 1984 that affected the northwestern shore of Honshu Island, Japan, caused failures very similar to those in Niigata in 1964.

The cases cited above are just a few of the many that have been

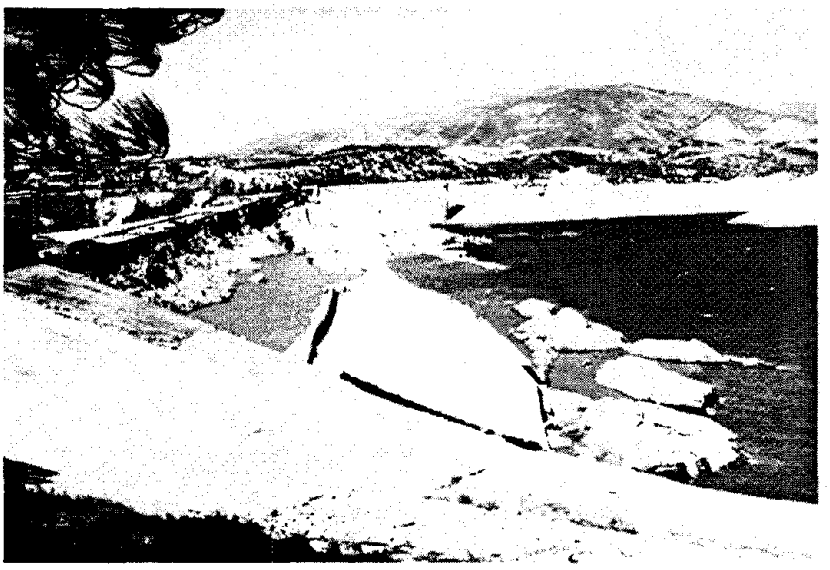

FIGURE 2-4 Failure of the Lower Van Norman San Fernando Dam during the San Fernando earthquake of 1971. Part of the upstream face of this 140-ft-high dam lost strength and slipped beneath the water. Eighty thousand people living below the dam in Los Angeles were evacuated from their homes for several days until the water level behind the dam was drawn down. Photograph: Courtesy of R. V. Whitman.

documented (Youd and Hoose, 1977; Liao, 1985). They serve as reminders that the problem is frequent and widespread. There have, of course, been many cases of embankments and foundations on sand that did not fail during earthquakes, even when the ground motion was quite strong. Field observations that indicate the causes of such failures and identify the factors that determine whether or not a failure occurs are therefore of great interest.

The principal focus of this report is earthquake-induced liquefaction. There are, however, several other natural and artificial disturbances discussed in this report that can also generate liquefaction. These disturbances include loadings from storm waves in offshore environments; increases in pore water pressure due to rise of the phreatic level in a hydraulically connected water source; and man-made vibrations from explosions, construction operations such as pile driving, and heavy rail and highway traffic. Much of the knowledge and technology applicable to earthquake-induced liquefaction can be transferred to these other generative mechanisms. Conversely, behavior observed during failures induced by these other mechanisms has provided valuable information about liquefaction during earthquakes.

FIGURE 2-5 Damage to the San Fernando Juvenile Hall facility during the 1971 San Fernando earthquake. This building partially collapsed when soils under the foundation liquefied. Even though the building is on a relatively flat slope, uneven displacements occurred and essentially pulled the building apart. Note the surface cracks in the parking lot in the foreground. Photograph: Courtesy of G. W. Housner.

Failure Types

Many phenomena are associated with liquefaction, including rise of pore water pressure, sand boils, and various types of deformation. But only when deformations become large enough to damage constructed works do they have significance to engineering. Such deformation of the ground is called ground failure and may be manifested in several forms or types.

Sand Boils

Although not strictly a form of ground failure because alone they do not cause ground deformation, sand boils are diagnostic evidence of elevated pore water pressure at depth and an indication that liquefaction has occurred. During earthquakes, sand boils are formed by water venting to the ground surface from zones of high pore pressure generated at shallow depth by the compaction of granular soils during seismic shaking. The water, which may flow violently, usually transports considerable suspended sediment that settles and forms a conically shaped sand boil deposit around the vent (Figure 2-6). These

FIGURE 2-6 Sand boils near the town of El Centro from the 1979 Imperial Valley earthquake. These sand volcanoes, which spouted a mixture of sand and water, are evidence of extensive liquefaction at depth. Photograph: Courtesy of G. W. Housner.

deposits commonly litter the ground surface, marking areas of subsurface liquefaction. Sand boils generally cause no damage, but flooding and sediment deposition have caused economic loss and some damage. Housner (1958) gave an early discussion of the possible mechanism, and Scott and Zuckerman (1973) have studied the phenomenon in detail.

The pattern of sand boil formation is governed by the details of the soil deposit. Cohesionless and relatively permeable soil overlying the liquefied material causes a general settlement of the ground, with the uniformity of the settlement depending on the degree of homogeneity of the material. When the overlying layer of soil is cohesionless and of lower permeability, it becomes suspended on the fluid zone and settles nonuniformly, creating "cavities" filled with loose sand. Lenses of water may develop near the bottom of an overlying cohesive layer. If the cavities approach ground surface, the pressured soil-laden water in the cavity can break through almost explosively to form a waterspout or sand volcano, bringing sand with it from the liquefied zone. The greater the thickness of the overlying layer, the fewer and larger the boils,.because the breakthrough of the first vents inhibits concurrently developing cavities. In a thick layer, fewer cavities reach the surface.

When the material overlying the liquefied zone is cohesive, the

development of liquefaction and, possibly, continued shaking cause the upper layer to crack. Venting of the liquid occurs through the cracks, and irregular and elongated or two-dimensional sand boils form.

When the flow of soil and water to the surface is interrupted by the concrete foundation of a building, a roadway, or other paved surface, sand-water ejection and sand boils appear around the edge of the structure. Venting of the liquefied soil may be influenced by the presence of animal holes, burrows, or man-made openings such as trenches and ditches. The path to the surface is generally not vertical but convoluted, depending on the nonuniformity or anisotropy of the soil.

The volume of sand deposited on the surface from sand boils depends on the depth of liquefied material. If a coarser layer—e.g., gravel—overlays the liquefied region, the sand and water mixture may not vent at the ground surface but will be expended in the pores of the coarse material.

Fossil sand boils have been identified in the geologic column at the Pallett Creek site along the San Andreas Fault (Sieh, 1978, 1984) and in relation to the Charleston earthquake of 1886 (Obermeier et al., 1985). They have been used to date these events and thus establish the earthquake frequency at the sites.

Flow Failures

Flow failures are the most catastrophic ground failures caused by liquefaction (Figure 2-7a). These failures commonly displace large masses of soil for tens of meters, and at times large masses of soil have traveled tens of kilometers down long slopes at velocities ranging up to tens of kilometers per hour. Flows may be composed of completely liquefied soil or blocks of intact material riding on a layer of liquefied soil. Flows usually develop in loose saturated sands or silts on slopes greater than 3 degrees. The failure of the upstream slope of the Lower San Fernando Dam during the 1971 San Fernando earthquake is a notable example of flow failure (Seed et al., 1975d).

Flow failures have often affected mine-waste tailings dams built of loose and saturated crushed rock debris. A recent example, shown in Figure 2-7b, occurred during the Central Chile Earthquake of March 3, 1985. Flow failures have also occurred in these tailings waste piles and in other very loose man-made earth structures, during construction, and without any earthquake taking place (Casagrande, 1936).

Many of the largest and most damaging flow failures have developed in coastal areas. For example, flow failures, mostly under water, carried away large sections of port facilities at Seward, Whittier, and Valdez, Alaska, during the 1964 earthquake and generated large sea waves that caused additional damage and casualties along the coast.

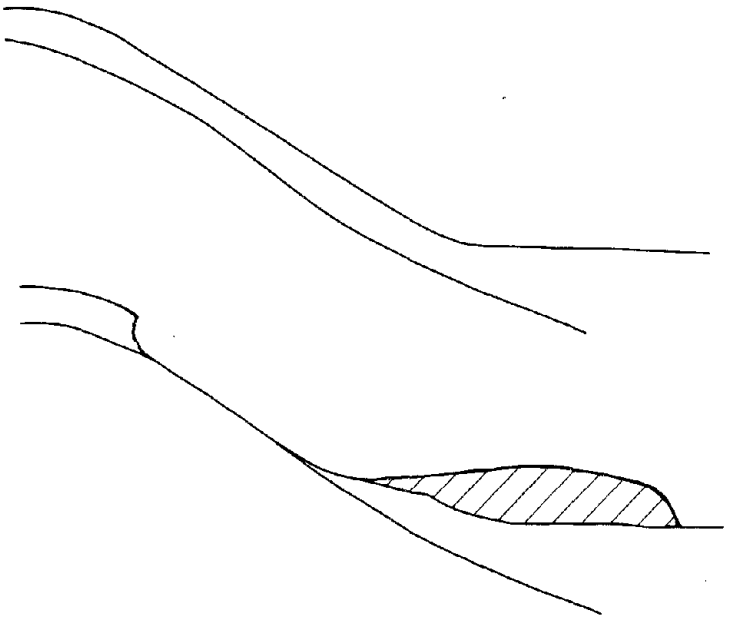

FIGURE 2-7a Diagram of a flow failure. Liquefaction develops beneath the ground surface, causing the soil to lose strength and flow down the steep slope. On land the liquefied soil and blocks of intact soil riding on the flow commonly come to rest as a mass when the flow reaches the bottom of the steep slope. Beneath water some flows have traveled many kilometers down long gentle slopes. Source: Youd (1984b).

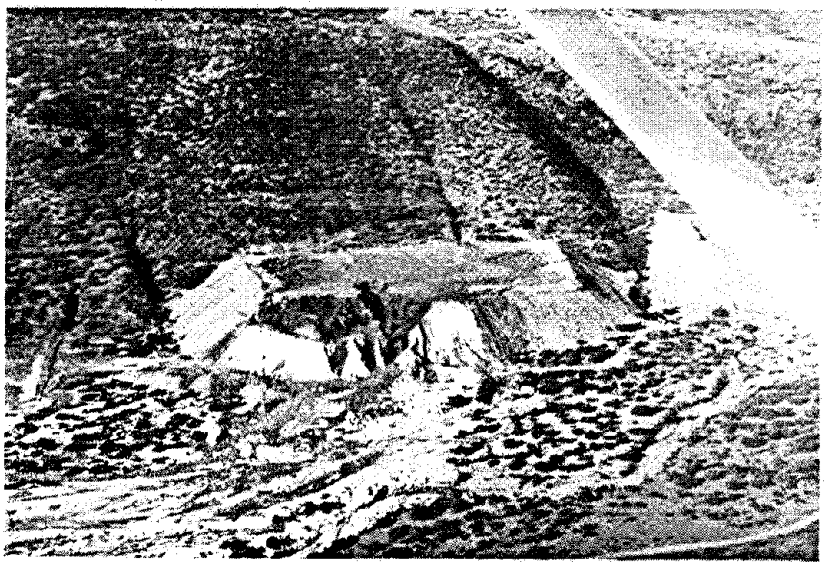

FIGURE 2-7b Liquefaction failure of a tailings dam in Cerro Negro, Chile, from the March 3, 1985, earthquake. Photograph: Courtesy of G. Castro.

Flow failures of natural soils on land are commonly called debris flows, and they have been more catastrophic, though less frequent, than submarine failures. Massive flow failures in collapsible, partially saturated loess deposits were reported during earthquakes in China and Russia. The flow failures triggered by the 1920 earthquake affecting Kansu, China, ranged up to 1.6 km in length and breadth. Some failures flowed downslope for several kilometers. The flowability of these soils was attributed to pressures generated in entrapped air rather than in water. An estimated 200,000 people were killed in these loess flows.

Lateral Spreads

Lateral spreads involve lateral displacement of large, superficial blocks of soil as a result of liquefaction in a subsurface layer (Figure 2-8). Movement occurs in response to the combined gravitational and inertial forces generated by an earthquake. Lateral spreads generally develop on gentle slopes (most commonly between 0.3 and 3 degrees) and move toward a free face, such as an incised river channel. Horizontal displacements on lateral spreads commonly range up to several meters, but can extend up to several tens of meters where slopes are particularly favorable and ground shaking durations are long. Ground shifted by lateral spreading usually breaks up internally, causing fissures, scarps, horsts, and grabens to form on the failure surface. Lateral spreads commonly disrupt foundations of buildings located on or across the failure (Figure 2-9), rupture sewers, pipelines, and other utilities in the failure mass, and compress or buckle engineering structures crossing the toe of the failure.

Damage caused by lateral spreads, though seldom catastrophic, is severely disruptive and often pervasive. For example, during the Alaska earthquake of 1964, more than 250 bridges were damaged or destroyed by spreading of floodplain deposits toward river channels. The spreading compressed bridges over the channels, buckled decks (Figure 2-10), thrust stringers over abutments, and shifted and tilted abutments and piers.

Cumulatively, more damage has been caused by lateral spreads than by any other form of liquefaction-induced ground failure.

Ground Oscillation

Where slopes are too gentle to allow lateral displacement, liquefaction at depth commonly decouples overlying soil blocks, allowing them to jostle back and forth on the liquefied layer during an earthquake (Figure 2-11). This jostling of blocks produces an oscillation often seen by observers as ground waves. The oscillations are accompanied by opening and closing fissures and ground settlement, which can inflict

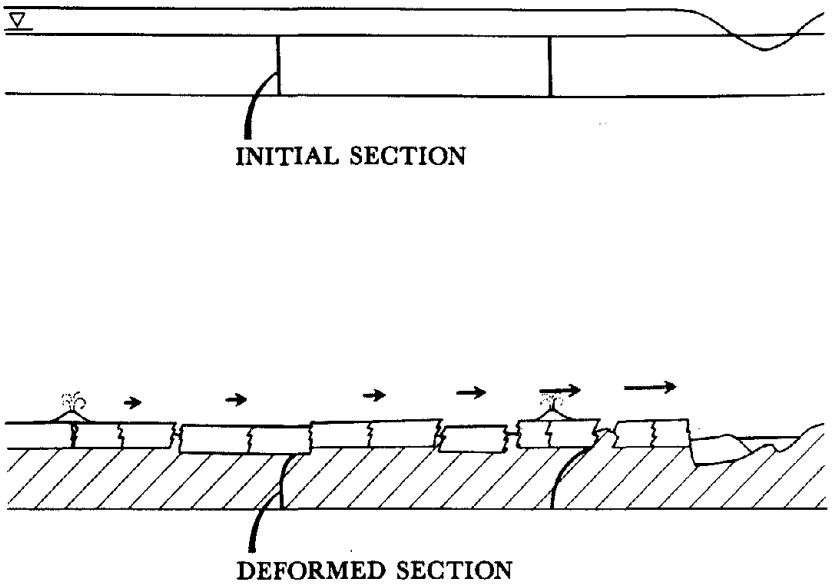

FIGURE 2-8 Diagram of lateral spread before and after failure. Liquefaction occurs in the cross-hatched zone. The surface layer moves laterally down the mild slope, breaking up into blocks bounded by fissures. The blocks also may tilt and settle differentially with respect to one another. Source: Youd (1984b).

FIGURE 2-9 Building pulled apart by lateral spreading during the 1964 Niigata earthquake. Source: Kawasumi (1968).

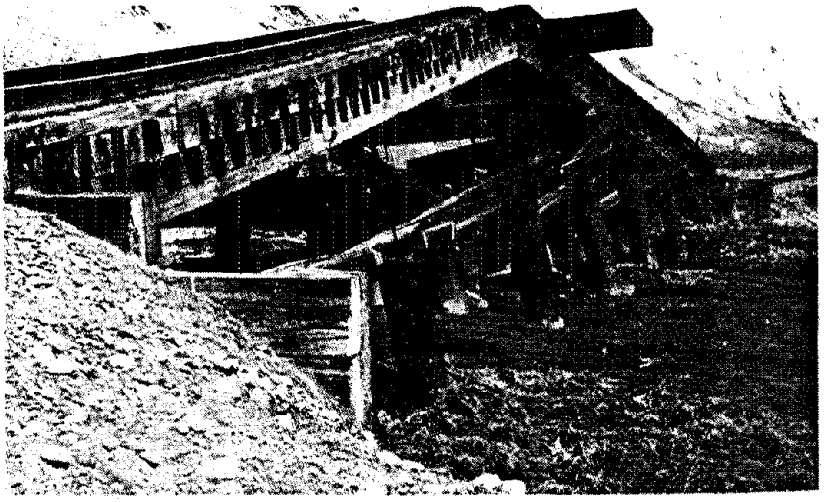

FIGURE 2-10 Bridge compressed and buckled by lateral spreading during the 1964 Alaska earthquake. Photograph: Courtesy of the U.S. Geological Survey.

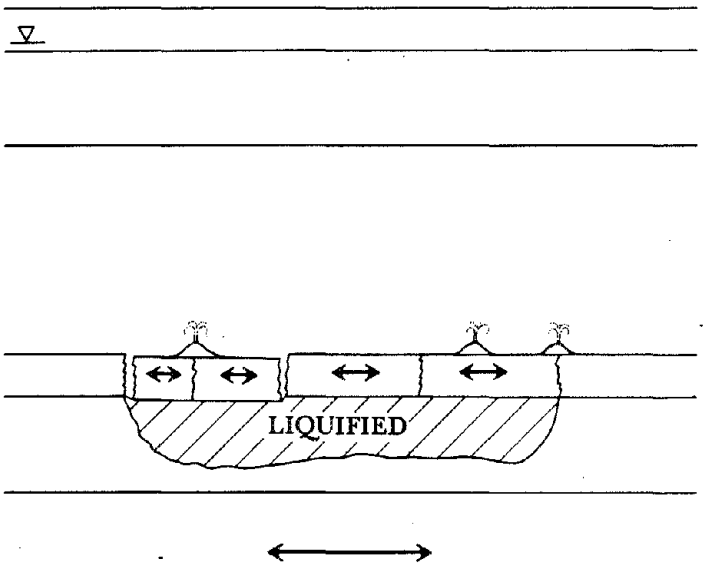

FIGURE 2-11 The mechanism of ground oscillation. Liquefaction occurs in the cross-hatched zone, decoupling the surface layer from the underlying firm ground. The decoupled layer vibrates in a different mode than the underlying and surrounding firm ground, causing fissures to form and impacts to occur between oscillating blocks and adjacent firm ground. Traveling ground waves and opening and closing fissures are commonly seen during ground oscillation. Source: Youd (1984b).

serious damage to overlying structures and to pipelines and other facilities buried in the ground.

Loss of Bearing Capacity

When the soil supporting a building or other structures liquefies and loses strength, large soil deformations can occur, allowing the structure to settle and tip (Figure 2-12). During the Niigata, Japan, earthquake of 1964, spectacular bearing failures occurred at the Kawagishicho apartment complex, where several four-story buildings tipped as much as 60 degrees (Figure 2-2). Apparently, liquefaction first developed in a sand layer several meters below ground and then propagated upward through overlying sand layers. The rising wave of liquefaction weakened the soil supporting the buildings and allowed the structures slowly to settle and tip. Most of the buildings were later repositioned upright, underpinned with piles, and reused.

Buoyant Rise of Buried Structures

Tanks, pipelines, cut-off timber piles, and other buried structures that are lighter in weight than the surrounding soil rise buoyantly when the surrounding soil liquefies. Spectacular emergences of several buried tanks have occurred during earthquakes in Japan (Figure 2-13). In other instances, old bridge piles have shot upward a meter or so, marking the past location of a long-forgotten structure. Damage caused by buoyant rise of structures is seldom catastrophic, but can have important consequences to lifelines and restoration of community services.

Ground Settlement

Several classic examples of ground settlement caused by earthquake shaking occurred in Alaska in 1964. While subsidence from tectonic movement occurred over a wide area, densification of sediment added significantly to the total subsidence in several local areas. For example, the well casing illustrated in Figure 2-14 shows the portion of subsidence attributable to densification at a location near Portage. Settlement lowered the ground surface sufficiently so that houses and railroad and highway grades were inundated at high tide. Ground settlement at the Jensen Water Filtration Plant after the San Fernando earthquake of 1971 caused considerable damage. Densification and ground settlement is commonly associated with and enhanced by liquefaction.

Failure of Retaining Walls

It is common practice to backfill with sand behind retaining walls. This is particularly true for quay walls and bulkheads at port facilities.

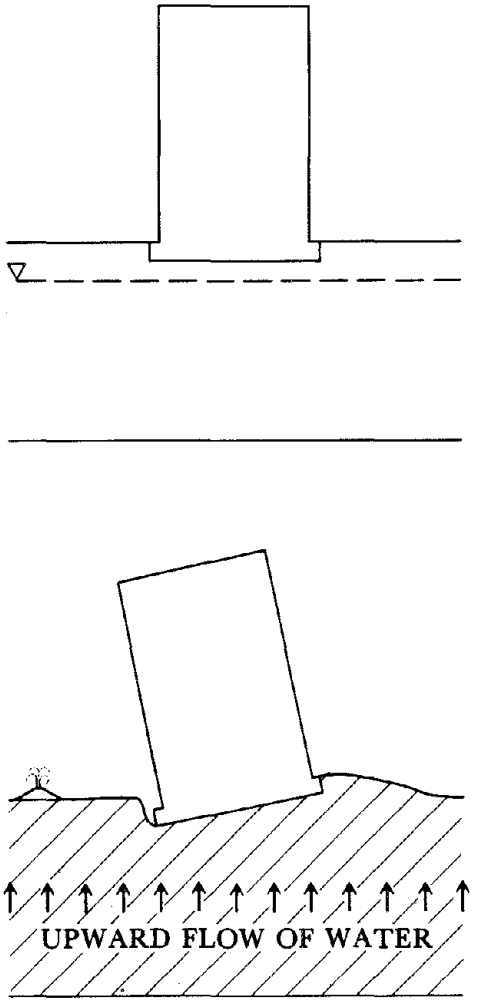

FIGURE 2-12 Tilting of a building from liquefaction and loss of bearing strength in soil. Liquefaction weakens the soil, reducing the foundation's support and causing the building to settle and tilt. Conversely, buried empty tanks and pipes may float upward through the liquefied soil. Source: Youd (1984b).

Liquefaction of the sand backfill increases the lateral stresses on the walls; this, combined in some cases with the drawdown of the ocean level caused by a tsunami, has led to failure of walls during several earthquakes (Figure 2-15). Spectacular failures of this type occurred in Chile during earthquakes in 1960 and 1985.

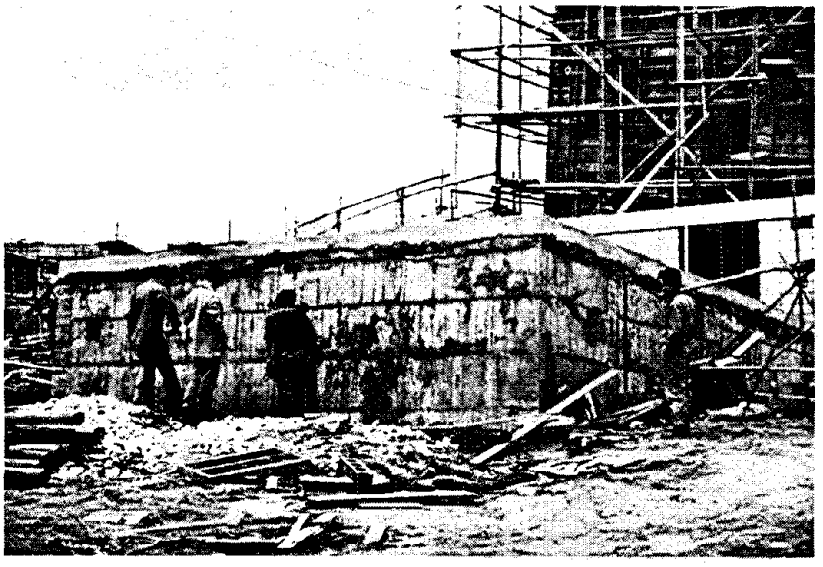

FIGURE 2-13 A concrete tank floated from the ground because of liquefaction of the surrounding soil. This concrete tank had been constructed with its top level with the ground surface. It was empty at the time of the earthquake and relatively bouyant with respect to the liquefied soil. Photograph: Courtesy of G. W. Housner.

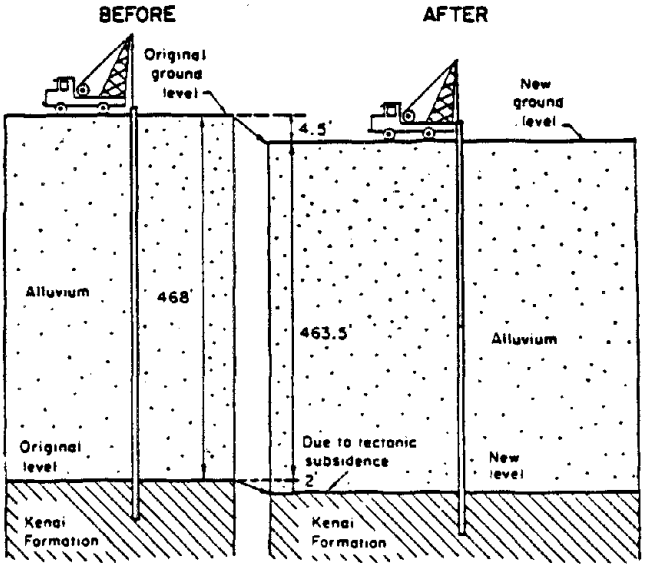

FIGURE 2-14 Ground settlement around well casing at Homer during the 1964 Alaska earthquake. Source: Grantz et al. (1964).

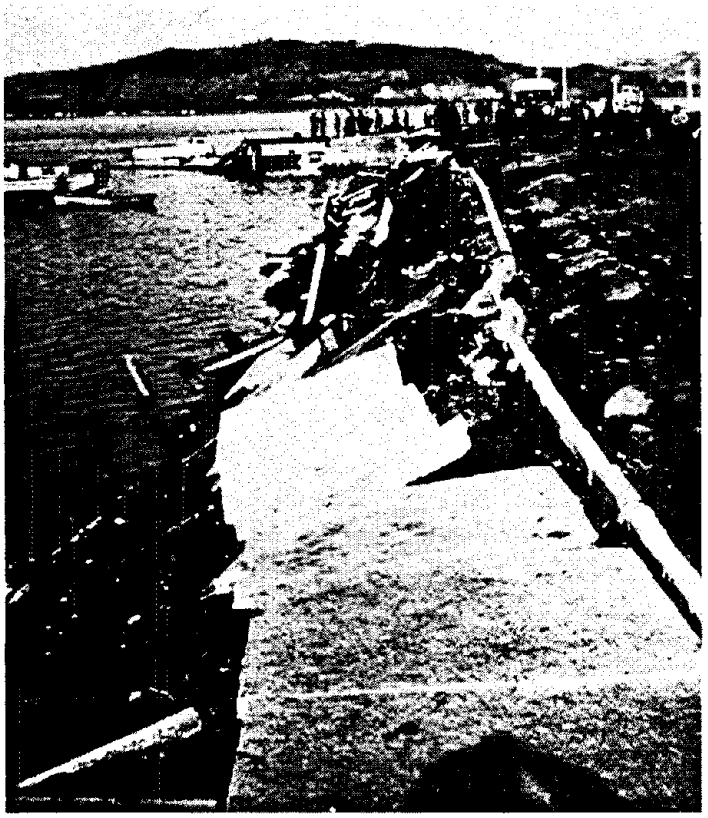

FIGURE 2-15 Example of a quay wall failure in Puerto Montt due to liquefaction during the 1960 Chilean earthquake. Photograph: Courtesy of G. W. Housner.

Some Observations of Liquefaction Phenomena During Earthquakes

Both direct and indirect field evidence confirm that pore pressures are elevated by earthquake shaking. Such evidence includes sand boils (previously described), measurement of pore pressures, ground motion records, and delayed failures.

Direct Measurements of Excess Pore Pressures

Direct measurements of excess pore water pressure induced by an earthquake were made below a railroad embankment during the Tokachioki earthquake of 1968 (Ikehara, 1970) and within an artificial island (Owi Island) in Tokyo Bay in 1980 by Ishihara et al. (1981). Similar measurements have also been made in the United States (Harp et al., 1984; Mavko and Harp, 1984; Tepel et al., 1984). Attention here is focused upon the data from Owi Island.

Owi Island No. 1 was constructed over a period of eight years, from 1961 to 1969. Dredged materials from a nearby seabed were pumped to the site until a water depth of 10 m was reached. At this point, waste materials from construction sites were dumped on top of the dredged fill. Piezometers were installed at depths of 6 m and 14 m, and a two-component accelerograph was placed on the ground surface. Figure 2-16 shows the soil profile at the location of the instruments.

The Mid-Chiba earthquake, with a magnitude of 6.1, shook the Tokyo Bay area on September 25, 1980. It had a focal depth of 20 km, and the epicenter was located about 15 km southeast of Chiba. The earthquake was the largest in the area since 1929. The pore pressures and accelerations recorded during this event are shown in Figure 2-17. During the first four seconds after triggering, there were small fluctuations in the pore pressure, presumably the result of changes in total stress during the small initial accelerations. About four seconds after triggering, the strong shaking began (approximately 0.1 g in the north-south directions and 0.065 g in the east-west directions), and the pore pressure suddenly rose. The maximum pore pressure increases measured by the instruments were about 15 percent of the initial vertical effective stresses. The subsequent decay in the pore pressure was caused by the dissipation of excess pore pressures by drainage. This decay was fairly rapid at the 6-m depth, but slower at the 14-m depth because the sand at this depth was overlain by a clay layer and the permeability of the sand at the 6-m depth was greater than that at the 14-m depth.

There was an aftershock about two hours after the earthquake, by which time the excess pore pressures had completely dissipated. The measured peak acceleration during this aftershock was 0.04 g, and no excess pore pressures were generated.

Ground Motions Recordings

If the stiffness and strength of sand are decreased by shaking, the ability of sand to transmit shear waves from depth to the surface should decrease. In an extreme case where nearly all stiffness is lost, ground motions occurring at the surface of a sand should be greatly reduced. This phenomenon was observed in an accelerograph record made in Niigata in 1964 (Figure 2-18). For about the first seven seconds, the record showed the usual character of ground accelerations measured during earthquakes. Then the accelerations suddenly decreased and the period of the motion lengthened.

Time of Failure

In many instances of liquefaction-caused failure, the actual failure was observed to occur following the end of the earthquake ground shaking.

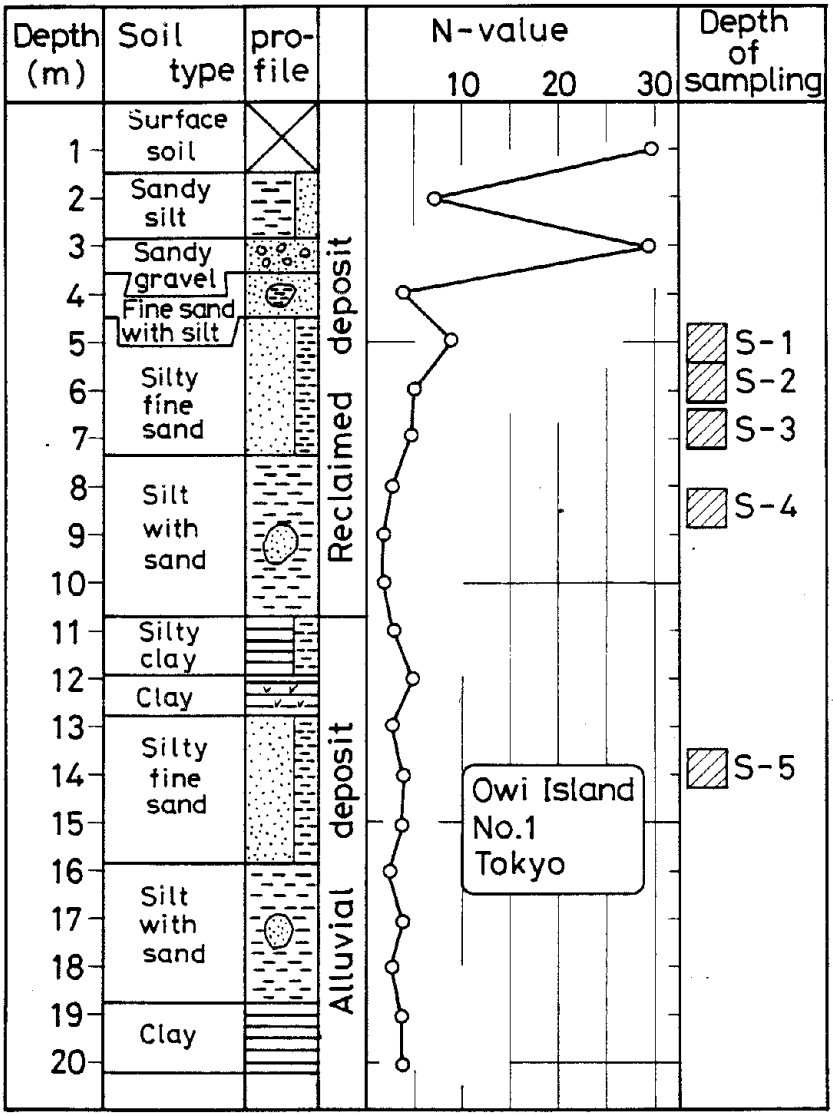

FIGURE 2-16 Soil profile at Owi Island during the September 25, 1980, Mid-Chiba earthquake. Source: Ishihara et al. (1981).

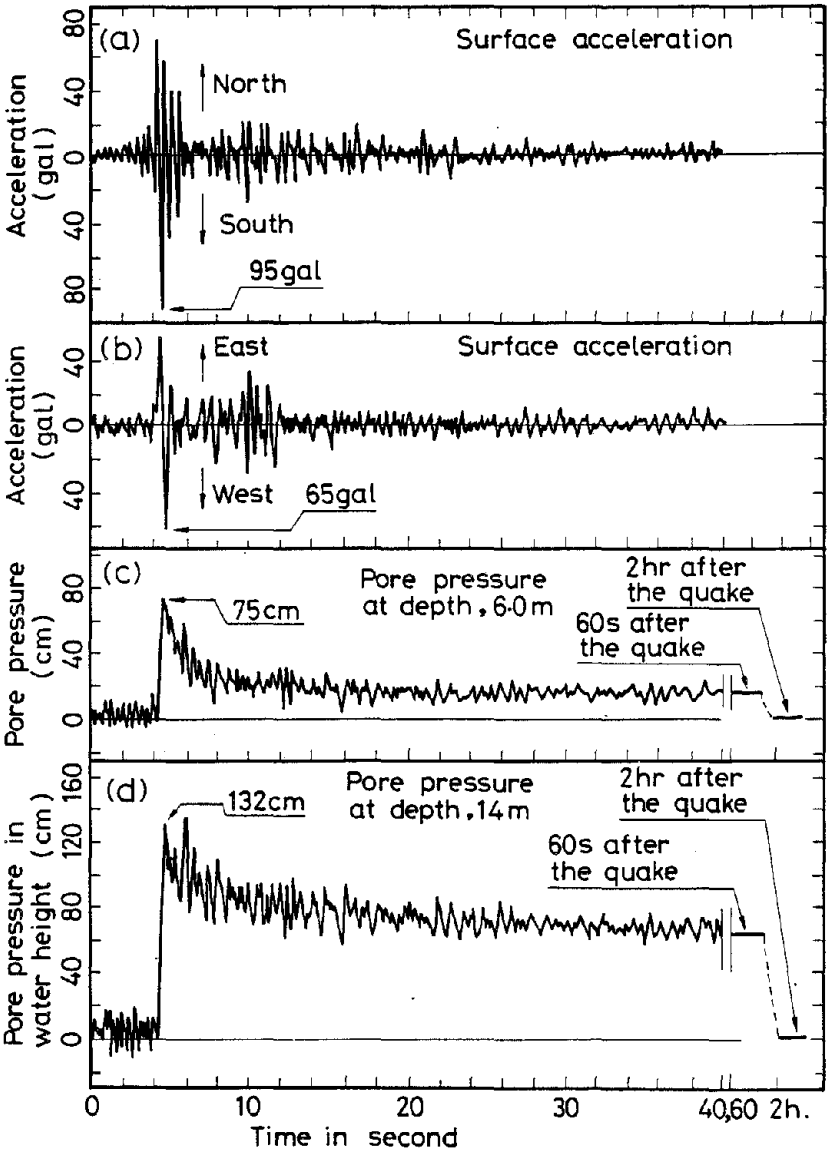

FIGURE 2-17 Instrument recordings of surface accelerations and pore water pressures at Owi Island recorded during the September 25, 1980, Mid-Chiba earthquake. Source: Ishihara et al. (1981).

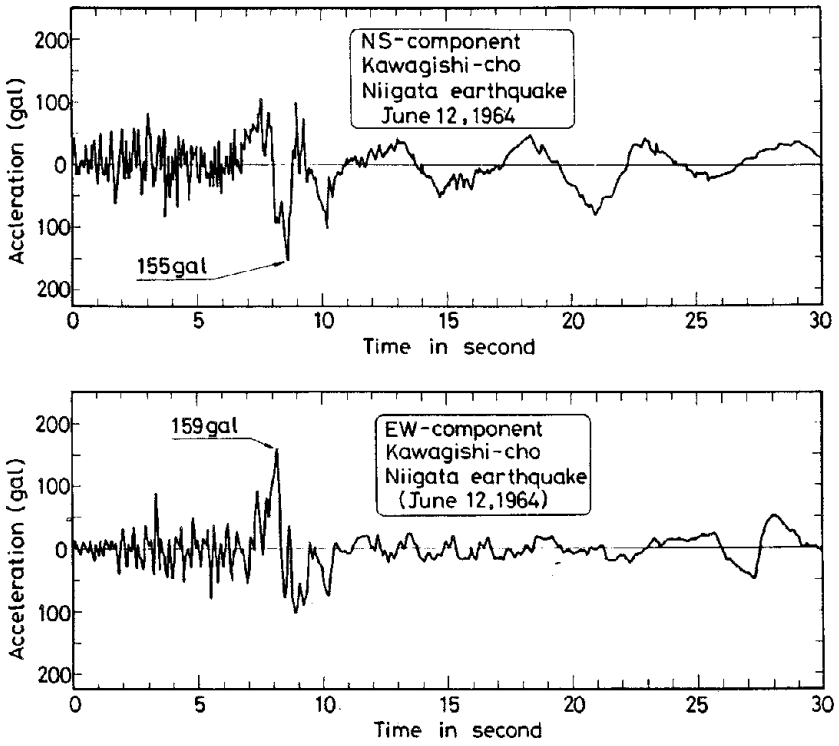

FIGURE 2-18 Accelerations measured in Niigata during the 1964 Niigata earthquake. Note the high-frequency oscillations at the beginning of the record compared with the low-frequency oscillations at the end. The change in frequency is associated with a reduction in the stiffness of the ground resulting from liquefaction. Source: Ishihara (1985).

In the case of the Niigata earthquake, large sand boils erupted near a school about three minutes after the cessation of shaking. The sudden and dramatic failure of the Lower San Fernando Dam (Figure 2-4) is reported to have occurred about 30 seconds after the end of strong shaking (Seed, 1979b). Failure of a tailings dam in Japan on the Izu Peninsula took place about 25 hours after a major aftershock of the Near Izu Oshima earthquake in 1978 (Okusa et al., 1980; Ishihara, 1984). These are important observations bearing upon the mechanisms involved in the liquefaction phenomenon.

Geological and Geotechnical Observations

Based on the results of sieve analyses on soils that did or did not liquefy during past earthquakes, Tsuchida (1970) proposed the grain

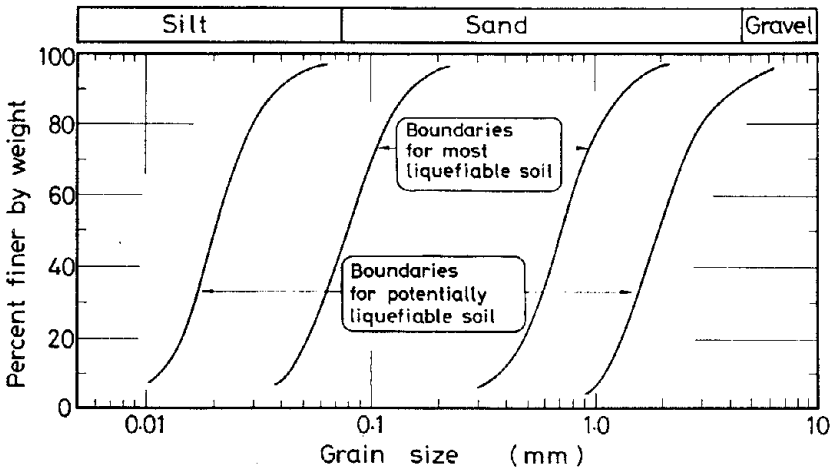

FIGURE 2-19 Limits in the gradation curves separating liquefiable and unliquefiable soils. Source: Tsuchida (1970).

size distribution boundary curves in Figure 2-19 to identify soils that are and are not susceptible to liquefaction. Subsequent work (discussed later in this section) suggests that even finer soils may liquefy if the fines are totally nonplastic.

Earthquake-induced instabilities involving cohesionless soils occur most frequently in geologically recent deposits (Youd and Hoose, 1977). Riverbank deposits and alluvial fans, especially those formed within the last several hundred years, are most susceptible to such failures. Few, if any, failures have occurred in soils deposited earlier than the late Pleistocene. A high water table has also been noted as an essential condition. These observations have formed the basis for procedures to map the susceptibility to liquefaction (see Chapter 4).

Youd (1984a) has examined geological evidence historically concerning the important question: Can a soil that has once liquefied liquefy again during a subsequent earthquake? The answer appears to be yes. Several cases are cited in which a loose layer has been left in the topmost portion of a sand deposit as a result of one liquefaction event, with the layer remaining susceptible to liquefaction again during another strong shaking.

Engineering Correlations

The many documented instances of liquefaction and nonliquefaction on level ground have been used to construct correlations involving the intensity of ground shaking, the depth of the water table, and the

resistance of the soil. Resistance has most commonly been evaluated using the standard penetration test (SPT). These studies have provided the most reliable basis for evaluating the susceptibility of a site to liquefaction (see Chapter 4). However, difficulties in using such correlations arise because the characterization of earthquake strong ground motion is a problem as complex as liquefaction. Thus, the geotechnical engineer concerned with liquefaction is confronted with the problem of understanding two complex processes, even before beginning to address the effect of liquefaction on a structure.

Historically, geotechnical engineers have used earthquake magnitude and peak acceleration to characterize earthquakes. Acceleration and duration of strong ground motion, the parameters of primary interest in liquefaction investigations, have been correlated with magnitude and distance to the earthquake source (Seed, 1979a). The correlations, however, are far from perfect, and the reasons for the deviations are not fully understood. McGarr (1984) has argued that accelerations near earthquake sources are a function of both crustal stress state and magnitude. Thus, earthquakes with identical magnitudes, but in radically different stress regimes, may have different capabilities for liquefying susceptible materials.

Variations in shaking duration appear to be related primarily to the manner in which earthquakes are generated. Earthquakes consist of energy released and radiated from fracture along faults as slippage propagates along the fault. Complexities, particularly delays, of the propagation of the rupture cause important variations in duration and acceleration that are not reflected solely by earthquake magnitude.

Another useful scale for inferring peak acceleration at sites with liquefaction, but for which strong ground motion records are not available, is the Modified Mercalli Scale of 1931 (Wood and Neumann, 1931). It is a qualitative scale, ranging from I to XII, that is based on all observable seismic effects at a site, including, for the highest level, structural damage. Comparison at sites with measured strong ground motion indicate a rough correlation between peak horizontal acceleration and intensity (Trifunac and Brady, 1975). Although liquefaction effects have occurred at intensities as low as Intensity VI, liquefaction becomes common at Intensity VII if susceptible deposits are present. This suggests a typical threshold acceleration of about 0.1 g,* although smaller accelerations associated with long-duration earthquakes may cause liquefaction where soil conditions are particularly susceptible.

*The observable effects of liquefaction are among the factors used to determine the Modified Mercalli Intensity, and so this correlation results partly from circular reasoning.

Liquefaction Offshore

Soil deposits located offshore are subject to liquefaction from earthquakes in the same way as onshore soils. Also, during storms submerged soils are subject to many cycles of repeated wave loading, which can generate excess pore pressures even though the individual cyclic loads are modest. Such loadings occur over a much longer time than those due to earthquakes, and the mechanisms of diffusion and consolidation can decrease the pore pressures substantially even while they are being generated (Rahman et al., 1977).

Liquefaction and large deformation from cyclic loading are also significant phenomena to be considered in the design of offshore gravity and pile-founded structures. Experience in the North Sea has shown that rocking of gravity offshore platforms during storms can cause increased pore pressures in the soil under the edges of the structure and a corresponding tendency for the soil to flow out from these zones. Typical design measures for gravity platforms include drainage wells to reduce pore pressures in any sand immediately beneath the structure (Eide and Andersen, 1984).

Submarine slope failures are also of concern. There are recorded instances of enormous flow failures. Andreson and Bjerrum (1967) discussed the occurrence of such failures in cohesionless soils. Slope movements in cohesive soils off the Mississippi Delta, causing the total loss of several offshore platforms and pipelines (Bea and Audibert, 1980; Bea et al., 1980; Henkel, 1982), appear to have a similar nature.

There is also evidence that pipelines buried offshore have failed due to liquefaction of the overlying soil or because of the loss of much of its strength during a storm (Christian et al., 1974).

Blast-Induced Liquefaction

Clear evidence of liquefaction has been observed (Melzer, 1978; Blouin and Shinn, 1983) when explosives have been detonated near the ground surface in the presence of saturated soils to produce a crater (Figure 2-20). Fountains of water and sand boils (Figure 2-21) have occurred, and excess pore water pressures have been measured. Slumping and flow of soils toward and into the initial crater have significantly changed the crater profile. Significant settlement of the ground surface surrounding the initial crater has also occurred. Small buried explosives have been used to densify loose sand deposits (Kok, 1981). An important aspect of the densification process is the liquefaction of subsurface soils (Mitchell, 1981).

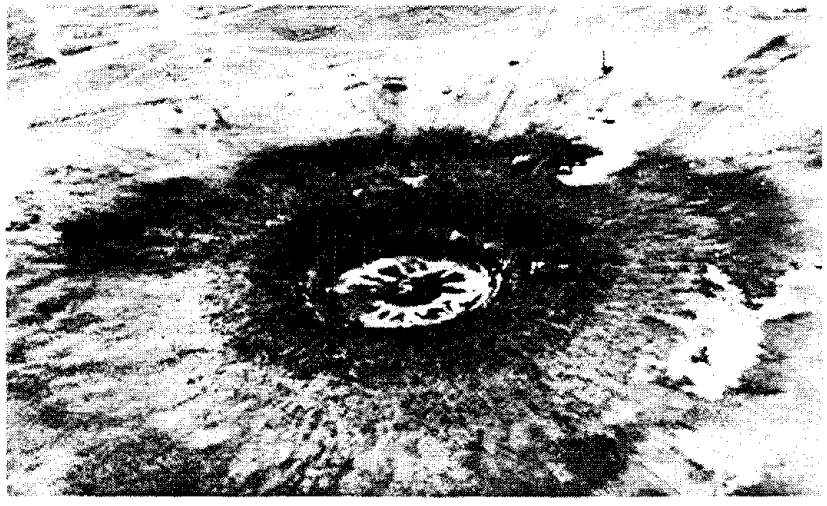

FIGURE 2-20 Example of explosion-induced liquefaction. A large, 1,100-ft-diameter, shallow crater was produced with explosives. Photograph: Courtesy of G. W. Housner.

FIGURE 2-21 Liquefaction is evident from the geysering of water and sand (about 1 m high) through an instrument borehole in an explosion-produced crater. Photograph: Courtesy of G. W. Housner.

Knowledge from Laboratory Tests on Elements of Soil

There is much literature reporting results from tests, using cyclic or earthquake-like loadings, on an element of soil. Some results, discussed herein, provide a basis for (1) understanding the phenomena of liquefaction, (2) identifying the factors that control resistance to liquefaction, and (3) indicating the accuracy and reliability with which resistance can be measured in the laboratory.

Densification by Cyclic Loading

Figure 2-22 shows the progressive densification of a sand by repeated back-and-forth straining in a simple shear test in which drainage occurs freely. Each cycle causes further densification, at a decreasing rate, until the sand assumes a very dense state. This densification is the result of the soil particles being rearranged during the back-and-forth straining. Actually, each half-cycle of straining generally causes some expansion (dilation) of the sand as particles are forced to roll or slide up on adjacent particles, but the particles are able to form a still denser packing upon unloading.

The process of densification is controlled by the amplitude of the cyclic strain rather than by the magnitude of cyclic stress (Silver and Seed, 1971; Youd, 1972). However, for practical work, the amount of densification is often predicted using the ratio of cyclic stress to the vertical or octahedral effective stress. Such practice represents an approximation valid over a limited range of effective stress.

Both cyclic simple shear and shaking table tests of dry sands have shown the existence of a threshold shear strain, γ_t (approximately equal to 0.01 percent), below which no densification takes place regardless of the number of cycles (Dobry et al., 1981a). This behavior was first demonstrated in resonant column tests by Drnevich and Richart (1970) and later confirmed in direct simple shear tests by Youd (1972), and is illustrated by the simple shear results in Figure 2-23. Therefore, cyclic straining below this level is nondestructive, since no rearrangement of soil grains occurs.

Small increases and decreases in effective octahedral stress usually do not result in significant densification of a sand. This statement becomes less valid as the magnitude of the loading increases. With increasing stress the fraction of the strain that remains after unloading also increases (Figure 2-24) because crushing and breaking of soil particles play an increasingly important role.

Buildup of Pore Pressure During Undrained Cycle Loading

Decreases in volume caused by cyclic loading cannot occur if a soil is saturated with an incompressible fluid and movement of the fluid

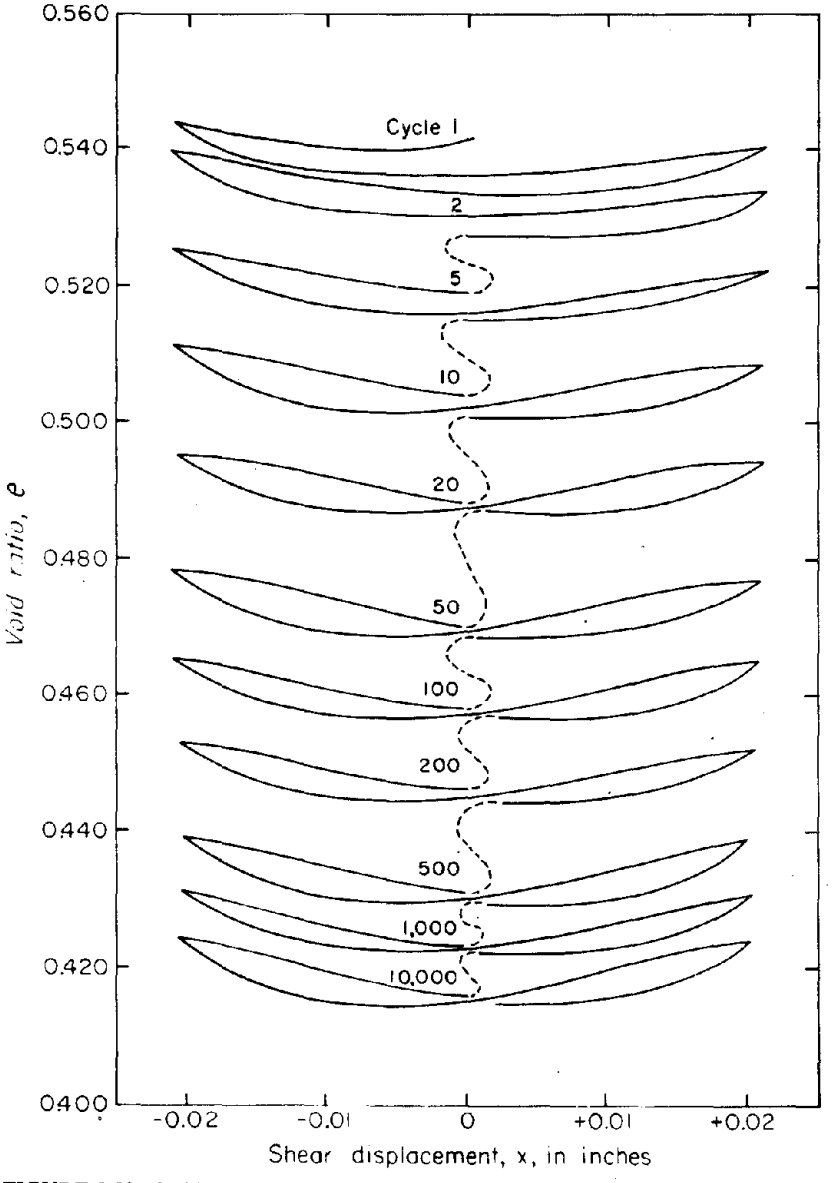

FIGURE 2-22 Void ratio versus cyclic shear displacement showing densification of a sand with successive cycles of shear. Source: Youd (1972).

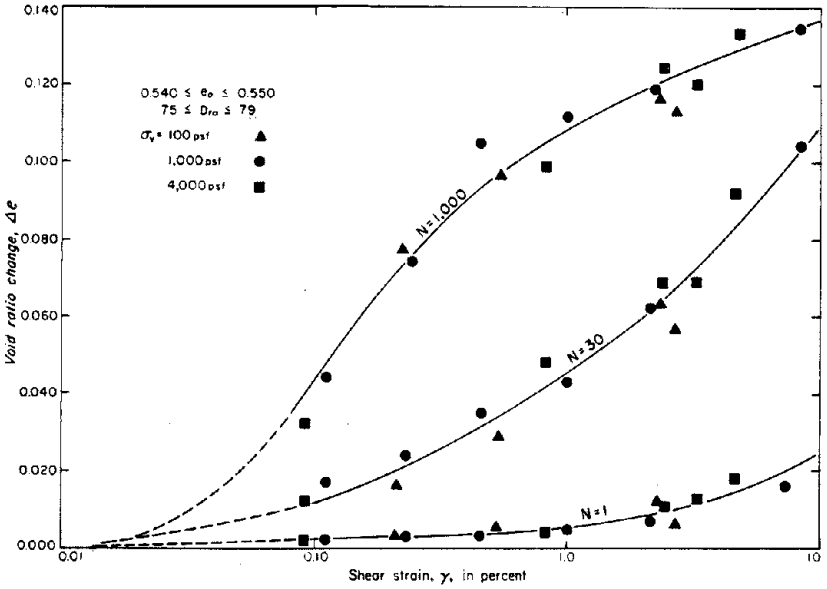

FIGURE 2-23 Void ratio change for a sand as a function of cyclic shear strain and number of cycles. Source: Youd (1972).

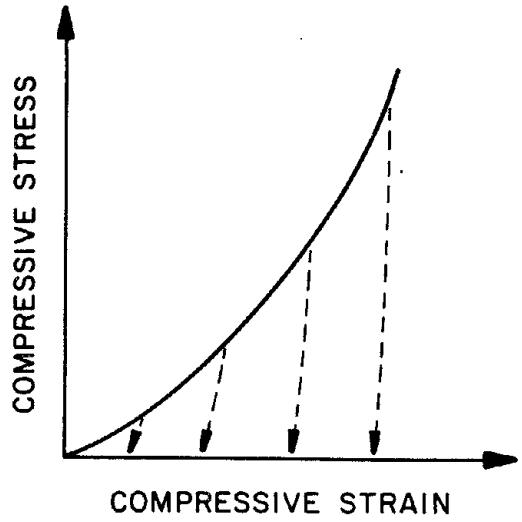

FIGURE 2-24 Load-unload curves from high-pressure tests in oedometer.

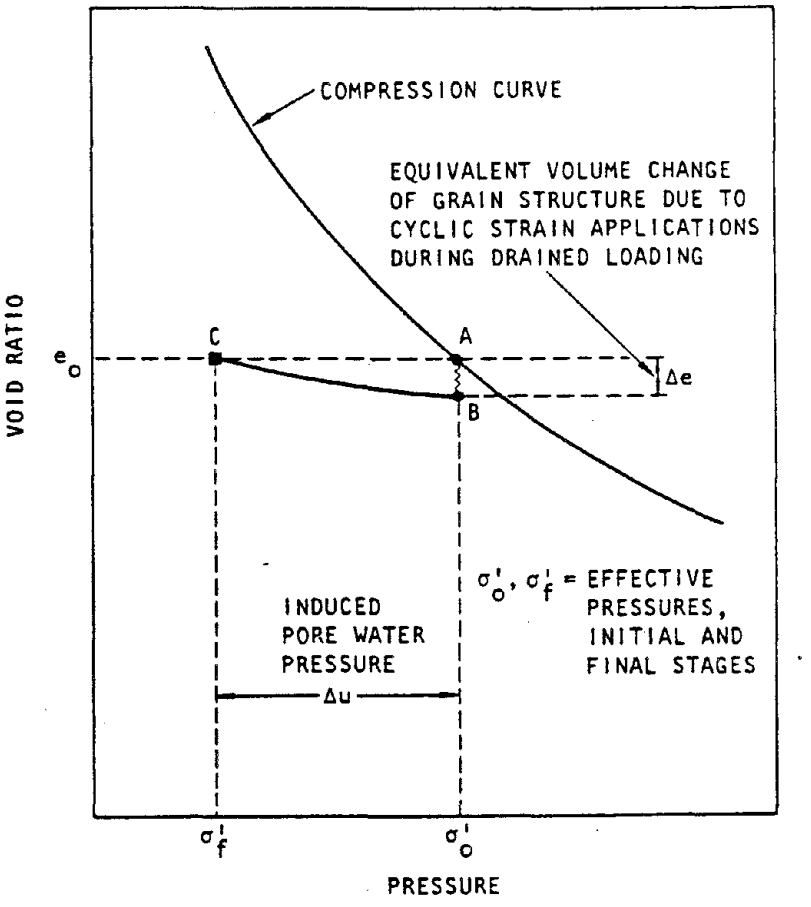

FIGURE 2-25 Schematic illustration of mechanism of pore pressure generation during cyclic loading. Source: Seed and Idriss (1982).

within or from the soil is prevented. Instead, the tendency to decrease in volume is counteracted by a decrease in effective stress. This situation is shown schematically in Figure 2-25. With a constant total stress, a decreased effective stress means an increased pore pressure. In effect, cyclic straining causes the soil skeleton to try to decrease its volume, and part of the applied stress is transferred to the less compressible pore water.

Seed and Lee (1966) first demonstrated and investigated the pore pressure buildup in sand subjected to cyclic loading. Figure 2-26 shows several of their classical results for tests in which the initial consolidation stresses are isotropic; that is $q = 0$ initially. (The stresses in level ground and in a triaxial testing apparatus are illustrated in Figure

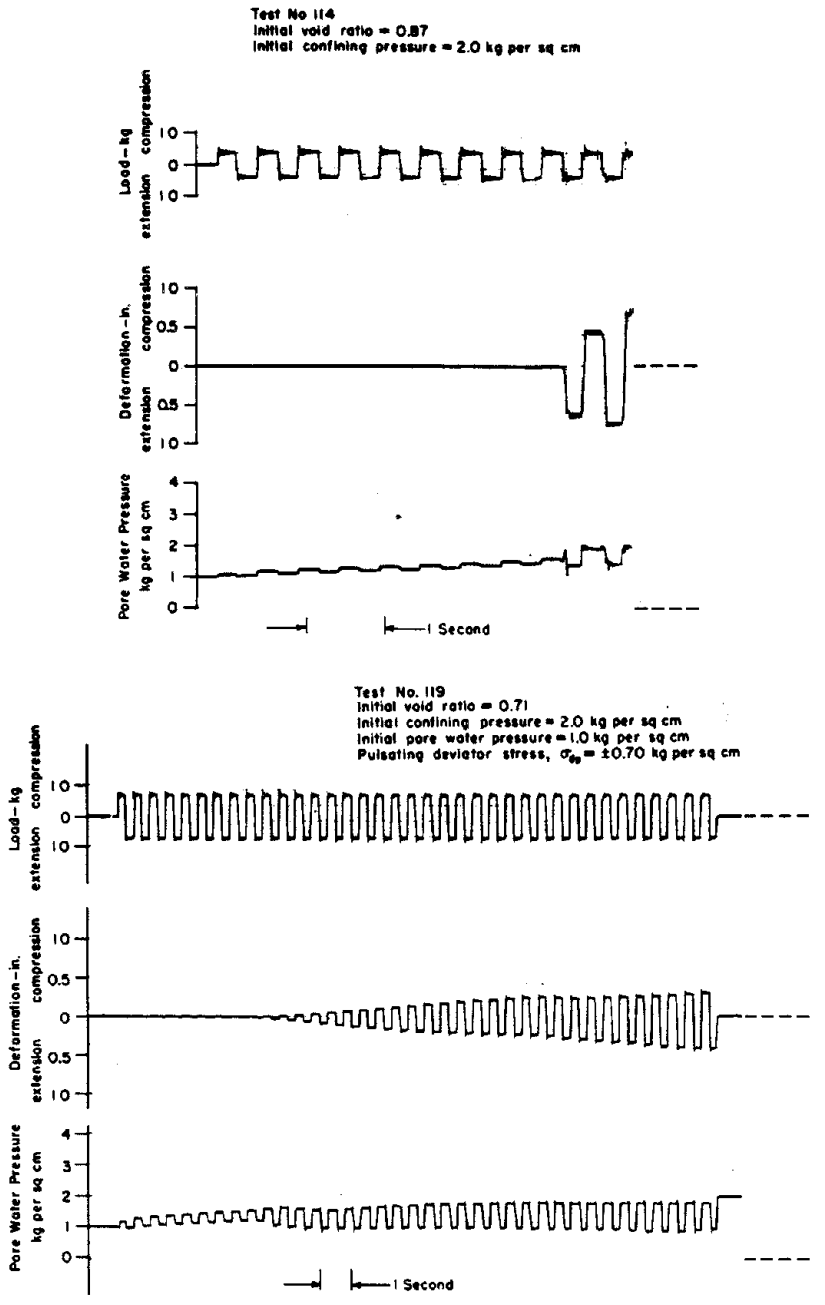

FIGURE 2-26 Results from isotropically consolidated cyclic triaxial tests. The top test (114) is for loose sand; the bottom test (119) is for dense sand. Source: Seed and Lee (1966).

2-27.) As cycling continues, the pore pressure increases progressively until finally it reaches, during part of each subsequent cycle, the total stress acting upon the sand. Thus, there are momentary conditions of zero effective stress. The first time this condition occurs is often referred to as *initial liquefaction*. In this report the symbol $\sigma' \simeq 0$ is used to denote this condition.* Cyclic simple shear tests produce similar results, as shown in Figure 2-28, but the initial liquefaction ($\sigma' \simeq 0$ condition) is now defined as occurring when the pore pressure equals the vertical total stress.

In Figure 2-26 there is a cyclic variation of pore pressure prior to reaching the $\sigma' \simeq 0$ condition, superimposed upon the overall trend for a steady increase. This cyclic variation is caused by the change in octahedral stress during each cycle—a change that is immediately reflected in the pore pressure. This strong cyclic effect is absent in the results from the simple shear tests (Figure 2-28). The pore pressure continues to cycle after first reaching the $\sigma' \simeq 0$ condition, which can only occur in the absence of shear stress. Application of shear stress causes dilation and decrease in pore pressure; thus, the pore pressure cycles as the applied shear stress cycles.

The number of cycles required to reach the $\sigma' \simeq 0$ condition is a function of the density (among other factors) of the sand and of the magnitude of the applied cyclic stress (or strain). A typical relationship is reproduced in Figure 2-29. Here the intensity of loading is represented by the ratio τ_c/σ'_{vo} where τ_c is the cyclic stress and σ'_{vo} is the initial vertical stress. The value of τ_c/σ'_{vo} required to reach $\sigma' \simeq 0$ in a given number of cycles is not a constant, but rather decreases with increasing σ'_{vo}. This decrease is related to the fact, noted above, that the tendency to densify is controlled by cyclic strain rather than cyclic stress.

As shown in Figure 2-30, cyclic shear strains must exceed a threshold level before any excess pore pressures are generated. This threshold strain corresponds to that required to begin densification and is about

*The approximately equal symbol ($\simeq$) indicates that the decreased resistance to straining associated with initial liquefaction can occur when the effective stresses are still slightly greater than zero. Two methods for denoting effective stress (total stress minus pore pressure) are in common use: σ with a bar ($\bar{\sigma}$) or with a prime (σ'). They will be used interchangeably in this report.

There was considerable discussion during the workshop concerning the best shorthand notation for denoting the condition of initial liquefaction. An alternate notation receiving strong support was $r_u \simeq 100$ percent, where r_u is the ratio of pore pressure to total vertical stress. This notation, which is not used in this report, clarifies a potential confusion in the use of $\sigma' \simeq 0$: What effective stress is meant? Vertical? Horizontal? In fact, when initial liquefaction occurs, the effective stress must be nearly zero in all directions. Therefore, $\bar{\sigma} = \sigma' \simeq 0$ and $r_u = 100$ percent represent essentially the same conditions.

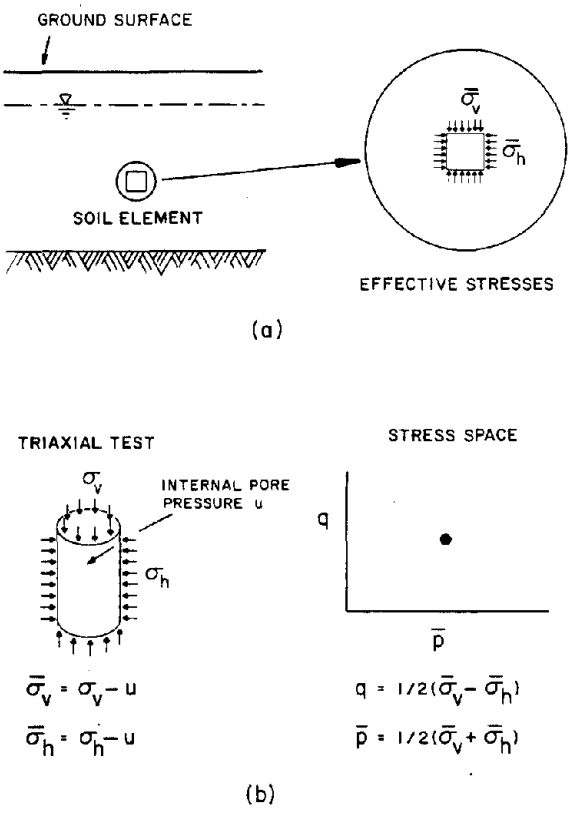

FIGURE 2-27 Illustration and mathematical notation of stress states in the ground (a) and in the triaxial test, with definitions of q and p parameters (b).

10^{-4} (0.01 percent) strain for a wide variety of sands (Dobry et al., 1981a, 1982; Dyvik et al., 1984).

Once the $\sigma' \simeq 0$ condition is reached in tests in which the cyclic stress is controlled, the cyclic strains become larger. For looser sand the increase in strains is quite sudden. For denser sand the increase is less dramatic. It appears that there is a limiting cyclic strain that can develop following initial liquefaction, as indicated in Figure 2-31.

Figure 2-32 shows the effective stress path during a typical cyclic triaxial test. (The definitions of q and p are illustrated in Figure 2-27.) The gradual buildup in pore pressure causes the stress path for each cycle to progress toward the failure lines. Once a failure line is reached (typically during the extension portion of a cycle), pore pressure and strain development accelerate. After the $\sigma' \simeq 0$ condition occurs, the stress paths run up and down the failure lines, passing through or near

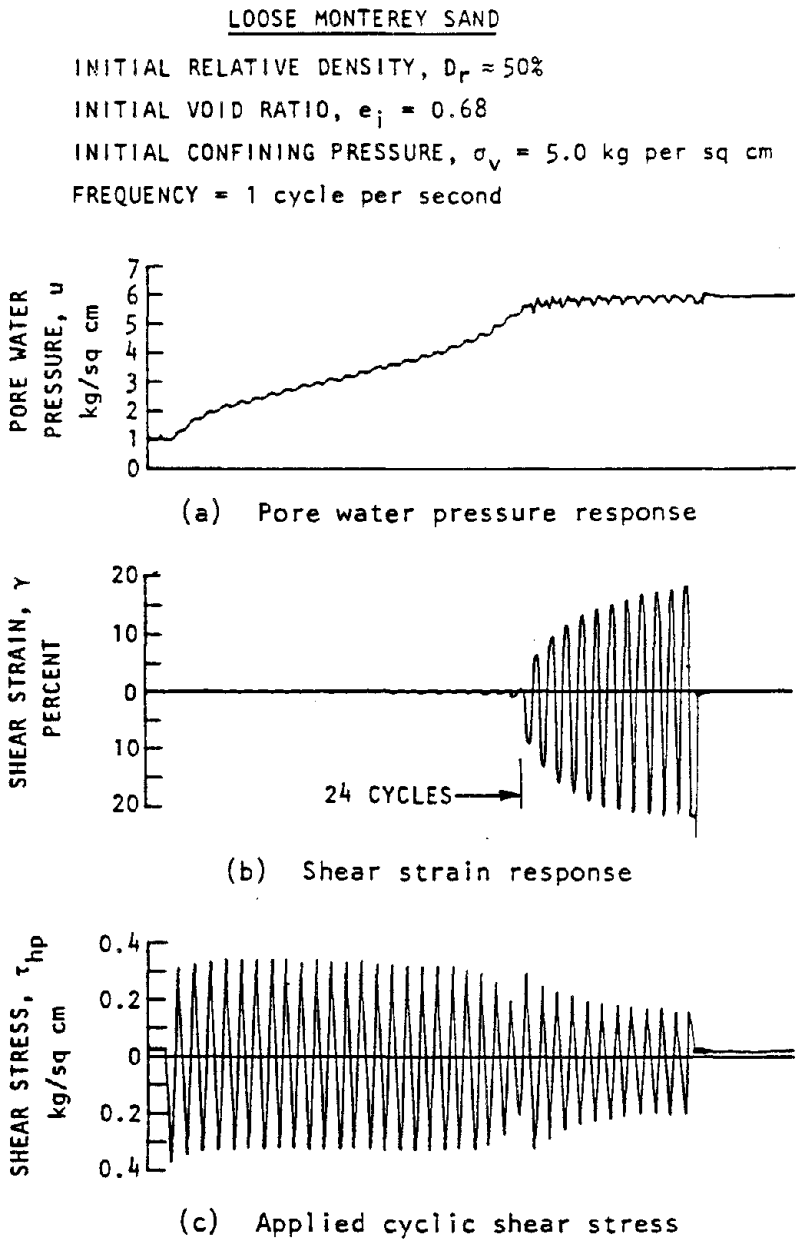

FIGURE 2-28 Results from a typical simple cyclic shear test on a loose sand. Source: Seed and Idriss (1982).

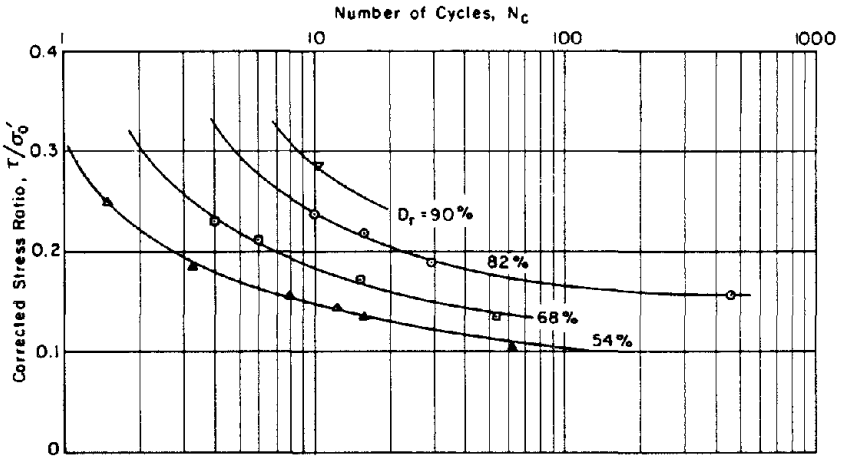

FIGURE 2-29 Stress ratio τ_d/σ'_{vo} versus number of cycles to initial liquefaction, from tests on a shaking table. Source: DeAlba et al. (1976).

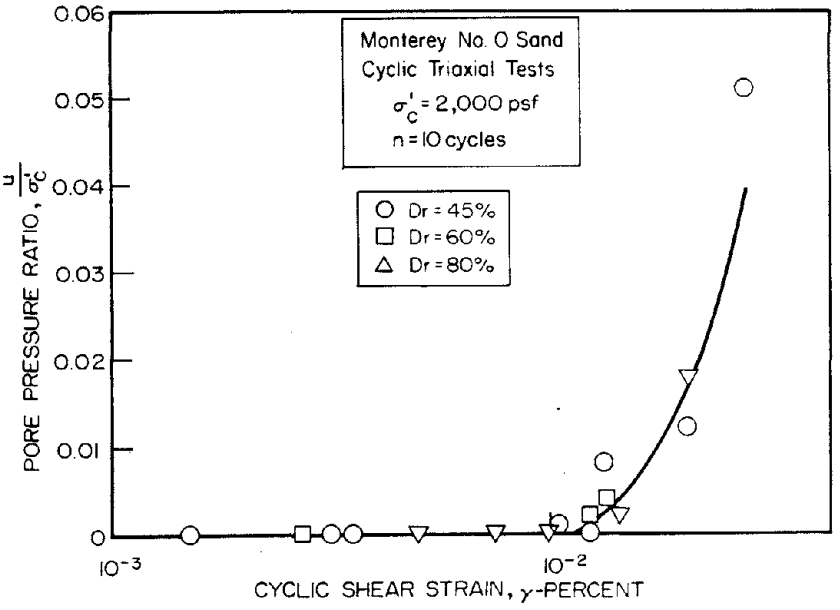

FIGURE 2-30 Pore pressure ratio versus cyclic shear strain, illustrating the concept of a threshold strain required to cause generation of excess pore water pressures. Source: Dobry et al. (1981a).

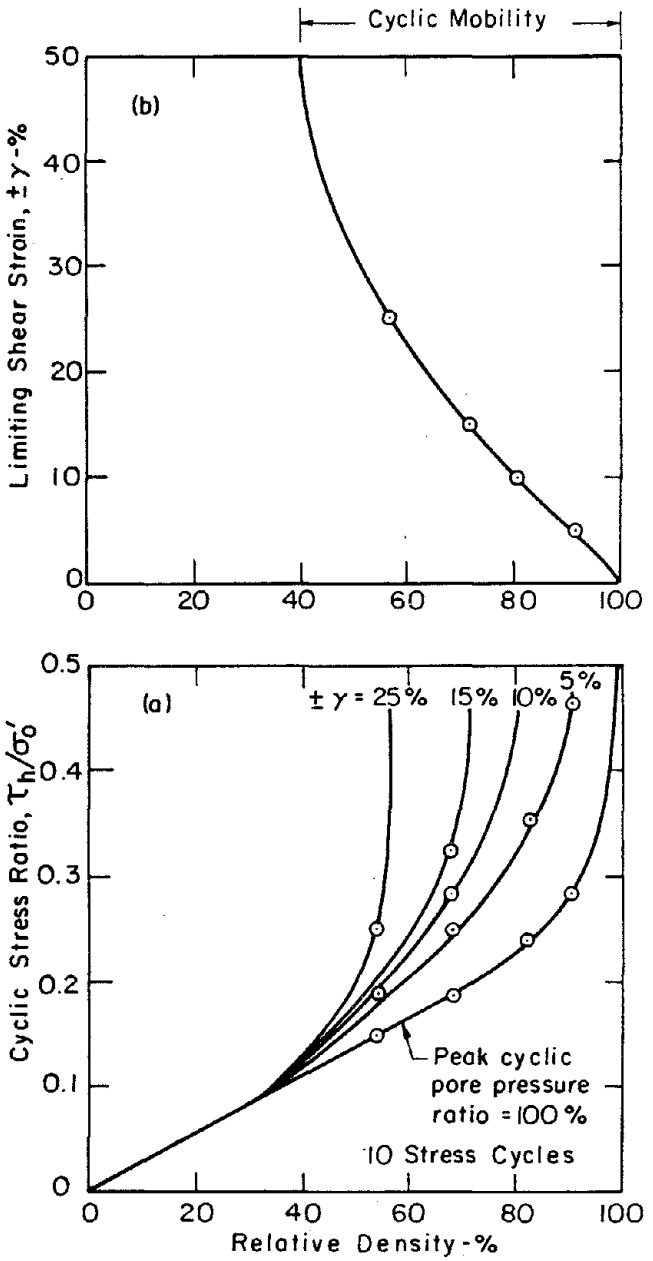

FIGURE 2-31 Limiting shear strains during shaking table tests. Source: Seed (1976).

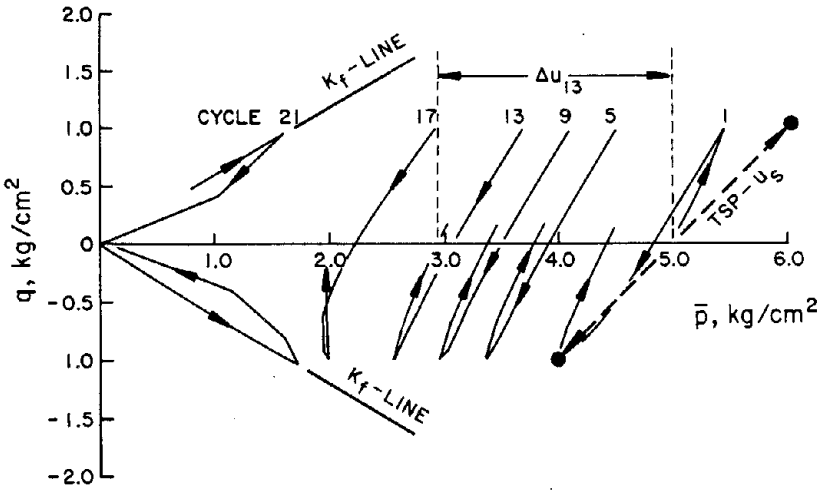

FIGURE 2-32 Effective and total stress paths for isotropically consolidated fine sand (relative density = 55 percent) in a triaxial test. Note that units are in kgf. Source: Hedberg (1977).

the origin twice each cycle. This behavior corresponds to the contraction-dilation phases in densification, as shown in Figure 2-22, and explains the fluctuation of pore pressure subsequent to reaching the $\sigma' \simeq 0$ condition. This fluctuation typically has a frequency twice that at which the stresses or strains are applied. Typical stress-strain loops for the post $\sigma' \simeq 0$ condition are shown in Figure 2-33.

Influence of Static Shear Stress

The foregoing results come from triaxial tests with isotropic consolidation or from simple shear tests with zero sustained shear stress. Anisotropic consolidation in triaxial tests, or the presence of a sustained shear stress in simple shear tests, can have a profound effect on the nature of the results (Vaid and Chern, 1983; Mohamad and Dobry, 1983). This is illustrated by the data from cyclic triaxial tests following anisotropic consolidation, presented in Figure 2-34. Cycling of the deviator stress causes the pore pressures to increase so that the effective stress path shifts progressively to the left, toward the failure line. Once the stress path reaches the strength envelope, it tends to stabilize so that the pore pressure does not build up further. Thus the $\sigma' \simeq 0$ condition is never reached in such a situation. However, there is an accumulation of permanent strain, which continues after the stress path has stabilized at the strength envelope.

The behavior of the stress path upon reaching the strength envelopes and the associated development of strains are affected greatly by the

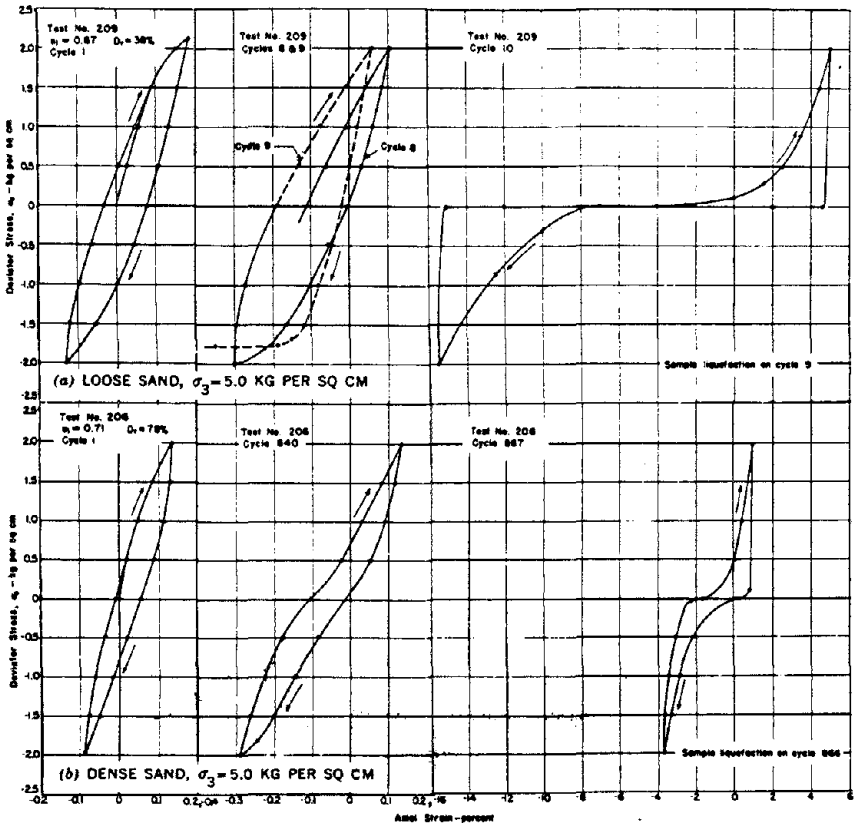

FIGURE 2-33 Hysteresis loops before and after initial liquefaction of loose and dense sands in triaxial tests. Source: Seed and Lee (1966).

minimum deviator stress occurring during cyclic loading and by the density of the sand. Figure 2-35 shows results from a case where the deviator stress just barely reverses. A $\sigma' \simeq 0$ condition develops. If the minimum deviator stress does not drop to zero or if the direction of the deviator stress does not reverses, however slightly, then the behavior is as reflected in Figure 2-34.

When there is a static shear stress, it is in general not possible to express resistance to cyclic loading in terms of the loading that causes a $\sigma' \simeq 0$ condition to be reached. This is the case when the soil is in a slope or is loaded by the foundation of a building. The shear stress is caused by an external load that must be resisted before, during, and after cyclic loading. [The initial shear stresses in a horizontal layer of soil that has been consolidated anisotropically (K_o not equal to 1) may be adjusted internally during cyclic loading and do not have to be

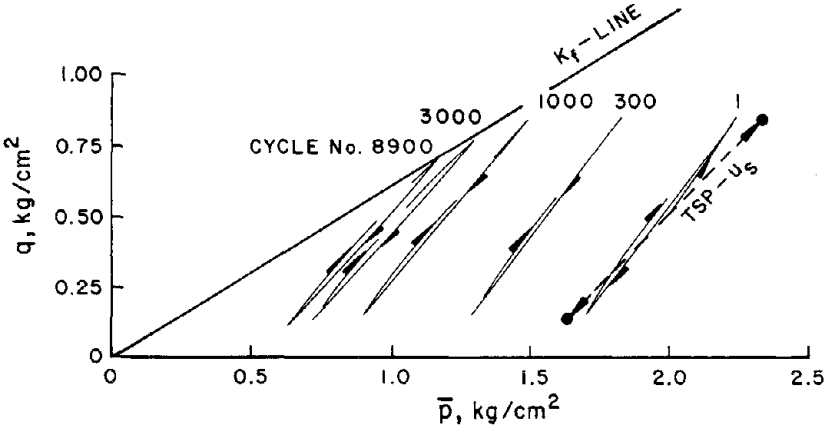

FIGURE 2-34 Effective and total stress paths during cyclic triaxial compression test on fine sand (relative density + 42 percent). Note that units are in kgf. Source: Hedberg, (1977).

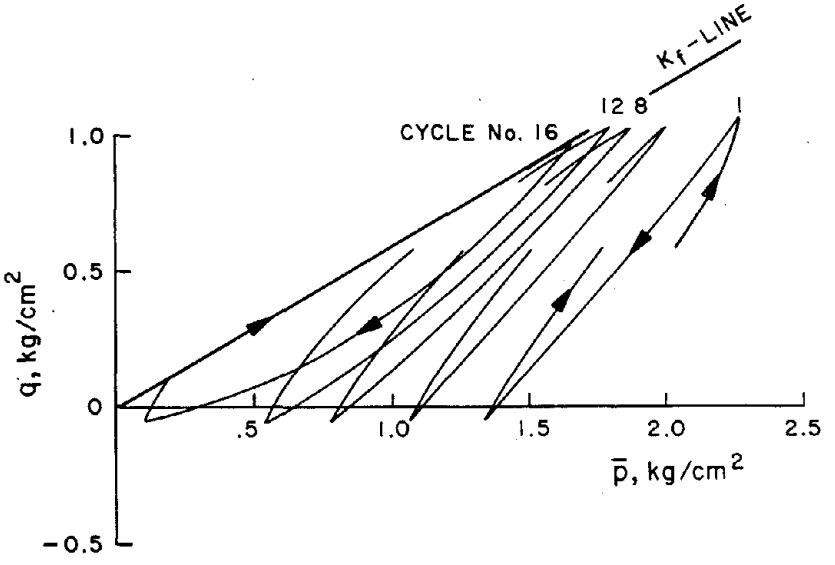

FIGURE 2-35 Effective stress paths from cyclic triaxial test in which deviator stress barely reverses. Source: Hedberg (1977).

resisted.] In this circumstance, resistance is usually expressed (as in Figure 2-29) by the combinations of cyclic shear stress and number of cycles causing a specified strain (cyclic or permanent), such as 2 percent or 5 percent strain.

Cycling Compressive Stress

Usually the application of a cycle of hydrostatic compressive stress under undrained conditions in a triaxial cell, or of axial stress in an oedometer, does not cause any residual increase in the pore pressure. The pore pressure does increase and decrease during a cycle, but the effective stress does not change significantly because of the relative incompressibility of the pore water compared to the soil skeleton.

However, when the total stress increase is sufficiently intense, the volumetric strain in the pore water may become greater than the elastic rebound of the soil skeleton. This unloading may lead to the development of residual pore water pressure that can equal the total stress. This phenomenon is illustrated in Figure 2-36. A major cause of this behavior is the crushing and breaking of particles, leading to higher susceptibility in calcareous versus quartz sands (Fragaszy et al., 1983). The response to compressive loading is a significant factor in the development of blast-induced liquefaction in laboratory experiments conducted with quartz and calcareous sands (Charlie et al., 1983).

Strength Following Cyclic Loading

Even though a $\sigma' \simeq 0$ condition develops in a sand during cyclic loading, the sand may still exhibit considerable resistance to shear during a subsequent undrained loading. This is illustrated by the curves in Figure 2-37. Previous cycling influences the early portion of the stress-strain curve, but the shear strength after loading is still essentially the same. Figure 2-37b shows the results from a test with cyclic loading superimposed upon an initial deviator stress. After cycling, the sand still possesses a substantial margin of strength to support the sustained loading.

This behavior may be understood using the concept of steady-state strength. After a sufficiently large unidirectional undrained deformation, a soil reaches a condition of steady state of deformation* whereby

*The steady state of deformation (Poulos, 1971, 1981) for any mass of particles is that state in which the mass is continuously deforming at constant volume, constant normal effective stress, constant shear stress, and constant velocity. The steady state of deformation is achieved only after all particle orientation has reached a statistically steady-state condition and after all particle breakage, if any, is complete, so that the

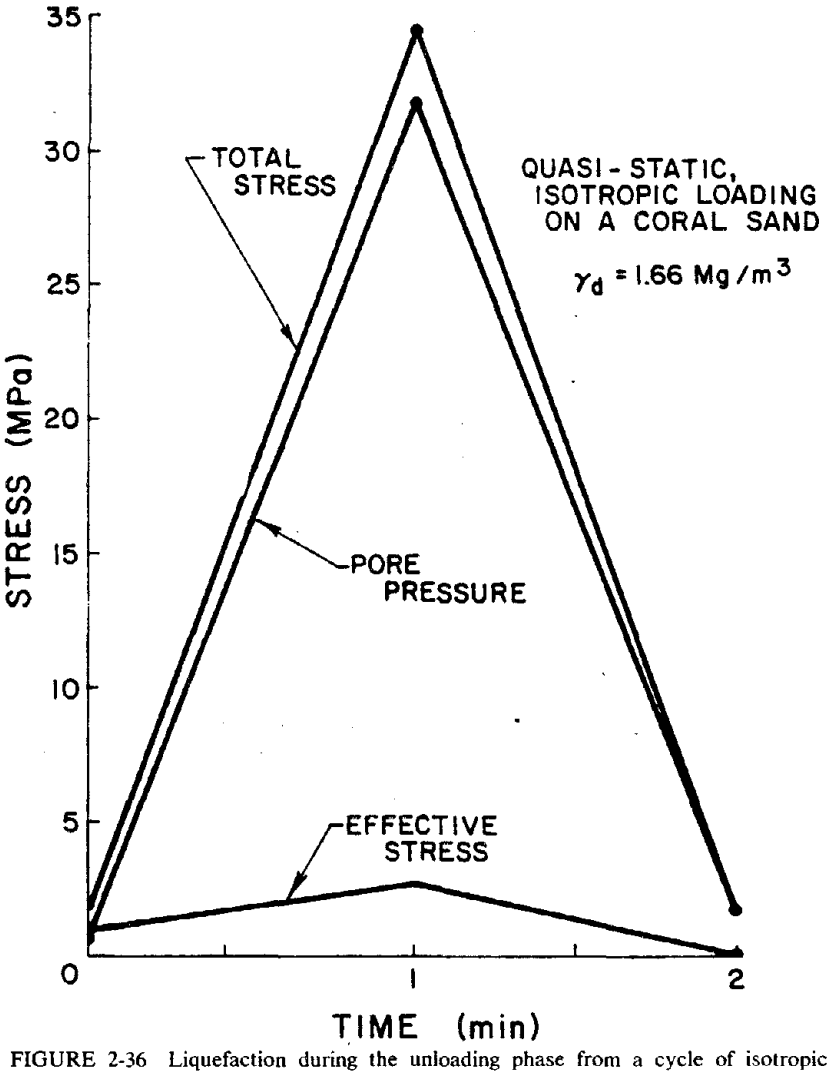

FIGURE 2-36 Liquefaction during the unloading phase from a cycle of isotropic compressive loading. Source: Fragaszy (1985).

shear stress needed to continue deformation and the velocity of deformation remain constant. The steady state of deformation is the same concept as envisioned by Casagrande (1936, 1938) when he proposed the existence of a critical void ratio, or critical density, for sands. The concept, which is similar but subtly different from residual and critical state strength, applies to all particulate materials.

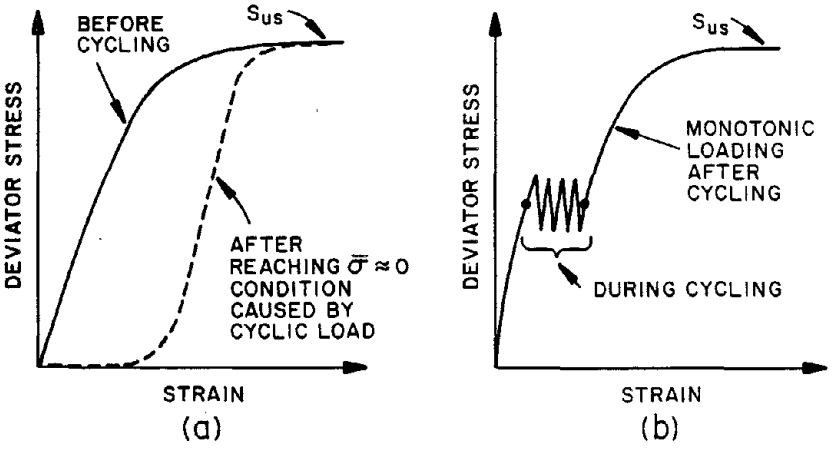

FIGURE 2-37 Undrained stress-strain curves for medium dense or dense sand. S_{us} denotes undrained steady-state shear strength.

the strength is only a function of its void ratio and is independent of stress history and initial structure (Castro, 1969; Castro et al., 1982). Thus, even though a $\sigma' \simeq 0$ condition may develop, the soil does not lose its undrained steady-state strength.

The behavior shown in Figure 2-37a is typical of a dense or medium dense sand consolidated under a relatively low confining stress. If, however, a sand is very loose, or if the consolidation stress is very large, the value of the undrained steady-state strength can be low enough so that it is smaller than the applied static shear stress. Thus, the stress-strain behavior can be as shown in Figure 2-38a. There is an initial loading applied under drained conditions. The subsequent curve for undrained loading exhibits a distinct peak, after which the shearing resistance decreases until the undrained steady-state strength is reached. If such a sample is subjected to an undrained cyclic loading in addition to a sustained deviator stress, it may collapse (Figure 2-38b). That is, it will no longer be able to resist the sustained shear stress.

In very loose sands, undrained cyclic or monotonic strains permit the particles to rearrange so that their resistance to steady deformation is less than the initial loading. The typical test results sketched in Figure 2-38b correspond to a conventional triaxial test. A similar behavior, discussed in Chapter 4, has been observed by Dobry et al. (1984) by superimposing small torsional strains on an anisotropically loaded triaxial specimen of loose sand.

The distinction between the types of behavior illustrated in Figures 2-37 and 2-38 is very important, and will be returned to later. With

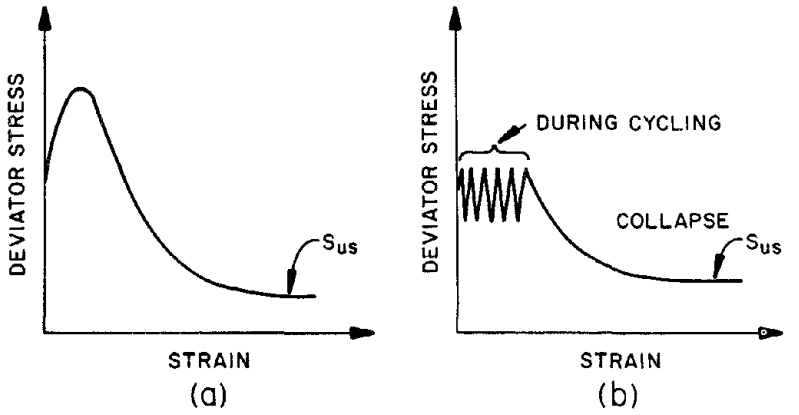

FIGURE 2-38 Undrained stress-strain curves for very loose sand. S_{us} denotes undrained steady-state shear strength.

the behavior shown in Figure 2-37, total collapse is not possible with truly undrained conditions. Large strains, both cyclic and permanent, may result from a cyclic loading. Casagrande (1975), Castro (1975), and Castro and Poulos (1977) have suggested that such a response corresponds to a problem of deformation rather than of strength and should be called *cyclic mobility*. They have maintained that the behavior shown in Figure 2-38, in which total collapse and unrestrained deformation can occur from the loss of strength, is the only true form of liquefaction.

Other Aspects of Behavior

Sample Disturbance and Preparation

Several studies have emphasized the great influence of the method of sample preparation upon the deformations caused by stress-controlled cyclic loading (Mulilis et al., 1975; Ladd, 1977). Figure 2-39 shows a typical set of results (note that all specimens were tested at substantially the same void ratio). Various studies have shown that laboratory-prepared specimens, and also ordinary tube samples, commonly have considerably different resistance than specimens obtained from block samples or from samples frozen in situ, even though the laboratory-prepared specimens are at the in-situ void ratio (Yoshimi et al., 1984). This is illustrated in Figure 2-40. An extensive study at the U.S. Army Engineering Waterways Experiment Station has revealed that substantial nonuniformities are induced in the specimens under cyclic loading. Figure 2-41 compares the density distribution for unstrained specimens (control specimens) with a specimen (number 68) subjected

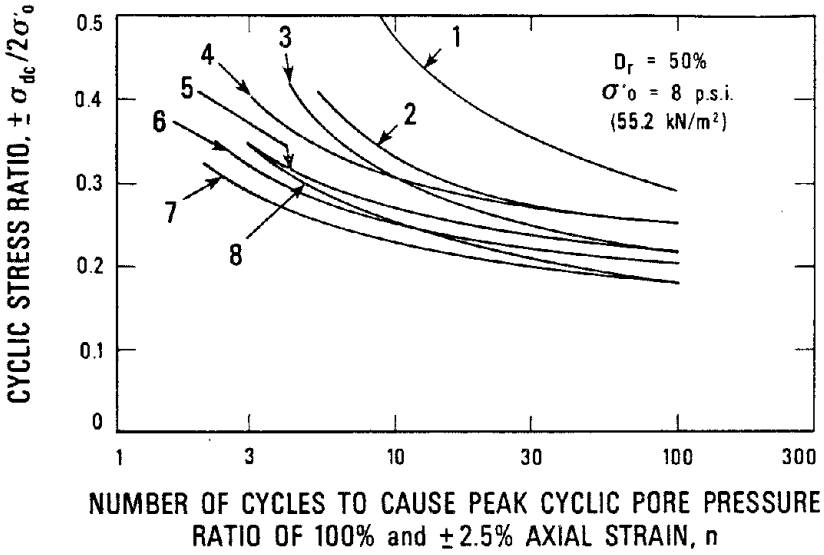

Curve No.	Method of Compaction
1	High frequency vibrations on moist samples
2	Moist tamping
3	Moist rodding
4	Low frequency vibrations on dry samples
5	High frequency vibrations on dry samples
6	Pluviated-water
7	Pluviated-air
8	Dry rodding

FIGURE 2-39 Cyclic stress ratio versus number of cycles for different compaction procedures for specimen preparation. Source: Seed (1976).

to cyclic loads that resulted in a maximum double amplitude strain of 22 percent. Similar results had been shown by Castro (1969).

These several results emphasize the uncertainties involved when laboratory tests are used to measure in-situ deformations resulting from cyclic loading.

Stress History

Laboratory tests have shown that the deformations are influenced significantly by previous overconsolidation, by the duration of a confining stress prior to cyclic loading (Seed, 1979a), and by previous densification by less intense ground shaking. It appears that the influence of such effects upon in-situ resistance may be retained in

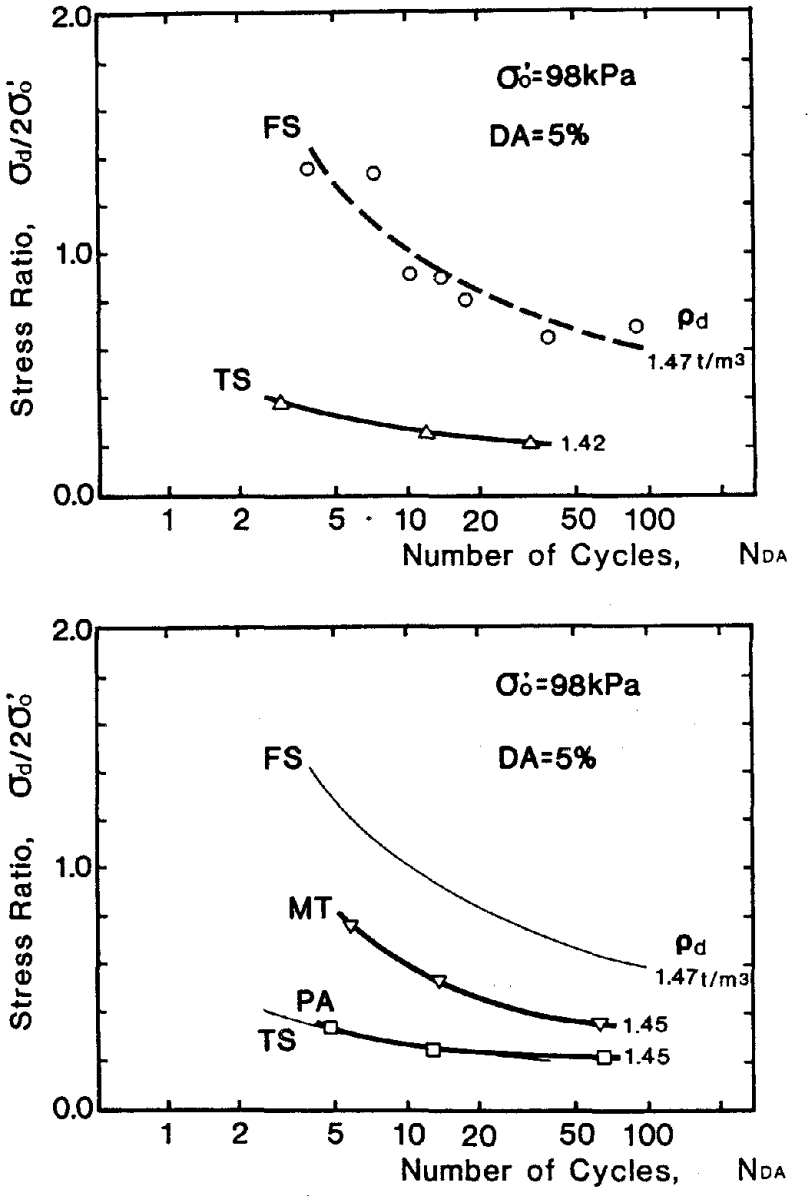

FIGURE 2-40 Undrained cyclic strength of in-situ frozen sample (FS) compared with those of conventional "undisturbed" tube sample (TS) and reconstituted samples (PA: pluviation through air; MT: moist tamping). DA: Double amplitude axial strain. Source: Yoshimi et al. (1984).

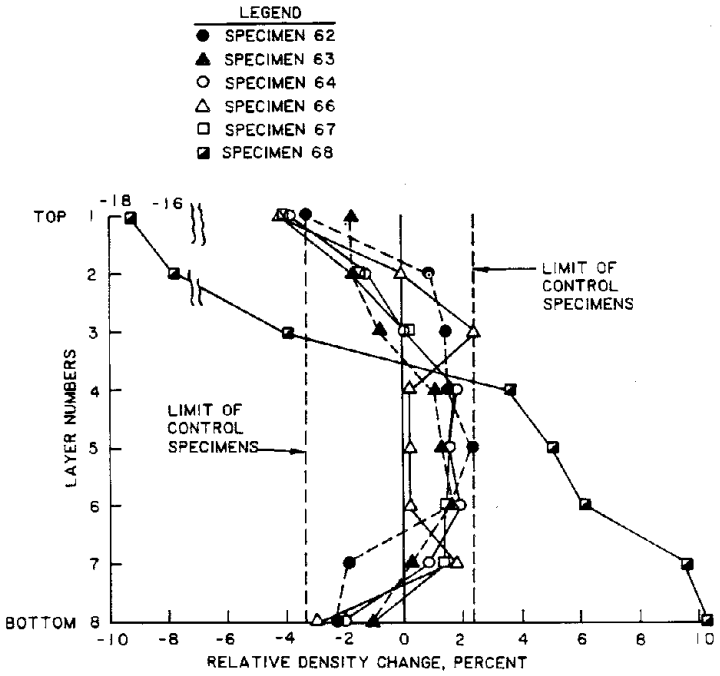

FIGURE 2-41 Relative density versus height in cyclically loaded specimens at nominal 40 percent relative density. Source: Gilbert (1984).

high-quality undisturbed samples obtained by in-situ freezing provided that freezing progresses without impeding drainage at the freezing front, the sands do not contain too much fines, the effective confining stress is adequate, and only a part is used of the frozen sample taken far from a possible zone of disturbance where the freezing pipe has been inserted (Yoshimi et al., 1978; Singh et al., 1982; Yoshimi et al., 1984).

Particle Size, Gradation, and Shape

Tests have revealed that a wide variety of clean cohesionless soils can develop large cyclic strains under cyclic loading if evaluated at comparable densities and if loaded under undrained conditions. (Earlier results suggesting greater resistance in coarser soils involved an experimental error associated with membrane penetration.) On the other hand, the presence of significant amounts of fines—especially cohesive fines—can impede particle rearrangement during cyclic straining and thus provide increased resistance to cyclic loading.

Poulos et al. (1985) state that particle shape is a significant factor in determining steady-state strength.

Ishihara (1984, 1985) has reported results from tests on mine tailings with substantial fractions of fines (see Figures 2-42 and 2-43), but of low plasticity. In cyclic triaxial tests these soils developed significant strains at stress ratios as small as those found for clean sands (Figure 2-43).

General Nature of Cyclic Loading

It is well known that isotropically consolidated triaxial tests measure a greater resistance to deformation than simple shear tests, if both tests are performed using the same initial vertical effective stress and controlled cyclic stresses. The difference is thought to be associated primarily with the different horizontal effective stresses in the two types of tests as well as with larger strains in the extension phase of triaxial loading. Simple shear tests simulate more closely the in-situ resistance beneath level ground, and hence it is appropriate to correct values of resistance measured using triaxial tests (Peacock and Seed, 1968; Seed and Peacock, 1971).

Actually, an ordinary simple shear test simulates the effect of cyclic straining in one direction only, whereas multidirectional straining is present during actual earthquakes. Special simple shear tests with straining in two orthogonal directions, and tests made upon a shaking table, have provided measures of the importance of multidimensional shaking (Seed et al., 1975e; Seed et al., 1977; Casagrande and Rendon, 1978; Ishihara and Yamazaki, 1980). The resistance during multidirectional straining is about 80 percent to 90 percent of that during one-dimensional straining.

Detailed Nature of Cyclic Loading

While ordinary laboratory tests involve uniform cycles of loading, the time history of stress or strain during an earthquake is quite irregular. Methods for converting irregular cycles to equivalent regular cycles have been developed (Ishihara and Yasuda, 1975; Annaki and Lee, 1977; Haldar and Tang, 1981). For most earthquake ground motions, the maximum pore pressure buildup is reached at the time when the largest peak ground acceleration occurs, and hence only the history of loading to that moment must be considered when evaluating the equivalent number of cycles. This ceases to be true when there are subsequent peaks of acceleration almost as large (i.e., greater than 80 percent) as the largest peak.

Minor details of a stress or strain time history can significantly influence the buildup of excess pore pressure and the development of cyclic strains (Nemet-Nasser, 1982; Nemet-Nasser and Takahashi, 1984; Wang and Karazanjian, 1985). Such details are very important

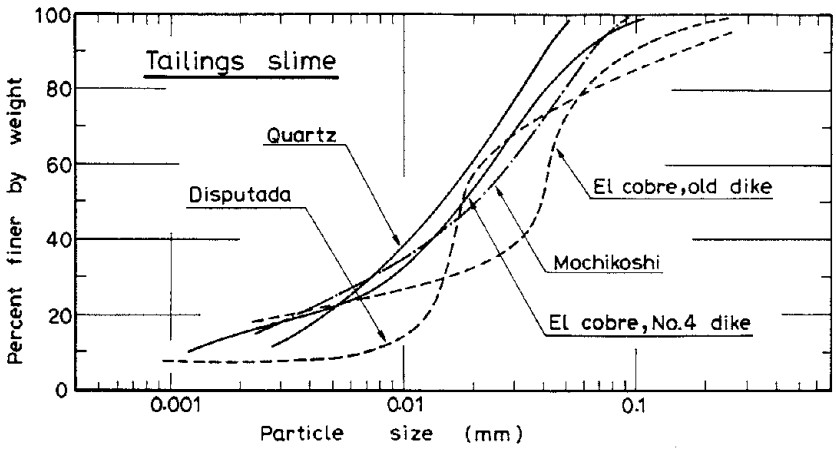

FIGURE 2-42 Graduation curves of tailings slimes used in tests on low-plasticity index tailings slimes. Source: Ishihara (1984).

in formulating numerical analyses designed to predict response to an irregular loading.

Repeated Shakings

Laboratory studies have shown that a history of previous shaking may make a sand either more or less susceptible to liquefaction, depending upon the strength of previous shakings (Finn et al., 1970). In these tests, involving loose sands, samples were allowed to reconsolidate between undrained cyclic loadings. A series of small previous shakings, either too weak to cause liquefaction or just barely strong enough to cause a $\sigma' \simeq 0$ condition, allow the soil to densify uniformly and increases subsequent resistance to liquefaction. However, a very strong shaking may cause uneven densification, leaving a topmost looser layer with increased susceptibility to liquefaction.

Knowledge from Centrifuge Testing

Tests have been performed with shaking tables to investigate basic phenomena and to validate theories. Examples are contained in Finn et al. (1971) and Yoshimi and Tokimatsu (1977). A major difficulty with more detailed experimentation on shaking tables is that the stresses arising from the weight of the soil are much less than those in prototype situations. It is well known that the stress-strain behavior of soil is very nonlinear. Certain aspects of this behavior—such as dilatancy—are quite different for the small static stresses typically encountered in models than for the stresses associated with actual earth structures and foundations.

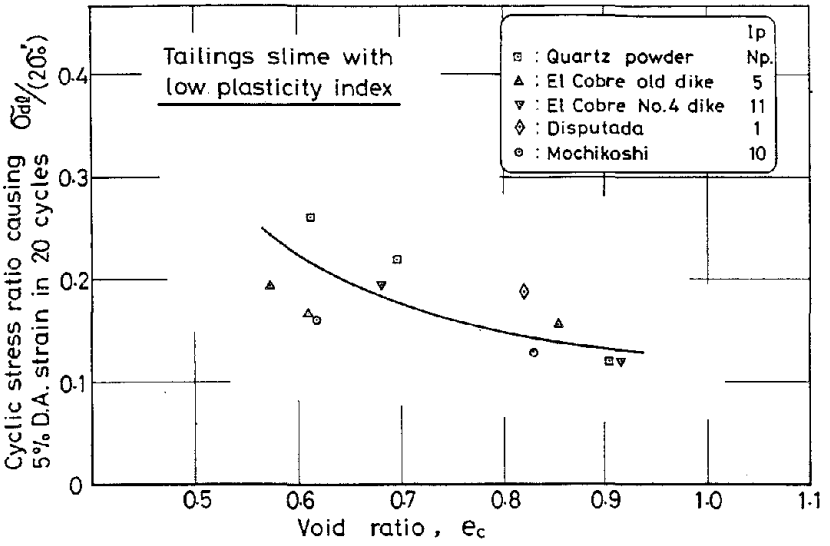

FIGURE 2-43 Relationship between cyclic strength and void ratio for tailings slimes. Source: Ishihara (1985).

One way to overcome this difficulty is to test models on a centrifuge where they are subjected to an increased gravitational field. Consider a dam that is actually 100 ft high. If a model is constructed with a height of 1 ft and is tested on a centrifuge at a centrifugal acceleration of 100 g, then the stresses at corresponding points in the model will be the same as those in the full-scale dam. If stresses are the same, and if the soil is the same in both model and prototype, then the strains and the overall pattern of the deformations should be the same. While various practical problems may preclude the making of exact scaled models of specific prototype situations, centrifuge model tests make it possible to observe the general patterns of response of soil masses to ground motions and to provide data against which methods for evaluating response may be checked.

The typical arrangement for a centrifuge model test is illustrated in Figure 2-44. The container holding the model rests upon a platform that is free to rotate upward as the speed of the centrifuge increases; thus the gravitational acceleration vector always acts along the vertical axis of the model. Cheney et al. (1983) have presented a survey of centrifuge experiments in which the effects of earthquake shaking have been simulated.

Experiments Using Stacked-Ring Containment

In experiments at both Cambridge University and the University of California at Davis (Whitman et al., 1982; Arulanandan et al., 1983),

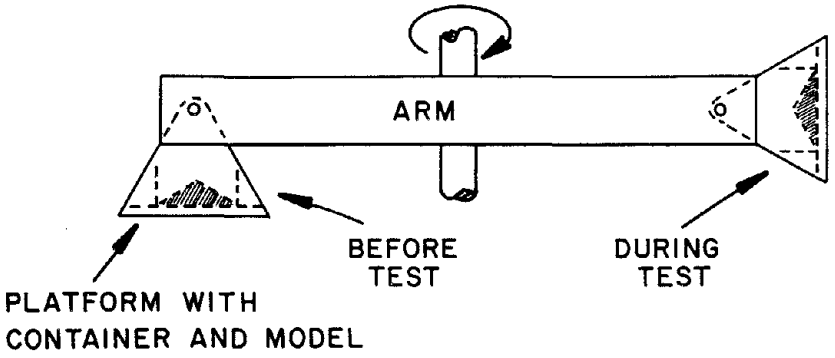

FIGURE 2-44 Schematic of centrifuge arm with swinging platform, soil container, and soil model. The platform is shown both in the stationary position before a test and in the test position while the arm is rotating.

saturated sand has been shaken within a stack of rings (Figure 2-45) to simulate the behavior of a column of soil within a horizontal stratum being shaken at its base. Figure 2-46 shows observed patterns of pore pressure increase during shaking and dissipation after the end of shaking. There was a threshold of acceleration required to cause any increase in pore pressures. While there was some unknown influence of the stack of rings, this threshold corresponded to prototype accelerations of 0.05 g to 0.1 g. In tests with strong shaking, the pore pressures increased until they equaled the total vertical stress; that is, a $\sigma' \simeq 0$ condition was reached. It was observed (Figure 2-47) that subsequent horizontal accelerations within the sand could no longer follow the accelerations applied at the base of the sand. This experimental result can be compared with the Niigata record shown in Figure 2-18. These results have confirmed hypotheses formulated on the basis of cyclic triaxial and simple shear tests and the available field observations.

Several detailed studies concern the process of dissipation of excess pore pressures following the occurrence of a zero effective stress condition. Consider the case of a uniform sand deposit that has completely liquefied during an earthquake and is subsequently "solidifying" through the dissipation of pore pressures. Model tests show that "solidification" will begin at the bottom of the soil deposit (even if the bottom boundary is impervious) and then propagate upward. This constitutes a horizontal solidification front separating soils still liquefied from soils that have "solidified." This has been observed in model soil deposits (Scott and Zuckerman, 1973; Heidari and James, 1982). Above this front the effective stress is zero and the soil particles are in suspension while they settle out. The usual process of consoli-

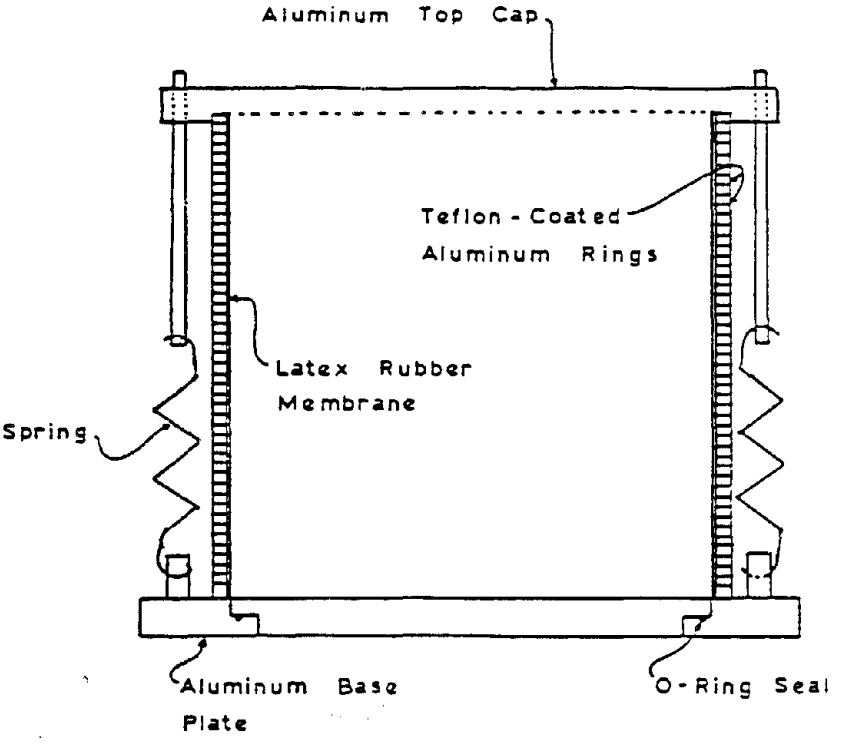

FIGURE 2-45 Schematic of stacked ring container for modeling soil profiles in a centrifuge. Source: Lambe and Whitman (1985).

dation applies only within the sand below this front, although the response of the entire sand mass can be modeled using a very nonlinear consolidation theory (Whitman et al., 1982).

Pore Pressures Within Foundations and Embankments

Results from centrifuge model tests demonstrate the complex patterns of pore pressure that may develop within foundations and embankments of saturated sand by earthquake ground shaking. Dilatancy and pore pressure spreading, as a result of complex interactions between different zones within the soil, are evident.

Figure 2-48 shows results from a test with a structure founded upon a saturated sand subjected to an input similar to that shown in Figure 2-47. The sand was contained within a box. The structure was simulated by lead shot placed within a frame with a flexible membrane as a bottom, and extended across the entire width of the box. The average bearing pressure was 130 kPa (1.3 tons/ft^2). The water table was located

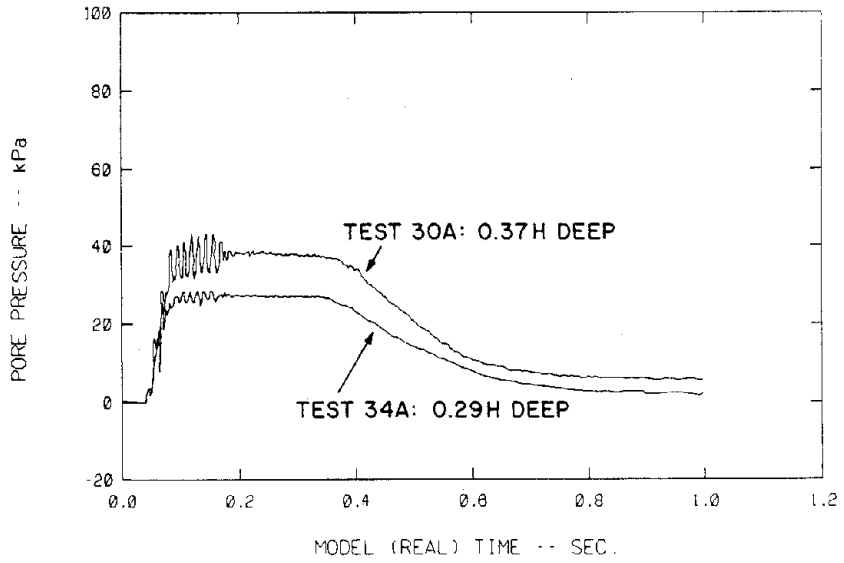

(a) IN UPPER PART OF SOIL

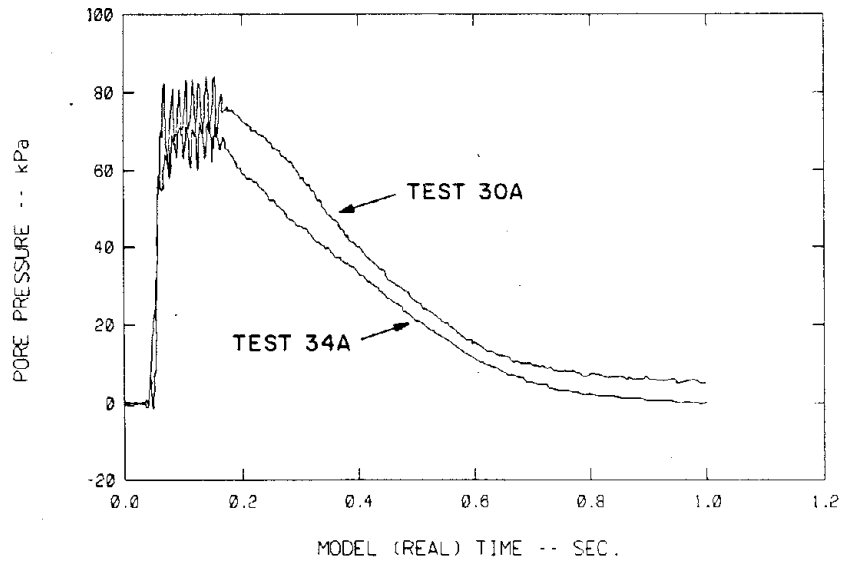

(b) AT BOTTOM OF SOIL

FIGURE 2-46 Pore pressure measurements in a saturated soil column contained within a stacked ring subjected to shaking in a centrifuge. Source: Whitman and Lambe (1985a).

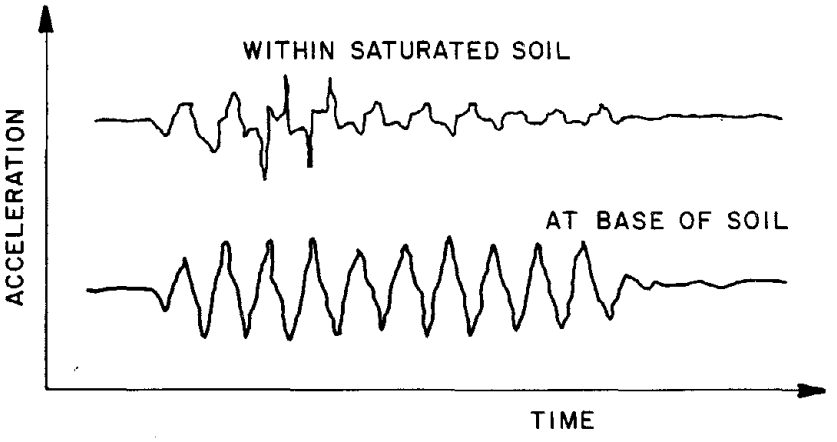

FIGURE 2-47 Acceleration record in a soil column shaken in a centrifuge. Liquefaction in the soil results in a reduced ability to transmit acceleration. Source: Whitman and Lambe (1985b).

at the surface of the sand, which had a relative density of about 65 percent. Several features of the results on the model structure are of note:

- At point E in the "free field" away from the structure, the pore pressure rapidly increases until it reaches the total vertical stress; that is, a zero effective stress condition occurs at this point.
- At points C and D beneath the structure, the excess pore pressure is less than in the free field and much smaller than the total vertical stress at these points. Thus, the presence of the structure has inhibited the buildup of pore pressures.
- At points C and D the pore pressure during shaking fluctuates about the mean trend. This is from the total stress fluctuating at these points, much as in a cyclic triaxial test, because of inertial loading from the structures. This does not occur at points A and E, where the stress conditions are similar to those in a cyclic simple shear test.

Figure 2-49 shows pore pressures measured during shaking of a model dam of sand, with water standing on both sides of the dam. In this and the two subsequent examples, the sand is at a relative density of about 55 percent. At point A on the centerline the pore pressure rose steadily during shaking. At points B, C, and D there was a cyclic component superimposed upon the mean trend of increasing pore pressure. This cyclic component may come from changes in the mean total stress at these points caused by rocking of the dam. At point D the pore pressure initially increased, but then the mean trend reversed and the excess pore pressure became negative. Following the end of

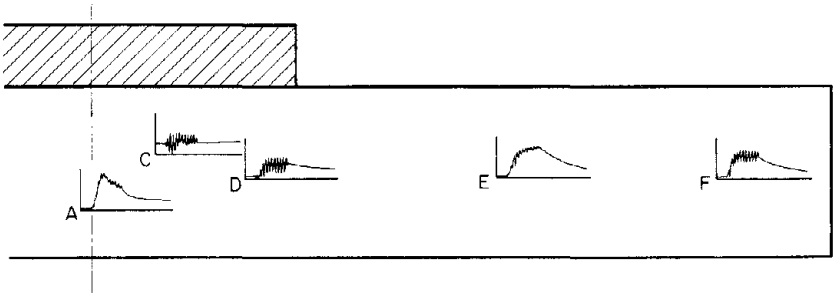

FIGURE 2-48 Pore pressures (vertical) versus time (horizontal) at several points beneath and outside the foundation of a model structure shaken in a centrifuge. The scales are the same for all plots. Source: Whitman and Lambe (1985a).

shaking the excess pore pressure at this point rose and became positive again before beginning to dissipate. Apparently, the mean shear strain at point D became large enough during shaking to cause the sand to dilate.

Figure 2-50 depicts a steel plate resting upon an embankment of sand, with the plate and embankment both submerged. This arrangement simulates a structure resting upon a sand island. The model embankment was 90 mm high with side slopes 3:1 and a crest width of 200 mm. The centrifuge acceleration was 40 g, and the resulting contact pressure from the steel plate was from 15 to 31 kPa. At points X and Y the pore pressure rose steadily during shaking. Immediately beneath the plate the pore pressure reached the total stress, and thereafter the acceleration transmitted to the plate decreased markedly. At point Z the excess pore pressure was strongly negative during early stages of shaking, indicating strains large enough to dilate the sand. Toward the end of shaking the pore pressure began to rise as water seeped toward this point from regions with positive pore pressure, and this trend continued after shaking ceased.

The final case shown in Figure 2-51 involves an embankment of silt resting upon sand, with fluid flowing through the sand. At points 38, 42, and 52 the pore pressure rose during shaking and then began to dissipate following shaking. However, at point 68 the pore pressure remained small during shaking and then rose when shaking ceased.

Settlements and Permanent Distortions

Figure 2-48 involved a situation where initial liquefaction clearly developed within the free field and yet a structure remained stable. There were settlements of the structure, occurring entirely while shaking continued. Adjusted to prototype scale, these settlements were

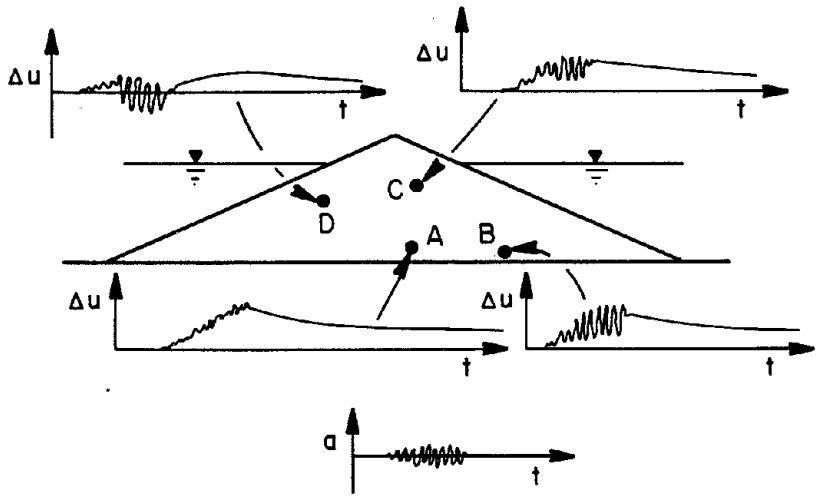

FIGURE 2-49 Pore pressure measured in a model dam shaken in a centrifuge. The vertical scales for the several pore pressure (Δu) records are different. Acceleration (a) versus time at the base of the dam is shown at the bottom. Source: Adapted from Dean and Schofield (1983).

about 80 mm (3 in.), for a structure with a width of 20 m (66 ft). These are large but not necessarily damaging settlements.

Problems with embankments involved noticeable settlements and permanent distortions, but the embankment remained stable despite the development of very large excess pore pressures within large zones of the soil. Clearly the occurrence of large pore pressures and even a zero effective stress condition does not necessarily imply failure of a foundation or embankment.

Theory Based on Microscopic Considerations

Since sands are composed of assemblages of solid particles, experimenters explain the behavior of granular media under stress by examining discrete or particulate models. The simplest of these models are composed of circular disks in two dimensions, or spheres in three dimensions in regular packings. These were used by Thurston and Deresiewicz (1959), Rowe (1962), Scott (1963), and Horne (1965) to demonstrate certain properties allied to soils. Such regular models cannot, however, divulge complex behavior that is qualitatively similar in important aspects to a random arrangement of loose or dense soil particles of irregular shape and a wide range of sizes. In particular, the phenomenon of liquefaction is too complex for these models.

On the other hand, confirmation of some experimental results can

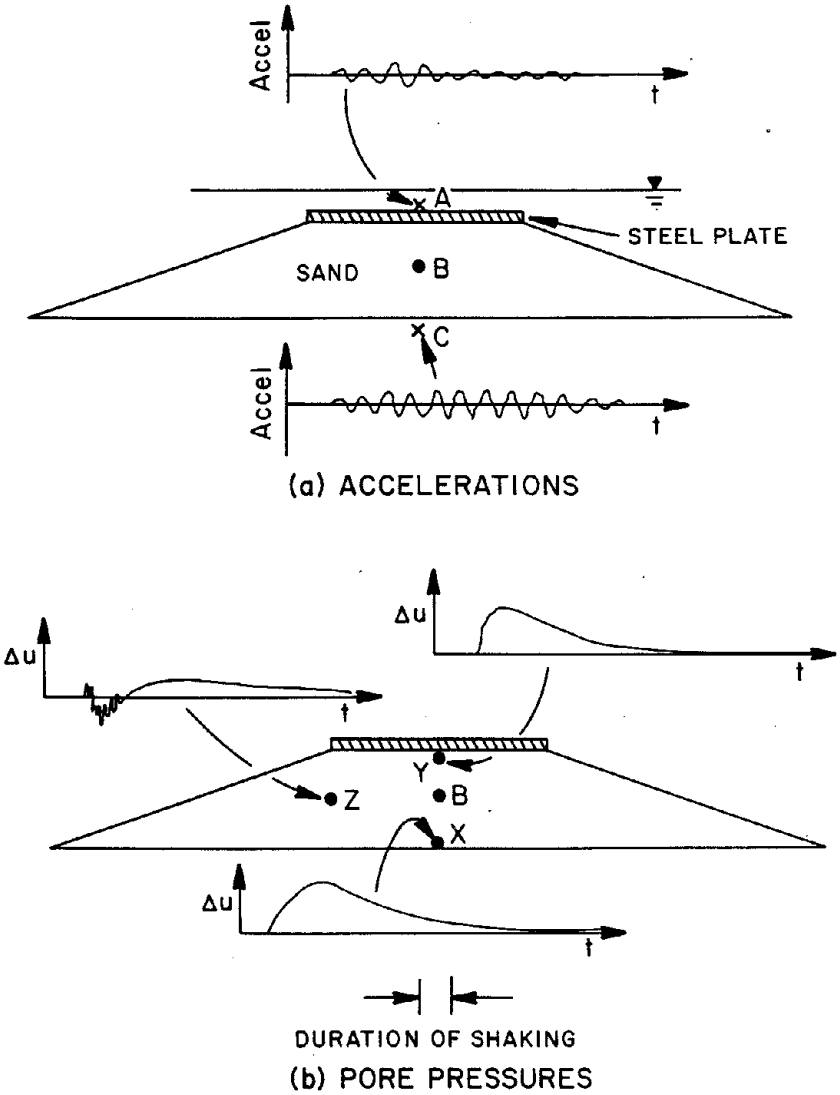

FIGURE 2-50 Accelerations (upper diagram) and pore pressures (lower diagrams) measured in a model structure consisting of a steel plate resting on a soil embankment submerged below the water. This arrangement simulates a structure resting on a sand island in the ocean. The vertical scales differ among the several plots, and the time scales are different for the upper and lower diagrams. Source: Adapted from Lee and Schofield (1984).

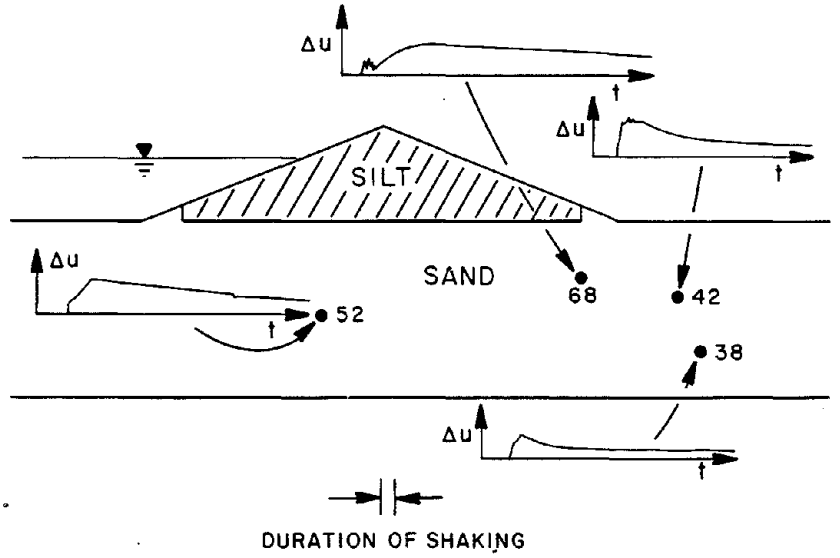

FIGURE 2-51 Pore pressures (Δu) measured in a model of a silt embankment resting on a sand foundation shaken in a centrifuge. Flow is occurring through the sand. The vertical scales are not the same for all plots. Source: Adapted from Schofield and Venter (1984).

be obtained by examining some regular arrays, as demonstrated by a theoretical study performed by Dobry et al. (1982). This clarified the reason for the existence of a threshold shear strain, $\gamma_t \simeq 0.01$ percent, below which no rearrangement of grains takes place, and thus no densification or pore pressure buildup can occur. The model used is the simple cubic array of identical quartz spheres, subjected to an all-around pressure σ (see Figure 2-52). The spheres are elastic and rough (i.e., the contacts can support tangential forces). If a monotonically increasing stress increment τ is then applied, tangential forces T appear at the contacts and create a relative motion δ between centers of adjacent spheres. The load-displacement relation T versus δ for any constant can be obtained using Mindlin's Theory, and is shown in Figure 2-53. At a "threshold" value, $\delta = \delta_1$, all contacts of the array slide simultaneously.

A theoretical expression for the corresponding threshold strain of the array can then be obtained:

$$\gamma_t = 2.08 \frac{(2 - \nu)(1 + \nu)f}{(1 - \nu^2)^{1/2}(E)^{2/3}} (\sigma)^{2/3} \quad \text{(in./in.)} \qquad \text{(Eq. 2-1)}$$

where E and μ equal the elastic constants of the spheres and f equals

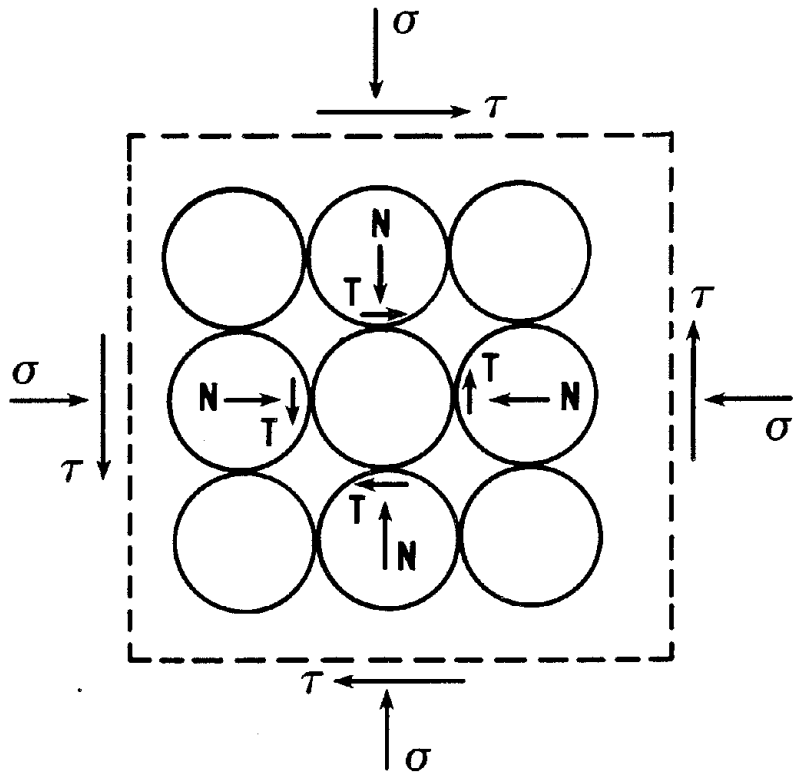

FIGURE 2-52 Stresses and forces on a simple cubic array of equal spheres. Source: Dobry et al. (1982).

the friction coefficient. When the known material properties for quartz are used in Eq. 2-1, an expression is obtained for quartz sands relating γ_t and σ:

$$\gamma_t = 1.75 \times 10^{-4}(\sigma)^{2/3} \qquad \text{(Eq. 2-2)}$$

where σ is in psf. Eq. 2-2 is plotted in Figure 2-54. For the range of confining pressures of most practical interest ($500 < \sigma < 4{,}000$ psf), γ_t is between 0.01 percent and 0.04 percent, close to the experimental values measured in actual sands. For sands made up of grains that are not quartz, Eq. 2-1 permits γ_t to be predicted if the grain's material constants E, μ, and f are known.

Studies have used packing arrangements and contact angles of more realistic granular media to provide preliminary data toward the construction of models more closely identified with real soils (Oda, 1972; Oda and Konishi, 1974). These investigations clarified the microscopic mechanisms developed during shear of soils. More recently, statistical

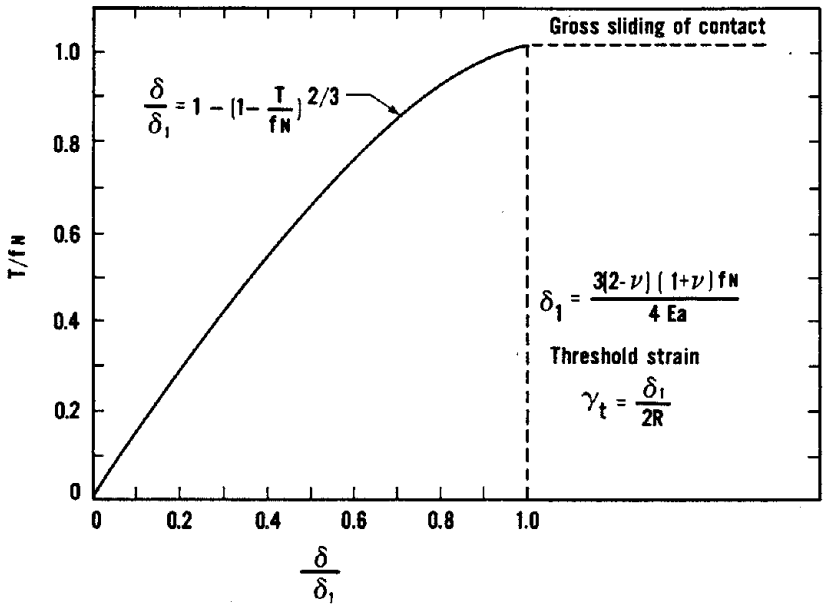

FIGURE 2-53 Tangential force-displacement relation for two elastic spheres under constant normal force N. Source: Dobry et al. (1982).

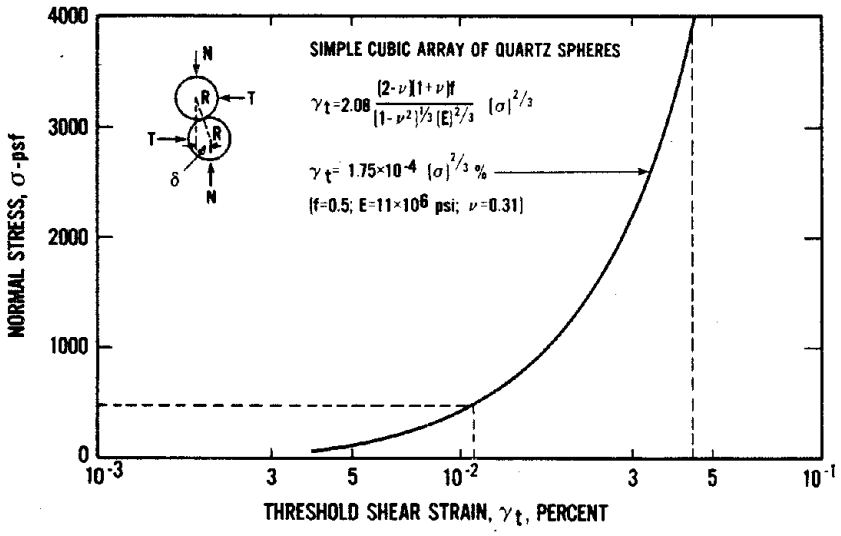

FIGURE 2-54 Calculated threshold shear strain as a function of isotropic confining stress for a simple cubic array of quartz spheres. Source: Dobry et al. (1982).

models have been proposed, based on these preliminary investigations, and have been used to give qualitative and partially quantitative descriptions of behavior in cyclic drained and undrained simple shearing tests (Nemat-Nasser and Shokooh, 1979; Nemat-Nasser, 1980; Oda et al., 1980).

From these studies, Nemat-Nasser and Takahashi (1984) have drawn certain conclusions regarding the behavior of soils in drained and undrained cyclic shearing tests. In particular, they find that the liquefaction resistance of a sample that has been prestrained or previously liquefied is increased if the previous load cycles are terminated at zero shear strain, whereas it is reduced if the cycles terminate in a state of zero shear stress. The results seem to be confirmed by tests and can be explained by examining the effects of anisotropy, through consideration of the soil fabric, or the distribution of soil particle contact angles, in conjunction with their micromechanical model.

Two types of anisotropy are to be distinguished: inherent anisotropy in particle arrangements because of sample preparation or natural deposition, and induced anisotropy from particle rearrangements by previous cycles of loading. It appears that the induced anisotropy is erased when the shear strain returns to a zero state, but not when the shear stress is zero. This is the cause of the changes in liquefaction resistance indicated above. The variation of anisotropy associated with various sample preparation techniques also affects the soil's response to cyclic loading.

3
A Framework of Understanding

The preceding survey of field observations, key results from laboratory tests upon soil elements, model tests, and theory will establish a general framework of understanding to identify any fundamental disagreements and gaps in defining the liquefaction problem and to discuss the state of the art in analysis and evaluation of particular sites or earth structures. This framework provides a synthesis of what is generally known about the behavior of saturated cohesionless soils when subjected to a transient disturbance and the possible consequences of this behavior.

Engineers are concerned primarily with circumstances that cause excessive deformations—those large enough to render some building, transportation system, or facility unuseable, either temporarily or permanently. Essentially their focus is on a possible failure. High pore pressures are symptomatic of a possible failure, and in some cases may be said to cause the failure. Thinking in terms of pore pressures and effective stresses can aid in understanding a problem, but the evaluation of possible deformations and movements of earth must be organized around failure mechanisms.

Two types of behavior constitute "failure." *Flow failure* describes the condition where a soil mass can deform continuously under a shear stress less than or equal to the static shear stress applied to it. Such a condition will cause slope instability or bearing capacity failure. Equilibrium is restored, if at all, only after enormous displacements or settlements. The failures of the tailings dams in Chile in 1965 and 1985, the failure of the Lower San Fernando Dam in 1971, and the bearing capacity failures in Niigata in 1964 are examples of flow failures.

Deformation failures involve unacceptably large permanent displacements or settlements during (and/or immediately after) shaking, but the earth mass remains stable following shaking without great changes in geometry. Examples are settlements of oil tanks and the slumping and cracking of earth dams. Such movements can, if sufficiently large, be the cause of damaged tanks or excessive dam seepage.

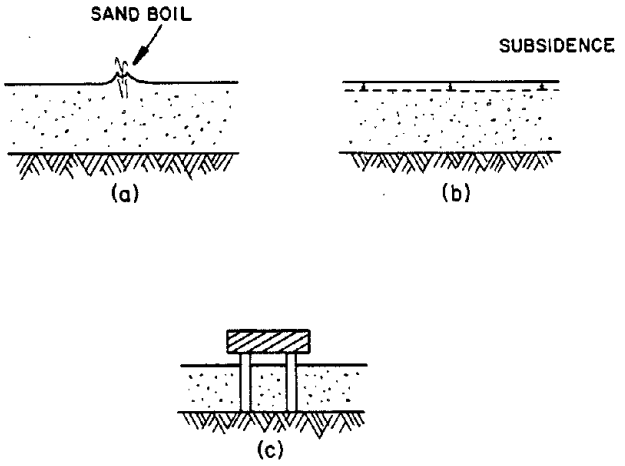

FIGURE 3-1 Possible mechanisms of failure induced by liquefaction on horizontal ground without any significant stresses other than due to the self-weight of the soil: (a) sand boil; (b) subsidence of the ground; (c) a situation where differential transient motions may be damaging.

Liquefaction Failure Mechanisms for Horizontal Ground

For purposes of this discussion, horizontal ground is characterized by: (1) a horizontal surface of very large extent, and (2) the absence of any superimposed or buried structure that imposes significant stresses in the ground. Thus, essentially all of the stress within the soil stems from the self-weight of the soil. Any static shear stresses that may be present in the ground are from the depositional process and subsequent loading history. However, these shear stresses are not needed for equilibrium of the mass, and the shear stresses can therefore change as a result of shaking and even become zero.

Suppose that excess pore pressures suddenly develop within horizontal ground. Such pressures might result from earthquake shaking, from intense compressive loading, or just from a sudden increase in pore pressure imposed at the base of the stratum. Three possible failure mechanisms can be envisioned (see Figures 3-1a, 3-1b, and 3-1c).

Sand Boils

An upward flow of water is established when excess pore pressures develop at some depth. If the upward gradient is large enough, the flowing water will buoy up the soil particles. With a homogeneous soil, this could result in a widespread quicksand condition. It is more likely, however, that the flow will break through to the surface in places where the topmost stratum is especially thin or where there are

cracks or other weaknesses in the superficial soil. Soil particles are carried upward with water at these locations and will be left on the surface as sand boils.

Sand boils alone seldom constitute a failure, although their sudden appearance is frightening. There can be rupturing of thin pavements. There may also be minor subsidence of the area around a boil, associated with the volume of soil deposited on the surface.

Subsidence and Settlement

Dissipation of the excess pore pressures will be accompanied by densification of the soil and settlement of the surface. It is this tendency to densify that causes development of the excess pore pressures by earthquake or blast loading. Such settlement quite likely will be uneven and may result in damage to pavements, railroad tracks, and some structures, especially pile-supported bridges. If the site lies adjacent to a river, lake, or ocean, permanent flooding may result.

Differential Transient Motions

Figure 3-1c depicts a structure overlying the soil and supported on end-bearing piles. The excess pore pressures cause the stiffness of the soil to be reduced, and hence differential motions of many inches or even feet can occur between the top and bottom of the soil during earthquake shaking. Such relative motions may damage the piles or any pipes running vertically through the soil. Since such large transient motions likely would be nonuniform in horizontal directions, buried pipes or tunnels might also experience excessive bending.

Most failures of horizontal ground are problems of excessive deformation, possibly a significant concern in its own right. Deformations may be responsible for a large proportion of liquefaction-induced failures even though they are not the most dramatic aspects of the liquefaction problem. The greatest threat to people involves slopes and foundations. Since a structure often rests upon level ground, the response of such ground (the "free field" away from the structure) often is analyzed to indicate whether or not liquefaction might threaten the structure. Reaching the $\sigma' \simeq 0$ condition in the free field, however, does not necessarily mean excessive settlement of a structure.

Flow Failures of Slopes and Foundations

Figure 3-2 depicts several situations involving a nonhorizontal ground surface, or where a load from a building or embankment is superimposed on otherwise level ground. The common characteristic of these situ-

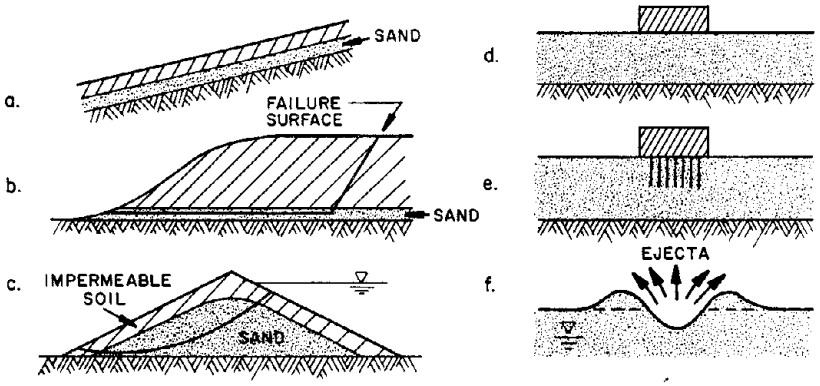

FIGURE 3-2 Examples of situations involving the existence of significant shear stresses in the soil: (a) sloping ground (potential failure mechanism A); (b) embankment on level ground (potential failure mechanism A); (c) earth dam (potential failure mechanism A, B, or C); (d) structure supported on shallow foundation (potential failure mechanism A, B, or C); (e) structure supported on friction piles (potential failure mechanism D); (f) explosion-caused cavity (potential failure mechanism C).

ations is that the saturated cohesionless soil must, if a flow failure is to be avoided and stability is to be preserved, still sustain shear stress once the transient disturbance ceases.

Soils are distinguished on the basis of the shape of their stress-strain curve during *undrained* monotonic straining. For anisotropically consolidated conditions, two possible forms of stress-strain behavior relate to the potential for a flow failure, as shown in Figures 3-3a and 3-3b (Poulos, 1971; Castro, 1975; Castro et al., 1982).

Type I Stress-Strain Behavior

The first type of stress-strain behavior consists of the undrained loading defining a peak strength followed by a decrease in resistance to a value of steady-state (or residual) strength that is lower than the consolidation value of shear stress. During shear, the soil experiences a continuous increase in pore pressure until a condition of steady state is reached, namely continuous deformation at constant resistance, constant effective normal stresses, and constant volume. A point representing the steady-state parameters is shown in the state diagram (the e versus σ'_3 plot) and lies on the steady-state line, which is unique for the soil. The steady-state line is only a function of the soil; it is not a function of the stress history or initial structure. [These concepts concerning type I stress-strain behavior had their genesis in the work of Casagrande (1936, 1938, 1965, 1975).]

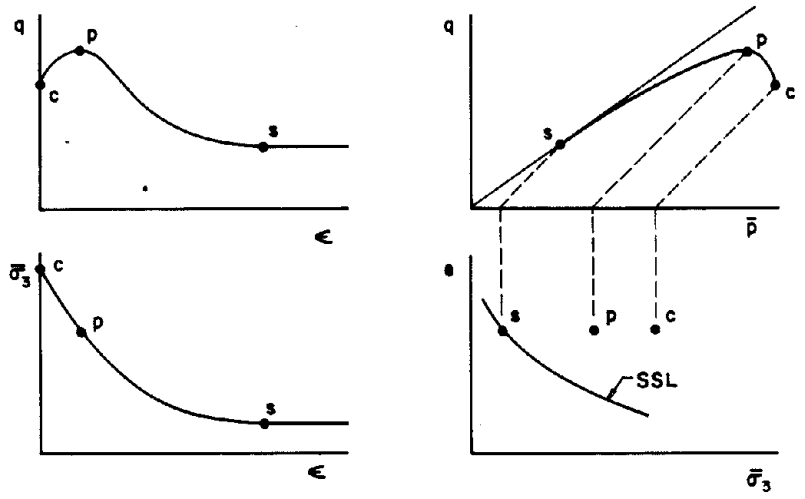

(a) UNDRAINED STRESS STRAIN BEHAVIOR, Type I

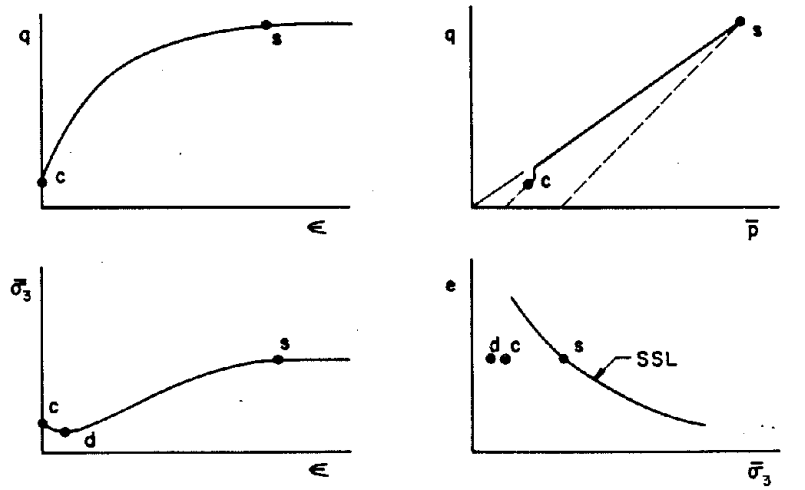

(b) UNDRAINED STRESS STRAIN BEHAVIOR, Type II

Legend: SSL = Steady State Line, s = steady state, c = consolidation state, p = peak strength.

FIGURE 3-3 Comparison of two basic types of stress-strain behavior found in soils under undrained monotonic shear: (a) stress-strain behavior type I; (b) stress-strain behavior type II. Source: Adapted from Poulos (1971), Castro (1975), and Castro et al. (1982).

Type II Stress-Strain Behavior

The second type of stress-strain behavior consists of the resistance initially rising sharply and then more gradually, with a constant resistance being reached generally after a large strain. While the pore pressure may initially increase, after some straining it decreases and the excess pore pressure becomes negative to counteract the tendency of the sand to dilate. It is the gradually decreasing pore pressure and the corresponding increase in effective stress that give rise to the gradually increasing shear resistance. Typically, the effective stress path first bends to the left as in the case of loose sand, but before reaching the failure line it bends back to the right and then runs up along (or close to) the strength envelope until finally a maximum resistance is reached. (In dense sand this maximum resistance may be quite large, possibly being associated with crushing of grains, and cavitation of pore water may occur before it is reached.)

Determinants of Stress-Strain Behavior

The same sand can exhibit either of the two types of stress-strain behavior depending upon the void ratio, the effective normal stress, and the shear stress (or deviator stress) prior to undrained shear. For the sand to exhibit type I behavior it must: (1) plot to the right of the steady-state line in the e versus σ'_3 state diagram, and (2) have a sufficiently high static shear stress so that it exceeds the value of the undrained steady-state or residual strength. The so-called "quick" clays, which are really loose clayey silts, can develop type I stress-strain behavior, as would any sensitive clay.

Four Mechanisms for Flow Failures

With the background given above, four types of flow failures may be identified.

Mechanism A

If the sand beneath a slope or a building has a stress-strain curve of type I, there clearly is a potential for a flow failure. A cyclic loading of sufficient amplitude and duration can "push the soil over the peak" of the stress-strain curve (Figure 3-4). Once this condition is reached, progressive failure will occur, pore pressure will continue to increase, and the shear resistance will continue to decrease until the steady-state or residual strength is reached.

Consider the infinite slope of Figure 3-2a. If the undrained steady-state (residual) strength is smaller than the shear stress required for

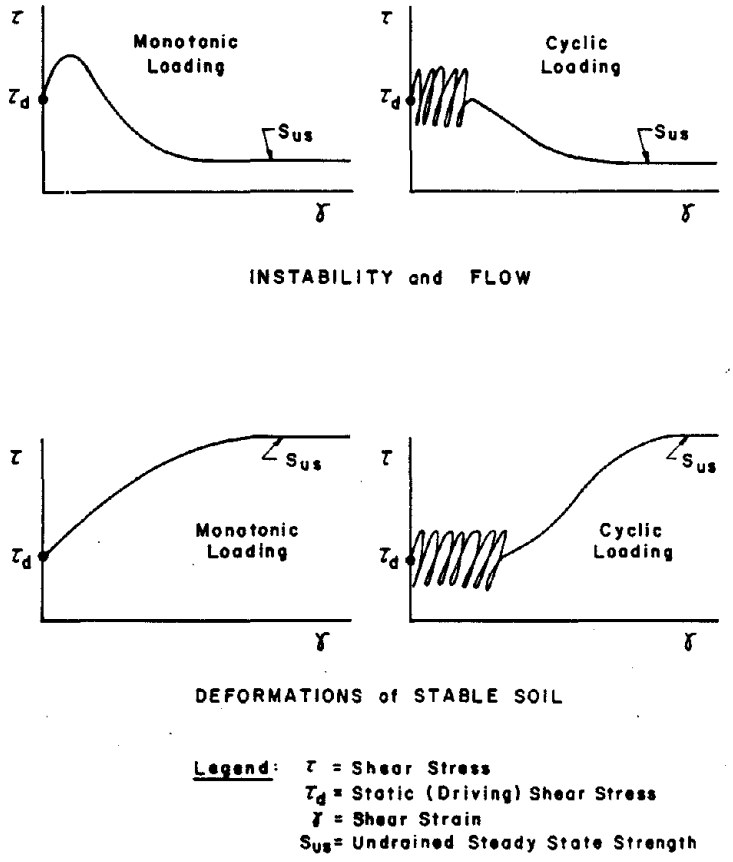

FIGURE 3-4 Unstable and stable behavior under static and cyclic loading. Source: Castro (1976).

static equilibrium, the slope will be destabilized and a flow slide will occur. For the situation depicted in Figure 3-2b, reduction of the shear resistance within the layer of sand may cause the overall slope to become unstable. Similar statements can be made concerning situations c and d. Thus, with a soil having type I stress-strain behavior, a progressive failure can occur with no volume change (i.e., truly undrained conditions) at any point within the earth mass.

On the other hand, if the sand within the slope has a stress-strain curve of type II under truly undrained conditions, there cannot be a flow failure. Cyclic loading may cause some permanent strain and some permanent downhill movement, but it cannot change the value of the undrained steady-state (residual) strength. Thus, at the end of the transient loading, the ever-present static stress is still less than the peak shear resistance and downslope movement will be arrested.

Mechanism B

If the soil overlying the sand is effectively impervious during the duration of the earthquake, the sand as a whole must remain at constant volume. However, a sand whose particles have been rearranged by cyclic straining (or by intense compression) naturally tends to settle under the pull of gravity. If it settles away from the overlying soil, leaving a liquid film at the interface, an unstable situation results. Actually, it is only necessary for a thin layer atop the sand to loosen enough so that its steady-state strength becomes less than the static shear stress that must continually be sustained. Such a situation could result in a failure of an infinite slope or of a slope containing one or more seams of saturated sand (a and b in Figure 3-2).

This process involves changes in void ratio within the sand—loosening of the upper portion and densification of the lower portion with some flow of water upward from the lower portion to the topmost zone (Figure 3-5). The result is a reduction in the steady-state strength of the sand in the upper portion (Figure 3-6). In this case the steady-state strength through the weakest part of the soil will differ from the undrained steady-state strength at the original void ratio. Such a redistribution of void ratio has been observed in laboratory tests (Castro, 1975; Gilbert, 1984) and could be expected in the field as well.

Mechanism C

The high excess pore pressures developed within cohesionless soils will tend to spread into overlying soils, thus reducing their shear resistance. Upward pressures may well cause overlying cohesive soils to crack, allowing sand to be carried upward into these cracks. The result is a loss of strength of the cohesive soil as a whole (and, incidentally, the formation of sand boils). This mechanism may be the cause of failure in a dam or slope having an interior region in which high pore pressures develop (Figure 3-7).

Reduction of strength in the outer crust, together with loosening of the upper portion of the sand associated with upward flow of water, reduces the total shear resistance along a potential failure surface. A similar situation may develop beneath a foundation, as pore pressures developed in soil beneath or to the sides of the foundation spread laterally and/or upward into stronger, cohesive, or nonsaturated soils near the free surface. In these cases there are global changes in void ratios involving soil other than the sand in which high pore pressures originated. Undrained conditions obviously no longer exist. In the case of slopes, transformation of apparently solid ground into a soil avalanche occurs much more rapidly than would be calculated from diffusion through pores of the soil because of the change in permeability when tension cracks open up (Schofield, 1980).

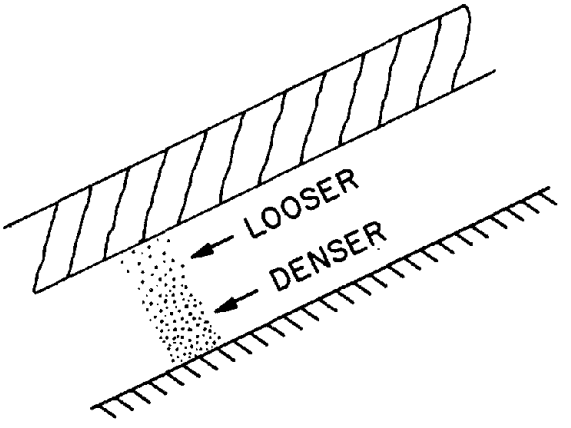

FIGURE 3-5 Example of a potential situation for mechanism B failure arising from the rearrangement of the soil into looser and denser zones. Local volume change occurs, but the sand as a whole remains at a constant volume and is "globally" undrained.

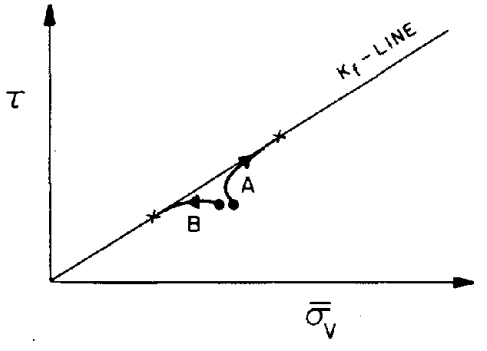

FIGURE 3-6 Change in the undrained stress path that a soil follows as a result of becoming loosened because of local volume change. Path A depicts the stress path without loosening. Path B depicts the stress path after loosening occurs.

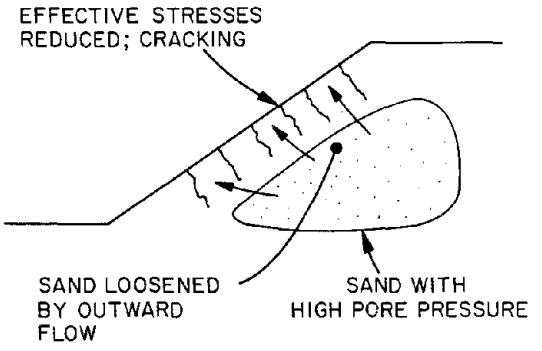

FIGURE 3-7 Examples of a potential situation for mechanism C failure resulting from spreading of pore pressure and global volume changes.

The instability and large change in geometry following the generation of a cavity by an explosion in a saturated sand (Figure 3-2f) is a special case of this mechanism. Water will immediately begin flowing toward the cavity, carrying soil particles with it—much as with a classic piping failure at the toe of a dam. The surrounding soil will be loosened and hence weakened by this flowing water so that slumping is possible.

Mechanism D

A situation where there is a well-defined interface between sand and a stiff body is another special case. A friction pile foundation (Figure 3-2e) is an example. Increased pore pressure can cause a plunging failure of such piles (De Alba, 1982, 1983a,b). In principle, such a failure can occur with the surrounding sand having either type I or type II stress-strain behavior. It only is necessary that the pore pressure rise sufficiently to reduce the shear resistance at the interface below that needed for static equilibrium (Figure 3-8). It is not necessary for there to be any volume change in the sand adjacent to the wall.

This same argument has been applied to infinite slopes, and might be valid if a plate with a very smooth surface rested upon an inclined stratum of saturated sand. In nature, however, the interface between sand and overlying soil is not abrupt, and the two soils grade into one another to some extent. Hence, if the overlying soil is stronger than the sand, failure must take place through the sand via mechanism B. Thus, mechanism D is closely related to mechanism B. Indeed, small localized changes in the void ratio alongside a pile may be necessary to permit a plunging failure since the surface of a pile is often somewhat rough.

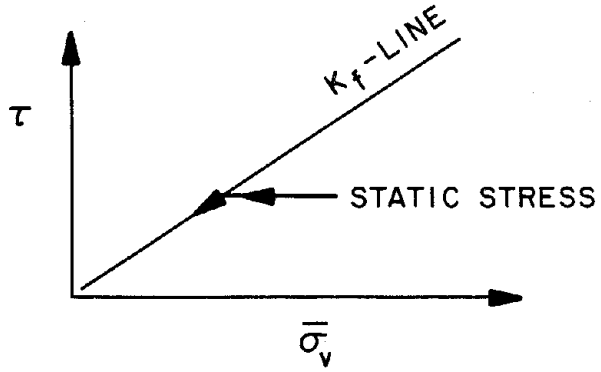

FIGURE 3-8 Effective stress path for element of soil next to friction pile during earthquake shaking. Pore pressure increases and effective stress decreases with constant soil-pile friction until the failure line is reached. Thereafter, further pore pressure increase causes loss of strength and plunging failure (failure mechanism D).

Discussion

The foregoing analysis has identified three primary mechanisms of flow failure in saturated cohesionless soils subjected to cyclic straining (Figure 3-9):

1. A loss of static shear resistance, associated with progressive failure, during truly undrained shear; i.e., undrained globally and locally.
2. A loss of static shear resistance within a portion (usually the upper portion) of a mass of cohesionless soil owing to redistribution of density within the soil.
3. A loss of static shear resistance within ground adjacent to cohesionless soil in which high pore pressures develop, owing to reduction of effective stress and possibly cracking as pore pressures push outward from the zone of high pore pressure.

While any of these mechanisms by itself could be the cause of a flow failure, all three may be present to some degree in any given case.

All three mechanisms can contribute to a failure while shaking continues, although it is probable that failures involving mechanism C will occur soon after the end of shaking. A failure associated with mechanism C may also occur hours later. If failure occurs solely as a result of mechanism A, it must occur during or very soon after the end of shaking.

Mechanism B is somewhat more speculative than mechanisms A or C. It is difficult to study the phenomenon in the laboratory because

<table>
<tr><td rowspan="3">DRAINAGE CONDITIONS</td><td colspan="3">STRESS–STRAIN BEHAVIOR</td></tr>
<tr><td>TYPE I</td><td colspan="2">TYPE II</td></tr>
<tr><td colspan="2">FLOW</td><td>DEFORMATION</td></tr>
<tr><td>UNDRAINED LOCALLY</td><td>MECHANISM A</td><td>NOT POSSIBLE</td><td rowspan="3">EXCESSIVE DEFORMATION BUT NOT INSTABILITY</td></tr>
<tr><td>UNDRAINED GLOBALLY</td><td rowspan="2"></td><td>MECHANISM B</td></tr>
<tr><td>DIFFUSION OF PORE PRESSURE</td><td>MECHANISM C</td></tr>
</table>

FIGURE 3-9 Classification scheme for various mechanisms of failure. Source: Modified from Whitman (1985).

membranes and other restraints on deformation inhibit a direct modeling of the actual situation. It is not known if the existence of a static shear stress in, say, a direct shear test can inhibit soil from settling away from the top cap. Various factors—the time required for such settlement, the effect of the thickness of the sample, and the influence of the roughness of the top cap—are poorly understood.

It is believed that all observed flow failures have resulted from one or a combination of the mechanisms discussed above.

Deformation Failures of Slopes and Foundations

Even though an earth mass does not fail totally and move large distances, there may be permanent deformations large enough to constitute failure in an engineering sense. In discussing such cases the focus is upon sands with type II stress-strain behavior, since with type I there generally is a narrow margin between experiencing very little permanent deformation and suffering a flow failure.

There are several different reasons why an element of soil might experience permanent deformation during a cyclic loading (Figure 3-10).

- An attempt is made to apply a cyclic stress that, together with the sustained static stress, is greater than the maximum shear resistance

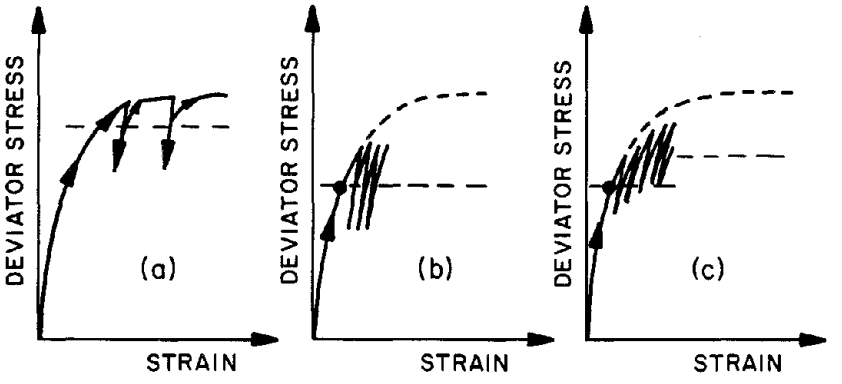

FIGURE 3-10 Three different types of loading that can cause permanent deformations: (a) attempted application of a combined static and cyclic stress that is equal to or greater than the maximum resistance; (b) application of a constant level of combined static and cyclic stress that is less than the maximum resistance; (c) an increasing level of combined cyclic and static stress due to load transference from other portions of the soil mass that may have decreased in stiffness.

of the soil. When the combined stress reaches the maximum resistance, plastic flow begins to occur. If the soil is transmitting stress to a mass that can move together, as soil within an infinite slope, the amount of plastic deformation will be determined by the interval of time over which the excessive stress acts. The method of analysis proposed by Newmark (1965) is aimed at evaluating the amount of such displacement. If the element of soil is surrounded by other soil that is not being stressed to the maximum resistance, the permanent deformation of the element will be determined by the deformation of the surrounding soil.

- The combined static plus cyclic stress remains less than the maximum resistance. Permanent deformation accumulates gradually as a result of the rearrangement of soil particles.
- The sustained static stress acting upon the element increases as a result of the cyclic loading because additional stress has been transferred to the element from other portions of the soil mass that have decreased in stiffness.

All three actions may be occurring together and are potentially important, but the second action is of the most interest to this discussion.

The deformation of an element of soil may be either in the form of "uniform" distortion or it may be concentrated on slip lines. Schofield (1981) has used the diagram in Figure 3-11 in discussing this point. In this diagram the curve OABC represents the limits to the stress that

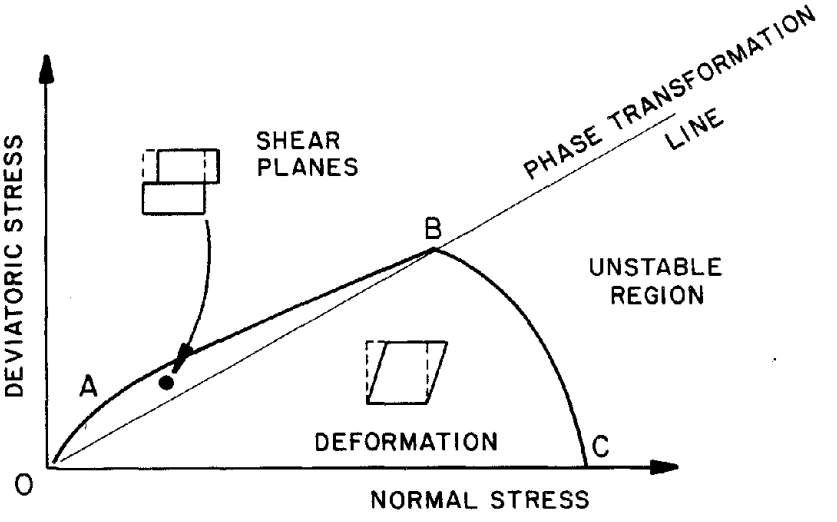

FIGURE 3-11 Diagram indicating combinations of shear and normal stress causing different deformation conditions for a soil at a given void ratio.

can be sustained in a stable manner by a soil at a particular void ratio. If the stresses remain in the sector OBC, then the deformations will be "uniform." However, if the stresses fall within the area OABO, then deformations will tend to concentrate in narrow zones.

The rate of increase of permanent deformation caused by an undrained cyclic loading may increase as the stresses approach the line OB in Figure 3-11. As long as the stresses remain safely below this line, the permanent deformations are likely to be small (except at very small effective stresses where the stiffness of the sand becomes small). Once the stress path during cyclic loading approaches this line, deformations may begin to increase significantly and experimental errors in laboratory tests simulating this condition may become a problem. Resisting the cyclic shear requires a decrease in pore pressure—that is, a dilatant action—and further movement of the soil particles is required for this to happen.

The line OB represents a broad concept. There are several lines variously referred to in the literature as the characteristic line (Luong and Sidaner, 1981), phase transformation line (Ishihara et al., 1975), critical state line (Schofield and Wroth, 1968), and steady-state line (Poulos, 1981). These various lines are not necessarily identical, but certainly are related. Despite the ambiguity of this concept, it serves as a framework for tying together basic concepts concerning deformations caused by cyclic loading.

A Summary

If some of the soil within an earth mass has type I behavior, there clearly is the potential for a catastrophic flow failure, and it is of great value to know whether or not soil exists in this state. However, flow failure can only occur if pore pressures and strains large enough to trigger the failure are caused by undrained cyclic or monotonic loading.

In many practical problems the soil will have type II behavior. It still is possible that there may be a flow failure, but only as a result of deviations from undrained conditions, which may be difficult to analyze. Even if the earth mass is safe from a flow failure, the possibility of excessive deformations must be considered. The likelihood of having large permanent or cyclic deformations may be related to how closely the characteristic line (or phase transformation, critical state, or steady-state line) is approached during the loading.

Procedural Differences in Evaluation of Liquefaction Effects

While there is general agreement on the principles described above, there are differences in the extent to which different workers ascribe failures to the different mechanisms. This influences the methods proposed for evaluating these effects. These methods will be treated in some detail in Chapter 4. The following discussion examines the methods and differences in general terms.

Level Ground Case

In evaluating this problem, the primary goal is to identify the state for reaching the $\sigma' \simeq 0$ condition in the soil profile, thereby triggering the development of liquefaction effects at the ground surface. Consequently, the dynamic shear stress induced in the soil is compared to the shear stress (intensity and number of cycles) required to reach the $\sigma' \simeq 0$ condition. This resistance may be evaluated using in-situ measurements, such as the standard penetration test (SPT) or the cone penetration test (CPT) or cyclic-load laboratory tests upon undisturbed samples of very high quality.

Flow Failures of Slopes and Foundations

Concerning the importance of the several mechanisms of failure, some experts focus primarily upon failure under undrained conditions (mechanism A), while others feel that flow failures can result from the redistribution of pore water and localized volume changes. The methods of analysis and evaluation of safety against flow failure are simplified

if it is assumed that such failures occur under completely undrained conditions. Methods for analyzing this situation are coming closer to being reliable. However, given the state of knowledge today, a study cannot exclude the possibility of failures occurring under circumstances that depart from the undrained conditions.

Even for the undrained case there are procedural differences. It is, in general, necessary to determine the following factors:

- The residual or steady-state strength of a soil, should a flow failure be triggered.
- If there is a potential for a flow slide, the loading conditions required to trigger the increases in pore water pressure that would lead to progressive failure and flows.
- The best procedures for determining the permanent deformations that will occur in saturated soils subjected to earthquake shaking if a flow failure cannot develop.

To evaluate these effects, Seed (1984) determines the pore pressure generation characteristics and triggering potential of soils using either cyclic load tests on high-quality undisturbed samples or SPT data, circumventing the problems associated with sample disturbance. He then evaluates the residual strength of a liquefied soil on the basis of in-situ SPT data and previous case histories, and investigates the possibility of flow by stability computations. Preference is given to SPT and field case data for the determination of residual strength on the grounds that (1) the residual strength is extremely sensitive to small changes in density that cannot be completely avoided in even the best-quality undisturbed samples of sands (in the absence of freezing); (2) effects, such as mechanism B, may play some role in the determination of residual strengths in full-scale structures, but are not necessarily reflected by the results of laboratory tests;* and (3) laboratory test programs on a limited number of samples may not provide representative data for soil properties over an extensive area such as that covered by a major earth structure. Deformations in soils not subject to flow failures are investigated by cyclic triaxial tests using stress conditions representative of field loading conditions and the strain-potential concept, or by Newmark-type deformation analysis.

On the other hand, Castro et al. (1982) and Poulos et al. (1985) evaluate the undrained steady-state strength by means of static load tests on high-quality undisturbed samples combined with a procedure

*Thus, in practical work, Seed's residual strength may differ from steady-state strength for the in-situ void ratio.

to correct the test results for the effects of changes in the volume of the samples. The measured values of in-situ steady-state strength are related to field index tests, such as SPT or CPT, so that an assessment can be made of the variability of strengths in the zone of interest. Conventional slope stability analyses are then used to evaluate the possibility of flow failure. Laboratory tests are used for the direct determination of steady-state strengths because any correlation between steady-state strengths and index tests are likely to be different for different soils.

When the steady-state strengths are small enough so that a flow type failure is possible, the cyclic loads required to trigger liquefaction are determined by means of cyclic triaxial tests. In these tests an attempt is made to properly represent the potential for the flow failure by having the appropriate ratio of applied static shear stress to undrained steady-state shear strength (which in this case is larger than one). If the strength values are higher than the static shear stress, the yield strength is determined using the results of cyclic tests, and deformations are estimated by a Newmark-type analysis.

The major reason for these procedural differences is related to the problem of taking into account the inevitable effects of sample disturbance on the properties of sandy soils, the variability of natural deposits, and the ability of SPT values to reflect soil properties appropriately. Seed (1984) places greater emphasis on the properties of soils indicated by previous case studies and their relationship to SPT values, while Castro et al. (1982) and Poulos et al. (1985) place greater emphasis on laboratory test procedures. In fact, however, both groups use both types of procedures to some extent in their evaluations.

Permanent Deformations

Prediction of deformation in soils not subject to flow failures is a very difficult and complex nonlinear problem, which is still far from being resolved. Hence, various approximate methods exist, as discussed in Chapter 4. There are significant procedural differences between these, and the state of the art is such that only crude estimates of permanent deformations are possible at this time.

Final Comments

The relative merits of these different approaches to the determination of the liquefaction characteristics of soils are not likely to be resolved by conducting laboratory test programs on small samples of soil. Furthermore, theoretical calculations, while they may provide some

useful insights, will not by themselves resolve the differences among preferred approaches.

What is needed are observations on actual earth structures subjected to earthquake shaking. Cases involving failure are especially instructive, but instances in which strong shaking does not cause failure are also valuable. Given the infrequent opportunities to obtain such data, there is also an important role to be played by small-scale tests conducted on centrifuges.

4

The State of the Art In Analysis and Evaluation

This chapter assesses the current state of the art in the analysis and evaluation of liquefaction at a specific site or within a small region. The process of evaluation is indeed an art, requiring considerable judgment and experience as well as testing and analysis. Enormous advances have been made during the past two decades in understanding liquefaction and in developing tools to help assess safety against liquefaction, but many aspects of the problem remain uncertain.

Evaluating the likelihood of liquefaction involves two parts:

- Liquefaction potential or liquefaction susceptibility—assessing the chance that liquefaction will occur given earthquake ground shakings of various intensities.
- Ground shaking hazard analysis—assessing the various intensities of ground shaking that could occur or assigning a specific intensity that is required as a basis for design.

The emphasis in this report is upon the first of these parts. However, the importance of the second part is not to be dismissed. Indeed, many engineers feel that the greatest difficulties in evaluating liquefaction arise because unrealistically conservative ground motions are prescribed.

The following sections discuss various methods for analyzing and evaluating liquefaction susceptibility, beginning with the methods that require the least testing and analysis and proceeding to the more complex.

Mapping Based upon Geological Criteria

The U.S. Geological Survey has recently been engaged in mapping liquefaction susceptibility in several regions, primarily in California. The procedure now being followed is based upon a methodology developed by Youd and Perkins (1978). It has also been adapted and applied by engineers employed or retained by several communities.

Evaluations of liquefaction susceptibility based on the geology of a region are distinguished from site-specific liquefaction evaluations in terms of scope, objectives, and applications.

Regional studies of liquefaction susceptibility delineate areas where liquefaction could occur given a sufficiently large earthquake. Such regional studies are valued primarily by persons or agencies having planning, regulatory, or emergency response functions. They are not substitutes for site-specific evaluations of liquefaction hazards, but they do indicate areas where site-specific evaluations may be desirable.

The initial step is to make a map showing superficial geologic deposits according to one or more mappable properties that correlate with liquefaction susceptibility. In the following example from southern California, susceptibility to liquefaction generally decreases as the geologic age of the alluvial fan and floodplain deposits increases, as indicated by standard penetration test (SPT) studies performed in the mapped deposits and by observations and follow-up studies of actual occurrences of liquefaction during earthquakes. Among alluvial deposits in the San Fernando Valley the following age distinctions are made:

- Latest Holocene: 0-1,000 years
- Earlier Holocene: 1,000-10,000 years
- Late Pleistocene: 10,000-130,000 years

Identification of age is based chiefly on landform analyses, flood inundations, radiocarbon analyses, relation of interfleuves to the drainage network, and charactersitics of weathering profiles that develop in the sediment or become preserved by burial beneath younger sediments.

Latest Holocene deposits are most closely related to the natural drainage network and typically have a history of inundation by floods. Rates of deposition exceed rates of weathering, resulting in undeveloped or minimally developed profiles. In contrast, areas of earlier Holocene deposits present a more dissected landscape because they no longer receive frequent increments of floodborne sediment. Progressive weathering has resulted in thicker, better defined, distinctively oxidized profiles containing small but appreciable amounts of translocated silt and clay.

Late Pleistocene deposits typically have been tectonically deformed in this continental margin regime, they are more dissected by streams than earlier Holocene deposits, and weathering profiles contain conspicuous amounts of iron oxyhydroxides, iron oxides, and translocated and authigenic clay. Deposits older than late Pleistocene are assumed to be not susceptible to liquefaction on the basis of experience during actual earthquakes.

TABLE 4-1 Considerations Used in Producing a Map of Liquefaction Susceptibility in the San Fernando Valley

	Depth to Groundwater (ft)		
Age of Deposit	0–10	10–30	<30
Latest Holocene	high	low[a]	nil
Earlier Holocene	moderate	low	nil
Late Pleistocene	low	nil	nil

[a]Latest Holocene deposits in this basin generally are not more than 10-ft thick. Saturated deposits in the 10- to 30-ft interval are earlier Holocene sediments.
SOURCE: Youd et al. (1978).

Stratigraphic distinctions using degrees of pedogenesis or weathering-profile development in the Los Angeles area have been made in accordance with principles discussed by Birkeland (1984), McFadden (1982), and McFadden and Tinsley (1982). Rates of weathering and pedogenesis may proceed elsewhere at different rates owing to climate, vegetation, parent materials, and topographic position. Other basins outside of southern California may contain sediments with different physical properties or geologic histories, and criteria for assigning geologic age, thickness, or other mapping criteria may need modification to distinguish degrees of liquefaction susceptibility (Anderson et al., 1982). Hence, caution is required if the criteria are transferred to other areas.

The next step is to develop a map giving the depth to groundwater. Such information is assembled using data from wells and other sources, and interpolated and extrapolated by studying general patterns of groundwater flow. In doing so, it is necessary to take into account seasonal variations and to select some standardized basis for constructing the map.

The geologic map and the groundwater map are then superimposed to produce a map of liquefaction susceptibility, using considerations of deposit thickness and criteria such as those presented in Table 4-1. An example of a liquefaction susceptibility map produced in this way appears in Figure 4-1. Provided susceptible materials are present, a rough interpretation of "high" susceptibility is that liquefaction will occur as a result of ground motion with 0.2 g and 10 equivalent cycles (M = 6.5).* "Moderate" susceptibility implies liquefaction by 0.5 g and 30 equivalent cycles (M = 8). Liquefaction might also occur, of course, with other equivalent combinations or accelerations and numbers of cycles. By introducing results from a ground motion hazard

*Magnitude is defined loosely in this report. Generally it is either surface wave magnitude (M_S) or Richter magnitude (M_L), whichever is greater.

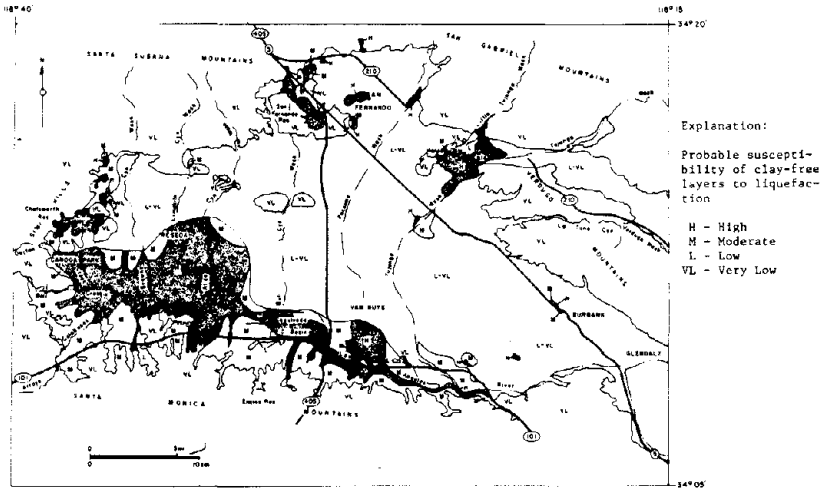

FIGURE 4-1 Zonation map for the San Fernando Valley showing probable susceptibility to liquefaction. Source: Youd et al. (1978).

analysis, "high" and "moderate" can be converted to rough estimates for the average recurrence interval for liquefaction.

In the approach developed above, analysis using measured penetration resistance in deposits of various ages have been used to "calibrate" and confirm the rankings and ratings of liquefaction susceptibility. Such studies provide an improved evaluation of susceptibility at the specific locations where penetration resistance has been measured, but inevitably such sites are too sparsely distributed to permit a direct mapping of susceptibility of heterogeneous sediments on a regional scale. These studies also can potentially provide information leading to more quantitative statements concerning the probability of liquefaction within a geologically defined deposit. (However, because the data bases are so sparse there has been a reluctance to pursue the probabilistic approach more deeply.) These geologic techniques provide a stratigraphic basis for recognition of areas where susceptible material may occur, but they are neither a substitute for site-specific evaluations of liquefaction potential nor a basis for design.

Liquefaction susceptibility maps have been or are being developed, for several regions:

- San Francisco Bay area (Roth and Kavazanjian, 1984; Kavazanjian et al., 1985)
- San Fernando Valley (Youd et al., 1978)
- Los Angeles Basin (Tinsley et al., 1985)
- Riverside area (Carson and Matti, 1982)

- San Diego (Power et al., 1982; Idriss et al., 1982)
- Salt Lake City area (Anderson et al., 1982)
- Memphis, Tennessee (Sharma and Kovacs, 1982)
- San Mateo County, California (Youd and Perkins, 1985)

Inevitably, it has been necessary to adapt this basic approach in light of local geologic conditions, the availability of maps, data concerning depth to the water table, and seismic characteristics of each region.

An alternative approach to the problem of regional evaluation of liquefaction, for example, has been employed by Anderson et al. (1982) along the Wasatch Front, Utah. They evaluated liquefaction potential from existing subsurface data and from supplementary subsurface investigations performed during their study. Liquefaction potential was classified as high, moderate, low, and very low depending on the probability that a critical acceleration will be exceeded in 100 years. The critical acceleration for a given location is defined as the lowest value of the maximum ground surface acceleration required to induce liquefaction, estimated according to the methodology of Seed and Idriss (1982).

The categories of high, moderate, low, and very low correspond to probabilities of exceeding the critical acceleration in the ranges of greater than 50 percent, 10 to 50 percent, 5 to less than 10 percent, and less than 5 percent, respectively. Among the virtues in this approach are (1) the results are cast overtly in probabilistic terms, and (2) levels of risk can be identified chiefly on geographic groupings of critical acceleration values within a sedimentary basin in which mapped geologic units do not conform to clearly identifiable levels of liquefaction potential.

Simple Geotechnical Criteria

The simplest and crudest criteria to use for evaluating liquefaction susceptibility at a given site are the grain size characteristics of the soils (Figure 2-19). The lower boundary on particle size reflects the influence of fines in decreasing the tendency of soils to densify during cyclic loading. Plastic fines make it more difficult for sand particles to come free of each other and seek denser arrangements. However, nonplastic fines may not have as much of this restraining effect (see Figure 4-2).

The upper boundaries are associated with the more permeable nature of coarser soils, meaning that at least partial dissipation can occur even during earthquake shaking. These upper boundary curves must be used with care, however, because the rate at which excess pore pressures can dissipate is very much affected by the extent of the soil

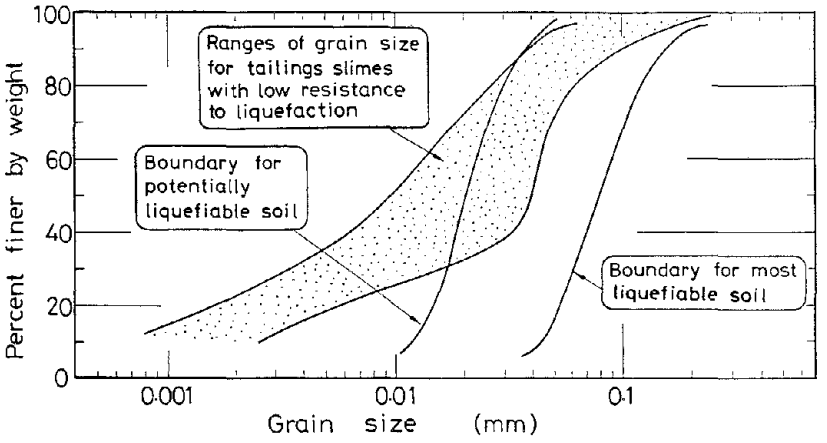

FIGURE 4-2 Ranges of grain sizes for tailings slimes with low resistance to liquefaction. Source: Ishihara (1985).

deposit, the presence of strata with lower permeabilities, and other factors. This matter has been examined in a preliminary way by Seed et al. (1976), who show that grain size can have a major effect upon dissipation of pore pressures for coarse sands with $D_{20} > 0.6$ mm. They conclude that it is unlikely that soils with $D_{20} > 0.7$ mm would ever develop a condition of initial liquefaction, provided there are no overlying or intervening layers of low permeability to inhibit drainage.

Empirical Correlations Using In-Situ Evaluation of Resistance

Since the Niigata earthquake, considerable field experience with liquefaction during actual earthquakes has been obtained and interpreted. This mass of data forms a basis for establishing empirical correlations relating the occurrence or nonoccurrence of liquefaction to the intensity of ground shaking and the principal characteristics of cohesionless soils.

Correlations Based on Standard Penetration Resistance

Figure 4-3 shows information applying to sites with clean sands and earthquakes with a magnitude of about 7.5. Each point corresponds usually to one boring record during some particular earthquake. The intensity of ground motion at the site is represented by the vertical ordinate τ_{av}/σ'_o, where τ_{av} is the average peak shear stress and σ'_o is the initial vertical effective stress. τ_{av}/σ'_o is computed from the peak

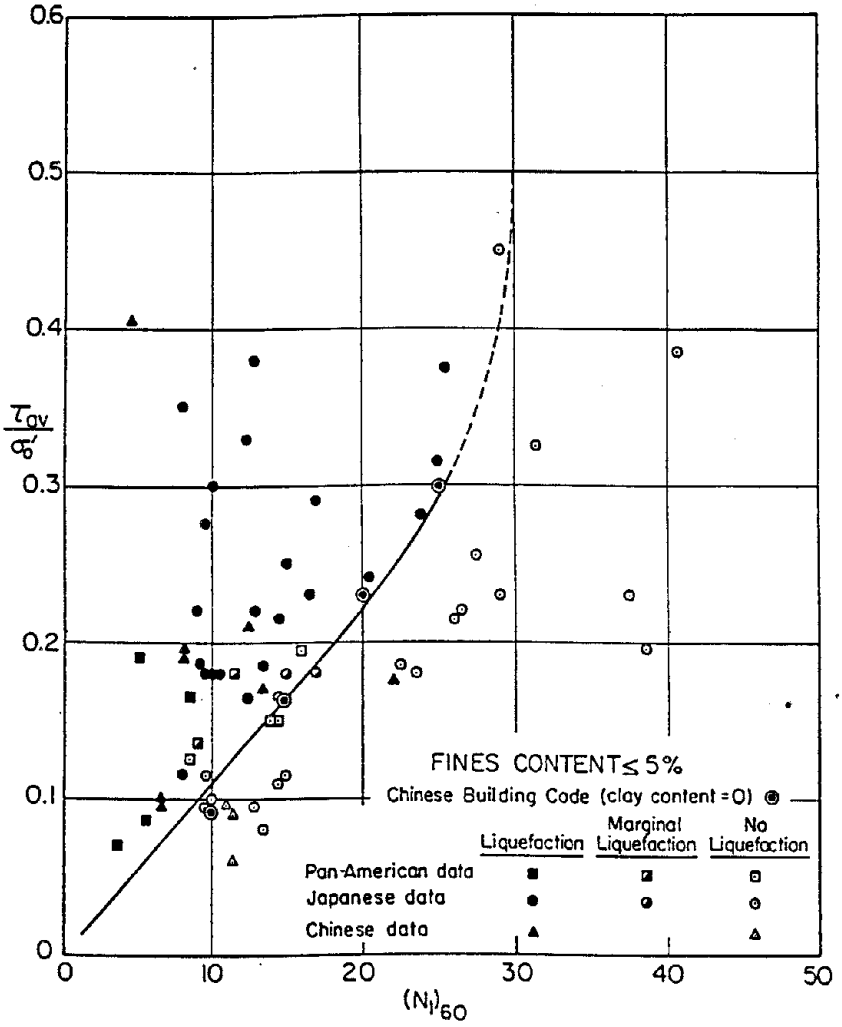

FIGURE 4-3 Relationship between stress ratios causing liquefaction and $(N_1)_{60}$ values for clean sands for magnitude 7.5 earthquakes. Source: Seed et al. (1984).

surface acceleration by a simple equation that accounts approximately for the relative importance of the many different acceleration peaks in a typical ground motion record (Seed and Idriss, 1971):

$$\tau_{av}/\sigma'_o = 0.65\, a_{max}\, \sigma_o\, r_d/\sigma'_o\, g \qquad \text{(Eq. 4-1)}$$

where a_{max} is the maximum acceleration at ground surface, σ_o equals the total overburden stress at depth under consideration, σ'_o is the effective overburden stress at this same depth, and r_d equals a stress

reduction factor that decreases from a value of 1 at the ground surface to a value of 0.9 at a depth of 35 ft.

The resistance of the soil is represented by the horizontal abscissa $(N_1)_{60}$, which is the blow count in the standard penetration test (SPT), corrected (as discussed later) for the depth of overburden and for certain details in the performance of the test. Both τ_{av}/σ'_o and $(N_1)_{60}$ are evaluated at the depth in the particular deposit most critical from the standpoint of liquefaction.

The curve drawn in Figure 4-3 is intended to divide zones corresponding to liquefaction and nonliquefaction. A new site would be evaluated by plotting a point corresponding to the blow count for the site and to the design earthquake ground motion. If the point plots on or above the curve, the site would be judged susceptible to liquefaction. If the point plots below the curve with an adequate margin of safety, the site is judged to be safe.

There is no general agreement on the appropriate margin of safety, primarily because the degree of conservatism thought desirable at this point depends upon the extent of the conservatism already introduced in assigning the design earthquake. If the design earthquake ground motion is regarded as reasonable, a safety factor of 1.33 or 1.35 on τ_{av}/σ'_o is suggested as adequate. However, when the design ground motion is excessively conservative, engineers are content with a safety factor only slightly in excess of unity.

The important effect of the duration of the ground shaking can be taken into account by a correction related to the magnitude of the earthquake. Statistical studies (Seed et al., 1975c) show that the number of cycles representative of different magnitude earthquakes is typically as in Table 4-2. Using a representative shape for the relationship between cyclic stress ratio and the number of cycles required to cause liquefaction, a factor with which to correct the ordinates of

TABLE 4-2 Representative Number of Cycles and Corresponding Correction Factors

Earthquake Magnitude (M)	Number of Representative Cycles at 0.65 τ_{max}	Factor to Correct Abscissa of Curve in Figure 4-3
8.5	26	0.89
7.5	15	1.0
6.75	10	1.13
6.0	5-6	1.32
5.25	2-3	1.5

SOURCE: After Seed and Idriss (1982).

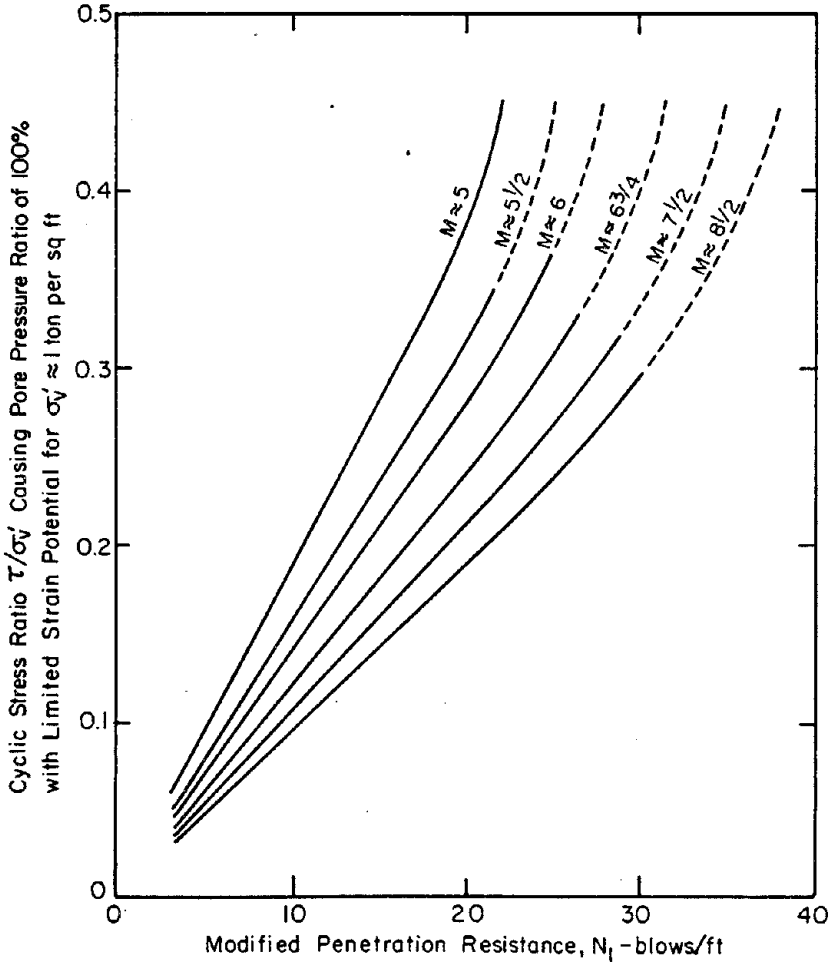

FIGURE 4-4 Chart for evaluation of liquefaction potential of sands for earthquakes of different magnitudes. Source: Seed and Idriss (1982).

Figure 4-3 can be deduced. These correction factors are also listed in the table. Using these factors leads to a family of curves such as those in Figure 4-4.*

The form of the plot in Figure 4-3 is well-grounded in theory. Laboratory tests and theoretical analyses have shown the general appropriateness of the ratio τ_{av}/σ'_o as a measure of resistance to liquefaction. Use of this ratio means that the depth of the water table

*Note that the curves for $M = 7\frac{1}{2}$ are somewhat different in Figures 4-3, 4-7, and 4-4, since the curves were based on different data sets. Figure 4-4 is included for illustrative purposes only; use of Figure 4-3 plus Table 4-2 represents the most up-to-date practice.

is automatically taken into account. The penetration resistance reflects various factors (e.g., relative density and horizontal effective stress) known from laboratory tests to affect susceptibility to liquefaction. This figure is the latest in a gradually evolving lineage of such curves (Seed and Idriss, 1971; Seed and Peacock, 1971; Whitman, 1971; Castro, 1975; Seed et al., 1975a; Seed, 1976; Seed, 1979a; Seed et al., 1983; Tokimatsu and Yoshimi, 1983; Seed et al., 1984) that have improved as more data have become available and as the interpretations of the data have been refined. Many eminent engineers regard use of plots such as Figure 4-3 as the best method available for assessing liquefaction susceptibility. This practice avoids the difficult problems and questions concerning undisturbed testing and sampling and makes the most direct use of actual experience during earthquakes.

Nonetheless, there are additional factors that must be considered.

Corrections to Blow Count

It has been apparent that the standard penetration test has not been standardized. There are important differences between the procedures used in different countries, and there can be significant differences in the practice followed within a country. It is important to understand and correct for these differences when preparing data such as that in Figure 4-3, and such understanding is vital when applying such results to evaluation of a new site. There are several aspects of the problem to consider: for example, the manner in which energy is delivered to the drill rod, the length of the drill rod, the effect of the type of sampling tube, the effective stress present at the depth where the blow count is being evaluated, and the drilling fluid (DeMello, 1971; Schmertmann and Palacios, 1979; Kovacs and Salomone, 1982; Kovacs et al., 1984).

The manner of delivering energy to the drill rod is especially important. Table 4-3 summarizes results from studies into the fraction of theoretical energy actually reaching the rod when using different hammer types and hammer release mechanisms. Most of the above difficulties can be eliminated by standardizing the test procedures, as recommended by Kovacs et al. (1983, 1984) and Seed et al. (1984), or by correcting results to this standardized procedure. This involves using the standard conditions shown in Table 4-4 and correcting results to an energy ratio of 60 percent and an effective overburden pressure of 1 ton/ft^2.

Figure 4-5 is a chart used to correct the observed blow count to that value, (N_1), which would be measured at an effective overburden stress of 1 ton/ft^2. Thus the combined correction is:

$$(N_1)_{60} = C_N \, ER_m \, N_m/60 \qquad \text{(Eq. 4-2)}$$

TABLE 4-3 Summary of Energy Ratios for SPT Procedures

Country	Hammer Type	Hammer Release	Estimated Rod Energy (Percent)	Correction Factor for 60 Percent Rod Energy
Japan[a]	Donut	Free-fall	78	78/60 = 1.30
	Donut	Rope and pulley with special throw release	67	67/60 = 1.12
United States	Safety	Rope and pulley	60	60/60 = 1.00
	Donut[b]	Rope and pulley	45	45/60 = 0.75
Argentina	Donut	Rope and pulley	45	45/60 = 0.75
China	Donut	Free-fall[c]	60	60/60 = 1.00
	Donut	Rope and pulley	50	50/60 = 0.83

[a]Japanese SPT results have additional corrections for borehole diameter and frequency effects.
[b]Prevalent method in the United States today.
[c]Pilcon-type hammers develop an energy ratio of about 60 percent.
SOURCE: Seed et al. (1984).

TABLE 4-4 Recommended SPT Procedure for Use in Liquefaction Correlations

Factor	Recommended Procedure
Borehole	Four-to five-in.-diameter rotary borehole with bentonite drilling mud for borehole stability
Drill bit	Upward deflection of drilling mud (tricone of baffled drag bit)
Sampler	O.D. = 2.00 in. I.D. = 1.38 in., constant (i.e., no room for liners in barrel)
Drill rods	AW for depths less than 50 ft; N, BW, or NW for greater depths
Energy delivered to sampler (rod energy)	2,520 in.-lb (60 percent of theoretical maximum)
Blowcount rate	Thirty to forty blows per minute
Penetration resistance count	Measures over range of 6 to 18 in. of penetration into the ground

SOURCE: Seed et al. (1984).

where N_m is the measured blow count and ER_m the corresponding energy ratio in percent. Both corrections were made to all observed blow counts in Figure 4-3. Other corrections were also applied in some instances.

With respect to the overburden correction factor C_N, it has been pointed out by Liao and Whitman (1985) that discrepancies exist with

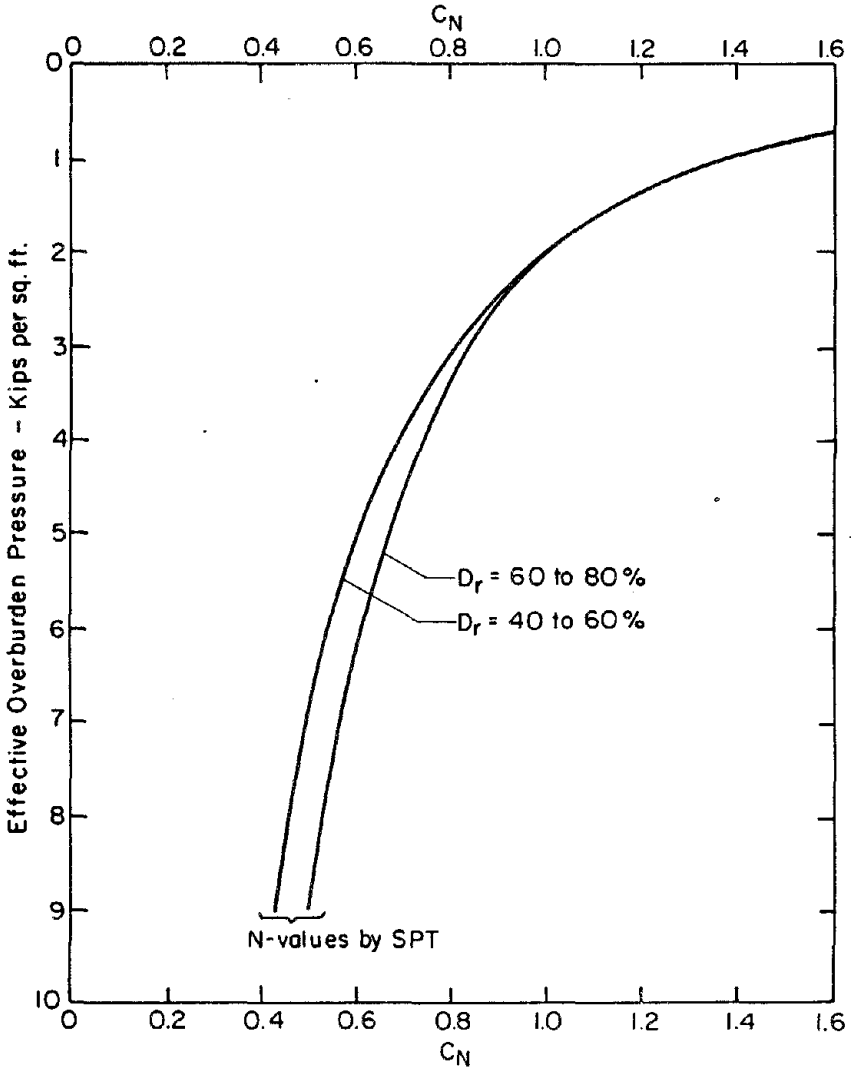

FIGURE 4-5 Charts for values of overburden correcting factor C_N. Source: Seed et al. (1984) based on data and analyses from Marcuson and Bieganousky (1977).

correction factors used in the past compared to what is the current state of practice, as represented by Figure 4-5. To some degree, this is a standardization problem in terms of SPT interpretation. As a simple useful approximation to the curves in Figure 4-5, Liao and Whitman suggest the following formula:

$$C_N = (1/\sigma'_o)^{1/2} \qquad \text{(Eq. 4-3)}$$

where σ'_o is in tons/ft^2 or kg/cm^2. They also suggest a more generalized formula of the form:

$$C_N = \{(\sigma'_o)_{ref}/\sigma'_o\}^k \qquad \text{(Eq. 4-4)}$$

where $(\sigma'_o)_{ref}$ is a reference stress (nominally 1 ton/ft^2) and k would be a value that depends on soil grain size, stress history, and other factors. However, more experimental measurements are needed to define k accurately.

The use of these procedures eliminates much of the uncertainty connected with nonstandardization of the SPT procedure.

Uncertainty in Interpretation of Correlation

There are several difficulties in the compilation and interpretation of field experiences. For example, the actual peak ground acceleration is not as well known in some cases as in others; the depth of the water table is not always accurate; and some of the data are from borings performed after the earthquake. There is also the question of how to choose the representative blow count for a boring (e.g., smallest value or average of three smallest). Indeed, there is some problem of deciding just which case study records are documented "well enough" to be included. Consequently, the data sets assembled by different engineers and researchers differ somewhat.

Finally, some judgment is involved in deciding where to draw the boundary curve separating liquefaction from nonliquefaction. Examination of Figure 4-3 shows that some points corresponding to liquefaction lie below the curve while some representing nonliquefaction lie above. Even more "misclassified" points appear in a data set compiled recently at the Massachusetts Institute of Technology (Liao, 1985) after an exhaustive and careful review of published catalogs, although the import of the results is not significantly different from that indicated in Figure 4-3.

There have been various attempts to use statistical techniques to aid in choosing the most proper location for the boundary curve (Christian and Swiger, 1975; Yegian and Whitman, 1978; Yegian and Vitelli, 1981a). One effort is under way at MIT (Liao, 1985) using sophisticated techniques developed in connection with other types of engineering and scientific problems. The particular class of methods selected for this purpose is called dichotomous regression (Cox, 1970; McFadden, 1974) and provides an estimate for the probability of liquefaction given a value for τ_{av}/σ'_o and $(N_1)_{60}$. A result from this analysis is given in Figure 4-6.

Effect of Fines

Thus far the discussion has focused on clean sands free of gravel and

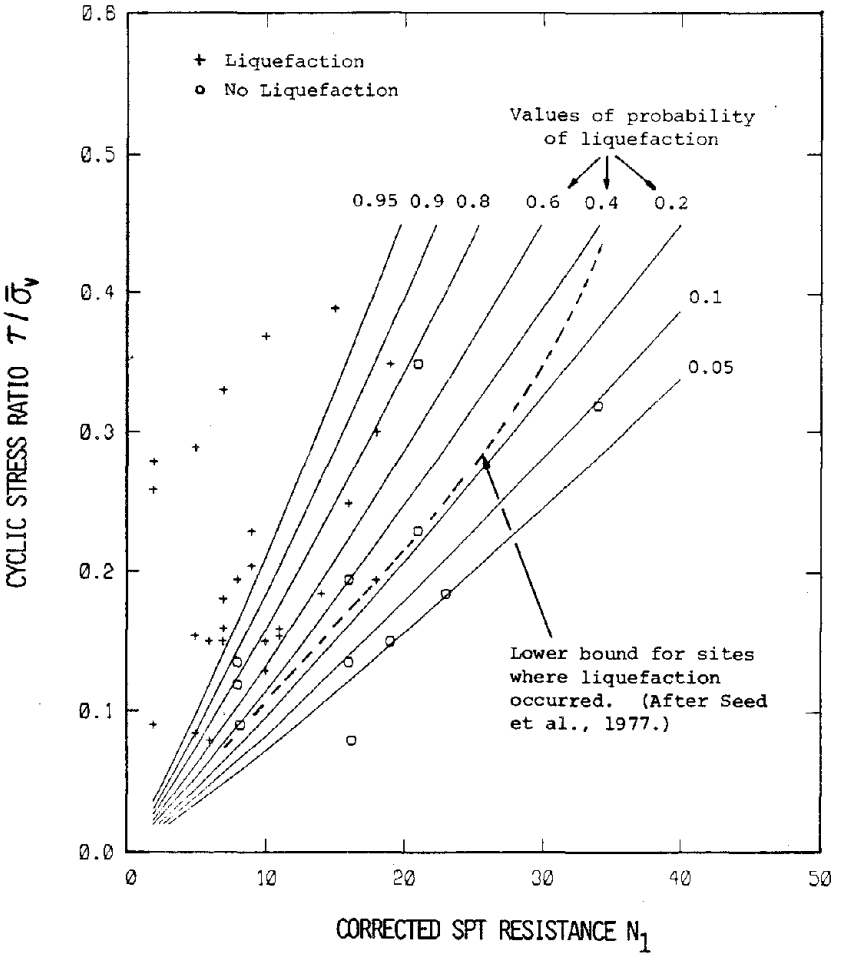

FIGURE 4-6 Preliminary results from a dichotomous regression technique showing contours of equal probability of liquefaction. Note that these results are preliminary partly because they are based on a relatively early data set from Seed and Idriss (1971). Source: Veneziano and Liao (1984).

with fines composing less than 5 percent of the soil. Deviations from these conditions require special treatment.

Figure 4-7 presents results from field observations of liquefaction or nonliquefaction involving silty sands with a content of fines greater than 5 percent. The number alongside each data point is the actual fines content. The curve labelled "$\leq$5 percent fines" is the same curve as on Figure 4-3. Clearly there are a number of instances of nonliquefaction that lie above this curve. The curves for 15 percent and 35

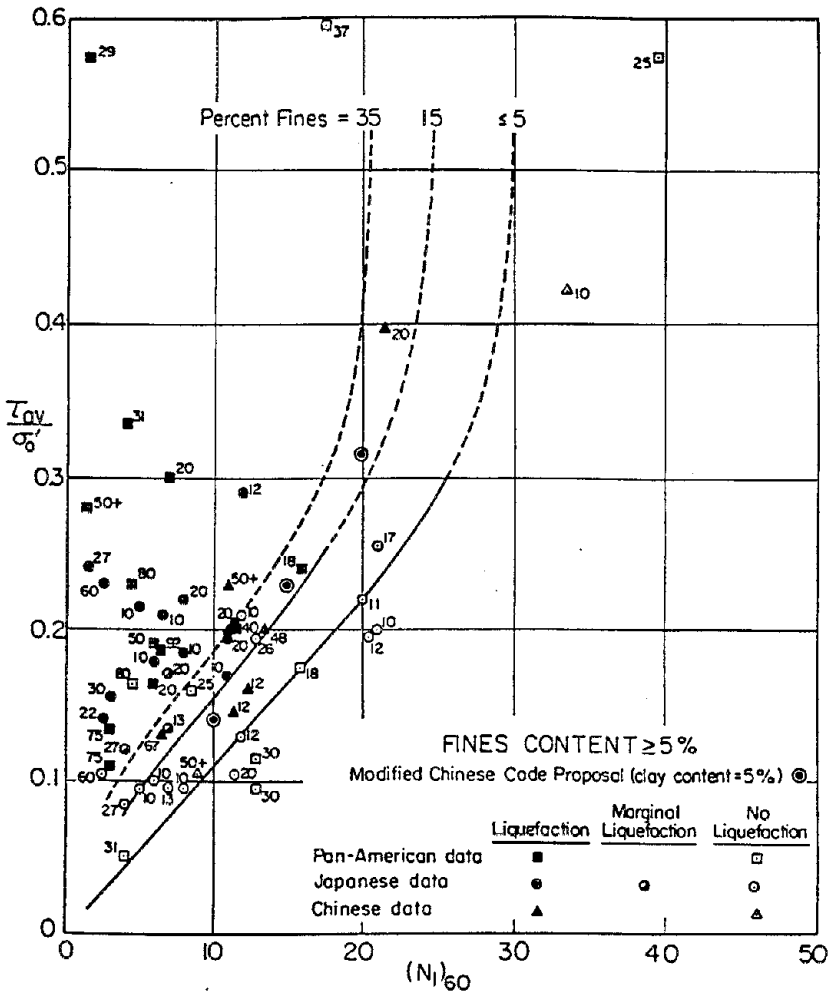

FIGURE 4-7 Relationships between stress ratio causing liquefaction and $(N_1)_{60}$ values for silty sands for magnitude 7.5 earthquakes. Boundary points specified by the Chinese Building Code are shown for comparison. Source: Seed et al. (1984).

percent fines drawn on Figure 4-7 represent the judgment of Seed et al. (1984). However, preliminary analysis using regression methods (Liao, 1985) confirms that there is a statistically significant effect of fines.

It is clear that ignoring the presence of fines can be conservative, and that the fines content should be noted in evaluating the liquefaction susceptibility of a deposit. However, it still is not possible to evaluate the likelihood of liquefaction of a silty sand with the same confidence as for a clean sand.

Gravel

Soils containing gravel have been observed to liquefy during earthquakes. However, it is not possible to evaluate the liquefaction susceptibility of such soils using the SPT; the presence of a small quantity of gravel can increase greatly the penetration resistance without having much influence upon the susceptibility to liquefaction.

This problem is undergoing study at the University of California at Berkeley. Part of the research is devoted to understanding when and how much gravel affects susceptibility. Another approach is to develop an alternate form of in-situ test, such as driving a larger sampling spoon, for which penetration resistance might be less sensitive to small amounts of gravel.

A Final Comment

From the general success of the correlation with SPT blow count, it would appear that penetration resistance is sensitive to the same factors (e.g., relative density, ratio of horizontal to vertical stress, and overconsolidation ratio) that affect resistance to liquefaction. Attempts to demonstrate this hypothesis by means of penetration tests under carefully controlled conditions in laboratory test tanks have generally been successful. There are exceptions, however. For example, Baldi et al. (1985) have found that blow count and cone penetration resistance are influenced only to a limited extent by past strain history, whereas resistance to liquefaction is affected by this factor. Nevertheless, the overall results of these studies have been encouraging.

Ishihara (1985) summarizes various studies in Japan of the correlation between penetration resistance and liquefaction resistance, as shown in Figure 4-8. (Neither axis in this figure is exactly the same as in Figure 4-3.) The curves from the Japanese code of bridge design and from Kokusho et al. (1983) are based on the correlations between resistance upon "undisturbed" samples as measured in the laboratory and in-situ penetration resistance. These tests have been useful in confirming the influence of fines upon the relationship of penetration and liquefaction resistance. Other sets of studies have related experiences during actual earthquakes to penetration resistance. The curve from Tokimatsu and Yoshimi, derived from field experience, has been confirmed by laboratory tests on in-situ frozen samples for an N_1 value of about 30 determined with a free-fall donut hammer.

Other In-Situ Methods

Cone Penetration Resistance

A cone penetrometer has a sharpened point that is pushed into the ground at a steady rate. Many engineers feel that a cone penetration

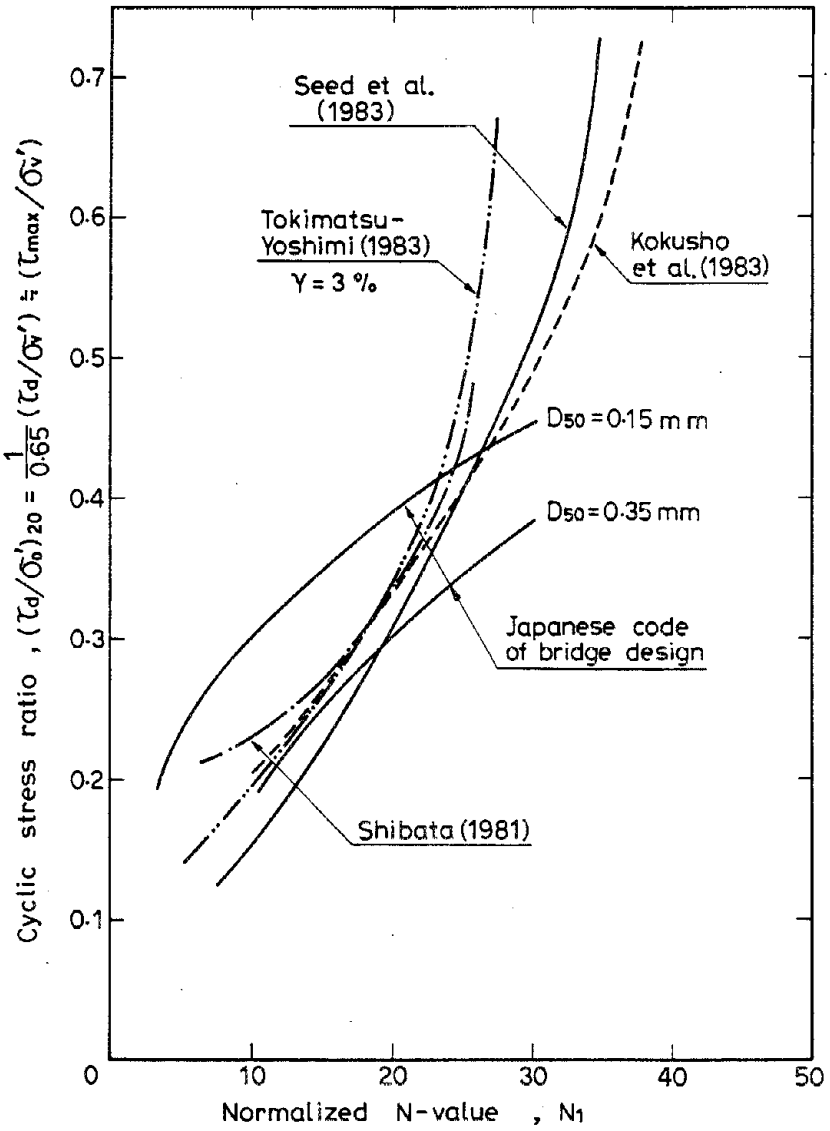

FIGURE 4-8 Summary chart for evaluating the cyclic strength based on the normalized SPT *N*-value. Source: Ishihara (1985).

test (CPT) provides a more consistent evaluation of the strength and stiffness of soils than does the SPT, and hence there is considerable interest in using the device to evaluate liquefaction susceptibility.

Cone penetration resistance has been measured at few sites where the occurrence or nonoccurrence of liquefaction during actual earth-

quakes has been documented. Consequently, it is not possible directly to develop charts such as those constructed using standard penetration resistance. The usual approach is to use a correlation between cone resistance and blow count N, and then enter charts such as those in Figures 4-3 and 4-7. Alternatively, one may use the correlation to correct the horizontal axis of such charts to penetration resistance.

There have been a number of discussions about the correlation between cone resistance and SPT blow count (Douglas et al., 1981; Seed and Idriss, 1982; Robertson et al., 1983; Kovacs et al., 1984; Baldi et al., 1985; Robertson and Campanella, 1985). Figure 4-9 indicates that the ratio of cone resistance to blow count increases with increasing mean grain diameter. As shown in Figure 4-10, there can be considerable scatter in the correlation even for a limited range of grain sizes. Seed et al. (1983) propose using:

$$q_{c1}/N_1 = \begin{cases} 4 \text{ to } 5 \text{ for clean sands} \\ 3.5 \text{ to } 4.5 \text{ for silty sands} \end{cases} \qquad \text{(Eq. 4-5)}$$

where q_{c1} and N_1 are values of cone resistance and blow count, respectively, corrected to an overburden stress of 1 ton/ft^2. The correction of q_c for overburden stress is sometimes forgotten. When it is included, usually the same correction factor (Figure 4-5) is used for both quantities, although Baldi et al. (1985) indicate that somewhat different corrections are appropriate. These authors also suggest the possible importance of the fines content in a soil.

With this somewhat convoluted procedure, which involved introducing additional uncertainty in the correlation between cone resistance and blow count, some or even all of the advantages of using the CPT may be lost. Figure 4-11 indicates the range of boundary curves separating liquefaction and no liquefaction, starting from Figure 4-3 and then applying different proposed correlations between q_c and N. In addition, the CPT by itself does not provide samples of soil for visual inspection or grain size analysis.

There are important potential advantages, however, to the use of the cone. Because it provides a continuous record of penetration resistance, it makes possible a more thorough interpretation of a soil profile. For example, Figure 4-12 compares the continuous profile of liquefaction resistance obtained from a CPT with values deduced from SPT and laboratory tests. Thus, it is a more sensitive device for locating pockets or thin strata of loose sand within a generally denser but heterogeneous deposit. The greater sensitivity of the CPT can provide better control over field methods for improving the resistance of a soil to liquefaction.

The CPT technology is rapidly improving. The introduction of the electric cone has also allowed the addition of pore pressure measure-

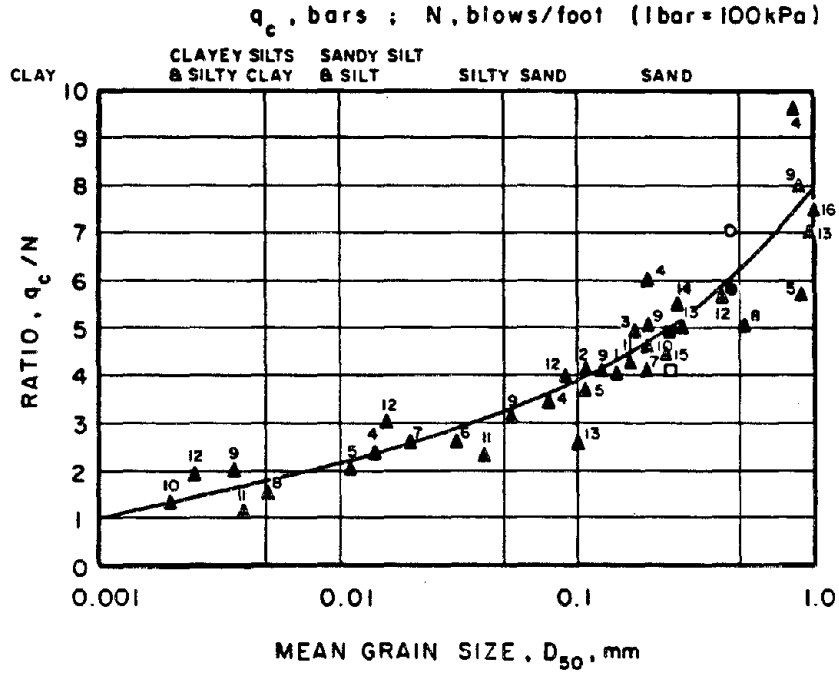

FIGURE 4-9 Relationship between q_c/N_{SPT} and median grain size D_{50}. Numbers next to data points indicate various sources of data. Source: Robertson et al. (1983).

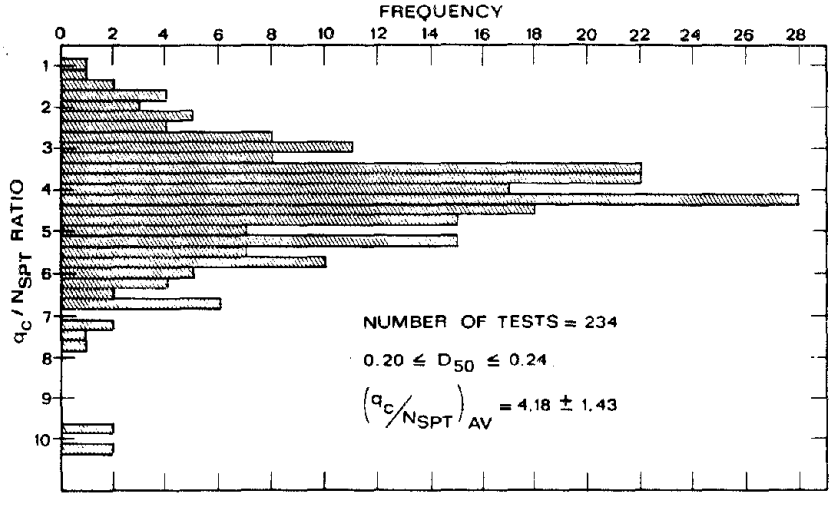

FIGURE 4-10 Histogram of q_c/N_{SPT} ratio for sands with a relatively narrow range of median grain sizes ($0.20 \leq D_{50} \leq 0.24$ mm). Source: Baldi et al. (1985).

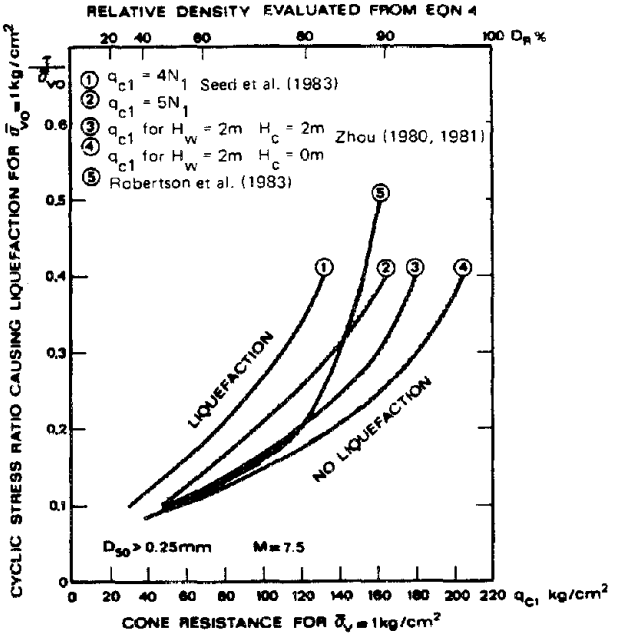

FIGURE 4-11 Various relationships for evaluation of liquefaction potential from q_c values. Source: Baldi et al. (1985).

ments during penetration, which aid in the interpretation of the soil profile. The procedure and equipment of the quasi-static electric cone penetration test are easily standardized (American Society for Testing Materials, 1984). Much of the CPT carried out in various parts of the world is performed according to European and American Society for Testing and Materials (ASTM) standards; thus, results are independent of operator variability. Therefore, data can be collected and compared with confidence to improve and upgrade existing design correlations.

Recently the Japanese Public Works Research Institute has introduced a cone with an internal vibrator; comparing resistance in adjacent borings with and without vibration apparently aids in detecting soils susceptible to liquefaction. Additional developments of this type can be expected. As more CPT results are obtained from sites of actual field experiences, the CPT will likely play an increasing role in site evaluations.

Electrical Measurements

Arulanandan (1977) and Arulmoli et al. (1985) have developed techniques for measuring the resistivity and capacitance of soil in situ, showing that these characteristics can be correlated to liquefaction

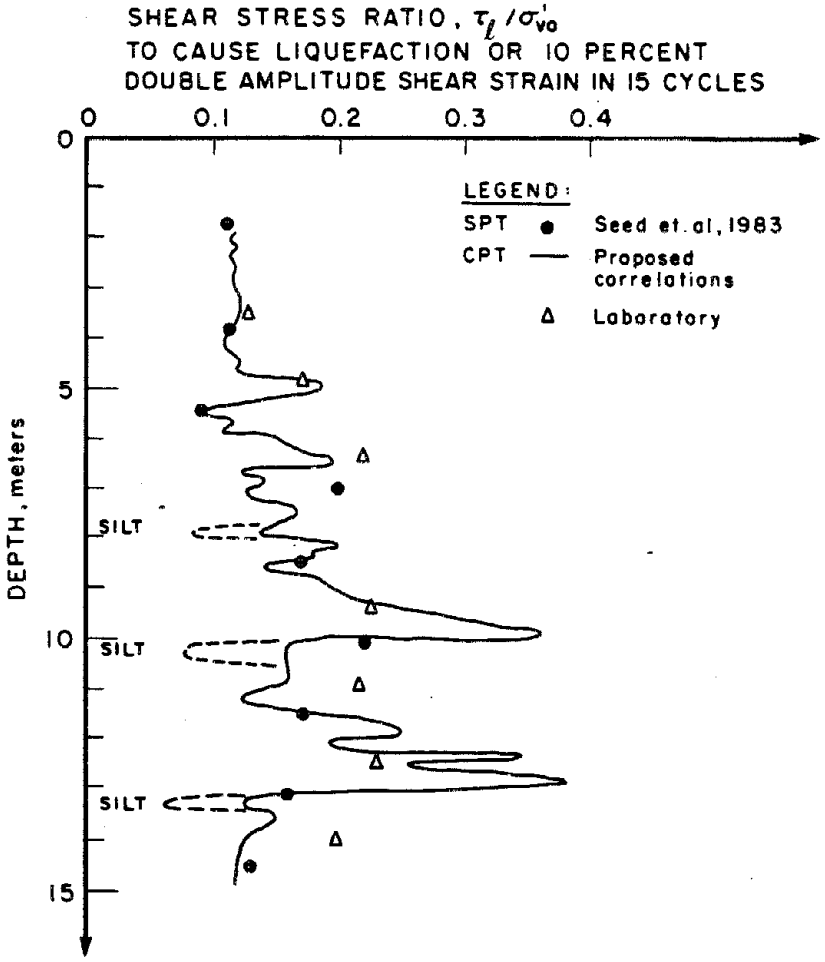

FIGURE 4-12 Comparison of predicted cyclic stress ratio from SPT, CPT, and laboratory testing at McDonald's farm site, Vancouver, B.C. Source: Robertson and Campanella (1985).

resistance as measured by cyclic load tests in the laboratory. Investigations have been made at several sites where liquefaction has occurred during earthquakes. More effort will be required to demonstrate that this tool is superior to the penetration methods now in use.

Shear Wave Velocity Measurements

Over the past 15 years, significant advances have been made in measuring shear wave velocities in the field. Accurate and detailed profiles can be determined with both the crosshole and downhole

seismic methods (Stokoe and Hoar, 1978; Woods, 1978). Shear wave velocity, V_s, is influenced by many of the variables that influence liquefaction, such as density, confinement, stress history, and geologic age. Thus, V_s has promise as a field index in evaluating liquefaction susceptibility. However, few data are available for correlating the occurrence of liquefaction with V_s. One such correlation for recent earthquakes in Imperial Valley, California, is shown in Figure 4-13. V_s also is the major in-situ parameter in the threshold strain approach discussed later and provides an alternative to relying on direct correlation.

Use of this approach requires evaluation of shear wave velocity, which in soil can be measured in situ with considerable accuracy and confidence (Woods, 1978). Crosshole and downhole methods can be relatively expensive. A newly developed method employing surface waves (Stokoe and Nazarian, 1985) overcomes the expense and drilling difficulties associated with the crosshole and downhole methods.

A new device combines a piezometer cone with a set of miniature seismometers built into the cone (Campanella and Robertson, 1984). The piezometer cone measurements are used to log the stratigraphy during penetration, and downhole seismic technique is performed during pauses in the penetration to provide a profile of the in-situ wave velocity. A set of such measurements is shown in Figure 4-14 together with values of V_s from the crosshole measurements.

One of the potential advantages of seismic methods is that they can be performed on hard-to-sample soils such as gravels. Another advantage is that seismic testing evaluates a fundamental soil property, i.e., the shear modulus in the initial portion of the stress-strain curve. However, the use of seismic velocity as an index test for liquefaction resistance is not yet a proven technique.

Influence of Overlying Liquefaction-Resistant Stratum

It has been presumed that the effects of a liquefaction at some depth within a soil profile will become manifest at ground surface, at least in the form of sand boils. However, the presence of a nonliquefiable surface layer may prevent the observable effects of an at-depth liquefaction from reaching the surface. This can occur when the surface layer is thick enough to resist upward pressure and the liquefying stratum is thin enough to provide only a limited reservoir of water.

Ishihara (1985) has assembled several case histories that give guidance on this matter. Figure 4-15 collects data from sites in Japan where there was a buried stratum of loose sand with blow counts less than 10. There was no evidence of liquefaction when the nonliquefiable surface layer had a thickness greater than 3 m. If the thickness of the underlying liquefiable stratum was less than 3 m, an even thinner

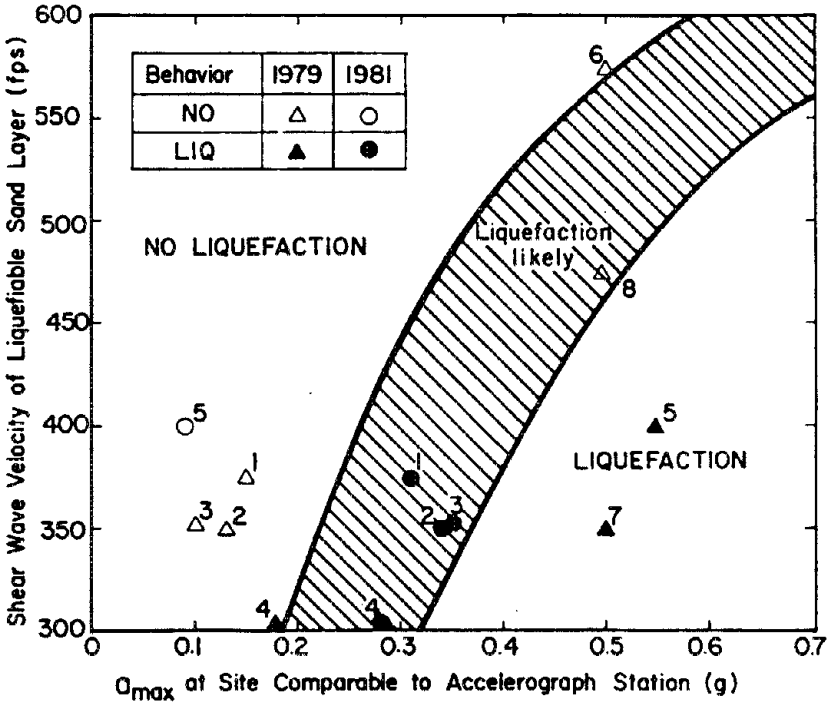

FIGURE 4-13 Influence of shear wave velocity on liquefaction potential of sands from field and parametric studies, Imperial Valley, California, $M = 5.5$ to 6.5. Source: Bierschwale and Stokoe (1984).

surface layer apparently masked any actual liquefaction. Based upon this and other experiences, Ishihara has suggested that the chart in Figure 4-16 may be used for sites having a buried liquefiable layer with $N < 10$.

Use of Threshold Strain

Laboratory tests (Chapter 2) show there is a level of cyclic shear strain below which straining does not cause a buildup of excess pore pressures. Thus, if it can be shown that the cyclic strains in a particular soil as a result of an earthquake do not exceed this threshold strain, liquefaction cannot occur during that earthquake. This provides a conservative evaluation, since liquefaction may not occur even if the strains do exceed the threshold.

The peak strain caused by an earthquake ground motion may be estimated with considerable accuracy using the equation:

$$\gamma = \frac{\tau}{G} = \frac{(a/g)\,\sigma_o\, r_d}{G} \qquad \text{(Eq. 4-6)}$$

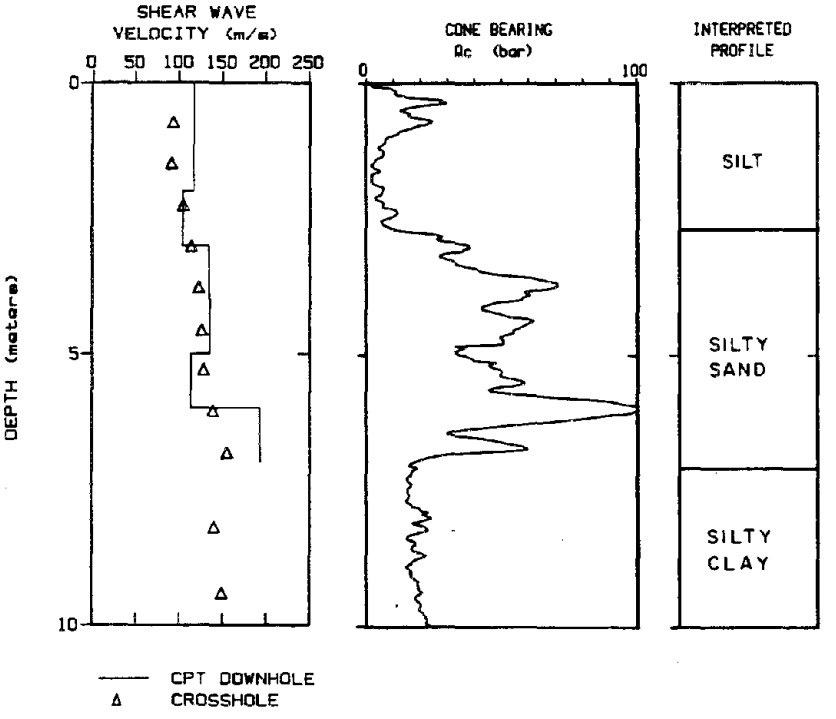

FIGURE 4-14 Comparison of seismic CPT downhole and crosshole data at Wildlife Site, Imperial Valley, California. Source: Campanella and Robertson (1984).

where γ equals strain, τ equals peak stress, G equals shear modulus, a equals peak acceleration at ground surface, g equals the acceleration of gravity, σ_o equals the total vertical stress at the depth of interest, and r_d is a stress reduction factor, which for this purpose has values between 0.92 and 1.0. Assuming that the mass density of the soil is approximately constant with depth, Eq. 4-6 can be rewritten as:

$$\gamma = \frac{a\, z\, r_d}{(G/G_{max})_\gamma V_s^2} \qquad \text{(Eq.4-7)}$$

where z equals depth, $(G/G_{max})_\gamma$ is a modulus reduction factor for strain, and V_s equals shear wave velocity. $(G/G_{max})_\gamma$ is itself a function of strain, so that iteration is necessary to solve Eq. 4-7. However, it often is reasonable to use $(G/G_{max})_\gamma = 0.8$. Combining this with an average value for r_d leads to:

$$\gamma = 1.2\, a\, z/V_s^2 \qquad \text{(Eq. 4-8)}$$

Hence, by measuring the shear wave velocity as a function of depth, γ can be evaluated as a function of depth. If γ thus computed for any

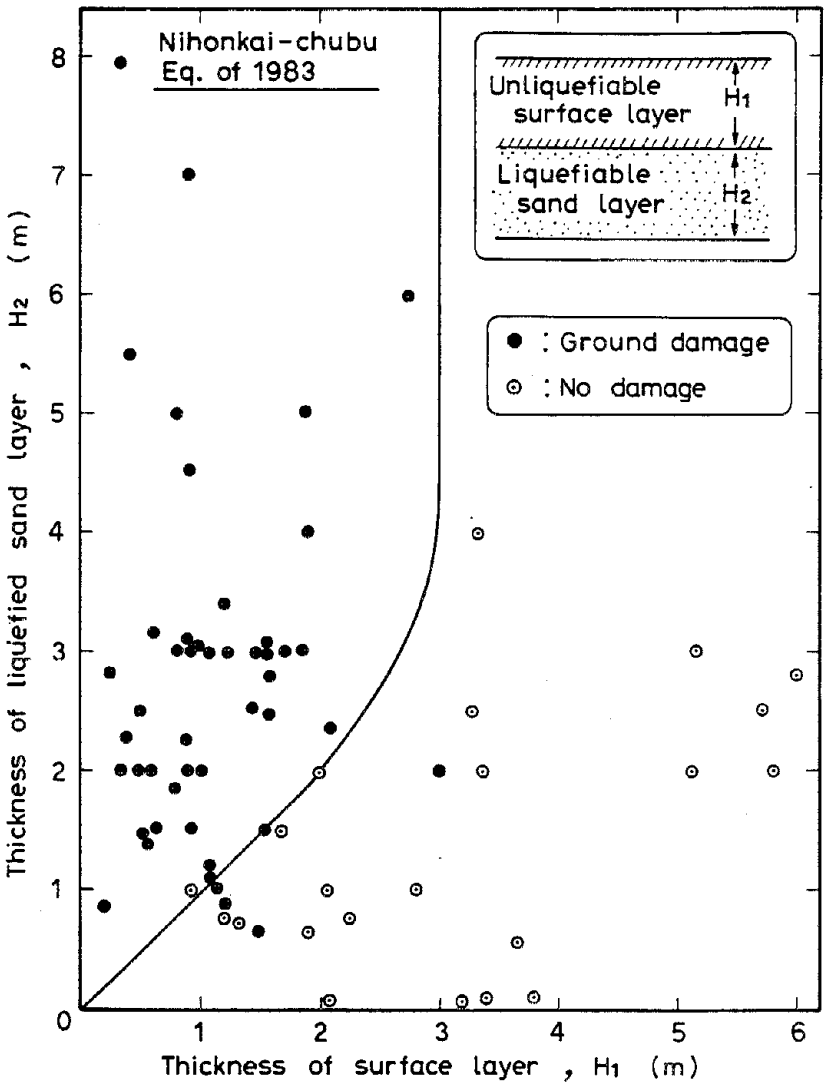

FIGURE 4-15 Conditions of subsurface soil stratification discriminating between occurrence and nonoccurrence of ground rupturing from liquefaction. Source: Ishihara (1985).

depth in a cohesionless deposit is less than the threshold strain (typically 0.0001, or 0.01 percent), then there is safety against liquefaction.

Dobry et al. (1981a) have assembled data for wave velocities in various saturated cohesionless soils and have found a clear trend for this velocity to increase with the geologic age of the deposit (Table

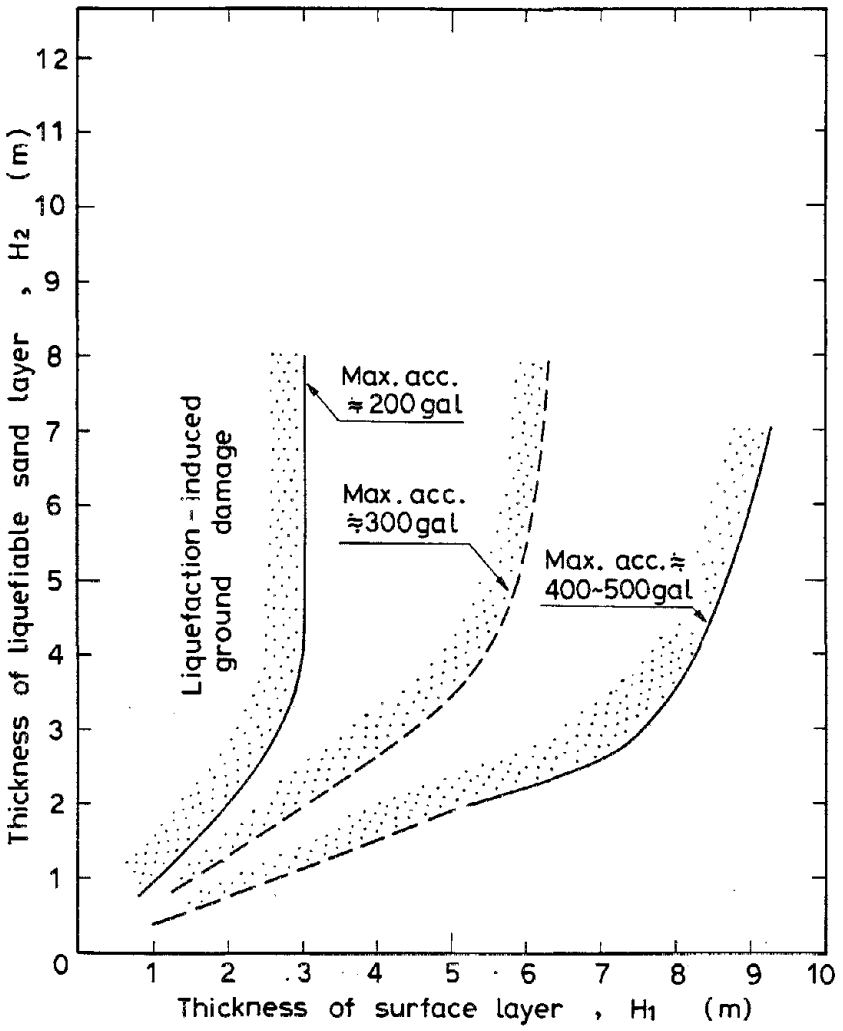

FIGURE 4-16 Proposed boundary curves for site identification of liquefaction-induced damage. Source: Ishihara (1985).

4-5). Since increasing velocity means smaller cyclic strain for a given peak surface acceleration, this trend is consistent with the geologic evidence concerning liquefaction susceptibility.

It is also possible to turn the foregoing equations around to evaluate the acceleration corresponding to the threshold strain. Using Eq. 4-7, Dobry et al. (1981a) have prepared charts giving the threshold peak surface acceleration as a function of shear wave velocity for different depths and for different values of threshold strain. Several examples

TABLE 4-5 Typical Ranges of V_s in Saturated Sands

Material	V_s
Very recent noncompacted sands	300 to 700 fps
Other Holocene sands (<10,000 years)	500 to 1,000 fps
Pleistocene sands (>10,000 years)	600 to 1,400 fps

SOURCE: Dobry (1985).

appear in Figures 4-17 and 4-18. It may be seen that the threshold accelerations are in general accord with experience.

The method outlined here provides an alternative to reliance upon penetration resistance for evaluation of liquefaction susceptibility, especially for sands containing gravel. It must be remembered, however, that in the form described here it is a conservative evaluation. The use of cyclic strain as a controlling variable can be extended beyond the threshold strain to predict pore pressure buildup to the $\sigma' = 0$ condition. This extension is described subsequently.

Instability at Constant Volume

As discussed earlier, instability can occur under constant volume (i.e., undrained) conditions only when the static shear stress that the soil must sustain exceeds the undrained steady-state strength. Then it is possible that a superimposed cyclic load may cause the available resistance to fall below the static stress. There are two key questions to be answered in analyzing a specific situation for the possibility of an undrained instability:

1. Does the soil have the type of stress-strain curve exhibited in Figure 3-3a, i.e., does the static shear stress exceed the undrained steady-state shear strength?
2. What combinations of cyclic stress amplitude and number of cycles of stresses will carry the soil "past the peak"?

Identification of Contractive Sands

A sand with the type of stress-strain curve in Figure 3-3a during undrained loading requires that the undrained steady-state strength (S_{us}) be lower than the drained strength; otherwise the static shear stress could not exceed S_{us}. Thus the sand must be contractive, i.e., it tends to decrease in volume when sheared. Whether or not a sand is contractive is determined by its void ratio and the minor principal effective stress applied to the sand.

The steady-state line relates the void ratio and minor principal

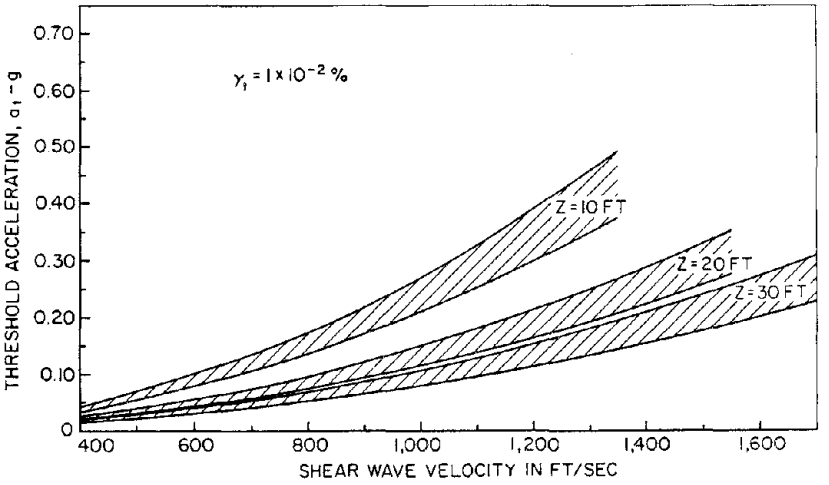

FIGURE 4-17 Simplified prediction chart for threshold acceleration for various depths, with threshold strain assumed to be 0.01 percent. Source: Dobry et al. (1981a).

effective stress during steady-state deformation; i.e., at constant shear stress and constant void ratio (Figure 4-19). The position of this curve depends only upon the grain size distribution and grain shape; it is not influenced by initial void ratio or the initial arrangement of the particles.

If a point representing the in-situ void ratio and the initial in-situ minor principal effective stress falls below the steady-state curve, the soil will be dilative, and its undrained strength would exceed its drained strength. Thus, a constant volume instability is not possible. If a point plots above the steady-state line, the undrained steady-state strength will be lower than the drained strength. Thus, it is possible for the static shear stress to exceed S_{us}. This implies a potentially unstable situation.

Figures 4-20 through 4-22 show steady-state lines for various soils, separated in groups based on grain angularity. The more rounded sands have flatter lines than sands with angular grains. The position of the line is sensitive to gradation, but the slope is primarily a function of grain angularity.

Evaluating Steady-State Undrained Strength

If the soil appears contractive based on blow counts or other index tests, then it becomes necessary to evaluate the undrained steady-state strength S_{us} for the soil in its in-situ condition. The strength S_{us} is sensitive to void ratio and thus to changes in density because of sampling, handling, and consolidation in the laboratory. A correction

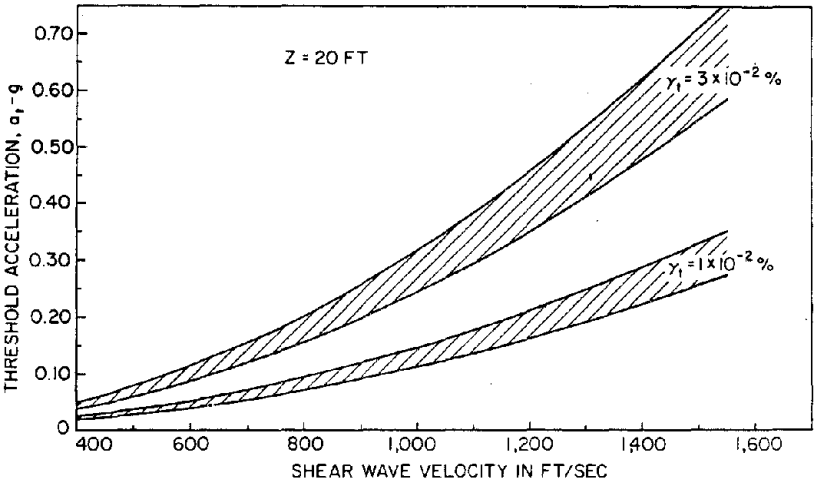

FIGURE 4-18 Simplified prediction chart for threshold acceleration for a depth of 20 ft, with various threshold strains. Source: Dobry et al. (1981a).

must be applied to strengths measured directly upon "undisturbed samples." Poulos et al. (1985) recommend the following procedure.

Step 1 Determine the in-situ void ratio. The in-situ void ratio must be determined for the specimens that are later used to determine their undrained steady-state strength. The best procedures are fixed piston sampling, freezing of the ground and coring, and sampling in test pits. The goals of a successful sampling procedure are to minimize volume changes and to allow measurements of the volume changes that do take place. If fixed piston sampling is used, the difference between the volume of sand sampled and the volume that is recovered is accurately measured. The difference is assumed to be caused by a change in volume during sampling unless a large difference occurs because of the samples sliding in the tube, rendering the sample useless.

Step 2 It is not possible to determine directly a correlation (steady-state line [SSL]) between void ratio and steady-state strength for the undisturbed specimens. However, the steady-state line for the remolded specimens is parallel but not identical to the line for the undisturbed specimens because the slope of the SSL is a function of angularity that is the same for remolded and undisturbed specimens, and position is a function of gradation that is slightly different for remolded and undisturbed specimens because of the ever-present stratification of natural deposits.

Step 3 Determine undrained steady-state strengths using the "undisturbed" specimens by means of consolidated undrained triaxial

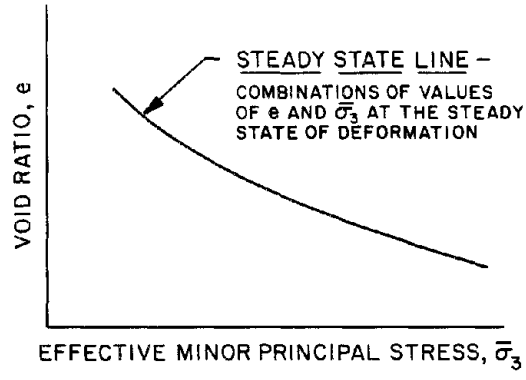

FIGURE 4-19 Schematic definition of the steady-state line.

tests, preferably using consolidation pressures that render the samples contractive.

Step 4 Correct the measured S_{us} to the in-situ void ratio using the procedure sketched in Figure 4-23. The strength measured at point A is corrected by drawing a curve parallel to the steady-state strength line obtained in Step 2, intersecting the in-situ void ratio at point B. This point defines the in-situ S_{us}.

A final step is to compare this S_{us} with the static shear stresses τ_d required for equilibrium, as determined from a static stability analysis. If $\tau_d > S_{us}$, then there is the potential for an undrained stability failure.

Because the curve of S_{us} versus void ratio typically is flat, uncertainty as to the actual in-situ void ratio has a large effect upon S_{us}. This is illustrated in Figure 4-24; an uncertainty of 3 pcf in density corresponds to a six- to sevenfold uncertainty in S_{us}! Thus, success in determining in-situ steady-state strength is dependent upon the accuracy with which in-situ void ratio or density can be measured. In addition to previously mentioned methods for evaluating in-situ density, use of a nuclear density meter or of electrical resistivity/capacitance is often urged. Several correlations have recently been developed to relate CPT data to soil dilatancy and thus directly to steady-state concepts (Been et al., 1985; Robertson, 1985). If it can be shown that these techniques can reliably measure in-situ density to within 1 pcf, it would be of great benefit to liquefaction analysis.

Conditions to Cause Undrained Failure

If it is found that S_{us} is less than the static stress required for equilibrium, it does not mean that failure will always occur during an earthquake.

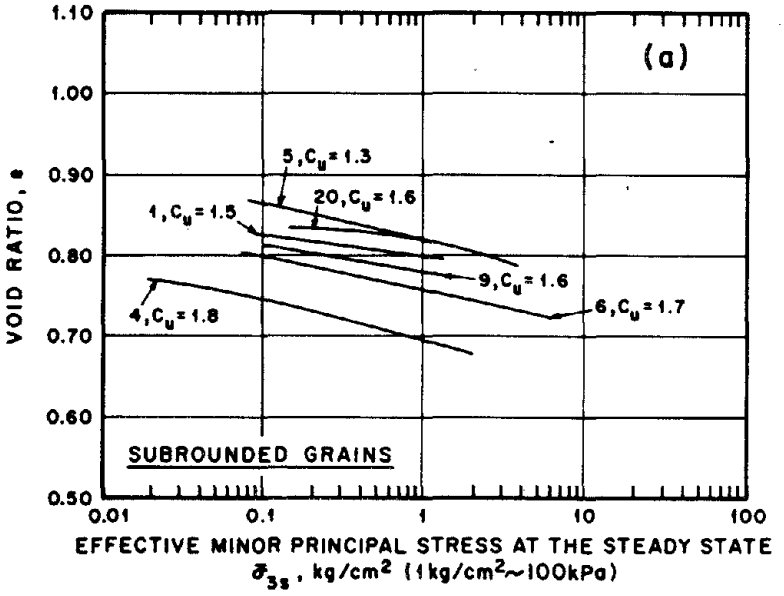

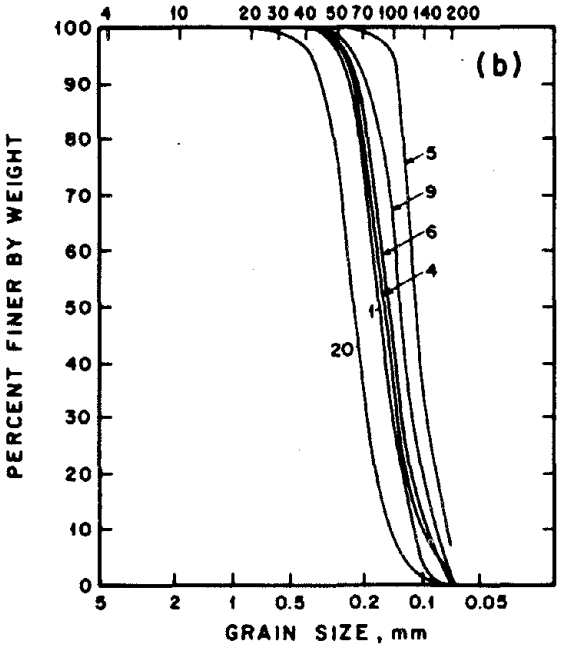

FIGURE 4-20 Steady-state lines for sands with subrounded grains. Source: Poulos et al. (1985).

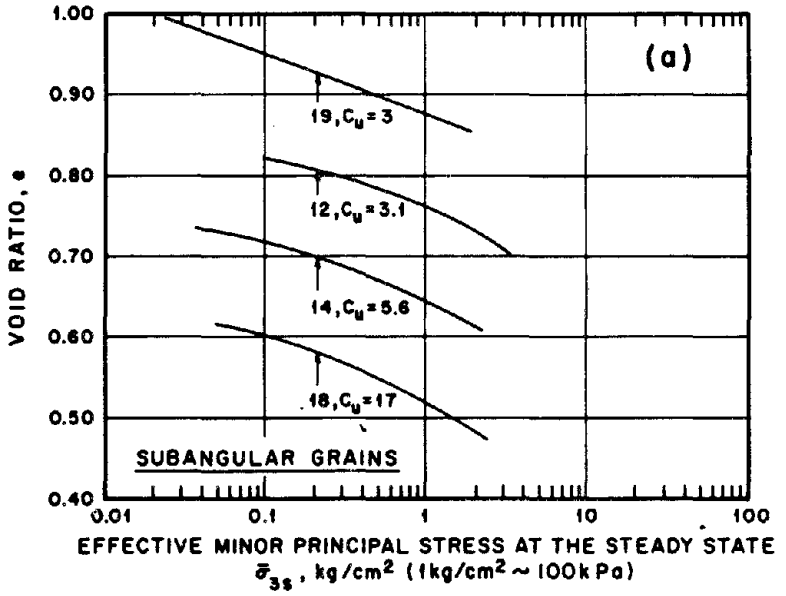

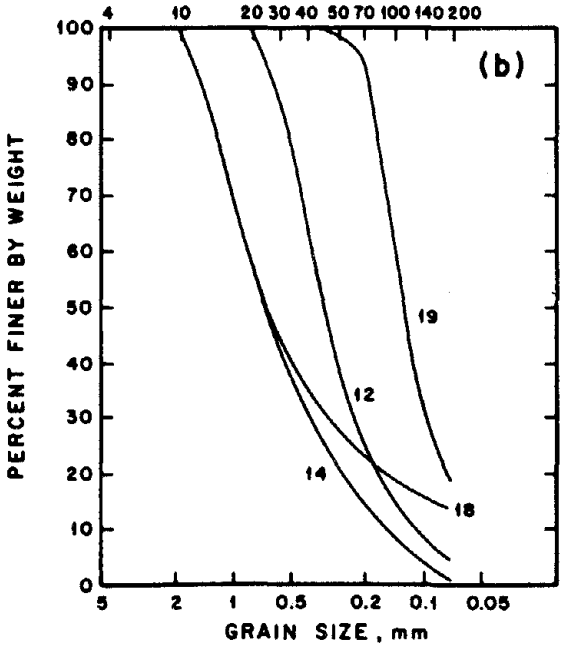

FIGURE 4-21 Steady-state lines for sands with subangular grains. Source: Poulos et al. (1985).

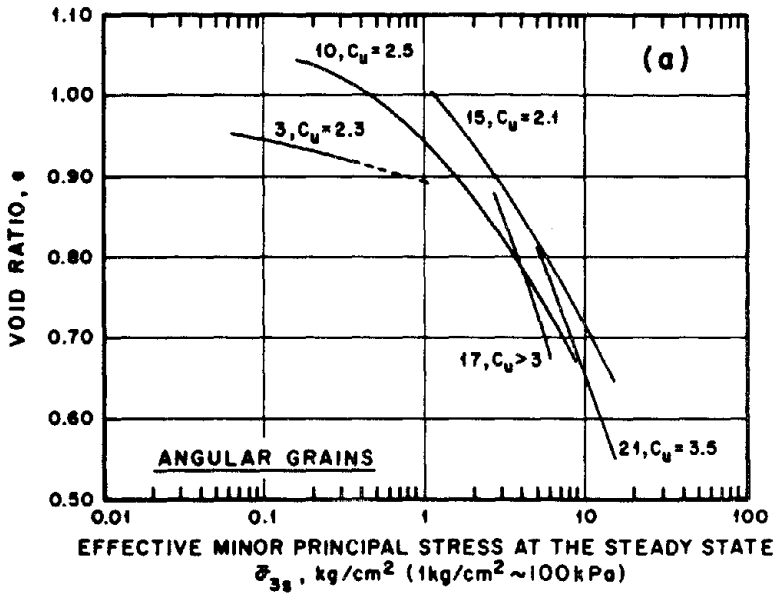

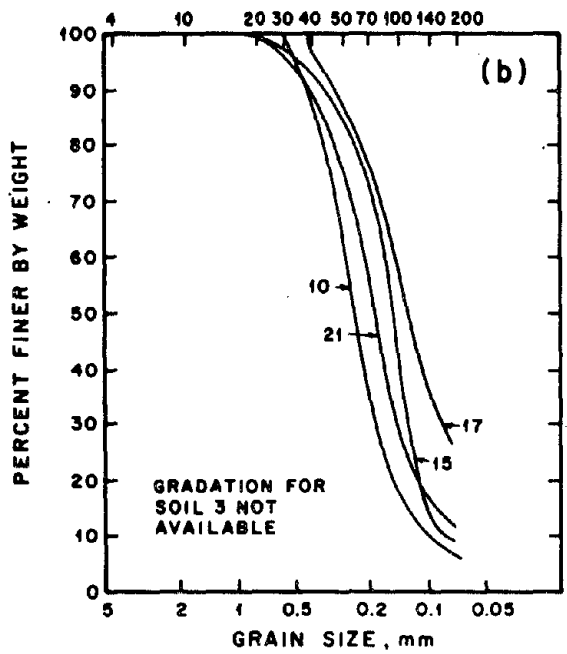

FIGURE 4-22 Steady-state lines for sands with angular grains. Source: Poulos et al. (1985).

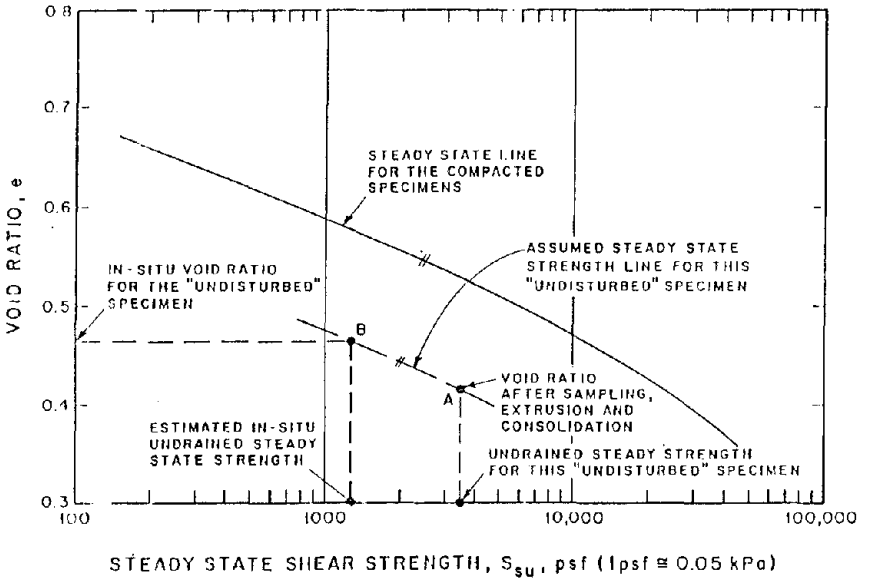

FIGURE 4-23 Correction procedure for measured undrained steady-state strength. Source: Poulos et al. (1985).

The earthquake must be strong enough to "push the soil over the peak" of the undrained stress-strain curve.

The magnitude and duration of the disturbance needed to cause liquefaction in a liquefiable mass is dependent on three principal factors (Poulos et al., 1985): (1) the ratio of the undrained steady-state strength to the driving shear stress (the lower the factor of safety against liquefaction, the smaller the disturbance needed to cause liquefaction), (2) the strain required to reach the peak undrained strength at the in-situ void ratio, and (3) the rate at which the peak undrained strength is lost with continued strain. These factors depend on the shape of the stress-strain curve in situ. Thus, the soil type, the initial soil structure, and the driving shear stresses all affect the intensity and duration of the disturbance needed to trigger liquefaction.

Three hypothetical stress-strain curves shown in Figure 4-25 illustrate the second and third of the above factors. In all three cases, τ_d/S_{us} is 0.25, i.e., much less than 1.0. The soil masses represented by these stress-strain curves are susceptible to liquefaction. Each represents a condition of unstable equilibrium. One would expect that a smaller disturbance is needed to cause liquefaction for case a than for case b because the peak strength, S_{sp}, is smaller for case a. If an earthquake is the disturbance in question, a less intense earthquake is needed to cause liquefaction in case a.

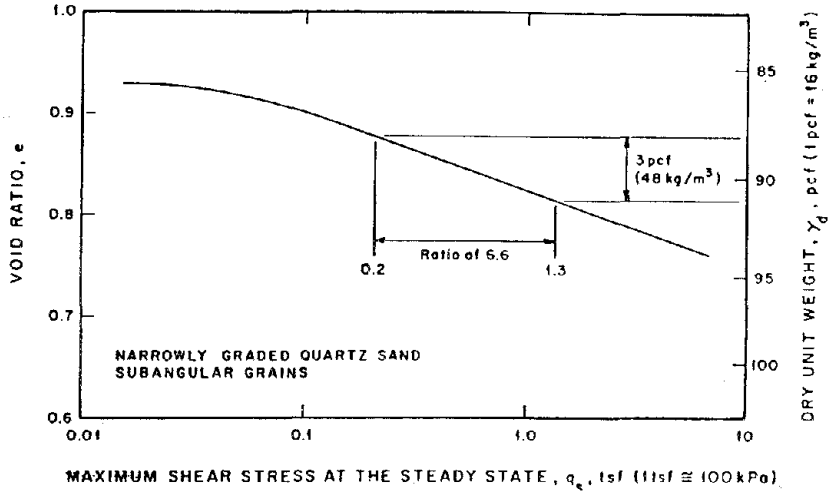

FIGURE 4-24 Schematic showing the sensitivity of the maximum shear stress at the steady state to variations in determination of the in-situ dry unit weight or void ratio. Source: Poulos et al. (1985).

Case c in Figure 4-25 represents the stress-strain curve for an undrained test on a clay or clayey silt, using the same scale for strain as for cases a and b. The peak strain is larger than for cases a and b, and a large strain is needed to reduce the strength to the steady-state strength. This soil could absorb many earthquakes that impose many cycles of shear stress in excess of τ_d (and well in excess of S_{us}) without failing. Thus, clayey materials (case c) are less susceptible to liquefaction. This laboratory finding is in agreement with field behavior.

Dobry et al. (1984) have investigated the cyclic stresses needed to trigger liquefaction using special tests in which cyclic torsional strains are superimposed upon a triaxial sample subjected to a static deviator stress. Figures 4-26 and 4-27 show a typical set of results. (Note that the relative density of this sand is very low.) At point T, after 109 cycles of small torsional moment, unidirectional flow deformation was triggered and the axial strain increased more than 15 percent in 0.32 s. It was found that this triggering of flow occurred when the effective stress, which constantly decreased during cycling, reached the failure line (Figure 4-27). Based upon these test results, Dobry et al. (1984) propose a method for determining the intensity of earthquake required to initiate failure in a dam.

Residual Strength from SPT

If the magnitude and duration of a disturbance are sufficient to push a liquefiable soil beyond the peak of its stress-strain curve, then an

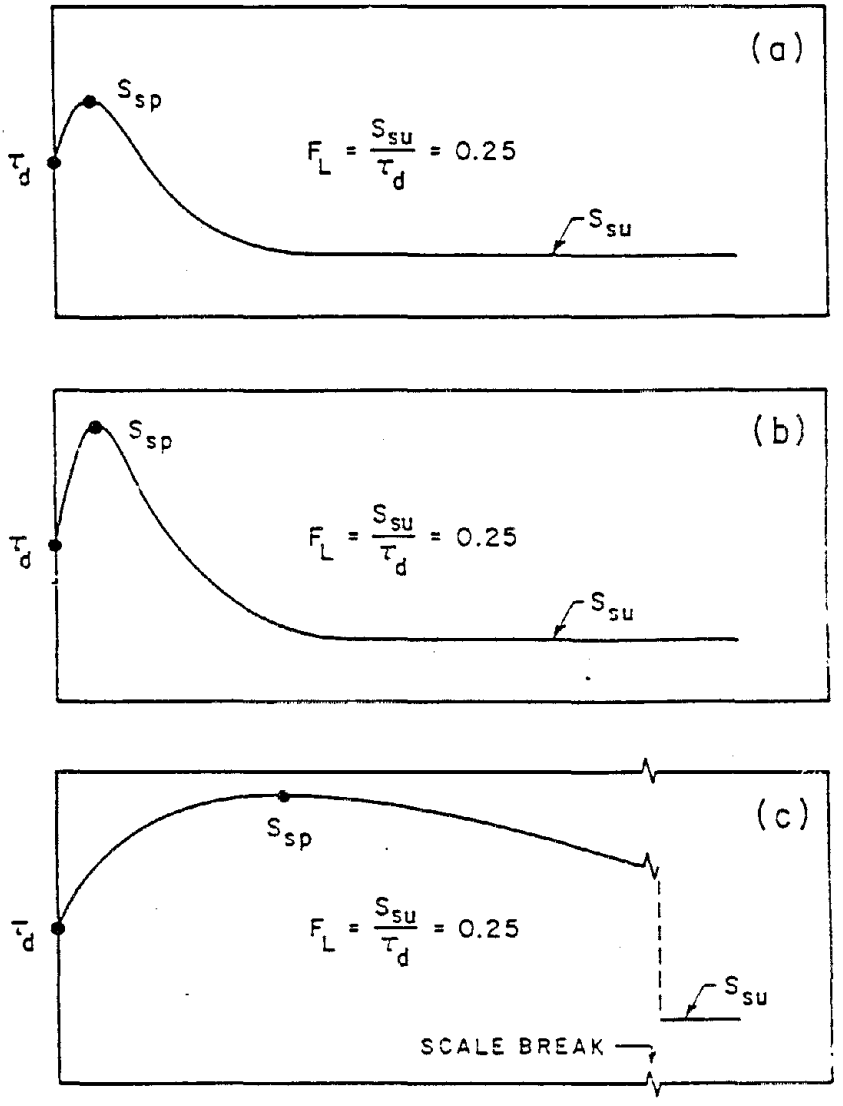

FIGURE 4-25 Hypothetical stress-strain curves illustrating various stress conditions causing undrained failure. Source: Poulos et al. (1985).

alternative approach to determining the steady-state strength is to use the residual strength determined from the relationship between residual strength and SPT N-values proposed by Seed (1984). In this method the residual strengths are based on back-analysis of liquefaction-type slides and the values are representative of known field behavior. This

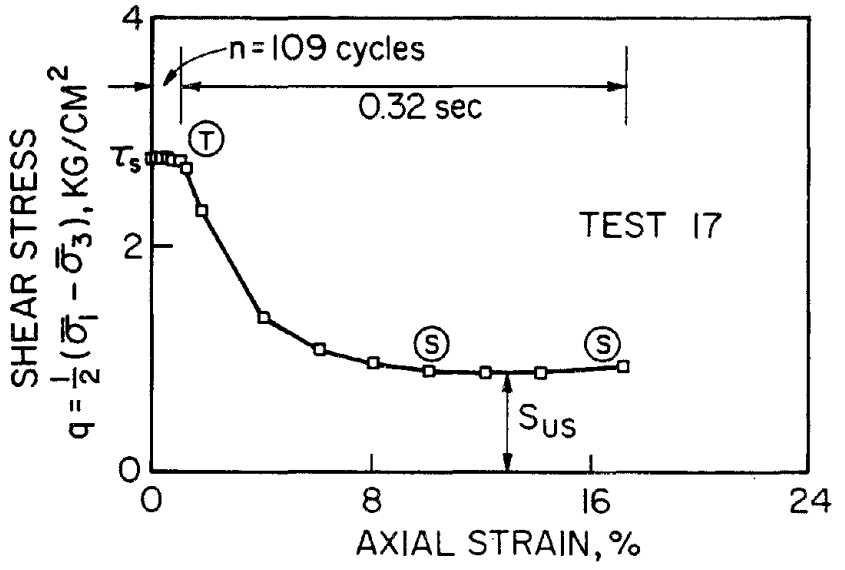

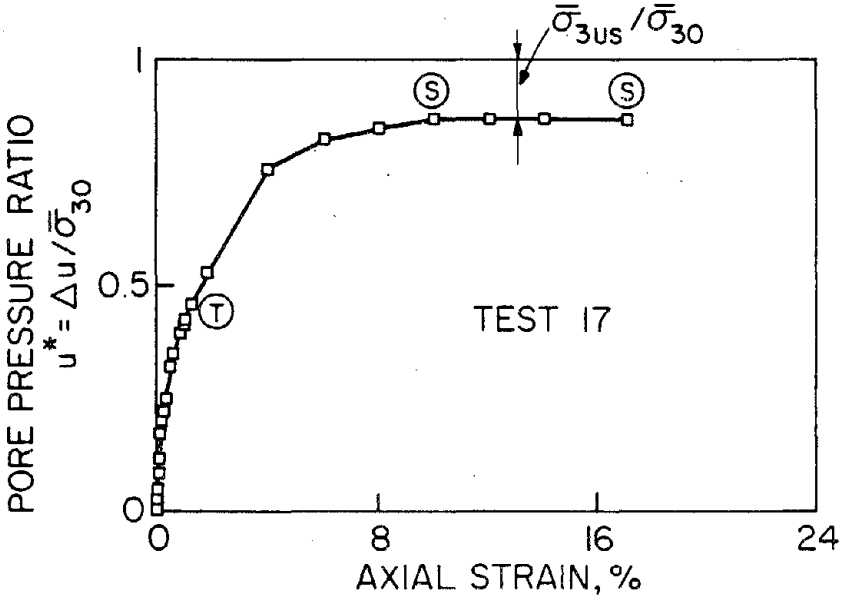

FIGURE 4-26 Typical stress-strain pore pressure response during a $C_y T$-$\overline{CAU}$ test on Banding sand (D_r = 23 percent, σ'_{30} = 5.5 kg/cm^2, K_c = 2). Source: Dobry et al. (1984).

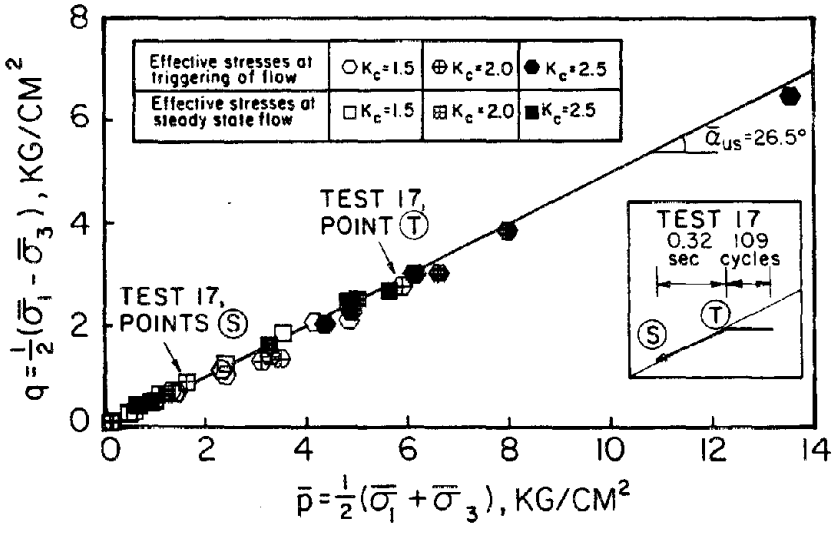

FIGURE 4-27 Effective stresses at triggering of flow and during steady-state flow from C_yT-$\overline{CAU}$ tests on Banding sand (D_r = 12 to 25 percent). Source: Dobry et al. (1984).

approach circumvents the problems associated with sample disturbance and the selection of representative samples for testing, since representative N-values can be developed for the soil over a substantial zone of a deposit. It involves the assumption, however, that the residual strength of a sandy soil is reliably related to its N-value.

As discussed earlier, Seed's residual strength is synonymous with undrained steady-state strength provided the soil is sheared at truly constant volume. There is no certainty that this condition actually exists, either in the cases studied by Seed or in any case of flow failure. Thus, the results shown in Figure 4-28 account in an empirical way for possible deviations from a constant-volume condition in field problems.

Buildup of Pore Pressures

Even though it is clear that the occurrence of liquefaction is intimately associated with the buildup of excess pore pressure, none of the evaluative techniques discussed have explicitly predicted this buildup. There are a number of reasons why it may be desirable or necessary to actually predict such pore pressures:

- On the practical side, it is necessary to predict excess pore pressures if an effective stress stability analysis is to be done. While there are major questions concerning the meaning and interpretation

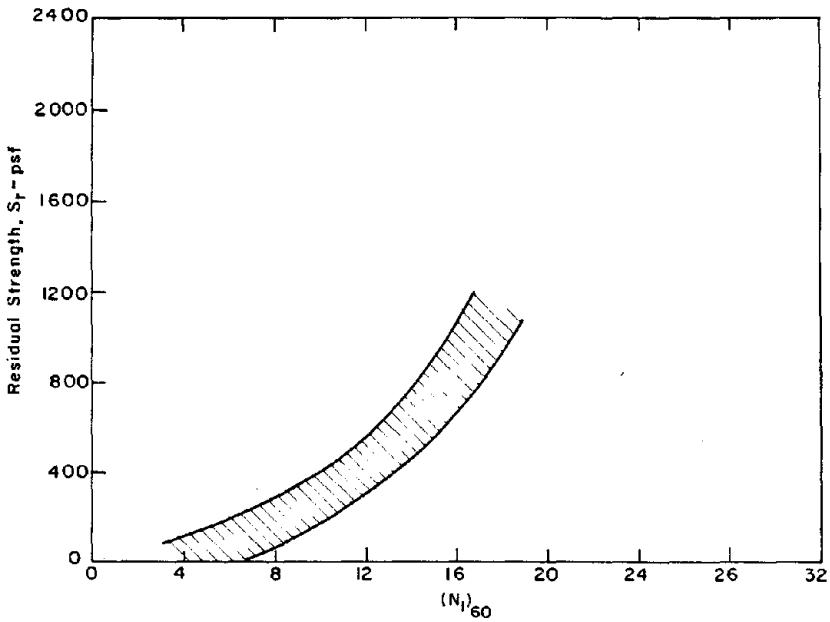

FIGURE 4-28 Tentative relationship between residual strength and SPT *N*-value. Source: Seed (1984).

of such an analysis, it is the only appropriate approach if the effects of deviations from undrained conditions (including outward spreading of pore pressures) are to be considered.

- The buildup of excess pore pressure can influence the amount of permanent deformation caused by an earthquake.
- On the academic side, an understanding of the liquefaction phenomenon is closely keyed to our understanding of the factors affecting the buildup of pore pressures.

Historically, the initial efforts to predict pore pressure increases dealt with a sand below a level ground surface (which in terms of this report means there is no structure on the surface). This situation involves deformations and pore pressures that vary only in the vertical direction; that is, it is a one-dimensional situation. The level ground case is primarily of academic interest. However, there are two strong reasons for developing methods for predicting pore pressure buildup in this case:

- To develop and test concepts and procedures for this simple situation before tackling the more realistic but more complicated two— and three-dimensional situations.

• To compare predictions with pore pressures actually measured during earthquakes to validate predictive theories.

A large variety of predictive methods and theories have been proposed. The following subsections summarize the key aspects of these approaches. Earlier summaries of work prior may be found in Valera and Donovan (1977) and Finn (1981).

It is convenient to think of an analysis as consisting of two parts:

1. Dynamic analysis to compute time histories of stress and/or strain at various points within a soil mass.
2. Computation of the generation (and perhaps dissipation) of pore pressures.

In some methods these two steps are indeed carried out separately; these are called decoupled analyses. In other methods the steps are effectively performed simultaneously; these are coupled analyses.

Pore Pressure Models

The major key to any analysis is a method for computing the increment of pore pressure caused by a cycle of stress or strain. In general, this increment of pore pressure will depend upon the prior history of stressing and straining as well as upon the intensity of the present cycle.

Direct Use of Laboratory Tests

Early studies of liquefaction made great use of cyclic load tests in the laboratory. Such tests provide curves relating cyclic stress to the number of cycles, N_l, to initial liquefaction (e.g., Figure 2-29), and to curves relating the pore pressure buildup $\Delta u/\sigma'_o$ to the ratio N_e/N_l, where σ'_o is the initial effective stress and N_e is the number of cycles of stress applied (Figure 4-29).

The relation between $\Delta u/\sigma'_o$ and N_l is more or less independent of the fabric of the sand, which means that the relation can be determined from tests upon undisturbed samples even when there actually is some disturbance. Thus, curves such as that in Figure 4-29 are used widely in the calculation methods discussed below.

The relation of N_l to τ_c/σ'_o may be very much affected by sampling disturbance (see the discussion in Chapter 2). For this reason, the value of N_l used in Figure 4-29 quite often is inferred indirectly from SPT or other in-situ tests. This effect of disturbance is emphasized by the scatter in the results in Figure 4-30 relating $\Delta u/\sigma'_o$ to τ_c/σ'_o for different numbers of cycles.

On the other hand, there is less scatter if $\Delta u/\sigma'_o$ is plotted against cyclic strain. This is shown by comparing Figure 4-30 (stress-controlled

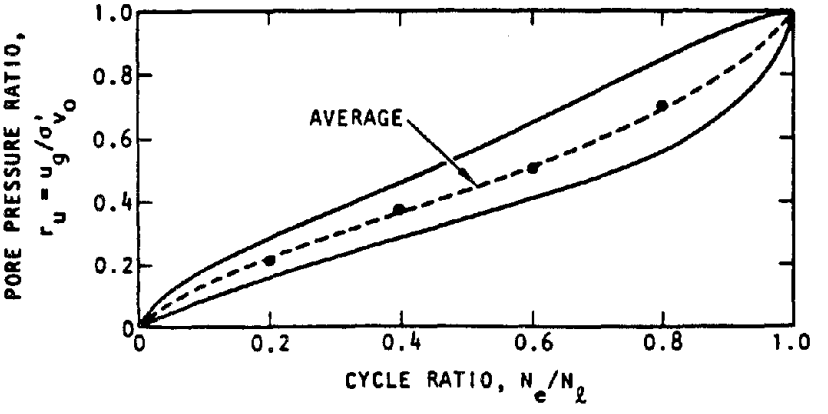

FIGURE 4-29 Rate of pore pressure buildup in cyclic simple shear tests. Source: Seed et al. (1976).

tests) with Figure 4-31 (strain-controlled tests); in both figures the same sand and specimen preparation techniques were used. Further evidence comes from Figure 4-32, compiled by Dobry (1985), which summarizes $\Delta u/\sigma'_o$ versus cyclic strain after 10 cycles of strain were obtained from 50 triaxial tests on saturated sands. The data in the figure include seven sands, and the tests were performed at three laboratories using $\sigma'_o = \sigma'_{30} = 500$ to 4,000 psf, on "undisturbed" and remolded, loose and dense sand specimens. Despite this wide range of materials and testing conditions, Figure 4-32 is remarkably consistent with, and confirms, the observation in Chapter 2 that cyclic strain is more fundamentally related to densification than is cyclic stress. Use of stress-controlled triaxial tests is further complicated by different strains during the compression and extension phases. This difficulty is avoided by using tests with controlled cyclic strain. For these reasons, some researchers suggest using cyclic strain as a basis for computation of pore pressures.

Computation from Data for Densification

Referring to Figure 2-25, it is in principle possible to compute induced pore water pressure from the densification that would occur if drainage was permitted together with the slope of the rebound curve. In equation form, this is expressed by:

$$\Delta u = \overline{E}_r \Delta \varepsilon_{rd} \qquad \text{(Eq. 4-9)}$$

where $\overline{E}_r$ is the rebound modulus and $\Delta\varepsilon_{rd}$ is the volumetric strain if drainage can occur. Martin et al. (1975) proposed procedures to evaluate $\Delta\varepsilon_{rd}$ and $\overline{E}_r$ using results from cyclic tests on dry sands and static

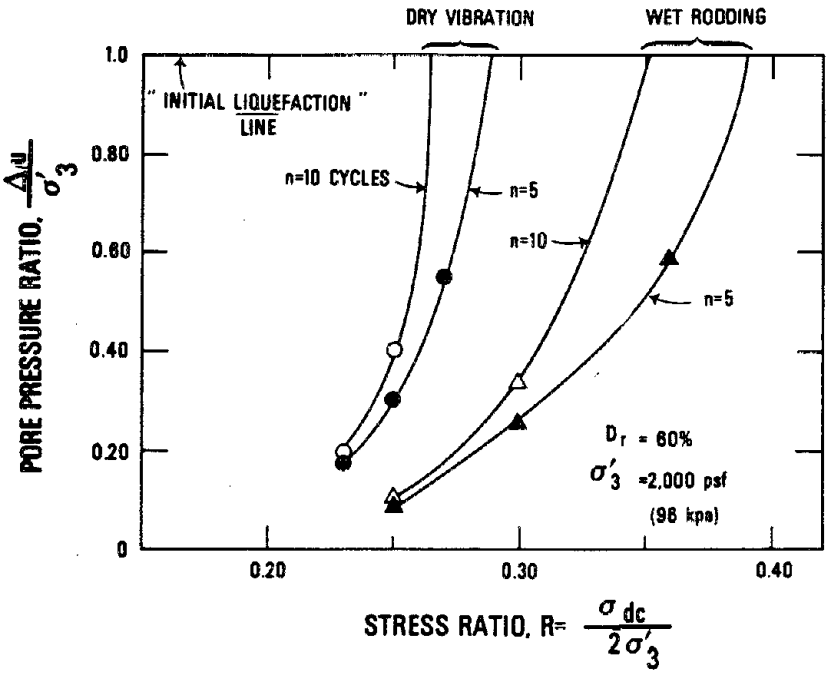

FIGURE 4-30 Stress-controlled cyclic triaxial tests of saturated Crystal Silica sand. The mathematical notation for the axes labels is different from that in the text, but the actual quantities are the same. Source: Dobry et al. (1982) modified from Park and Silver (1975).

rebound tests in a consolidation ring, respectively. The observed densification is fitted with an equation:

$$\Delta\varepsilon_{vd} = C_1(\gamma - C_2\varepsilon_{vd}) + C_3\varepsilon_{vd}^2/(\gamma + C_4\varepsilon_{vd}) \qquad \text{(Eq. 4-10)}$$

where γ is the cyclic shear strain, ε_{vd} is the current value of the volume change, and $C_1 \ldots C_4$ are experimentally determined constants. The rebound modulus is similarly modeled by the equation:

$$\overline{E}_r = (\sigma'_v)^{1-m}/m\ K_2(\sigma'_{vo})^{n-m} \qquad \text{(Eq. 4-11)}$$

where σ'_{vo} and σ'_v are the initial and current values of the vertical effective stress and K_2, m, and n are experimentally determined constants.

Finn (1981) has compared pore water pressures observed in cyclic strain tests with those predicted using these equations and has found very satisfactory agreement. The actually measured cyclic strain was used in making the predictions. These studies confirmed the close relation between densification under drained conditions and pore pressure buildup with saturated conditions.

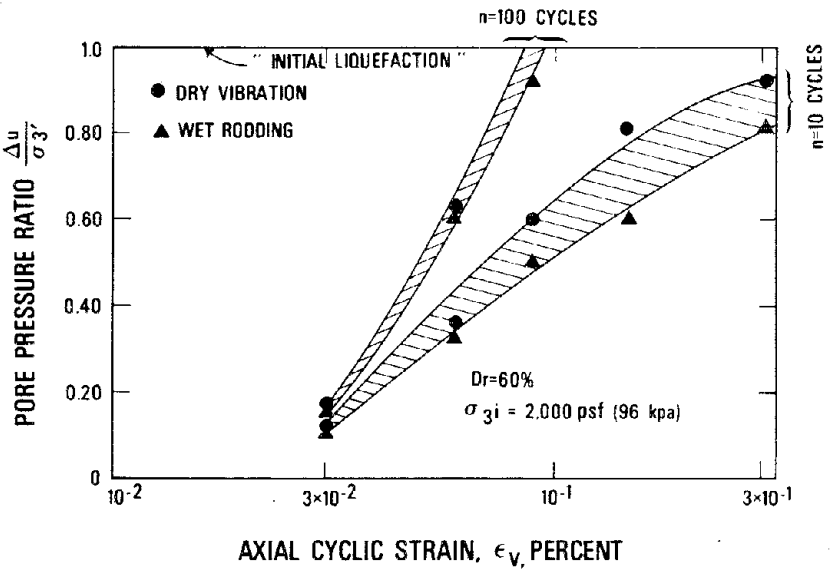

FIGURE 4-31 Strain-controlled cyclic triaxial tests of saturated Crystal Silica sand. The mathematical notation for the axes labels is different from that in the text, but the actual quantities are the same. Source: Dobry et al. (1982) modified from Park and Silver (1975).

An Endochronic Model

Finn and Bhatia (1981) developed an approach in which pore pressure buildup is predicted directly (without the intermediate steps using $\Delta\varepsilon_{vd}$ and $\bar{E}_r$) and is related to a single parameter, called a damage parameter, incorporating the influence of current cyclic strain and past strain history. The steps in this procedure are as follows:

1. An increment in the length of the "strain path" ξ is equated with an increment of deviatoric strain ε_{ij} by:

$$d\xi = \{1/2(d\varepsilon_{ij} \cdot d\varepsilon_{ij})\}^{1/2} \qquad \text{(Eq. 4-12)}$$

where $d\varepsilon_{ij} \cdot d\varepsilon_{ij}$ is in tensor notation; that is, it corresponds to the sum of several terms with i,j equal to 1,2,3 being alternated. The current value of ξ may be evaluated by integrating $d\xi$ with respect to the strain history.

2. The damage parameter κ is determined from the relation:

$$\kappa = \xi e^{\lambda\gamma} \qquad \text{(Eq. 4-13)}$$

where γ is the current value of the cyclic strain and λ is a constant whose value must be determined experimentally.

3. Tests have shown that pore pressure buildup during strain-

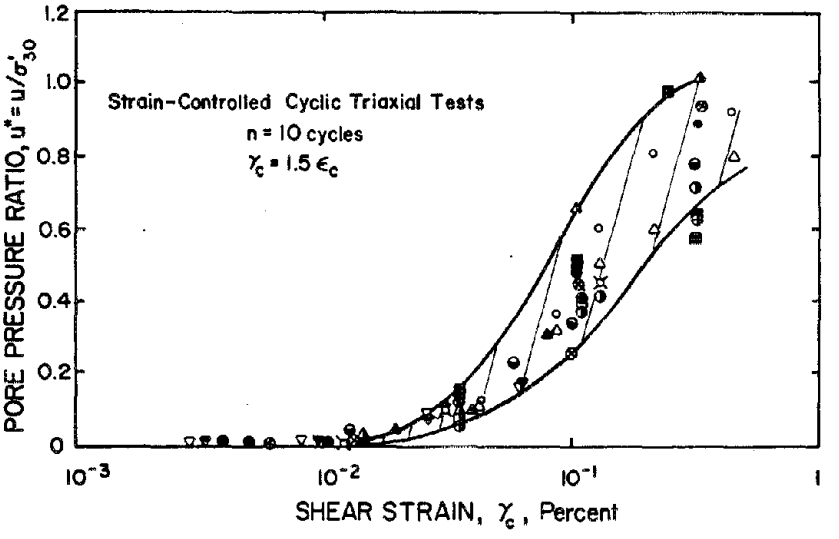

Symbol	Sand	σ'_{30} (psf)	D_r (%)	Samples/ Fabric	Measured u Peak (P) or Residual (R)
○	Crystal Silica	2,000	60	Dry Vibration	P
△	" "	2,000	60	Wet Rodding	P
▲	" "	2,000	60	Dry Vibration	P
▼	Sand No. 1	2,800	60	Moist Tamping	P
▽	" "	1,400	60	" "	P
○	Monterey No. 0	2,000	60	" "	P
●	" "	2,000	80	" "	P
□	" "	2,000	45	" "	P
■	" "	2,000	45	" "	R
▣	" "	533	60	" "	P
⊕	" "	4,000	60	" "	P
◎	" "	2,000	20	" "	R
•	Banding	2,000	60	" "	R
▲	"	2,000	40	" "	R
●	"	2,000	20	" "	R
●	Heber Road Point Bar	2,000	Dense	Tube Sample	R
◐	Heber Road Channel Fill	2,000	Loose	" "	R
⧓	Owi Island	2,000	40	Moist Tamping	R
⊖	" "	1,500	40	" "	R
⊖	" "	2,000	Medium Dense	Tube Sample	R
⊖	Mt. St. Helen Debris	2,000-4,000	50	Moist Tamping	R

FIGURE 4-32 Summary of results from strain-controlled triaxial tests on seven different sands with different specimen preparation techniques, showing consistent results when the pore pressure ratio is plotted against shear strain. The mathematical notation for the axes labels is different from that in the text, but the actual quantities are the same. Source: Dobry (1985).

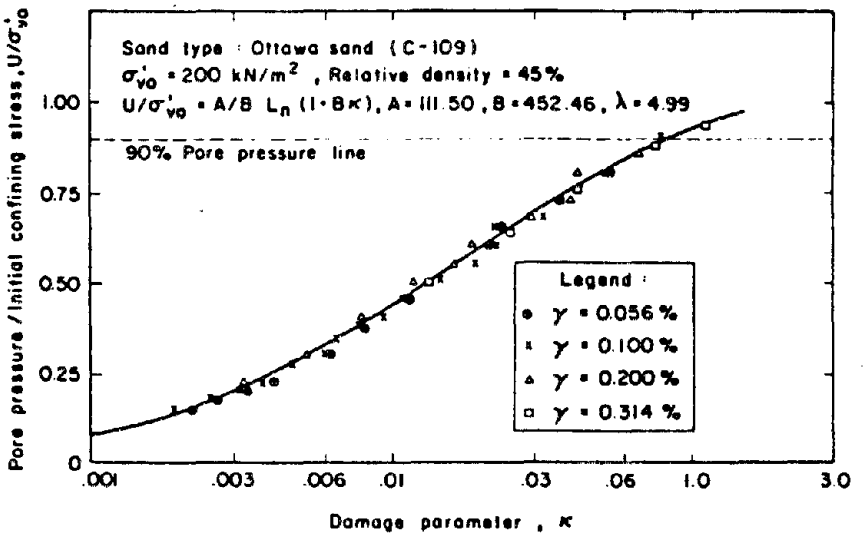

FIGURE 4-33 Pore pressure versus damage parameter k (logarithmic scale). Source: Finn (1981).

controlled cyclic load tests is uniquely related to κ (Figure 4-33). A curve of this type may be fitted by an equation of the form:

$$\Delta u/\sigma'_{vo} = (A/B)\ln(1 + B\kappa) \qquad \text{(Eq. 4-14)}$$

where the constants A and B are determined by nonlinear least-squares curve fitting. Alternatively, data relating pore pressure to κ plotted to an arithmetic scale may be fit by an equation of the form:

$$\Delta u/\sigma'_{vo} = \kappa(D\kappa + C)/(A\kappa + B) \qquad \text{(Eq. 4-15)}$$

with the constants again determined by nonlinear curve fitting.

The major advantages of the approach are that conventional test data can be used directly and a single equation can be used to represent response over a wide range of strains or stresses. A comparison between observed and predicted pore pressures is shown in Figure 4-34.

Stress Path Pore Pressure Models

These methods give rules for predicting the effective stress path (the relationship between shear stress τ and vertical effective stress σ'_o) during cyclic loading. The buildup of pore pressure is found from the difference between the total and effective stress (Figure 4-35).

This approach was developed by Ishihara et al. (1975) and subse-

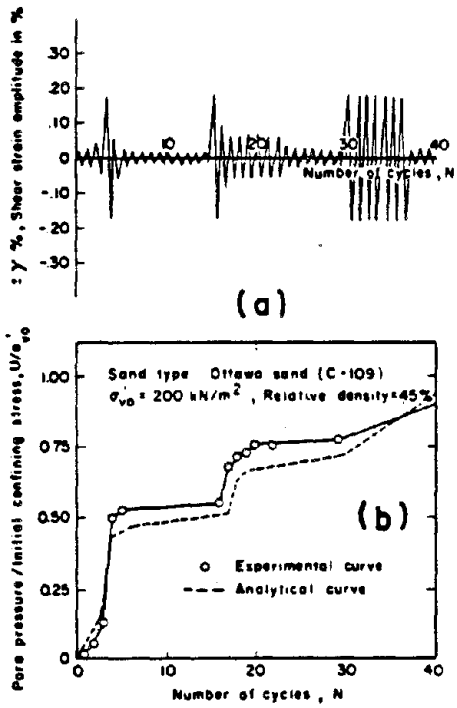

FIGURE 4-34 Comparison of computed and measured pore water pressures for irregular strain history based on an endochronic model. Source: Finn (1981).

quently refined several times (Ishihara and Towhata, 1980). The following types of rules are involved:

- During a virgin straining, the stress paths are described by parabolas (Figure 4-36). In early versions, circles were used. Ghaboussi and Dikmen (1978, 1984) and Dikmen and Ghaboussi (1984) assumed ellipses.
- For loading and reloading, various assumptions have been made. The early version assumed a vertical effective stress path upon reversal until the maximum previous shear stress in the opposite sense was reached, whereupon the appropriate curved path was followed (Figure 4-37). More recent versions use empirically determined relationships to define these portions of the stress path.
- Stress paths defined by these rules terminate when the phase transformation lines are reached (Figure 4-38). Rules are given for establishing the subsequent stress paths.

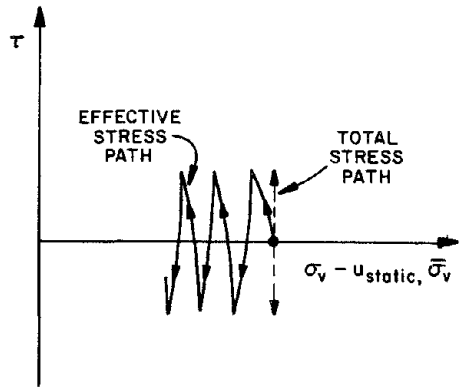

FIGURE 4-35 Schematic of basic concept of stress path models for predicting pore pressure buildup.

Success with this type of approach depends on the development of a satisfactory set of rules for handling the effect of stress reversals and the behavior once the phase transformation line is reached. These rules must be simple enough to be coded into a computer but accurately reflect actual behavior. This approach is complicated because pore pressure development is traced throughout every cycle of loading and unloading. Thus, the effect of each reversal of stress or strain must be taken into consideration. The experimental and theoretical work of Nemat-Nasser (1982) and Nemat-Nasser and Takahashi (1984) bears upon this complex problem.

Effects of a Sustained Shear Stress

The various methods just described have focused primarily upon the level ground case where there is no sustained shear stress. Emphasis has been given to test results from simple shear tests that simulate that situation.

It has, of course, been recognized that a sustained shear stress affects, and indeed can limit, the buildup of pore pressure. Based upon examination of measurements in triaxial cyclic load tests, a mathematical expression has been proposed (Figure 4-39) where $K_c = \sigma'_{10}/\sigma'_{30}$ reflects the presence of a sustained shear stress (Finn et al., 1978a). If K_c is large enough, a condition of initial liquefaction ($\sigma' \simeq 0$) is not reached. Hence the number of cycles, N_{50}, required to reach 50 percent of the minimum principal confining stress is used to normalize the horizontal scale in Figure 4-39. Similar behavior has been noted in simple shear cyclic tests (Finn and Byrne, 1976).

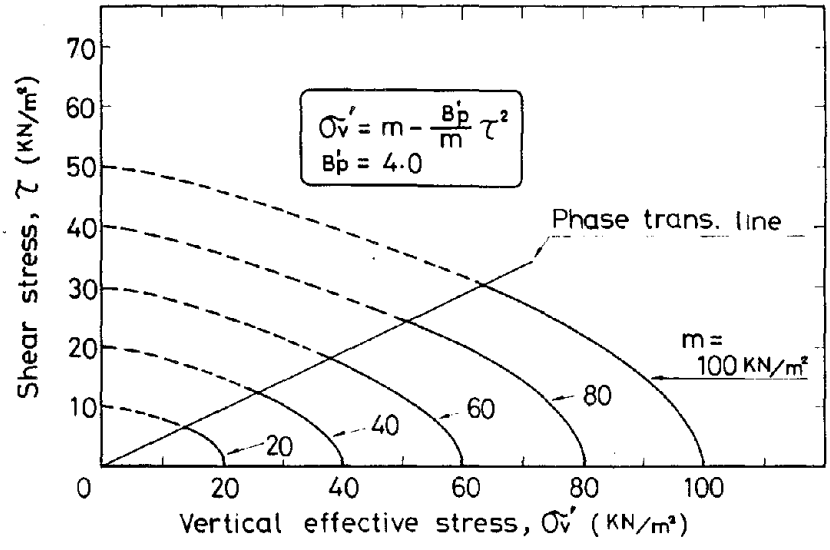

FIGURE 4-36 Parabolic stress paths during virgin loading. Source: Ishihara and Towhata (1980).

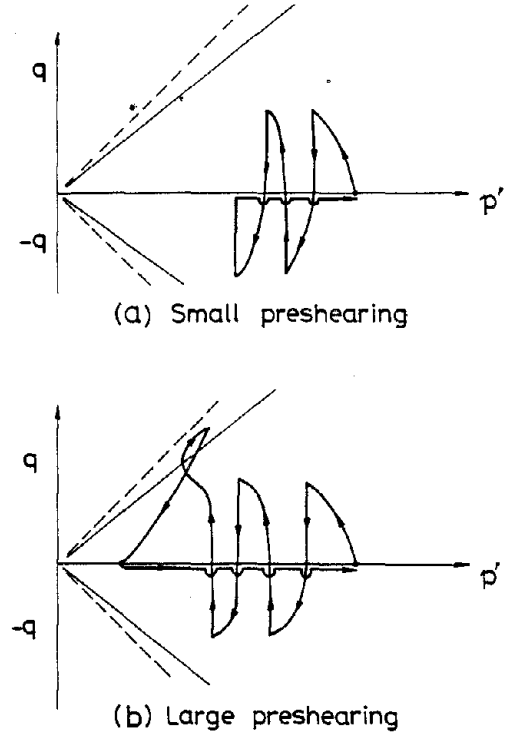

FIGURE 4-37 Rebound stress paths and small preshearing. Source: Ishihara and Towhata (1980).

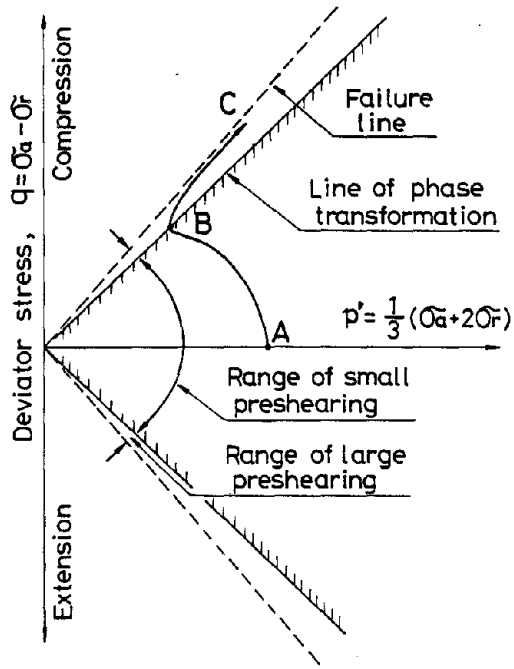

FIGURE 4-38 Phase transformation lines where rules for establishing stress paths change upon reaching these lines. Source: Ishihara and Towhata (1980).

This effect is incorporated into the Martin et al. (1975) model by adjusting the model parameters to match the liquefaction curves for various levels of static shear stress. These values are then used in the TARA program (described later). Stress path models can also be adapted for this purpose; it is necessary to develop a suitable set of rules that are not too complicated for practical work.

Multidimensional Straining

Few of the methods discussed above have dealt explicitly with the effect of multidimensional straining, an exception being that of Ghaboussi and Dikmen (1981).

Dynamic Analyses: Level Ground Case

These analyses use numerical methods for solving the dynamic equations of motion for a one-dimensional soil profile, employing various approximate representations for the nonlinear behavior. They are typically embodied within computer programs that handle variation of

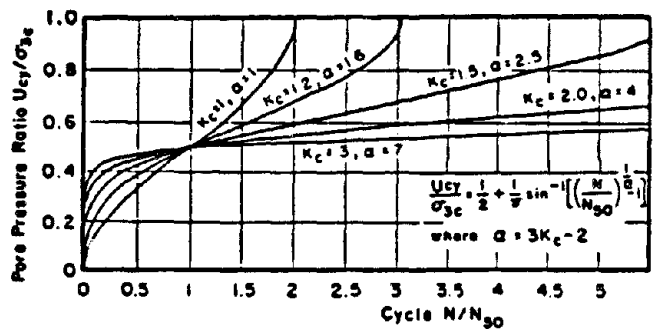

FIGURE 4-39 Normalized pore pressure curves for various values of K_c reflecting conditions where a sustained shear stress is present. Source: Finn (1981).

soil properties with position. The discussion first considers one of the more complete forms of analysis and then progressively simpler analyses. The final paragraphs survey a range of methods.

DESRA

This is a fully coupled program (Finn et al., 1977; Lee and Finn, 1975, 1978). The stress-strain behavior of soil is represented by a hyperbolic formulation that follows the Masing rules for unloading and reloading. The small strain term G_o in the hyperbolic equation is adjusted continuously for the current level of effective stress, assuming that $G_o = G_{oi}(\sigma'_o/\sigma'_{oi})^{1/2}$, where G_{oi} and σ'_{oi} are the values for G_o and σ'_o at the beginning of the analysis. The continuous soil profile is discretized using finite elements, and the solution of the equations is carried forward using a Newmark-type integration scheme. The analysis follows the details of each loading-unloading-reloading cycle, and irregular as well as regular motions may be used. A small amount of viscous damping (2 percent) is introduced to give stability to the computations.

There have been several versions of this analysis. In DESRA-1, pore pressure generation is computed using the densification model described previously. Actually, increments of pore pressure develop only during unloading from a peak in the strain-time history. DESRA-2 is similar, except that a transmitting boundary is included at the bottom of the soil profile so as to include radiation damping. Later, DESRA-2 was reprogrammed to use the endochronic model for pore pressure generation. Dissipation or redistribution of pore pressures simultaneously with generation can be included in the computation, if desired. Dissipation can be important in relatively free-draining material during prolonged shaking.

MASH-APOLLO

These are decoupled programs (Martin, 1975; Martin and Seed, 1979). MASH computes the dynamic response, while APOLLO computes pore pressure generation and dissipation.

The technique in MASH for solving the equations of dynamic equilibrium is similar to that used in DESRA. The program can accept as input a prescribed time variation for pore pressure, so that the small strain stiffness is varied as the computation progresses. Thus, it is possible to iterate back and forth between the MASH and APOLLO programs; that is, first MASH is used to predict time histories of dynamic stress at various points, then APOLLO is used to compute the corresponding time histories of pore pressure. Next, these computer pore pressures are entered into MASH and new time histories of dynamic stress are computed. Experience has shown, however, that usually only one iteration suffices, particularly if the stresses computed in the first run of MASH are reduced by a factor between 0.9 and 1.0 to compensate for the softening effect of induced pore pressures (Seed et al., 1976).

APOLLO generates pore pressures using an analytical expression fitted to data for $\Delta u/\sigma'_o$ versus N/N_l, as in Figure 4-29. This is done by converting short segments of the time history of stress into equivalent numbers of uniform cycles. The pore pressure buildup after each segment is determined successively. APOLLO is written to consider dissipation or redistribution of pore pressures simultaneously with ground motion shaking and the generation of pore pressure. Rules are suggested for choosing the parameters affecting dissipation, considering the effect of strains during an initial liquefaction ($\sigma' \simeq 0$) or a near-initial liquefaction condition.

SHAKE

The most widely used analysis has been a quasi-nonlinear (also called equivalent linear) total stress analysis, usually employing the computer program SHAKE (Schnabel et al., 1972). Nonlinear stress-strain behavior of soil is accounted for by adjusting modulus and damping, iteratively, until there is consistency between these parameters and the computed dynamic shear strains. Curves such as those in Figure 4-40 are used for this iterative procedure. The iterative adjustment is made at various depths within the profile.

This program provides a "total stress analysis"; that is, there is no provision for considering explicitly the softening effect of pore pressure buildup. It is an approximate method, using linear analysis, to account for the nonlinear behavior of soil. Fourier analysis techniques, with damping varying inversely with frequency to simulate the hysteretic behavior of soils, are used in the program. When originally written,

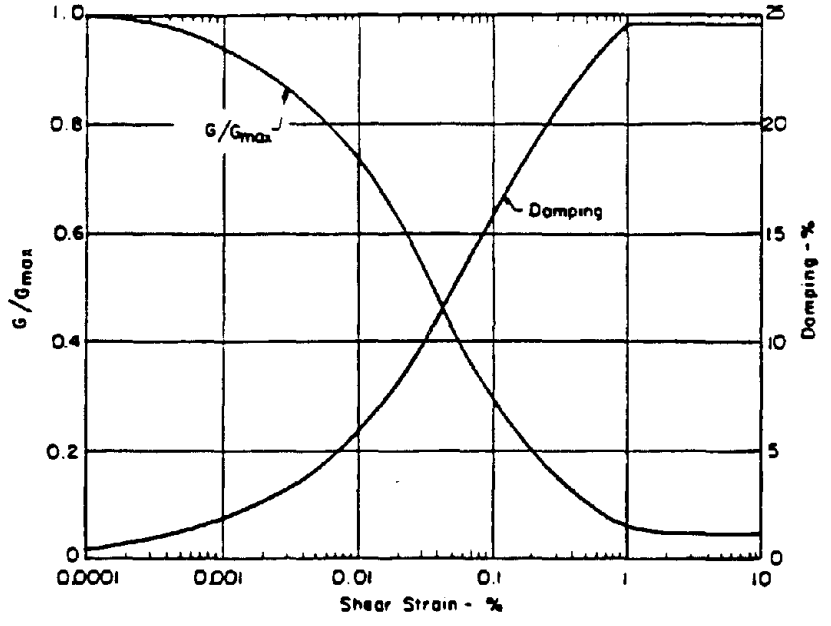

FIGURE 4-40 Relationships between shear modulus, damping, and shear strain typically used in the program SHAKE. Source: Makdisi and Seed (1978).

SHAKE provided an efficient and economical program for computing dynamic response. Today, however, it may be just as economical to use a nonlinear method.

Having evaluated the time history of stress at various points, corresponding pore pressures can be determined using the APOLLO program, or directly from relationships such as that in Figure 4-29.

Other Methods

CHARSOIL (Liou et al., 1977) uses the method of characteristics to solve the dynamic equations of motion. A Ramberg-Osgood model for nonlinear behavior is used, and the buildup of pore pressure is determined from an assumed relation between shear modulus and constrained modulus. Ghaboussi and Dikmen (1984) have presented an effective stress method, LASS-IV.

Comparisons Among Methods

Several studies (Finn et al., 1978b; Martin and Seed, 1979) have compared motions and pore pressures computed by the various methods. Differences in results arise because of variance in the assumed stress-strain behavior and in the model for pore pressure generation.

All the nonlinear models, when used in comparable total stress analyses, give similar results; MASH, DESRA, and LASS-IV give similar results in effective stress analyses. The principal differences between the programs relate to the properties required and the extent to which the necessary input parameters may be derived from conventional laboratory and site investigation data.

Finn and Martin (1979a,b) have investigated the validity of the equivalent linear method for determining the dynamic response of a nonlinear hysteretic soil by analyzing the response of level sites by SHAKE and the two nonlinear programs CHARSOIL and DESRA. The situation most suited to equivalent linear analysis is the response to steady-state sinusoidal motion. Maximum acceleration responses for a deep cohesionless site determined by SHAKE and DESRA are shown in Figure 4-41. The results are very similar except around a frequency of 1 Hz, where SHAKE shows a tendency toward resonant response.

The acceleration response spectra of ground motions at a sandy site 15 m deep (Figure 4-42) were computed by SHAKE, CHARSOIL, and DESRA and are shown in Figure 4-43. The spectra all show strong response around a period of 0.5 s, but SHAKE shows much stronger response than the nonlinear programs. This stronger response is also reflected in the magnitudes of computed dynamic shear stresses at various depths in the deposit (Figure 4-44).

This tendency toward resonant response in analyses based on the equivalent linear method has been noted in several comparative studies. Resonance occurs when the fundamental period of the input motion corresponds to the fundamental period of the site as defined by the final set of compatible properties in the iterative equivalent linear method of analysis. Since the analysis is carried out with this constant set of properties for the entire duration of the earthquake, there is time for resonant response to build up. In the nonlinear methods this tendency is controlled by the constantly changing stiffness properties. When strong resonant response is a function primarily of the method of analysis, it is called pseudo-resonance. Pseudo-resonance may lead to overestimates of dynamic response. This shortcoming can be compensated for by reducing slightly the shear stresses computed by SHAKE before using them to evaluate pore pressures.

The effect of pore water pressure may be seen from the plots of pseudo-acceleration spectra for 5 percent damping in Figure 4-45. The spectrum from a total stress analysis (by DESRA) shows a maximum at a period of about 0.35 s; the effect of increasing pore water pressure on the moduli is not included in this analysis. Increases in pore water pressure during seismic excitation lead to decreases in effective stresses and a softening of the moduli, which results in an increase in the

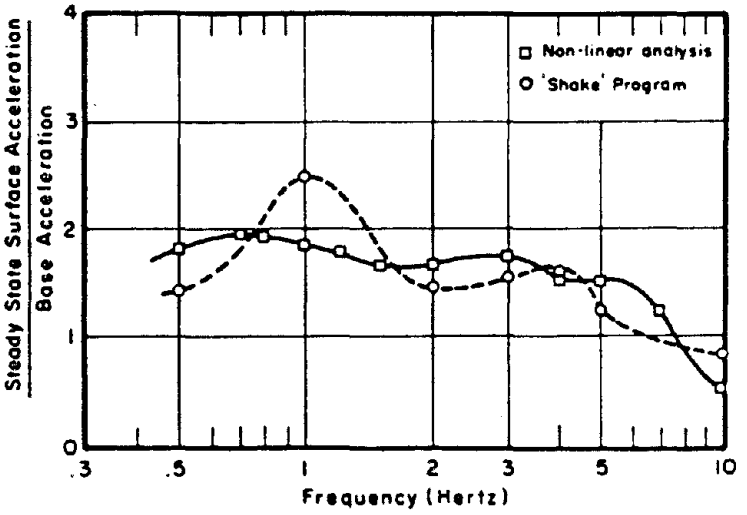

FIGURE 4-41 Comparison of acceleration responses for a deep sandy site using a nonlinear versus an equivalent linear analysis. Source: Finn et al. (1977).

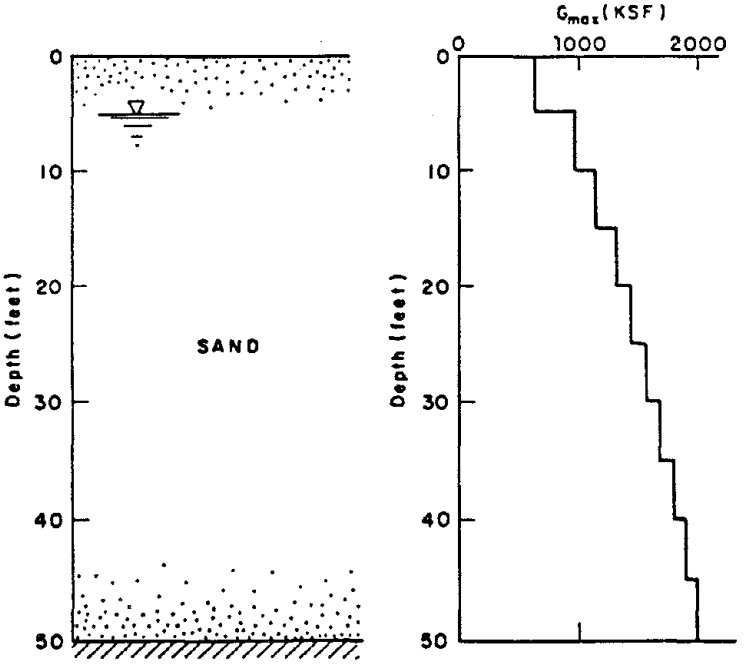

FIGURE 4-42 Soil profile used in comparative response analyses. Source: Finn et al. (1978).

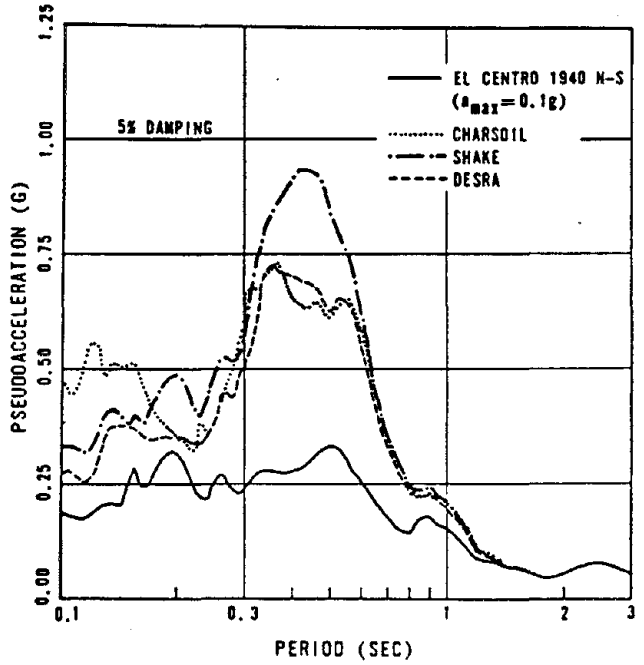

FIGURE 4-43 Comparison of acceleration response spectra computed by SHAKE, CHARSOIL, and DESRA—total stress analyses. Source: Finn et al. (1978).

fundamental period of the site to about 0.6 s. This shift in period is illustrated by the peaks in the spectra determined by nonlinear effective stress analysis, also using DESRA. The two effective stress spectra are for different assumptions about the dissipation of pore water pressure during excitation.

These effects of nonlinearity and pore water pressures have been confirmed using the one-dimensional nonlinear program MASH plus the program APOLLO for pore pressure generation (Martin and Seed, 1979). A comparison of shear stress distributions with depth for the site in Figure 4-42 computed by DESRA and MASH is shown in Figure 4-46.

Dynamic Analyses: Two-Dimensional Case

Methods for treating multidimensional cases are still in a relatively early stage of development and evaluation.

TARA

This is a fully coupled program (Finn et al., 1984; Siddharthan and Finn, 1982). Behavior in shear is treated exactly as in the level ground

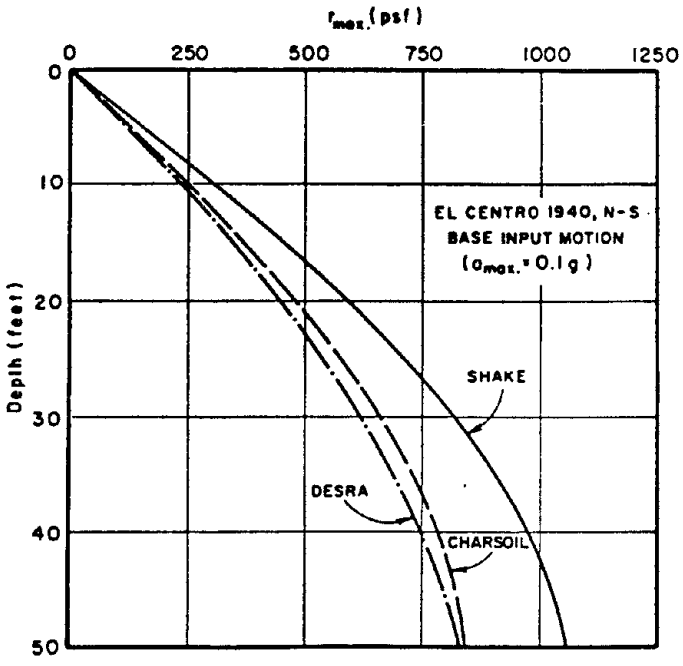

FIGURE 4-44 Comparison of maximum shear stress distributions computed by SHAKE, DESRA, and CHARSOIL—total stress analyses. Source: Finn et al. (1978).

case; that is, a nonlinear hyperbolic representation obeying the Masing criteria is used. The behavioral rule for response to changes in hydrostatic effective stress is nonlinear (i.e., stress dependent) but is essentially elastic compared to the behavior in shear. Pore pressures are determined by the volumetric strain model developed for the level ground case, extended to include the effects of an initial static shear stress. Two-dimensional space is discretized using finite elements, and solution proceeds by direct numerical integration. For analyzing problems involving contact between soil and rigid boundaries where high pore pressures may develop, provisions for slip elements have been incorporated into the program.

Quasi-Nonlinear Analyses

Seed et al. (1976) and Seed (1979a,b) have described the use of decoupled analyses, using equivalent linear techniques for the dynamic response analysis portion, to predict the buildup of excess pore pressures within earth dams. Shear stresses from the dynamic analyses are converted to equivalent numbers of cycles, and the generated

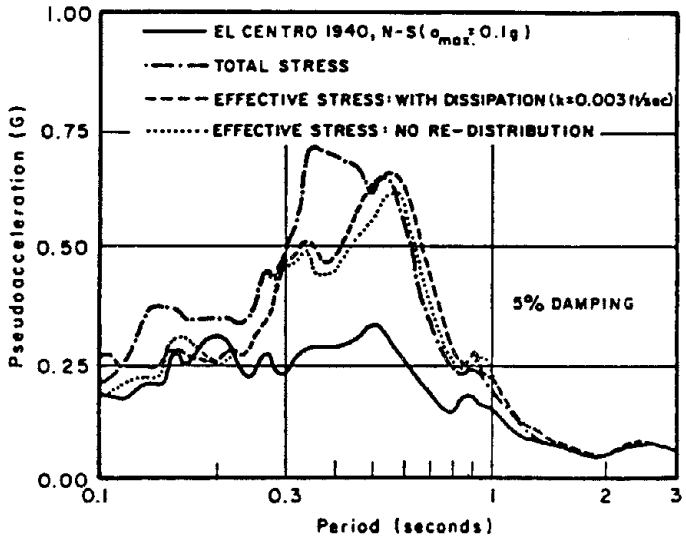

FIGURE 4-45 Comparison of acceleration response spectra computed using effective stress analyses versus total stress analyses. Source: Finn et al. (1978).

excess pore pressure is evaluated from curves for $\Delta u/\sigma'_o$ versus N/N_l, taking suitable account of the influence of initial shear stresses.

Actually, the analyses might be described as being partially coupled. After performing one dynamic analysis involving the entire cross-section (and this analysis itself might be run through several iterations to achieve compatibility of modulus, damping, and cyclic strain), the time at which one or more locations within the dam reaches the $\sigma' \simeq 0$ condition is identified. Then the dynamic analysis is restarted at this time, with zero stiffness now assigned to these locations. From this analysis the time that the next portions reach initial liquefaction ($\sigma' \simeq 0$) is found, and the analysis is restarted at this time with zero stiffness at these additional locations. This process is repeated until the end of shaking or until an instability occurs.

Dissipation of Excess Pore Pressures

The simultaneous generation of excess pore pressure from cyclic loading and its dissipation by the consolidation process present a difficult analytical problem. The governing equations are nonlinear because all of the parameters depend on the state of effective stress, often in complicated ways. It is also difficult to determine the correct values for the parameters.

One approach to this situation is to make the problem linear by assuming that stiffness and permeability are constant and specifying

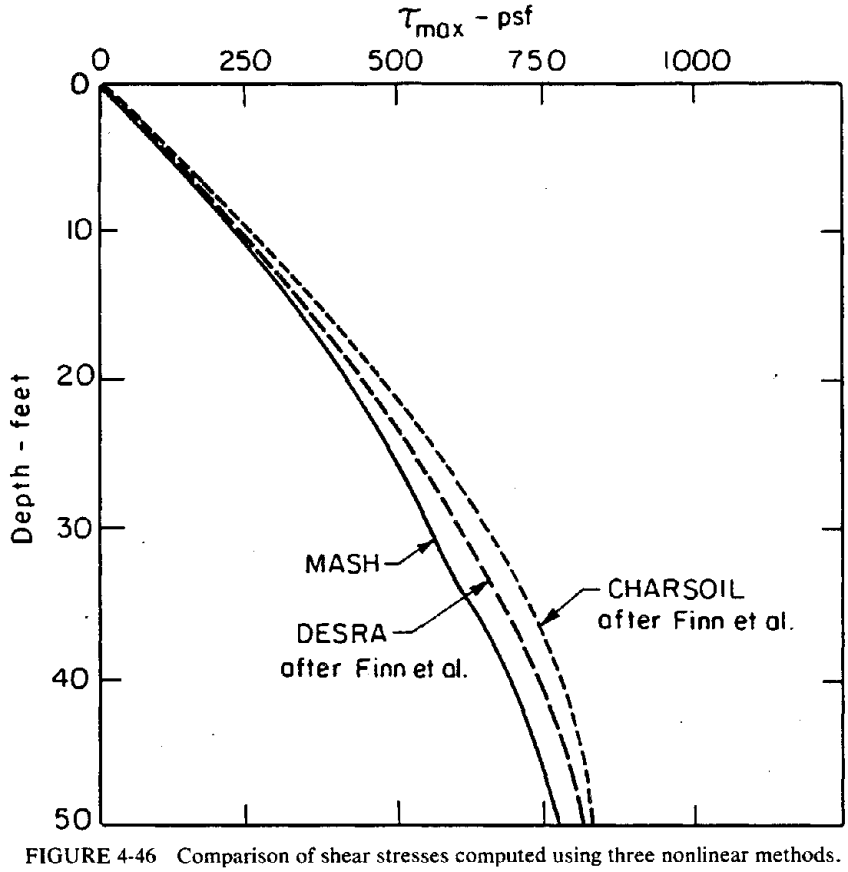

FIGURE 4-46 Comparison of shear stresses computed using three nonlinear methods. Source: Martin and Seed (1979).

the generation of excess pore pressure from the results of an earlier dynamic analysis. Such a linear, two-dimensional analysis of the generation and dissipation of excess pore pressures has been developed in the finite element program CLIP (Christian and Audibert, 1976). Its practical use requires that the values of the parameters be varied over a range of probable values to establish an expected range of results and their sensitivity to soil properties. Because of the difficulty of measuring linear or nonlinear properties (especially permeability), such a linearized parametric study can often provide results that are as useful for engineering purposes as those from more complex, nonlinear models. Marr and Christian (1981) describe one example of the use of the analysis for ocean wave loading. It is shown that very extensive redistribution of excess pore pressure can occur within a soil during the time of generation when the pressures are not generated uniformly.

Similar results have also been found in seismic problems involving coarse-grained soils.

The computer program GADFLEA is written to study the generation and dissipation of pore pressures in two dimensions (Booker et al., 1976). It is a finite element implementation of the general approach outlined above for the computer program APOLLO (Martin, 1975). The use of GADFLEA is suggested for use with nonlevel ground, to study the effects of drainage improvements, and in other situations. The computer programs APOLLO and GADFLEA have been modified to permit a fuller use of the analytically estimated site-specific earthquake response of soil deposits in studying pore pressure response in the deposit (Chugh and Von Thun, 1985a,b). The revised versions of these programs are named APOLLO-M1 and GADFLEA-M1. The changes, however, do not alter the basic formulation of the problem and the solution strategies implemented in the computer programs APOLLO and GADFLEA.

Visco-Elastic Analogy

This is a nonlinear coupled approach based upon an analogy between permanent strains developed during cyclic loading and creep under static loadings (Bouckovalas et al., 1984). It does not follow the strains during each cycle of loading, but rather uses the residual shear and volumetric strains caused by a cycle, or a packet of cycles, to characterize the stress-strain behavior. Empirical expressions, relating shear and volumetric strain to the amplitude and number of strain cycles, are used. The method has been developed for the case of cyclic loadings applied to a soil (e.g., by wave forces acting on a structure), but can be adapted to the situation of seismic loading.

Other Methods

Various other theoretical analyses have been developed and used to predict results for specific situations, but as yet these have had little impact upon practice in earthquake engineering.

Yoshimi and Tokimatsu (1978) conducted a two-dimensional analysis of the generation and dissipation of pore pressures in a level, saturated sand deposit (with or without a structure) during horizontal shaking.

A model based upon particulate mechanics and thermodynamics has been developed at the University of Massachusetts (Chang, 1981; Chang et al., 1983; Kuo, 1983) and applied to problems with undrained cyclic loading.

Several methods based upon plasticity theory have been proposed (Mroz et al., 1978; Prevost, 1978). These methods have the advantage of being very soundly based upon fundamental principles, but they become very complex when applied to cyclic loadings.

Final Comments

As noted at the outset of this subsection, the development of methods for analyzing the buildup of pore pressures in the two dimensional case is still in an early stage. For example, none of the methods described above really face the issue of the influence of rotation of principal stress directions, except as this effect happens to be approximated by the simple shear test.

Practical Analysis for Pore Pressure Buildup

The greatest difficulty with the methods described in the preceding subsections lies in the evaluation of the necessary parameters appropriate for a specific site.

Common to all methods is the determination of modulus and damping characteristics. The maximum (small strain) modulus is usually determined from in-situ shear wave velocity tests, or in some cases from tests in the laboratory on undisturbed samples or from correlations with relative density. For important projects the proper curves of G/G_{max} and the damping ratio are established using tests in the laboratory on undisturbed or reconstituted samples. For many projects, standard curves such as those shown in Figure 4-40 may be sufficiently accurate for G/G_{max} once a value of G_{max} is ascertained. Recent improvements in testing techniques have produced results indicating that the curves in Figure 4-40 are adequately representative for many soils, including clays, silts, sands, and gravels. These procedures are reasonably well established and reliable if carried out by competent investigators.

The major difficulty lies in the parameters relating to the rate of pore pressure generation. The earliest efforts to predict pore pressures used results from laboratory tests on specimens reconstituted to the in-situ void ratio or sometimes "undisturbed" samples. The practice of predicting pore pressures solely on the basis of laboratory tests, without the benefit of in-situ measurements such as SPT or shear wave velocity, is now recommended only if great precaution is taken to obtain samples with least disturbance. Such practice is particularly important for some types of soil for which there is as yet little or no experience. If circumstances allow, it is highly desirable to employ extraordinary measures such as ground freezing to obtain high-quality samples.

Indirect Use of Laboratory Pore Pressure Curves

An alternate approach is to use penetration resistance to determine N_l and then to enter curves such as those in Figure 4-29 to determine the pore pressure buildup during a particular earthquake. This approach

rests upon the assumption that the relationship between $\Delta u/\sigma'_o$ and N/N_l is affected little by disturbing or reconstituting the soil. Based upon Seed and Idriss (1982), the following steps are involved:

1. Determine the average cyclic stress ratio induced by the earthquake. Using charts such as Figures 4-3 or 4-7, together with a correction for magnitude (Table 4-2), find the magnitude of earthquake required to cause liquefaction.
2. By interpolation in Table 4-2, find the number of cycles corresponding to the liquefaction-causing magnitude. This is the number of cycles to liquefaction, N_l, for the induced stress ratio. (If the liquefaction-causing magnitude exceeds 8.5, use $N_l = 100$.)
3. Determine the number of effective stress cycles, N_e (at $0.65\tau_{max}$) induced by the earthquake. Various procedures for finding the effective number of cycles corresponding to an irregular earthquake ground motion have been proposed (e.g., Seed and Idriss, 1971). One method is simply to use Table 4-2 for the actual (design) earthquake.
4. Determine the cyclic ratio N_e/N_l, and read the induced pore pressure ratio from Figure 4-29 or from a similar curve obtained from cyclic tests on the sand of interest.

As an example, suppose that a magnitude 6 earthquake causes a cyclic stress ratio of 0.15 in a clean sand with a corrected penetration resistance of 13 blows/ft. For this sand the stress ratio just causing liquefaction is 0.20, so that the safety factor against liquefaction is 1.33. With the same induced stress ratio, a magnitude 7.5 earthquake with 15 equivalent cycles would be required to cause liquefaction. The actual earthquake has 5 to 6 cycles, so that $N_e/N_l = 0.37$. The pore pressure ratio is about 0.25 to 0.4. Thus, if the safety factor against liquefaction is satisfactory, the induced pore pressure will be relatively low.

Analysis Based upon Cyclic Strain

It has been noted that pore pressure buildup during undrained loading is more fundamentally related to cyclic strain than to cyclic stress. Accordingly, Dobry et al. (1982) have proposed a method based upon the following equation for computing the equivalent cyclic strain γ_c developed in the field by an earthquake:

$$\gamma_c = \alpha\left(\frac{a_p}{g}\right)\left\{\frac{\sigma_o r_d}{\rho V_s^2 (G/G_{max})_{\gamma_c, a^*}}\right\} \qquad \text{(Eq. 4-16)}$$

where a_p is the peak acceleration at ground surface, α is a factor ranging from 0.65 to 1.0 that accounts for the relative importance of other acceleration peaks, σ_o is the total vertical stress at the depth of

interest, r_d is the stress reduction factor discussed in connection with Eq. 4-1, and ρ and V_s are the mass density and shear wave velocity at the depth of interest. The modulus reduction factor (G/G_{max}) is a function of the cyclic strain and of the pore pressure buildup ratio $u^* = \Delta u/\sigma'_o$. This equation is a slightly modified form of Eq. 4-3. Use of this equation involves the following steps:

1. Choose suitable values for α, σ_o, r_d, and ρ, all of which can be evaluated with reasonable accuracy.
2. Measure V_s in situ. As discussed earlier, this wave velocity can be evaluated satisfactorily and reliably within ± 10 percent with good field techniques.
3. The modulus reduction factor G/G_{max}, which according to the authors has been found to be relatively insensitive to sample disturbance, may be evaluated using tests on reconstituted or "undisturbed" samples.
4. The equivalent number of strain cycles N is estimated using procedures similar to those used to compute an equivalent number of cycles of stress.
5. Having established N and γ_c, the pore pressure buildup ratio, which for a given cyclic strain is also relatively insensitive to soil fabric and sample disturbance (see Figure 4-31), is determined from charts such as Figure 4-32 or from strain-controlled tests on reconstituted or "undisturbed samples."

The main advantage claimed for this procedure is that the key parameter, V_s, can be measured in situ and is thus unaffected by sample disturbance, while the other essential data (for steps 3 and 5) are not very sensitive to the method for obtaining or preparing test specimens. Further study and research is needed concerning various aspects of the method. It still is not clear how the effect of pore pressure buildup upon the ratio G/G_{max} is best evaluated. From experience with evaluating the cyclic strain for ground response studies using equivalent linear modulus, it is known that the computed strain is rather sensitive to the curve of G/G_{max} that is used.

Use of DESRA and TARA

Moduli and strength parameters required as input for DESRA and TARA are obtained by conventional procedures. Parameters for the pore pressure model, if necessary for effective stress analysis, may be measured directly using good undisturbed samples or deduced from estimates of liquefaction resistance derived from index tests, such as the correlation between SPT or CPT and liquefaction resistance. The latter procedure is almost always followed in practice.

Use of Effective Stress Analysis for Analyzing Stability

As noted at the outset of this section, a primary purpose of predicting pore pressure buildup is to permit an assessment of stability in terms of effective stress. It is certainly a fundamental principle of soil mechanics that shear strength is controlled by effective stress. At the same time, there is also a fundamental problem in using an effective stress stability analysis to provide a numerical safety factor against a stability failure.

Consider the hypothetical slope and potential failure surface that have been sketched in Figure 4-47. Normal and shear stresses and pore pressures are distributed all along the failure surface, and all contribute to the stability of the overlying mass of soil. However, the average or typical condition may be represented by a single point A on a τ-σ' ($\sigma' = \bar{\sigma}$) diagram (Figure 4-48). This point might, for example, represent the conditions at the end of shaking in a slope that was undrained during the shaking. The conventional definition of safety factor would be obtained using the strength at point B. That is $FS = \tau_B/\tau_A$, where τ_B is the shear strength at the given effective stress.

To decide whether or not this definition of safety factor makes sense, it is necessary to envision just how and why there might be a failure even though the calculated τ_A-σ'_A point lies well below the presumed effective stress strength line. One possibility is that an error has been made in the evaluation of the strength, and that the actual strength is less (Figure 4-49). The conventional definition of safety factor does provide a sound indication of the margin of safety against a failure resulting from such an error. However, the location of the effective stress strength line is generally what is best known about the situation.

Another possibility is that the shear stress τ_A that must be sustained after shaking has been calculated incorrectly. The conventional definition of safety factor also gives a meaningful indication of the margin of safety against a failure caused by this error. But again the value of τ_A does not involve major uncertainty.

There is more uncertainty about the pore pressure induced by the earthquake, and hence about the average effective stress σ'_A. In this connection, it must be kept in mind that the average effective stress along the failure surface can decrease after the end of shaking, owing to spreading of pore pressure. It might make sense to define $FS = \sigma'_A/\sigma'_C$ (Figure 4-50), where σ'_C is the effective stress on the strength line corresponding to τ_A. However, few if any engineers will have much feeling for the significance of a safety factor defined in this way. Since most soils for which liquefaction is a problem have a strength line with little if any cohesion intercept, the safety factor defined in this way is essentially equal to the conventional definition of safety factor, that is: $\tau_B/\tau_A \simeq \sigma'_A/\sigma'_C$.

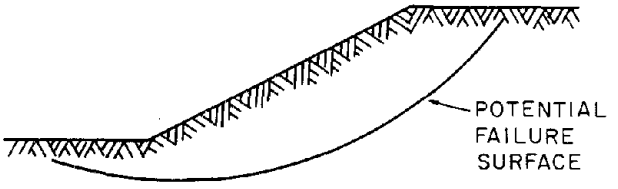

FIGURE 4-47 Hypothetical slope and potential failure surface.

Some engineers (e.g., Castro et al., 1982) argue that the safety factor should be defined in terms of the strength that can be mobilized if the soil is sheared undrained by monotonic loading starting from point A; that is, $FS = S_{uA}/\tau_A$ (Figure 4-51). Now the computed safety factor will depend greatly upon the undrained strength behavior of the soil. If the soil behaves as in Figure 2-38, the safety factor might be quite small, whereas if it behaved as in Figure 2-37 the safety factor could be quite large. Thus, from this viewpoint the margin of safety is closely related to the dilative versus contractive behavior of the soil.

The last-stated viewpoint, which in effect implies a total stress analysis, has considerable merit. However, there are also difficulties with this viewpoint. First, the need for great care in the evaluation of S_{uA} has already been discussed. Second and possibly more serious, part of the soil may increase in volume after the end of shaking in such a way that its shear resistance decreases.

This discussion does not mean that there is no value to an effective stress stability analysis, but rather that the result of it must be interpreted with care. One possible approach is to compute both $FS = \tau_B/\tau_A$ and $FS = S_{uA}/\tau_A$ and to focus attention on whichever is smaller. Use of $FS = \tau_B/\tau_A$ is a very approximate means (and perhaps a conservative one) for considering possible dilation of highly stressed zones within the soil. Its use also reflects the observations that strains begin to become large once an effective stress path reaches the strength line, even though there may still be a reserve of undrained strength.

Comparisons with Field Observations and Model Tests

Owi Island

The acceleration and pore pressure responses of Owi Island No. 1 to the Mid-Chiba earthquake (Figure 2-17) were investigated by dynamic effective stress analysis using the computer program DESRA-2 (Finn et al., 1982). The required input for the program consists of stress-strain properties, shear strengths on horizontal planes, and values of the parameters for the pore water generation and dissipation model. This input was developed using methods already described. Shear

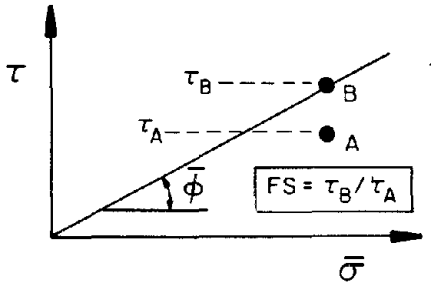

FIGURE 4-48 Conventional factor of safety.

wave velocities were estimated from the SPT values. Resistance of sands to liquefaction was evaluated using undrained cyclic triaxial tests performed on specimens from samples recovered using a large-diameter sampler. Parameters for the pore pressure model were selected to be consistent with results from those tests. Motions at the base of the fill were not recorded. However, because the acceleration levels were modest and the pore water pressures were low enough not to affect soil properties to a significant extent, it was relatively easy to develop an input base motion consistent with the surface acceleration.

The first 10 s of the recorded ground accelerations in the north-south direction are shown in Figure 4-52a. During the first 4 s, very low accelerations occurred. Significant accelerations developed between 4 and 6 s and, thereafter, only low-level excitation was recorded. The ground motions computed using DESRA-2 are shown in Figure 4-52b. Except for some minor differences in frequency and magnitude in the 8- to 10-s range, the computed record is very similar to the recorded motions.

The measured pore pressures are shown in Figures 4-53 and 4-54. In general, the agreement is excellent. DESRA-2 computes only

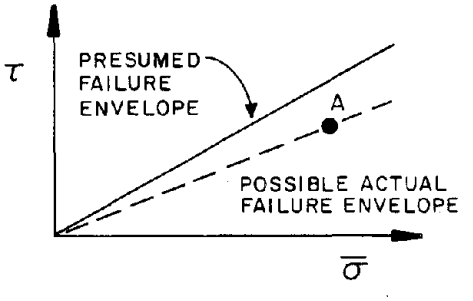

FIGURE 4-49 Rationale for definition of conventional factor of safety.

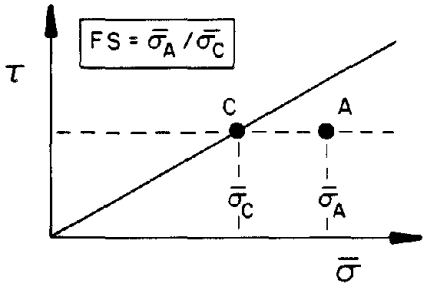

FIGURE 4-50 Factor of safety related to uncertainty in pore pressure (and hence in mean effective confining stress) with constant mean shear stress.

residual pore water pressures, so there are no fluctuations from changes in instantaneous total stress levels corresponding to ground accelerations, as actually occurred in the ground.

The pore pressure measurements at Owi Island also confirmed the concept of threshold acceleration, based on the existence of a threshold strain γ_t for sands in the laboratory. At Owi Island, no excess pore pressures developed in either sand layer between the triggering time and 4.2 s, with the exception of elastic fluctuations probably caused by initial, vertically propagating P-waves. At 4.2 s a large acceleration pulse occurred, and the pore pressures increased simultaneously at both depths. Ishihara conducted a very careful determination of the acceleration value at 4.2 s and concluded that the surface acceleration was 0.06 g when the pore-pressures began to increase. This indicates that, for this site and layers, the threshold acceleration, a_t, was 0.06 g. Two hours after the earthquake, and after the excess pore pressures had completely dissipated in the two layers, an aftershock occurred

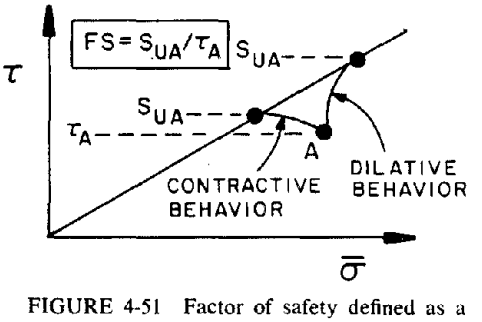

FIGURE 4-51 Factor of safety defined as a ratio of undrained strength to imposed shear stress.

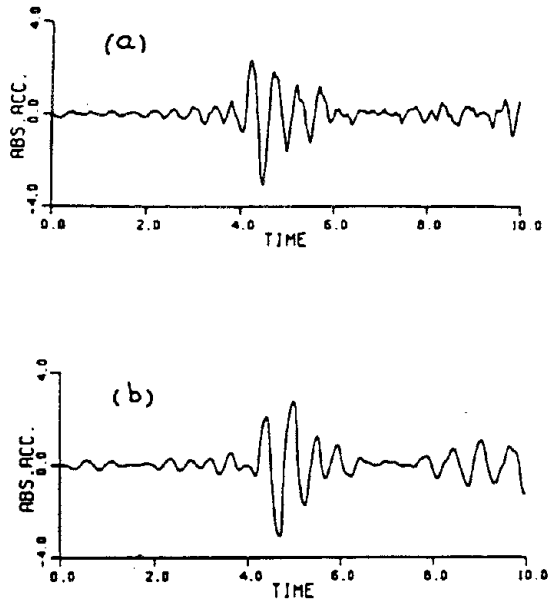

FIGURE 4-52 Comparison of measured ground acceleration at Owi Island during the 1980 Mid-Chiba earthquake with accelerations computed using DESRA-2 (acceleration in ft/s², time in seconds): (a) measured acceleration: (b) computed acceleration. Source: Finn et al. (1982).

with a measured a_p equal to 0.04 g. This aftershock did not induce any excess pore pressures in the sand layers, thus confirming the existence of a threshold acceleration with a value greater than 0.04 g.

The measured a_t at Owi Island agrees well with the predicted value for the two sand layers, based on γ_t determinations in the laboratory and in-situ V_s measurements (Dobry et al., 1981a). This $a_t \simeq 0.06$ g is also consistent with the range of a_t for recently deposited sands, as obtained from the charts in Figures 4-17 and 4-18. Further confirmation of these predicted values of a_t has been obtained from centrifuge tests, as illustrated by Figure 4-55, published by Arulanandan et al. (1983). This result shows no pore pressure buildup if $a_p < a_t \simeq 0.05$ g, even if a large number of shaking cycles (a long earthquake duration) are applied to the sand.

Shaking Table Tests

Yoshimi and Tokimatsu (1978) conducted a two-dimensional analysis of the generation and dissipation of pore pressures in a level, saturated sand deposit (with or without a structure) during horizontal shaking.

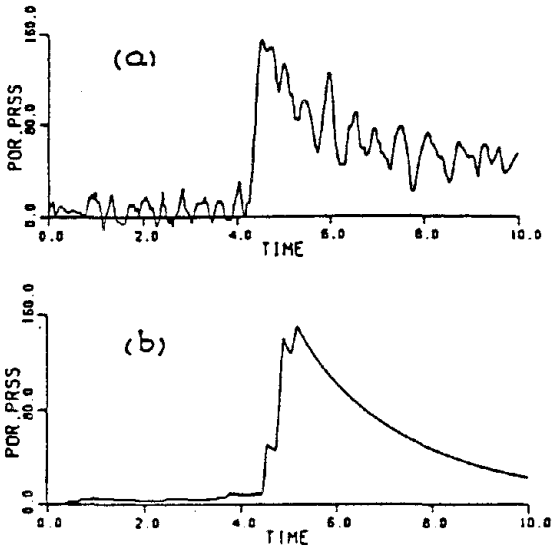

FIGURE 4-53 Comparison of measured pore water pressures at a depth of 6 m at Owi Island during the 1980 Mid-Chiba earthquake with pore pressures computed using DESRA-2 (pore pressures in lb/ft², time in seconds): (a) measured pore pressures; (b) computed pore pressures. Source: Finn et al. (1982).

The computed pore pressure time histories agreed reasonably well with the results of shaking table tests under normal gravity conditions, using an aqueous solution of glycerin in place of pore water.

Other liquefaction tests have been performed on the large shaking tables at the Public Works Research Institute in Tsukuba, Japan, but there have been only limited attempts to generalize the results.

Centrifuge Tests

Several comparisons have been made between pore pressures measured in sand confined within stacked rings (Figure 2-45) and shaken in centrifuge tests with those predicted using MASH-APOLLO and MASH-GADFLEA (Heidari and James, 1982; Whitman et al., 1982; Arulanandan et al., 1983). These studies have focused on the dissipation of excess pore pressures following shaking and have emphasized the very nonlinear nature of this process.

Finn et al. (1984) have compared predictions made using TARA-2 with results from the test shown in Figure 2-50 (see page 66) and with other centrifuge model tests conducted at Cambridge University. Analyses were conducted with and without slip elements between the

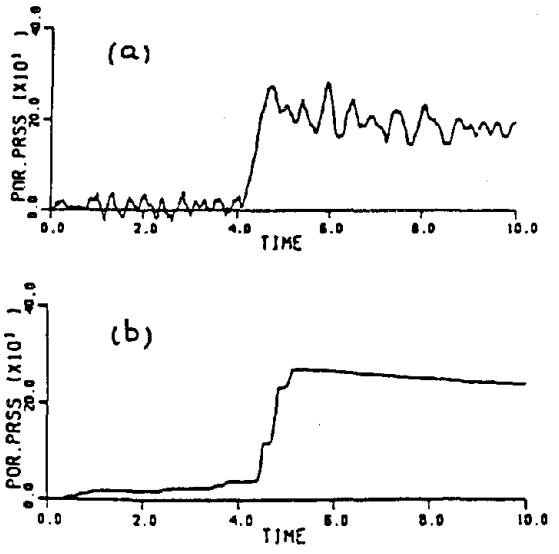

FIGURE 4-54 Comparison of measured pore water pressures at a depth of 14 m at Owi Island during the 1980 Mid-Chiba earthquake with pore pressures computed using DESRA-2 (pore pressures in lb/ft², time in seconds): (a) measured pore pressures; (b) computed pore pressures. Source: Finn et al. (1982).

surface of the "structure" and the embankment to determine the effect upon seismic response of relative motions across this interface.

Figure 4-56 compares measured and computed accelerations at location B, at mid-depth in the soil, in test 1. In this test the shaking was weak enough so that liquefaction did not develop. The agreement between measured and predicted motions is good, and slip at the interface had no influence upon pore pressures at this location.

Pore pressures measured in test 2 at location B are shown in Figure 4-57. This location is far enough from the structure to suggest that its response may not be greatly affected by slip between structure and plate. This is confirmed by dynamic analysis showing similar computed pore pressures whether slip elements were used or not. The computed pressures compare very well with those recorded.

Figure 4-58 shows pore pressures at location Y, at the top of the bank under the structure. At this location the effects of any decoupling between the motions of the structure and the bank would be greatest. This is clearly shown by the results of dynamic analysis. Analysis including slip elements predicts pore water pressures very close to those recorded. If slip is not allowed during analysis, only very low residual pore pressures are predicted.

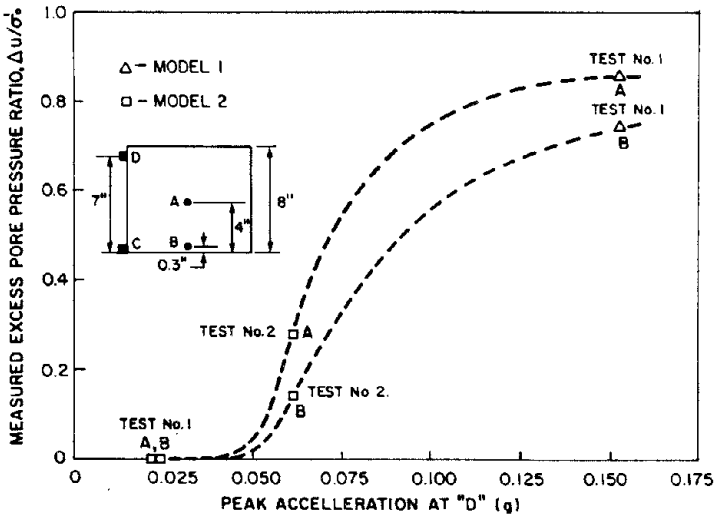

FIGURE 4-55 Relationship between measured excess pore pressure and peak acceleration at the top (point D) of a soil column shaken in a centrifuge. Data shown are for tests without prior straining due to previous shakings. Source: Arulanadan et al. (1983).

A complex part of the analysis is the proper transmission of accelerations from the embankment to the surface structure across the slip elements. In particular, the model should be capable of reproducing the rapid decay in acceleration after 4 s of shaking because of the loss in shearing resistance caused by very high pore pressures. The recorded and computed accelerations at point A on top of the plate (structure) are shown in Figure 4-59. The decay in acceleration after 4 s is modeled satisfactorily, but three peaks in the actual record are somewhat higher than those predicted. This may have been caused by partial embedment of the plate during shaking.

Blast-Induced Pore Pressure

While this section has dealt exclusively with pore pressures caused by earthquake ground motions, it should be mentioned that some study has also been made of pore pressures caused by explosionlike loadings. For example, two-phase, one-dimensional, dynamic finite element analyses based on laboratory-derived material properties have been conducted (Kim and Blouin, 1984). The results of these analyses (Figure 4-60) show a liquefaction "wave" following immediately behind the stress wave.

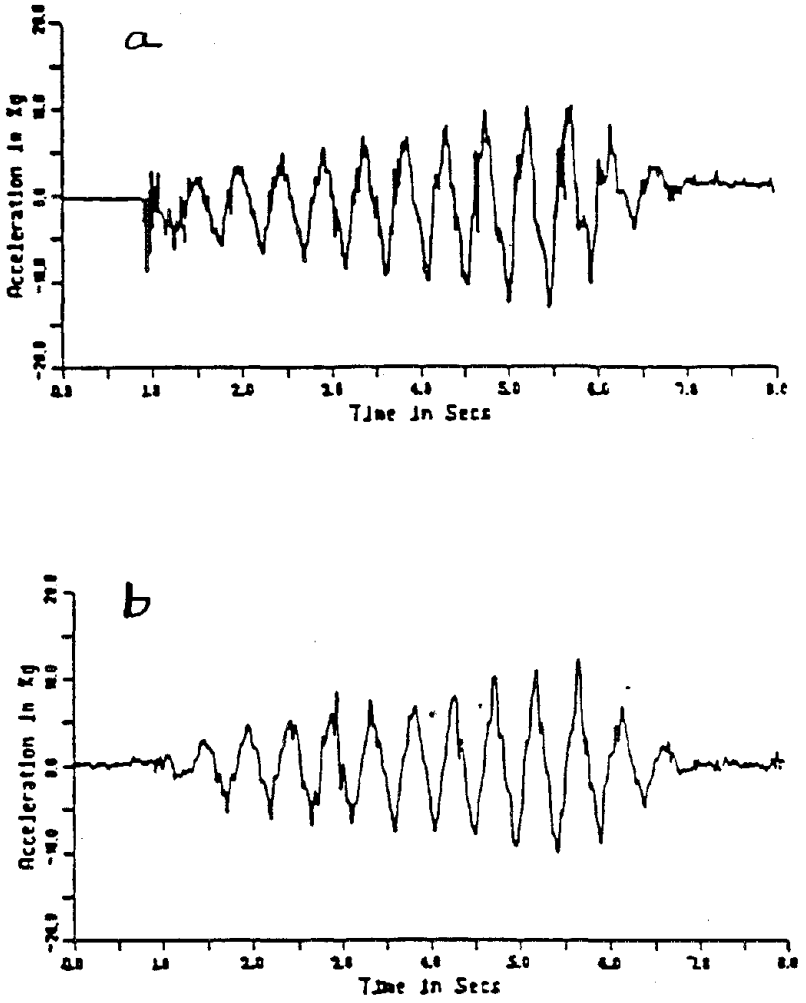

FIGURE 4-56 Comparison of accelerations recorded at point B (during test 1) for the centrifuge model shown in Figure 2-50 with those computed using TARA-2: (a) measured acceleration; (b) computed acceleration. The computations were made with and without incorporating slip elements. In this case, since the shaking was relatively weak, the use of slip elements produced no significant difference in the results. Source: Finn et al. (1984).

Deformations

Liquefaction-caused failure is really the result of excessive deformation. Transient (cyclic) displacements may cause a failure. This is

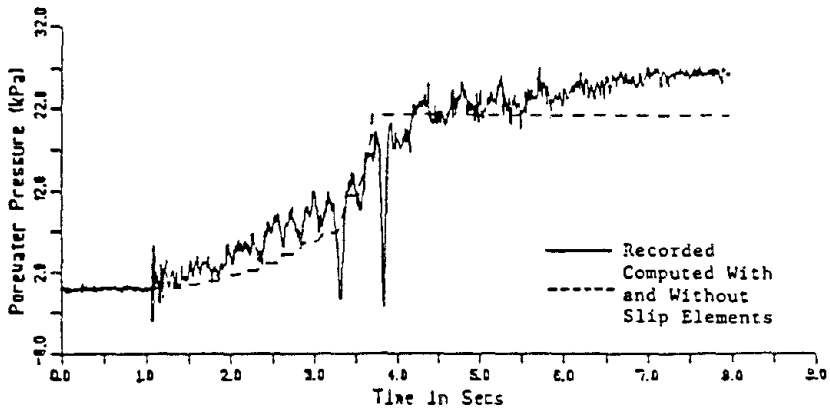

FIGURE 4-57 Comparison of pore pressures recorded at point B (during test 2) for the centrifuge model shown in Figure 2-50 with those computed using TARA-2. The use of slip elements did not affect the results. Source: Finn et al. (1984).

especially true in the case of offshore structures subject to wave loadings, where excessive transient movements of the platform relative to the seabed might cause conductor pipes to fail. However, with wave loading problems as well as with earthquake problems, failure generally takes the form of excessive permanent displacement, such as settlement or tilting of structures, excessive slumping or distortion, and (in the extreme) sliding of slopes.

The science of predicting deformations, especially permanent displacements, is still in its early years. The following discussion will draw upon developmental work done for offshore structures (generally for clayey soils) as well as that accomplished in earthquake engineering.

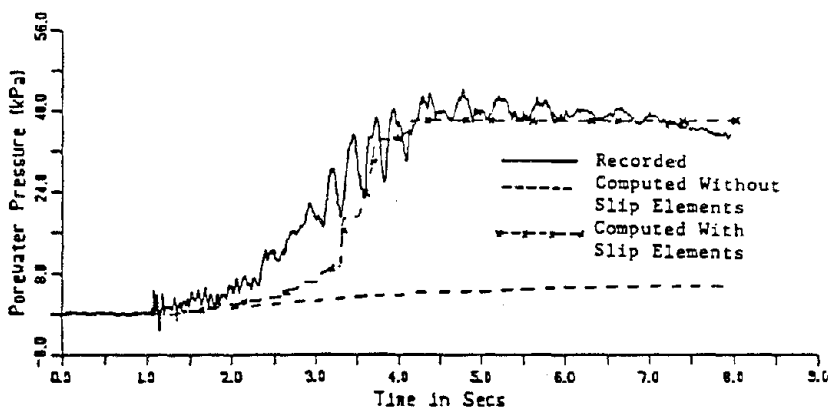

FIGURE 4-58 Comparison of pore pressures recorded at point Y (during test 2) for the centrifuge model shown in Figure 2-50 with those computed using TARA-2. Source: Finn et al. (1984).

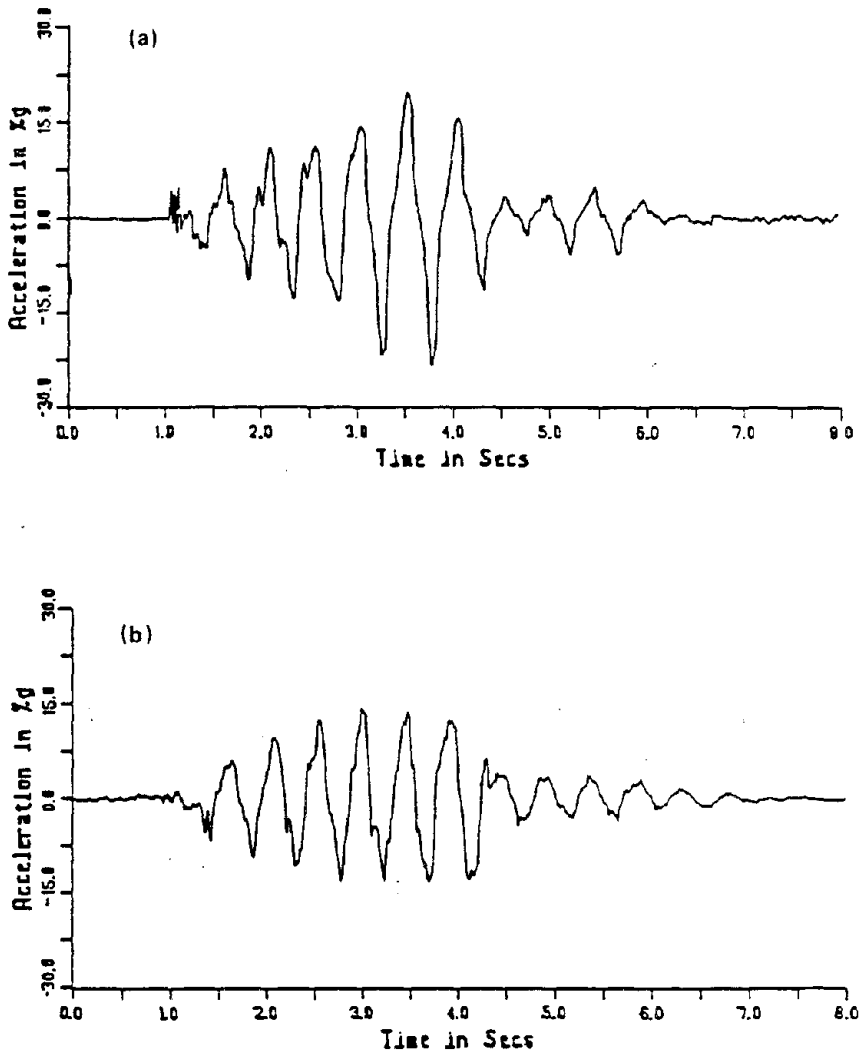

FIGURE 4-59 Comparison of accelerations recorded at point A (during test 2) for the centrifuge model shown in Figure 2-50 with those computed using TARA-2: (a) measured acceleration; (b) computed acceleration. Source: Finn et al. (1984).

Cyclic Deformations

Evaluation of cyclic displacements (or at least cyclic strains) is a key step for some of the methods discussed in this chapter for predicting the buildup of pore pressures. Such strains may be evaluated from a dynamic analysis using quasi-nonlinear (SHAKE) or nonlinear tech-

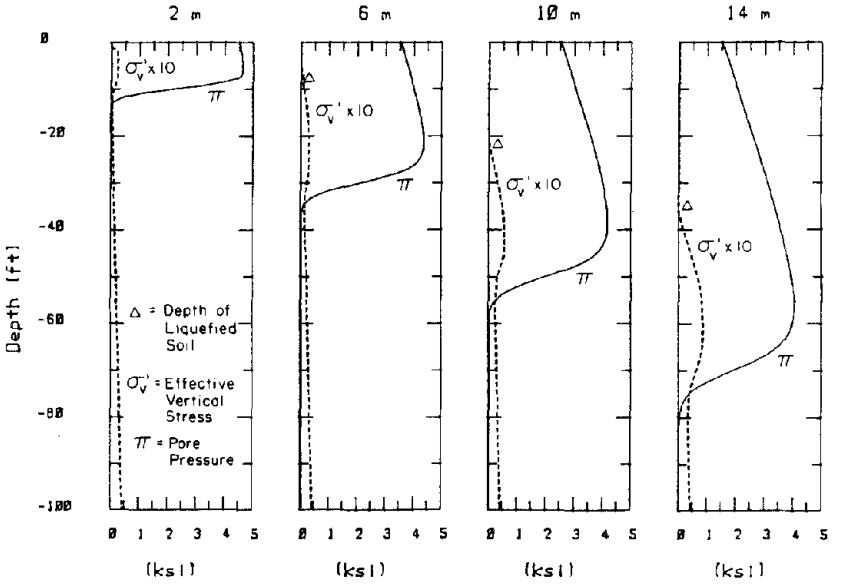

FIGURE 4-60 Predicted pore water pressures and effective stresses following a 5-ksi triangular loading of a saturated calcareous sand. Source: Kim and Blouin (1984).

niques (e.g., DESRA). Eq. 4-16, proposed by Dobry et al. (1982), provides an approximate method for computing cyclic strains.

Several empirical approaches have been developed in offshore engineering work. Based upon cyclic triaxial tests made on several sands, Marr et al. (1982) have proposed use of an equation of the form:

$$\gamma_c = C_1 + C_2(\Delta q/\bar{p}_o) + C_3\bar{p}_o \qquad \text{(Eq. 4-17)}$$

where Δq is the cyclic deviator stress, $\bar{p}_o$ is the average of the major and minor principal effective stresses, and C_1, C_2, and C_3 are constants to be evaluated from cyclic triaxial tests. Bouckovalas et al. (1984) compute cyclic strain using a hyperbolic equation, with some rather complex and ambiguous rules for choosing the ultimate strength required by this formulation. Data from simple shear tests upon clays have been obtained by Andersen et al. (1980) and by Goulois et al. (1985). Figure 4-61 shows contours of cyclic strain from tests having zero sustained stress, with the cyclic stress normalized by the conventional undrained strength during monotonic loading, plotted against the number of cycles. The degradation of stiffness with number of cycles is thought to be associated with the buildup of pore pressures. Figure 4-62 indicates the influence of a sustained (static) stress when cyclic stresses are superimposed. As a point of reference, Andersen

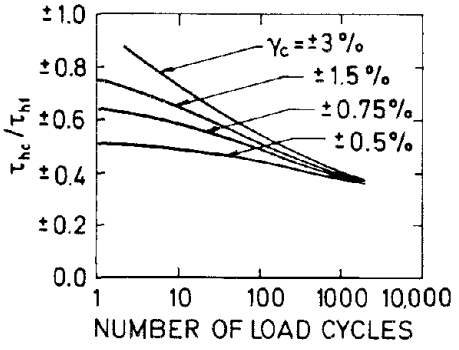

FIGURE 4-61 Contours of cyclic strain (γ_c) as a function of cyclic stress (τ_{hc}), normalized by the undrained strength during monotonic loading (τ_{hf}), and a number of cycles of loading, from simple shear tests on Drammen clay. Source: Andersen (1976).

(1976) has used a cyclic strain of 3 percent as an indication of failure in foundations for offshore structures.

There is indication that the $\sigma' \simeq 0$ condition may be associated with the onset of cyclic strains large enough to be considered excessive. Figure 4-63 shows curves for cyclic stress versus cyclic strain (single amplitude) from stress-controlled torsional tests upon a sand at various densities. The shaded area along each curve indicates the range of strains at which the $\sigma' \simeq 0$ condition is reached. This range, centered on 3 percent cyclic strain, is roughly the same for all densities. Thus, the $\sigma' \simeq 0$ condition may actually correspond to a failure situation.

Permanent Deformations

Sliding Block Analysis

A procedure for computing permanent ground displacements in the form of translatory landslides is based on Newmark's (1965) approach as augmented by Goodman and Seed (1966) and by Makdisi and Seed (1978). The procedure is summarized in Figures 4-64, 4-65, and 4-66.

In Figure 4-64, the soil blocks shown are assumed to be rigid. When the ground is accelerating in the direction away from the bluff, the soil block is free to move in the direction of the bluff as long as the active soil force plus the inertia force on the soil block is greater than the resisting force at the bottom of the soil block. However, when the direction of acceleration is toward the bluff, the soil block cannot move significantly because the passive soil pressure induced by the graben can be quite large.

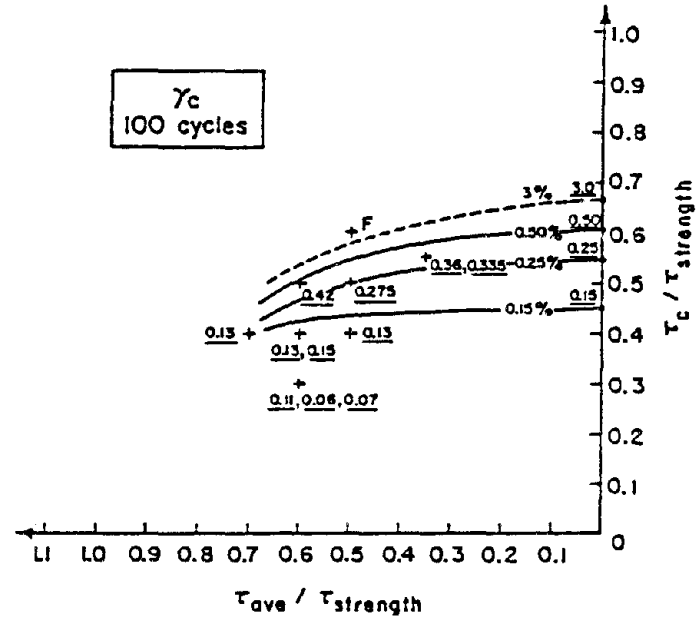

FIGURE 4-62 Contours of cyclic shear strain as a function of cyclic (τ_c) and sustained (τ_{ave}) shear stresses after 100 cycles of stressing from simple shear tests on Drammen clay. Both τ_c and τ_{ave} have been normalized by the undrained strength ($\tau_{strength}$) for monotonic loading. The symbol F denotes very large cyclic or permanent strains. Source: Goulois et al. (1985).

The maximum potential inertia force on the soil block is calculated by multiplying the total weight of the soil block by the maximum seismic coefficient. The maximum potential seismic coefficient, k_{max}, is the product of a free-field peak ground surface acceleration and a constant. The constant can include effects of the height of the soil block, bluff topography, the length of the soil block, and possibly other factors.

The resisting force available from the shear strength acting at the bottom of the soil block is computed by multiplying the length of the soil block by the average undrained shear strength of the soils involved. The average undrained shear strength of the soil depends on the level and length of shaking and the amount of displacement the soil block has undergone.

The yield seismic coefficient, k_y, is that seismic coefficient which, when multiplied by the total weight of the block, gives a large enough inertial force to make the total driving force equal to the total resisting

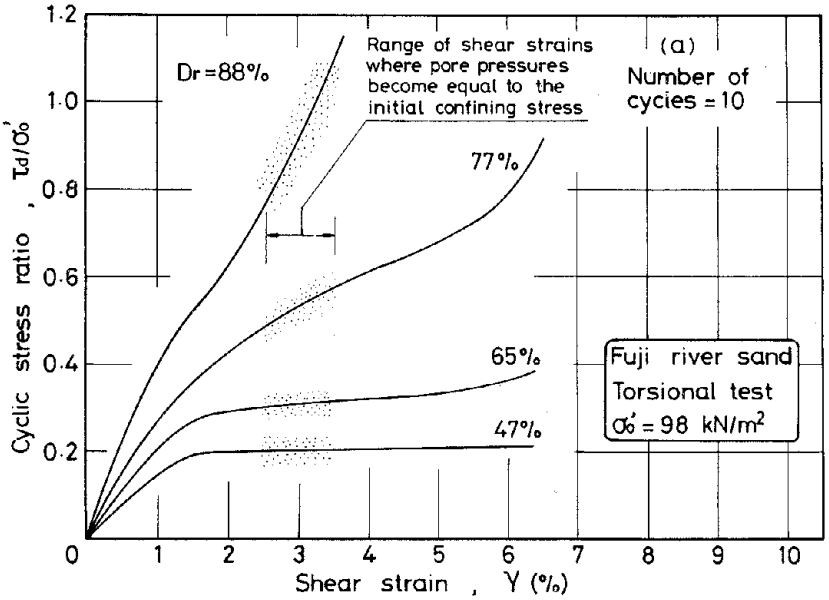

FIGURE 4-63 Relation of cyclic stress ratio to cyclic shear strain (single amplitude) from torsional tests on Fuji River sand. Source: Ishihara (1985).

force. This coefficient is calculated by the equation given in Figure 4-64.

Once the yield seismic coefficient and the maximum potential seismic coefficient k_{max} are known, the displacement of the soil block can be calculated. The basic process is shown schematically in Figure 4-65. Every time the soil block is shaken beyond the yield point (e.g., between t_1 and t_2) as represented by the yield seismic coefficient, relative velocity between the soil block and the underlying earth is initiated (time increment t_1 to t_3). By integrating this relative velocity, relative displacement is accumulated (from t_1 to t_3) in the direction of the bluff.

Based on the type of displacement calculation just described, Makdisi and Seed (1978) summarized graphically the expected displacement versus k_y/k_{max} for earthquakes of various magnitude, as shown in Figure 4-66. Similar plots have been prepared by Franklin and Chang (1977), Sarma (1979), and Whitman and Liao (1985). A basic assumption of all these studies is that k_y does not decrease with straining. If strength decreases only slightly with straining and if the strength versus strain relation is known, then the procedure can still be employed. If the strength decrease is more significant, the predicted movements

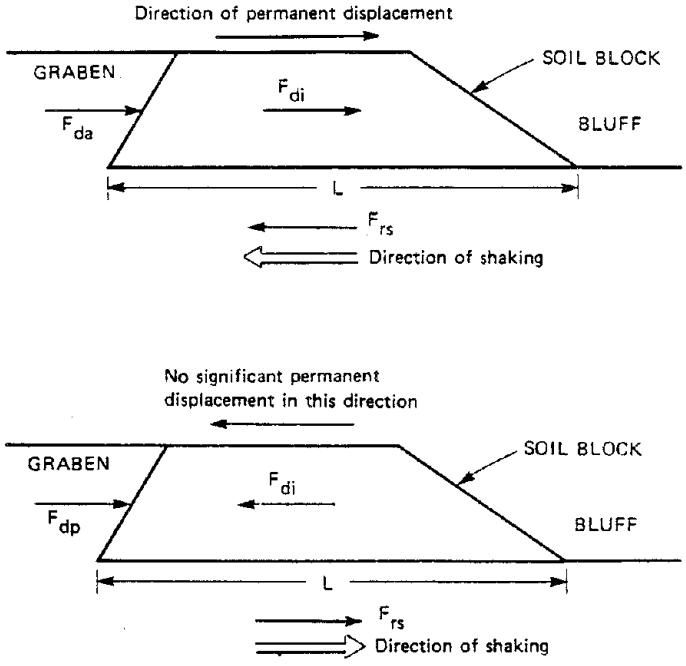

F_{da} = Driving force due to active soil pressure

F_{di} = Driving force due to earthquake inertia

F_{rs} = Resisting force due to soil shear strength

F_{dp} = Resisting force due to passive soil pressure

$$F_{di} = K_{max} W$$

where K_{max} = maximum seismic coefficient

W = weight of soil block

$$F_{rs} = S_u L$$

where S_u = average undrained shear strength of soil

L = length of soil block

Yield Seismic Coefficient

$$K_y = \frac{F_{rs} - F_{da}}{W}$$

FIGURE 4-64 Forces and equations used in analyses of translatory landslides for calculating permanent lateral displacements from earthquake ground motions. Source: Idriss (1985).

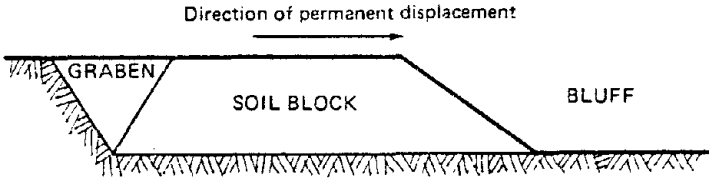

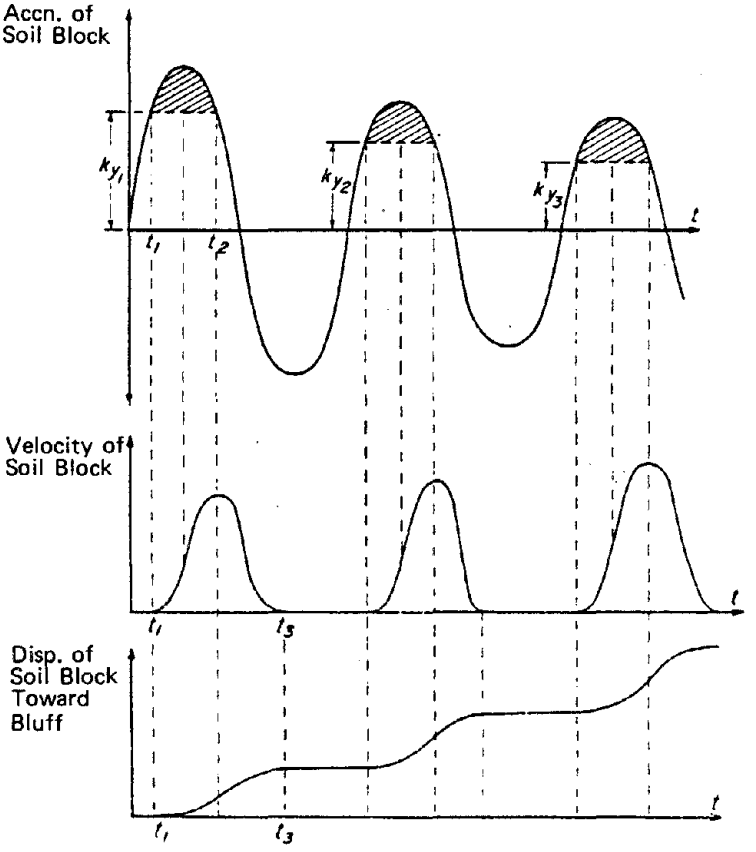

FIGURE 4-65 Schematic illustration for calculating displacement of soil block toward the bluff. Source: Idriss (1985) adapted from Goodman and Seed (1966).

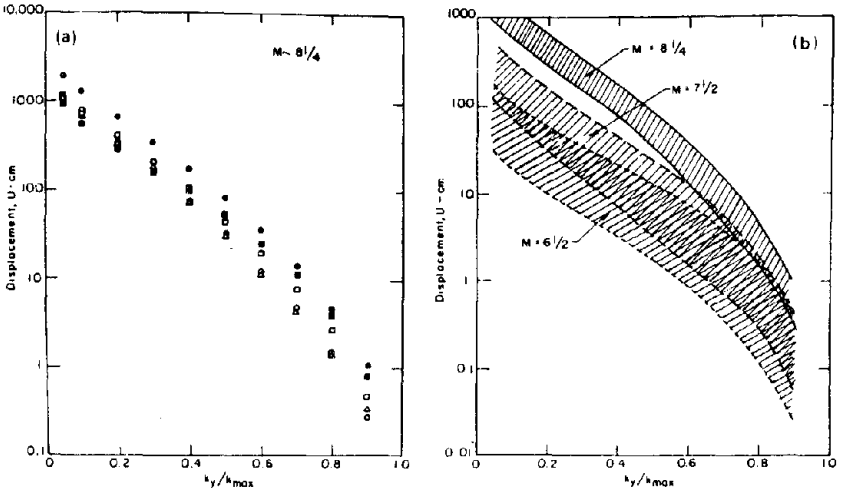

FIGURE 4-66 Permanent displacement from sliding block analyses: (a) results obtained using several input ground motions typical of earthquakes with magnitude 8.25; (b) summary of results from different magnitudes of earthquake. Source: Makdisi and Seed (1978).

become increasingly inaccurate. In the extreme case of large strength reduction (Figure 2-38) and flow failure, the procedure is not applicable and should not be used.

Some Approximate Solutions Using Elastic Analysis

While reasonably reliable procedures are available for estimating permanent deformations in soils that do not undergo significant strength loss, procedures for evaluating permanent deformations in soil deposits in which high pore pressures are generated by earthquake shaking are not nearly so well developed. One procedure for evaluating such problems is described by Seed et al. (1975b). It uses the concept of a strain potential; that is, the permanent deformation induced in representative soil elements in the absence of any constraint applied by neighboring elements. These values of strain potential are then interpreted to produce a compatible set of deformations and thence the deformed shape of the structure. This procedure has been shown to work reasonably well in the case of the deformations observed on the Upper San Fernando Dam in the 1971 San Fernando earthquake, where horizontal movements were of the order of 5 to 7 ft.

A similar approach is described by Marr and Christian (1981). The residual strains at each point of a finite element mesh at the end of the entire loading are determined (using an equation such as Eq. 4-18 in the next section) under the assumption that there are no changes in

total normal or shear stresses from beginning to end of the loading. These strains are then input to a special finite element program that restores the compatibility of displacement among the elements, producing the deformed shape of the earth mass.

A different approach has been used by Andersen (1983). Two finite element analyses using only static loading conditions are performed. The first uses a stress-strain curve for monotonic loading. The second uses a fictitious stress-strain curve drawn by connecting the final strains developed by superimposing a cyclic stress, having the correct magnitude and number of cycles, upon the sustained static stress (Figure 4-67). (This stress-strain curve is developed separately for a number of elements throughout the soil mass. The correct cyclic stresses at these elements are determined from an equivalent linear dynamic analysis.) The permanent deformation caused by the dynamic loading is the difference between the deformation from these two analyses. A somewhat similar form of analysis has been developed by Taniguchi et al. (1983).

While some of these methods were developed primarily for analysis of wave-loaded structures, extending their use to earthquake problems is straightforward.

Nonlinear Dynamic Analysis

Computer models such as DESRA or TARA can provide predictions of permanent deformation associated with residual shear strains. These models assume that degradation of stiffness during shaking results entirely from decreases in the effective stress as pore pressures build up and that these changes in effective stress are predicted correctly.

A version of DESRA for slopes called DONAL-2 has been used to estimate seismic deformations in underwater slopes in the Mediterranean (Finn, 1980). TARA has been used to estimate both cyclic and permanent displacements of a proposed gravity platform (Finn, 1985a) and of a tailings dam under earthquake loading (Finn, 1985b). Both TARA and DESRA may also be used to compute the settlements of structures under seismic loading (Finn, 1982, 1984).

The procedure proposed by Bouckovalas et al. (1984) for use with wave-loaded offshore structures also provides a direct prediction of permanent deformations (Marr et al., 1982). The increment of residual strain caused by a cycle (or a group of cycles) is given by an equation of the form:

$$d\gamma = B\, q \frac{|q|^{b-1}}{|\sigma'^{b}_{oct}|} \gamma_c^a N^c\, dN \qquad \text{(Eq. 4-18)}$$

where q is one-half the static deviator stress, σ'_{oct} is the octahedral effective stress, γ equals the cyclic strain, N is the number of cycles

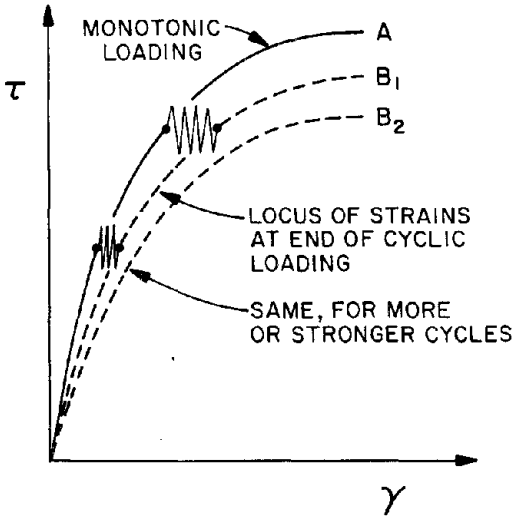

FIGURE 4-67 Stress-strain curves used in method of Andersen (1976) for computing permanent displacement. Curve A is the normal stress-strain curve for monotonic loading. Curve B is established from the total strain measured in a series of tests starting from different sustained shear stresses, with a specific cyclic stress and number of cycles. Curve B_2 is for a different combination of cyclic stress and number of cycles.

of strain, and a, b, and c are experimentally determined constants obtained by fitting results from drained cyclic triaxial tests with the cyclic load superimposed upon a sustained load.

This increment of residual strain is added to the elastic strain caused by any changes in the stresses at each point from beginning to end of the cycle, and the sum is used in equations satisfying dynamic equilibrium and compatibility. This method has the advantage that it is not necessary to integrate the equations of motion around entire cycles of stress; only the net effect of a cycle (or group of cycles) is considered. The trade-off for this advantage is that it is necessary to use a separate method for evaluating the cyclic strain.

Some Simple Guidance

Figure 4-68 indicates the range of limiting shear strains that can be experienced by sands with different densities if they reach the $\sigma' \simeq 0$ condition. Degrees of damage that can result are suggested.

Hedberg (1977), who performed undrained cyclic triaxial tests with sustained static stress, observed that the effective stress path typically reached the failure line (Figure 4-69) at an accumulated strain of about

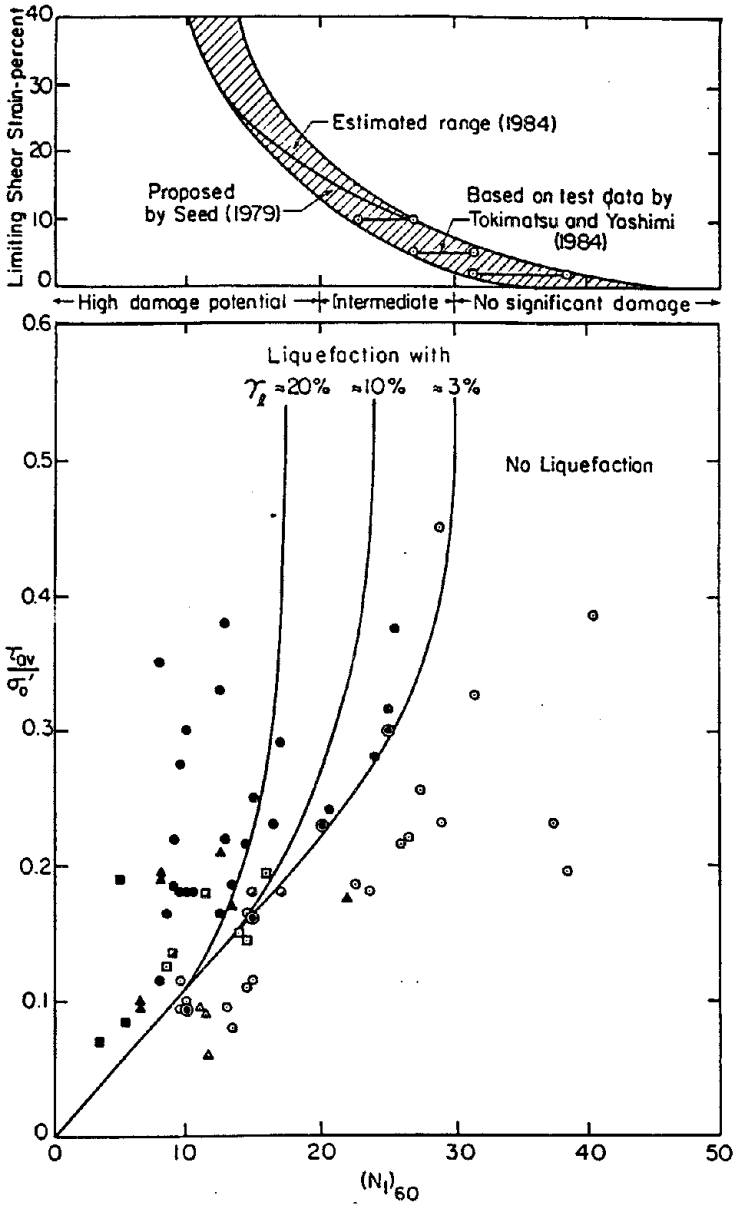

FIGURE 4-68 Tentative relationship between cyclic stress ratio, $(N_1)_{60}$ values, and limiting strains for natural deposits of clean sand. Source: Seed et al. (1984).

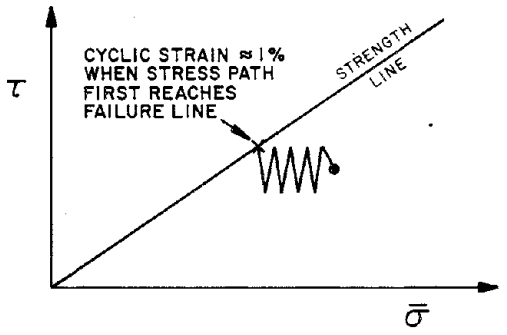

FIGURE 4-69 Typical effective stress path when a cyclic shear stress is superimposed upon a sustained shear stress. It has been observed (Hedberg, 1977) that the accumulated shear strain reaches about 1 percent when the effective stress path reaches the failure line.

1 percent. For some problems, this much strain can represent excessive deformation.

Figure 4-70 shows combinations of sustained (τ_{ave}) and cyclic (τ_c) stresses causing an accumulated strain of 3 percent during cyclic simple shear tests on a clay. Curves of this type provide general guidance concerning limiting combinations of sustained and cyclic stresses.

Plasticity Theory

Methods of analysis based upon the concepts of plasticity theory can be used to calculate permanent deformations (Andersen et al., 1978; Baldi and Rohani, 1979; Prevost, 1981). However, the procedures used in these methods to handle unload/reload cycles are often extremely cumbersome and are not yet regarded as giving reliable results. While there are great advantages to using methods of computation having a solid theoretical basis, plasticity-based methods have thus far found little favor for earthquake engineering problems.

Final Comments

It is clear that much further research and development is required before satisfactory methods for predicting permanent displacements will be generally available to engineers.

Role of Centrifuge Testing as an Evaluative Tool

As discussed in Chapter 2, centrifuge model tests can make valuable contributions by permitting general observations concerning the behavior of soil masses during simulated ground shaking and by providing

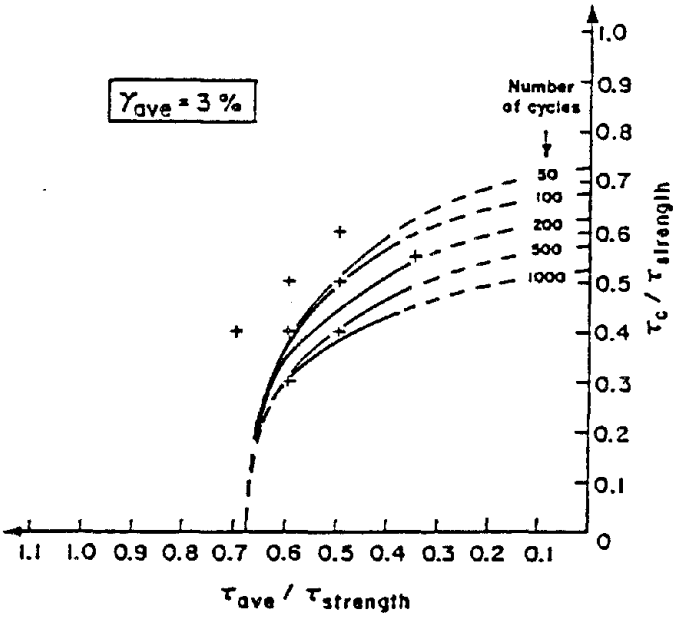

FIGURE 4-70 Contours showing combinations of cyclic shear stress (τ_c), sustained shear stress (τ_{ave}), and a number of cycles causing an accumulated shear strain of 3 percent, from simple shear tests on Drammen clay. Source: Goulois et al. (1985).

experimental data against which theoretical methods of analysis may be checked. As the discussion in the preceding sections has made clear, there is a great need for experimental data concerning the response of soil masses.

The possible role of centrifuge model testing in the analysis and evaluation of a specific site or project is less clear. One major problem is whether scaling requirements, especially those dealing with the scaling of time vis-a-vis flow of pore water, can be satisfied. The basic problem, of course, is the extent to which it is possible to get soil in a model to have just the same properties as will the actual soil in situ. This is certainly very difficult to do, and probably is impossible when the actual site involves complex stratigraphy and geologic history.

At present the use of theoretical models does appear to give greater flexibility in making controlled adjustments to assumed properties to see the effect of different assumptions about properties. With theoretical models, the input soil properties are at least known, whereas there are difficulties establishing the actual properties of soils in the centrifuge model. On the other hand, the centrifuge model incorporates aspects of actual soil behavior, such as the effects of rotation of principal

stress directions, that are poorly modeled in theoretical methods. Both theoretical analysis and centrifuge model testing therefore can provide valuable complementary insights into new and complex problems.

It appears at present that there is no direct role for centrifuge model testing in conventional engineering projects. However, if a project warrants a considerable theoretical analysis, and especially if theoretical methods still in the development stage are to be used, then centrifuge model testing to validate the theoretical analysis and perhaps to provide concepts for design is worthy of consideration.

Probabilistic and Statistical Analysis

Deterministic models of soil liquefaction give a yes or no answer as to whether liquefaction will occur or not, or an answer in the form of a factor of safety. In either case, some consideration of probabilities must be made—either implicitly or explicitly—to answer questions such as: Is the risk of liquefaction high enough to justify a large monetary expenditure to improve the ground at a project site, or should the investment already made at that project site be abandoned? Deterministic answers by themselves do not generally provide clear-cut decisions in cases where potential failure must be weighed against potential cost.

In the context of civil engineering projects, including those involving liquefaction, the existence of risks needs to be recognized and assessed. This point was emphasized recently by Whitman (1984) and earlier by Casagrande (1965). Probability and statistics are basically tools to augment—but not replace—the assessment of risk by human judgment, and to aid in making design decisions.

Probabilistic or statistical methods can be introduced at various stages of a liquefaction risk assessment. Depending on their objectives, various engineers have focused on one or two of the following sources of uncertainty:

- Uncertainty in the magnitude and location of earthquakes that can potentially affect the site.
- Uncertainty of the acceleration and duration of ground motion at a site, resulting from an earthquake but attenuated by distance and filtered by the site response.
- Uncertainty in the basic physical models of soil liquefaction behavior (model uncertainty).
- Uncertainty in the soil resistance parameters input to the physical model (the site characterization problem).

The Risk Analysis Framework

The general steps in earthquake risk analysis, as applied to the problem of liquefaction, are indicated in Figure 4-71. There are two essential

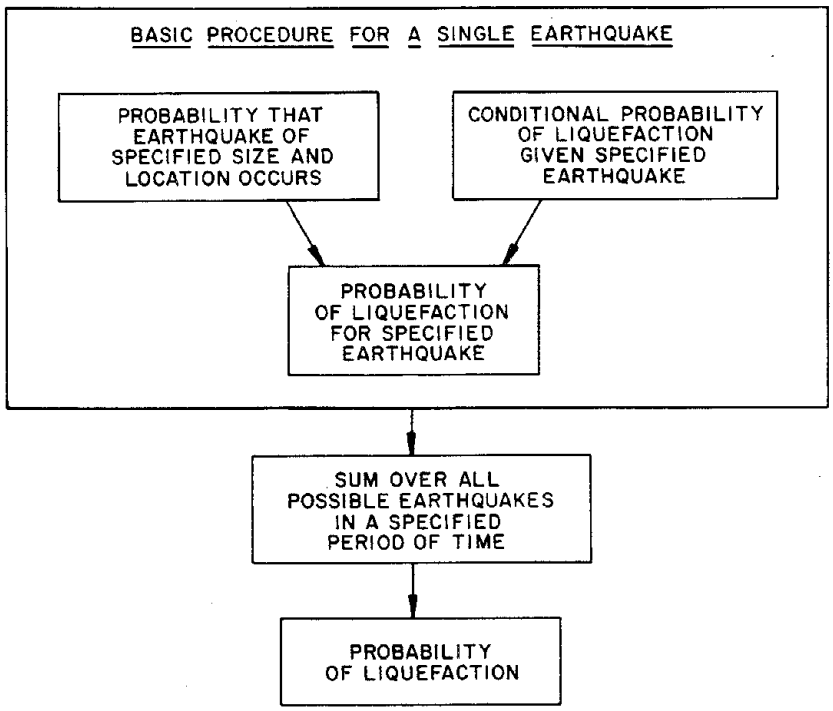

FIGURE 4-71 Schematic of the steps in a probabilistic liquefaction risk analysis. Source: Liao (1985).

parts. One deals with the probability that earthquakes occur; this portion is primarily the province of the seismologist. The second deals with the probability that there is liquefaction; this is primarily the concern of the geotechnical engineer, and tools used for this assessment have been discussed at length in previous sections. The probabilities from these two parts must be combined and summed over all possible earthquakes to give the probability of liquefaction.

Methods of liquefaction risk analysis have been proposed by McGuire et al. (1978, 1979), Yegian and Whitman (1978), Haldar and Tang (1979), Yegian and Vitelli (1981a, 1981b), Chameau and Clough (1983), Atkinson et al. (1984), and Kavazanjian et al. (1985), and they provide the major focus of this section. The question posed in such studies is: What is the probability of liquefaction at the project site during the life of the project (or during a specified time interval)? This phrasing reflects the fact that in a seismically active region, given enough time (e.g., thousands of years), at least one earthquake will occur that will be large enough and close enough to cause liquefaction at a susceptible site. Thus, discussion of probabilities of earthquake occurrence and liquefaction must be restricted to a specified time period, and results

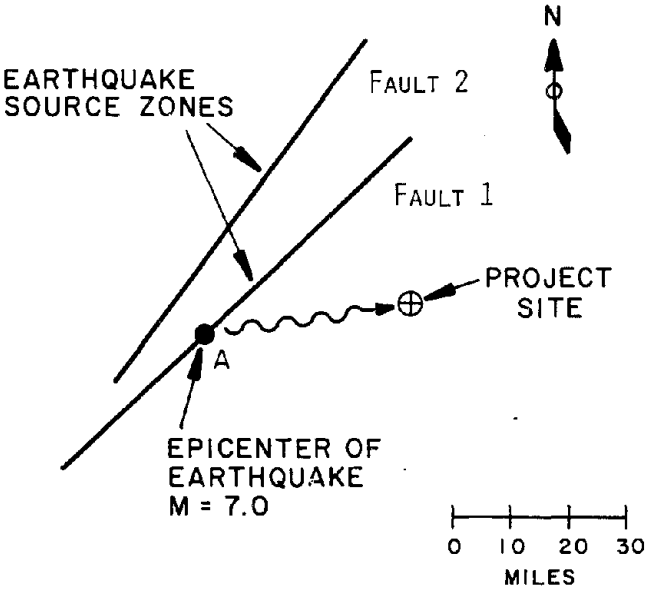

SEQUENCE OF QUESTIONS:

① P(EARTHQUAKE ON FAULT 1) = ?

② P(EARTHQUAKE AT POINT A) = ?

③ P(M = 7.0) = ?

④ $P\left(\begin{matrix}\text{LIQUEFACTION, GIVEN} \\ \text{ABOVE CONDITIONS}\end{matrix}\right) = ?$

FIGURE 4-72 Schematic of the sequence of questions that need to be answered as part of a typical liquefaction risk assessment. Source: Liao (1985).

are often given in terms of the probability of liquefaction during a year's period (i.e., annual probability).

To illustrate schematically the basic steps in a liquefaction risk analysis, a simplified hypothetical problem is shown in Figure 4-72. A project site is located in the vicinity of two active earthquake faults (linear "source zones"). It is assumed that the site is susceptible to liquefaction and that the probability of liquefaction occurrence within the next 50 years is to be evaluated. To begin the analysis, it is first asked: What is the probability of liquefaction resulting from an earthquake at a specific point (say point A) and having a specific

magnitude (say $M = 7.0$)? To answer this question requires answering the following sequence of questions:

- What is the probability that an earthquake will occur along fault 1 sometime in the next 50 years?
- If this earthquake occurs, what is the probability that the earthquake will have a magnitude of 7.0?
- If an earthquake of magnitude 7.0 occurs on fault 1, what is the probability that its epicenter will be located at point A?

To obtain the combined probability of occurrence of the specified earthquake, the probability estimates that answer the above questions are multiplied together. Then it is asked:

- If an earthquake of magnitude 7.0 occurs on fault 1 with its epicenter located at point A, what is the probability that liquefaction will occur at the project site?

The estimate of probability that answers the last question is often termed the "conditional probability of liquefaction," i.e., all of the loading conditions for the evaluation of the probability of liquefaction have been given. Multiplying this conditional probability by the probability of earthquake occurrence gives the overall probability of liquefaction being caused by the specified earthquake.

However, it is important to consider all possible earthquakes in the vicinity of the project site. Thus, the following possible situations must also be examined:

- Earthquakes can occur not only at point A but at several points on fault 1.
- Earthquakes of magnitudes other than 7.0 can occur.
- Earthquakes can occur not only on fault 1 but also on fault 2 (and possibly other source zones).

The probability of liquefaction associated with each and every combination of the above situations must be evaluated and summed to yield the total probability of liquefaction at the project site.

To formalize mathematically the preceding discussion, the following generalized notation is introduced:

- Let Ψ designate a set or "vector" of earthquake load parameters (e.g., $\Psi = (a,M)$, where a is the peak site acceleration and M is the earthquake magnitude).
- Let Ω designate a set or "vector" of liquefaction resistance parameters (e.g., $\Omega = ((N_1)_{60},PF)$, where $(N_1)_{60}$ is the normalized/corrected SPT resistance and PF is the percent fines content).
- Let Y be an indicator of liquefaction, i.e., $Y = 1$ if liquefaction occurs and $Y = 0$ if it does not occur.

Then the probability that liquefaction occurs at a specific site within a time period T can be generally expressed as:

$$P(Y = 1) = \int_{\Omega} \{1 - \exp(-\lambda T \int_{\Psi} P(Y = 1|\Omega,\Psi) g(\Psi) d\Psi)\} g(\Omega) d(\Omega) \qquad \text{(Eq. 4-19a)}$$

For the usual case of small values resulting from the integral over Ψ (which is the probability that any earthquake will result in liquefaction), P is well approximated by:

$$P(Y = 1) \simeq \lambda T \int_{\Omega} \int_{\Psi} P(Y = 1|\Omega,\Psi) \cdot f(\Omega) \cdot g(\Psi) d\Psi d\Psi \qquad \text{(Eq. 4-19b)}$$

where the integrals are over all values of the parameters in Ψ and Ω. In the equations above:

- $P(Y = 1|\Omega,\Psi)$ is the conditional probability of liquefaction.
- $g(\Psi)$ is the probability distribution of the earthquake load parameters, and represents the uncertainty of specific magnitudes and locations of earthquake occurrence.
- $f(\Omega)$ is the probability distribution of the soil resistance parameters, and represents the fact that site conditions are often spatially variable and inhomogeneous.
- λ is the overall rate of earthquake occurrence (e.g., earthquakes per year) from all potential seismic sources within the vicinity of the project site.

The terms $P(Y = 1|\Omega,\Psi)$ and $g(\Psi)$ have been discussed previously in the context of Figure 4-72. The variability of the soil liquefaction resistance was not discussed previously for the sake of simplifying the presentation. The integrals (usually evaluated numerically) represent the generalized summation of all the probabilities associated with each of the possible combinations of earthquake source zones, magnitudes, locations, and variable site conditions.

The above general formulation is the correct way of assessing the probability of liquefaction at a site and is adapted from the seismic hazard methodology originally proposed by Cornell (1968). All of the proposed methods of liquefaction risk assessment discussed in this section have the above framework in common. Where they differ are in the implementation of specifics in evaluating $P(Y = 1|\Omega,\Psi)$, $f(\Omega)$, or $g(\Psi)$ or in the summation or integration algorithm.

Earthquake Load Parameters

The variability in the earthquake load parameters are generally dealt with in the context of seismology and seismic risk models, such as

those by Cornell (1968) and Der Kiureghian and Ang (1977). The quantifications of earthquake risk is a discipline unto itself and is described briefly here in terms of how it interfaces with various aspects of liquefaction risk analysis. Practical examples of aspects of seismic risk evaluation have been presented by Christian et al. (1978) and by Donovan and Bornstein (1978).

Seismic Source Zones

The first step in evaluating seismic risk is in the definition or mapping of regions or where earthquakes originate. Seismic source zones can be faults that can be mapped on the earth's surface or planar regions within the earth that can be defined by analyzing patterns of earthquake hypocenters. It is usually assumed that an earthquake of a given magnitude has an equal probability of occurring anywhere within the seismic zone. In the absence of well-defined earthquake mechanisms in many geographic regions or for the sake of simplicity of analysis, it is sometimes assumed that the seismic source zone is circular and centered at the project site, as shown in Figure 4-73. In more sophisticated models or algorithms, where seismicity is relatively well defined, several irregularly shaped seismic source zones may be defined, as shown in Figure 4-74.

Rates of Seismic Activity

The rates of seismic activity in source zones are usually determined based on an analysis of past historical seismicity. These rates are then used in seismic hazard or liquefaction risk analysis, in which it is customary to assume that the occurrence of earthquakes is a stationary Poisson process in time. "Stationary" implies that the rate of earthquake occurrence (expected number of earthquakes per year) is constant over time. "Poisson" implies that the occurrence of any future earthquake is independent of any earthquakes that have occurred in the past. These two assumptions are generally not valid. In the framework of plate tectonics, after the release of strain in the earth's crust during a large earthquake, a certain period of time is required to build up enough strain to again cause another large earthquake rupture. Though the assumption of a stationary Poisson model for earthquake occurrence is commonly used, recent advances in seismology and earthquake prediction may offer better estimates of the probabilities of earthquake occurrence (Patwardan et al., 1980; Anagnos and Kiremedjian, 1984; Kiremedjian and Anagnos, 1984; Schwartz and Coppersmith, 1984; Sykes and Nishenko, 1984).

Seismic Source Mechanisms

There are two major seismic risk models in use, which differ in the modeling of the nature of the seismic source. The Cornell (1968) model

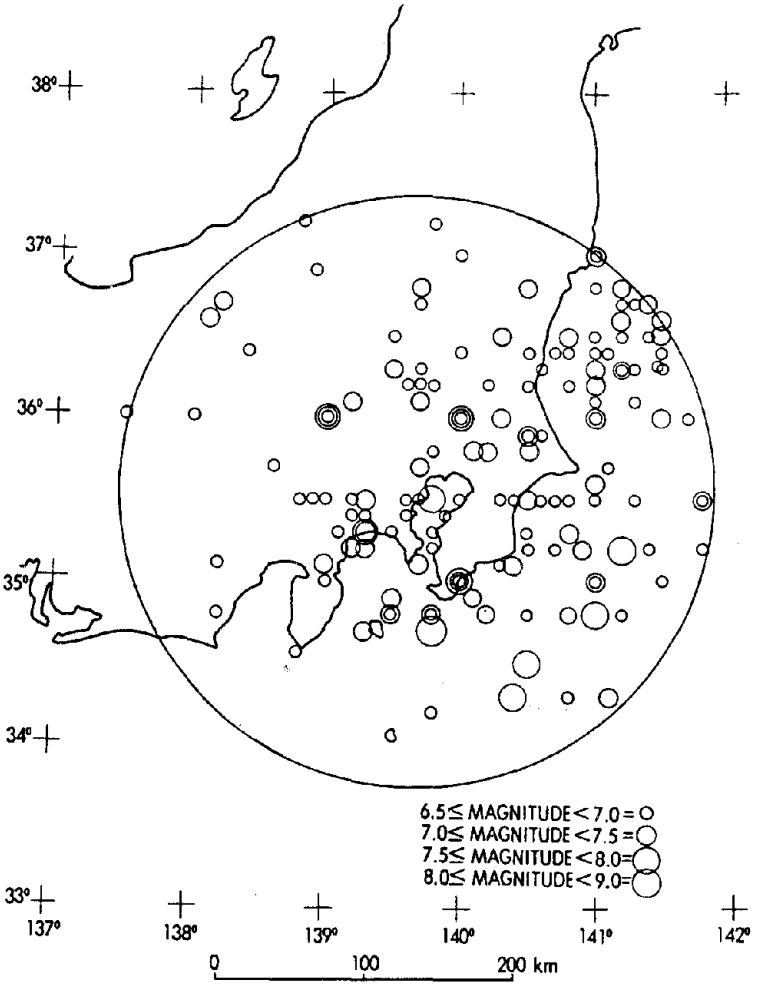

FIGURE 4-73 Circular seismic source zone centered at project site for liquefaction risk analysis. Source: McGuire et al. (1978).

assumes that the energy released during any earthquake (of the many that can possibly occur in the source area) is initially concentrated at a point and propagates outward from that point. In contrast, the model by Der Kiureghian and Ang (1977) assumes linear sources (faults) and that the energy released is not concentric about a point but rather propagates outward from a finite length of fault rupture. Thus, the largest contribution to earthquake intensity at a site may not be related to the location of the initial fault rupture, but rather to the slip that occurred closest to that site. The Der Kiureghian and Ang (1977) model

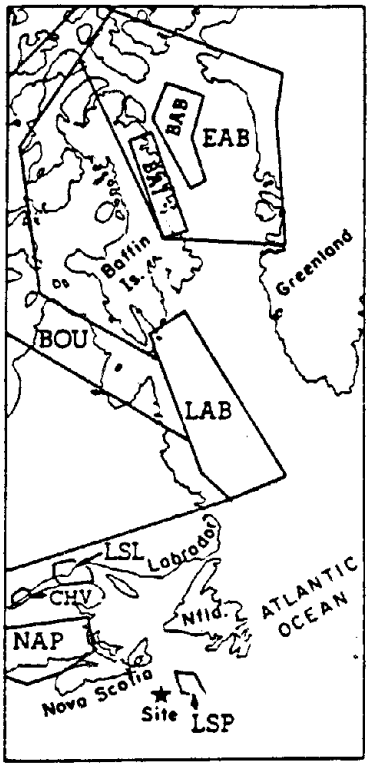

FIGURE 4-74 Complex set of irregularly shaped seismic zones (labeled LAB, BOU, etc.) for liquefaction risk analysis. Source: Atkinson et al. (1984).

is best suited for seismic regions such as California, where the strike-slip faults causing earthquakes are well defined and have been mapped extensively. However, in regions where the sources and perhaps even the nature of seismic activity is not well defined, the Cornell (1968) model is probably more appropriate.

A computer program presented by Atkinson and Finn (1985) for liquefaction risk analysis has the capability of using either the Cornell (1968) or the Der Kiureghian and Ang (1977) mechanism for its computations.

Load Parameters

Most analyses describe the intensity of earthquake shaking at the site in terms of peak acceleration and duration. This method (sometimes called the A&D approach) is represented by the methods proposed by

McGuire et al. (1978, 1979), Haldar and Tang (1979), Chameau and Clough (1983), Atkinson et al. (1984), and Kavazanjian et al. (1985). Acceleration is obtained from an attenuation law, giving acceleration as a function of magnitude and distance. Duration (usually in terms of number of equivalent cycles) is given by a correlation to magnitude. These two-load parameters are suitable for analyzing possible liquefaction at a site, using common methods of analysis. However, there is uncertainty in the correlations of these parameters to magnitude and distance, which should be taken into account. Formal treatment of uncertainty in attenuation was introduced by Cornell (1971) and has often been incorporated into analysis since that time. For example, Atkinson et al. (1984) consider a lognormal dispersion of acceleration around the expected value from the attenuation relationship. A range of attenuation relationships involving considerations of both hypocentral and closest distance to a fault are included in their computer program for liquefaction risk analysis.

An alternative approach, using magnitude (M) and distance (R) as the load parameters, sometimes called the M&R approach, is represented by the methods proposed by Yegian and Whitman (1978), Youd and Perkins (1978), and Yegian and Vitelli (1981a,b). The M&R methods are more data-based (empirical) and are more direct and arguably easier to use within a risk analysis framework, especially for large-scale mapping of liquefaction potential. However, their use requires that the possibility of liquefaction be related directly to magnitude and distance, which tends to obscure localized ground shaking site effects that may influence the occurrence of liquefaction.

Conditional Liquefaction Probability

As discussed previously, the conditional liquefaction probability expresses the probability that liquefaction occurs, given that an earthquake of specified location and magnitude or a ground shaking with specified acceleration and duration occurs. Some liquefaction risk procedures, such as those presented by Youd and Perkins (1978), McGuire et al. (1978, 1979), and Atkinson et al. (1984), do not account for any uncertainty in this factor. That is, they assume that the conditional probability function $P(Y = 1|\Omega,\Psi)$ can only take on values of 1 or 0 (liquefaction or no liquefaction), which represents a purely deterministic formulation. All the uncertainty in their liquefaction risk assessments arises from the uncertain nature of seismicity.

Actually, there is some uncertainty in any method used to determine the likelihood of liquefaction given an earthquake. The previous sections of this chapter have discussed the various problems involved in the analysis of a site. All such analyses involve some theoretical

model for the physical behavior of a site. Model uncertainty arises as a result of simplifications or assumptions made in formulating the model, and even if all the input parameters were known precisely there would still be some uncertainty about the outcome. An example is the original semi-empirical liquefaction model proposed by Seed et al. (1975a), represented by a plot of τ/σ'_o versus N_1. In that model, no provisions were made for duration effects of earthquakes, the differences in methods of obtaining N_1, or the effects of fines content. The neglect of these factors was the source of uncertainties in the original model. Even though these factors have since been incorporated into later versions of the model, some model errors still remain. In addition, there are uncertainties in the inputs to any model. For example, at a site where a large variation in N_1 exists, there are uncertainties as to which N_1 value should be used.

Approaches which have been used to obtain the conditional probability of liquefaction in other than yes or no terms can be categorized as probabilistic or statistical:

- Probabilistic methods involve the use of theoretical models to analyze for liquefaction at a site, estimating the inherent uncertainties in the parameters and propagating these uncertainties through the model.
- Statistical methods generally deal with the extraction of information from data; in the case of the liquefaction problem, "data" usually refer to field observations of instances of liquefaction or nonliquefaction.

Probabilistic Models

Haldar and Tang (1979) use a first-order second-moment (FOSM) method applied to the Seed and Idriss (1971) Simplified Method to obtain the conditional probability of liquefaction. Basically, this involved estimating the uncertainties (FOSM parameters) of the components of the Seed-Idriss model and propagating these uncertainties through the model. A more sophisticated FOSM model has been presented by Fardis and Veneziano (1982) incorporating the effects of pore pressure diffusion, soil stiffness reduction, and variations of soil properties within a stratum. In both models the assumption of normality or log-normality of load and resistance parameters is used in estimating the conditional probability of liquefaction. Estimation of the second-moment parameters (i.e, means and variances) is not trivial, and requires some judgment.

Probabilistic analyses based on pore pressure generation models have been presented by Chameau and Clough (1983). The accumulation of pore pressure is calculated using a nonlinear formulation, based either on laboratory data or on a basic constitutive physical model.

Their result for conditional probabilities $P(Y = 1|\Omega,\Psi)$ is equated to the probability that the pore pressure ratio r_u is equal to 1, and calculated assuming random arrivals of shear stress (or equivalent acceleration) peaks between positive zero crossing of the earthquake record. The distribution of the shear stress peaks has been modeled as beta, gamma, Rayleigh, or exponentially distributed. The number of positive zero crossings is a measure of duration and may also be treated as a random variable, as is done in the application of Chameau and Clough's method by Kavazanjian et al. (1985).

Earlier, Donovan (1971) proposed a similar model, assuming the variation of peak amplitudes of earthquake shaking to be distributed as a Rayleigh probability function. In his method the effects (damage) from the various peak accelerations in an earthquake record are calculated based on a total stress model of cyclic loading behavior and are summed or integrated with a weighting function proportional to the frequency of occurrence of the various peaks (Miner's Linear Damage Criteria). However, his method produces a deterministic criterion for liquefaction and not a conditional liquefaction probability.

An alternative to the assumption of a frequency distribution for shear stress peaks is to use the equivalent uniform cycle concept, which is commonly used in deterministic analyses. A statistical examination of this concept has been reported by Haldar and Tang (1981).

Another approach to the estimation of conditional liquefaction probability is the use of fuzzy set theory. This approach has been presented by Chameau and Gunaratne (1984), but it still requires considerable development before it can be applied usefully.

Statistical Analyses

One aspect of uncertainty in liquefaction analysis is the problem of how to draw the "best" boundary separating liquefaction and nonliquefaction behavior on a diagram such as Figure 4-75. This is known in statistics as a problem of classification or discrimination. This problem has been treated by Christian and Swiger (1975) using empirical data on site liquefaction behavior and a statistical method known as linear discriminant analysis (e.g., see Johnson and Wichern, 1982). Their results are shown in Figure 4-76 and have been interpreted (as a decision rule) to mean that:

$$P(Y = 1|D_r,A) = \begin{cases} 1 \text{ if } D_r < KA^{0.31069} \\ 0 \text{ if } D_r > KA^{0.31069} \end{cases} \qquad \text{(Eq. 4-20)}$$

where D_r is the relative density of the soil and A is a modified site acceleration. Of course, this is not strictly correct because the prob-

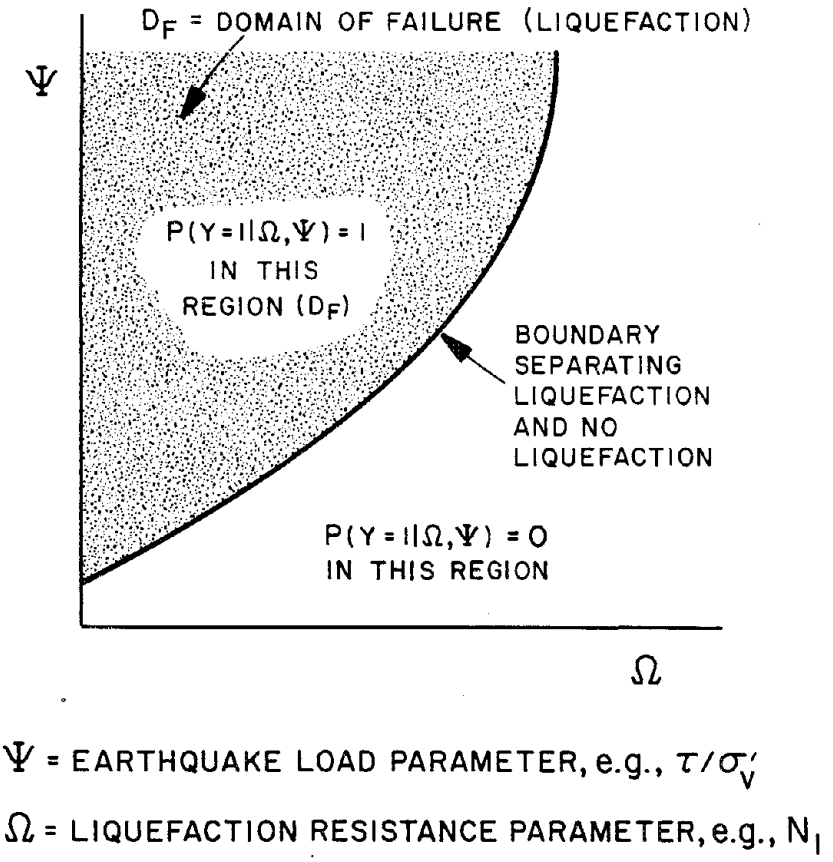

FIGURE 4-75 Schematic of the notation and results of a simple two-parameter classification problem.

ability $P(Y = 1|D_r,A)$ actually varies continuously from 0 to 1. The factor K is a function that depends on the probability of misclassifying a point as a site that would not liquefy, when in actuality it is a liquefaction point. This probability is denoted P in Figure 4-76, expressing the uncertainty in the location of the dividing line, and is not the conditional probability of liquefaction $P(Y = 1|\Omega,\Psi)$ previously defined, which in this interpretation of discriminant analysis scheme can only take on values of 0 or 1.

The results presented by Christian and Swiger are just an example of a variety of results that can be obtained using discriminant analysis. Other applications of discriminant analysis for studying liquefaction have been reported by Tanimoto and Noda (1976), Tanimoto (1977), Xie (1979), Wang et al. (1980), Davis and Berrill (1981, 1982), and Gu

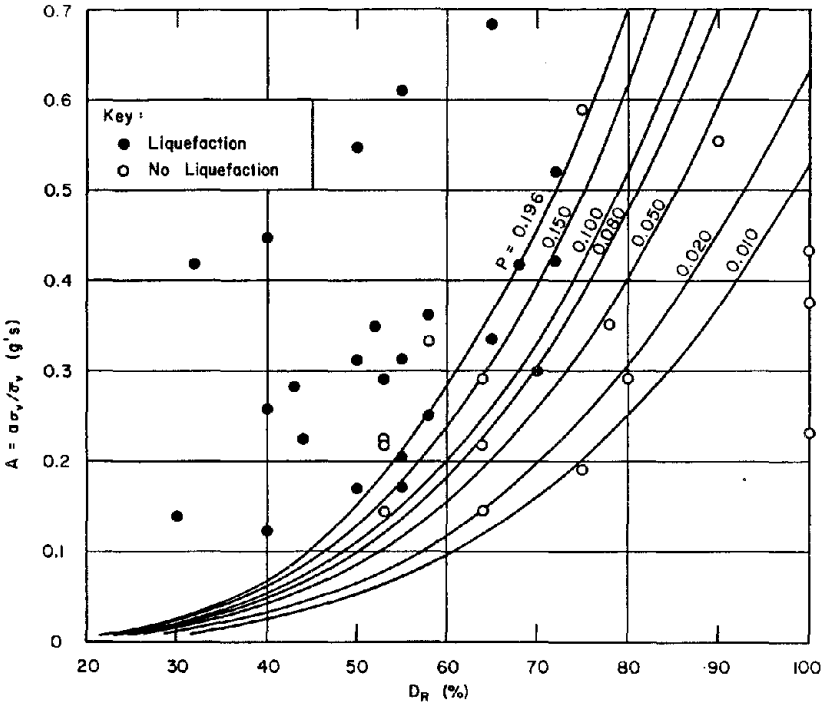

FIGURE 4-76 Example result from discriminant analysis of liquefaction data. Source: Christian and Swiger (1975).

and Wang (1984). Generally associated with the linear discriminant analysis methodologies are underlying assumptions of normality and randomness of data that are not satisfied by the available collection of liquefaction data. A concise discussion of these problems has been presented by Easterling and Heller (1976).

Yegian and Whitman (1978) presented a different classification method (developed by Yegian, 1976), termed the "least squares of the misclassified points." In essence, this method finds the boundary that best separates liquefaction from nonliquefaction based on minimizing the sum of the squared distances between the misclassified points and the boundary line. Atkinson et al. (1984) have used this method in part of their analyses, although their algorithm also accommodates the use of the more conservative lower bound curves from Seed (1979a) in their risk assessment procedure.

The problem with classification methods is that the discrimination criteria still give a deterministic yes-or-no type answer to whether liquefaction will or will not occur at a site, rather than a continuous conditional probability $P(Y = 1|\Omega,\Psi)$ that varies smoothly between 0

and 1. Within the framework of discriminant analysis, Bayes' Theorem can be used to obtain the desired conditional probability, provided that "prior" probabilities can be obtained based on the "global" probability distribution of liquefiable and nonliquefiable sites. This is, however, not an easy task. With respect to the method of "least square of misclassfied points," there is no formal theory to obtain the conditional probability of liquefaction, and the method used by Yegian (1976) to obtain $P(Y = 1|\Omega,\Psi)$ may be rational but is rather ad hoc.

Veneziano and Liao (1984) have presented a class of statistical methods that avoid many of the above problems discussed in estimating $P(Y = 1|\Omega,\Psi)$. Instead of treating the problem as a classification problem, the estimate of $P(Y = 1|\Omega,\Psi)$ is treated as a regression problem using Y as a binary (0 or 1) response variable. An advantage of this approach is that the probability distributions of Ω and Ψ do not need to be estimated and that $P(Y = 1|\Omega,\Psi)$ is directly evaluated with no need for appeals to Bayes' Theorem. One method known as logistic regression is well established for use in other applications (Cox, 1970; McFadden, 1974), but parametric assumptions (i.e., the mathematical forms of the probability function) must be made. More general nonparametric methods are being developed by Liao (1985), as well as further developments and applications of the logistic regression methods. An example of preliminary results from logistic regression analyses is shown in an earlier section (Figure 4-6).

The Site Characterization Problem

In the context of liquefaction analysis, site characterization refers to the problem of determining a representative value of a liquefaction resistance parameter (e.g., an SPT N-value) and the depth at which liquefaction is likely to occur. Soil deposits are generally highly variable, but for the sake of simplicity in analysis it is better to summarize the soil properties by a single number or a set of numbers such as the mean and standard deviation of the N-values.

Consider a fairly homogeneous sandy site where 10 borings have been drilled for purposes of liquefaction analysis. Suppose also that in each of the 10 borings, 10 SPT N_1-values are obtained along the boring profile, and there is some variability in the N_1-values in each boring. Since liquefaction involves both the generation and possible propagation of excess pore water pressures, liquefaction of the entire deposit may occur if the weakest part or sublayer of the deposit liquefies. Thus, to obtain a summary value of N_1 we could use the minimum of all the 100 N_1 values, the average of the minimum N_1 in each boring, the minimum average N_1 obtained at each depth, the average of all 100 N_1-values, or any multitude of similar combinations.

A practical example of where this problem was encountered has been presented by Jaime et al. (1981).

More details of this problem and how it affects the data base of case studies such as those presented by Seed et al. (1984) are discussed in the thesis by Liao (1985). However, this practical problem has not yet been addressed except in terms of appeals to "engineering judgment," which works well but is difficult to transfer from an "expert" to a less experienced engineer. Thus, the results of probability analyses are often given as functions of SPT blow count as in Figure 4-77.

The site characterization problem is one that is amenable to resolution by the use of statistical techniques and should deserve further research. This research would also be pertinent to the mapping of liquefaction potential over large areas, where geologic maps may need to be correlated with sparse SPT data. In such maps, site characterization may be extended to mean the characterization of widespread geologic units rather than a localized project site.

Comments on Probabilistic/Statistical Methods

The discussion in this chapter has concentrated on various aspects of assessing liquefaction probability considering uncertainties in the physical liquefaction models and site soil and earthquake conditions. Logically, the next step is to incorporate this evaluation of risk into a formal decision analysis framework, of which various examples have been given by Whitman (1984). This would entail the calculations of the expected probable costs of a liquefaction failure. One problem with this approach is that it is often difficult to assess the costs of failure, particularly if potential loss of human life is involved. Another problem is that numbers involving very small probabilities of failure (e.g., <0.001) cannot be assessed accurately (Whitman, 1984).

There are some significant advantages in using probabilistic methods to assess the potential for liquefaction. The risk of liquefaction can be compared in equivalent terms to the other risks to which a structure is exposed. Uncertainties in the different inputs can be treated systematically and uniformly, and those factors having the most influence on the risk can be more readily identified. For example, the analyses performed by Haldar and Tang (1979) point out the fact that there may be more uncertainty in liquefaction analysis arising from the earthquake loading parameters than from lack of understanding of the soil resistance parameters. Thus, probabilistic methods augment the decision process and enable a more effective transfer of experience based on subjective decisions. For all these reasons, probabilistic methods are considered to play a useful role in assessing the possibility of liquefaction. From the complexity of the foregoing discussion, however, it is evident that such methods should be employed with care.

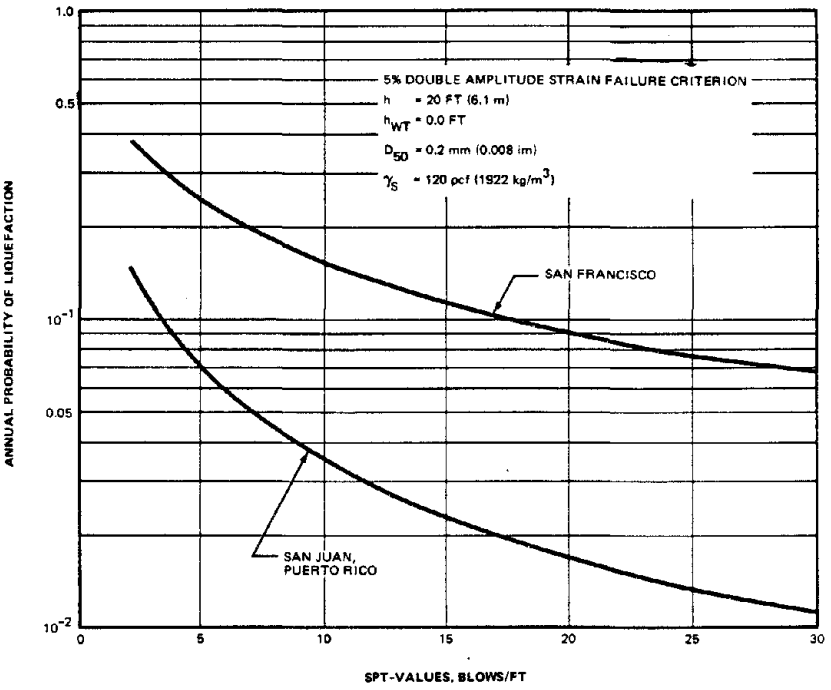

FIGURE 4-77 Example result from typical liquefaction risk analysis. Estimated annual probability of liquefaction for San Francisco and San Juan, Puerto Rico, as a function of SPT values. Source: Haldar and Tang (1979).

Summary and Perspective

From a practical point of view, it must be recognized that almost any saturated granular soil can develop increased pore water pressures when shaken, and that these pore pressures can become significant if the intensity and duration of earthquake shaking are great enough. The question that must be answered in a specific case is: What intensity and duration of shaking will cause liquefaction, or, conversely, can the soil survive the anticipated earthquake shaking without liquefaction? A wide variety of methods have evolved for assessing the likelihood of liquefaction at a specific site or within a small region. These techniques and their limitations are summarized below.

In considering these techniques, it should be remembered that evaluation of liquefaction hazard is an engineering art requiring judgment and experience in addition to testing and analysis. Important advances have been made during the past two decades in understanding liquefaction and in developing tools to help assess safety against liquefaction, but some aspects of the problem remain uncertain.

Level Ground

Level ground is characterized by a horizontal surface of very large extent and the absence of any superimposed or buried structure that imposes significant stresses in the ground. In evaluating this problem the primary goal is to identify the conditions for reaching the $\sigma' \simeq 0$ condition in the soil profile, which triggers the development of liquefaction effects at the ground surface. The case of level ground is of direct interest with regard to the safety of pavements, pipelines, building slabs on grade, and other objects. There are many situations in which evaluation of the level ground adjacent to a building or embankment appears to provide a conservative assessment of the potential of a foundation for failure. In such cases, however, it is difficult to assess the margin of safety in quantitative terms.

For level ground and sandy soils with little gravel, use of charts based on observed field performance together with a standard penetration test (SPT) or, with a lesser degree of certainty, a cone penetration test (CPT) can provide a practical evaluation of the degree of safety. In using this procedure the increased cyclic loading resistance associated with a larger content of silt and clay particles should be taken into account. It is desirable to adopt proposed procedures for standardizing the results of SPT tests for the purpose of evaluating liquefaction resistance. At a minimum, measured blowcount should be corrected to a common basis of energy delivered to the drill rod. The CPT is not as useful as the SPT for assessing safety against liquefaction, but it can be very valuable for locating loose pockets within a sand and for controlling efforts to improve the liquefaction resistance of a sand.

Flow Failures of Slopes and Embankments

The technology for analyzing the safety of slopes and embankments against a flow failure is not as well developed and agreed upon as in the case of level ground. Two general approaches are in use:

- Method 1 focuses first on the buildup of pore pressures that may trigger liquefaction. The susceptibility of the soil to such buildups is inferred from in-situ penetration resistance or from cyclic load tests on high-quality and disturbed samples. Various computational methods, from very simple and approximate to very sophisticated and complex, are available for predicting the buildup caused by a specific earthquake shaking. Zones where the $\sigma' \simeq 0$ condition occurs are identified, and a residual strength is assigned to those zones using correlations of observed residual strengths with in-situ penetration resistance. A static stability analysis is then performed. This method involves some uncertainties in the prediction of pore pressure buildup, but it has been

shown to provide results in good accord with some features of observed field performance in a number of cases.

- Method 2 focuses first on the potential for a flow failure. The evaluation involves the following: (1) determination of the in-situ steady-state strength of the soils by means of laboratory tests complemented with correlations between the measured steady-state strength and field index tests such as SPT or cone penetration; (2) if a potential for flow failure exists, an investigation of the conditions required to trigger the failure using results of laboratory cyclic tests and/or empirical correlations. Some uncertainties exist because determination of the in-situ steady-state strength is sensitive to changes in void ratio during sampling and testing. Thus it is necessary to correct results for these changes.

Both of these methods usually assume that constant volume conditions are maintained within the soil during the earthquake shaking. It has been hypothesized that flow failures can also occur if certain zones of the soil mass become weaker during and after an earthquake owing to redistribution of water content and spreading of pore pressures. The methods currently available to quantify the pore water migration and the associated volume changes are in a crude stage of development. These possible effects are included to some degree in the approach used in Method 1 and might in principle be incorporated into Method 2 as more case histories are used to calibrate the method.

Permanent Deformations

The prediction of deformation in soils not subject to flow failures is a very difficult and complex nonlinear problem that is still far from being resolved. Hence, various approximate methods exist:

- A procedure for computing permanent ground displacements in the form of translatory landslides is based on the approach of Newmark (1965). The mass above a failure surface is assumed to move only when the shear strength of the soil is exceeded and only during the time in which the strength is exceeded.
- The permanent deformations of soil elements are estimated from laboratory tests, assuming no constraint from adjacent elements. These are referred to as strain potentials. These strain potentials are then interpreted to produce a compatible set of deformations. Several techniques have been proposed for the laboratory testing as well as for producing compatible deformations.
- Dynamic computer models for nonlinear analysis and for plasticity theory produce estimates of permanent deformations. However, the proper modeling of soil properties for the analysis remains a formidable problem.

General Comments on Methods of Investigation

The following comments apply to cases of both level and sloping ground:

- Use of threshold strain provides a conservative assessment of the safety of foundations and earth structures to both triggering of flow failures and development of excessive deformations. The method is based on the values of shear modulus that can be measured in situ using wave propagation techniques. There is also evidence suggesting that this same approach, extended to larger strains by cyclic-strain-controlled laboratory tests, can be used to predict the development of pore water pressures in the field.
- For soils with a significant content of gravel, there is currently no satisfactory procedure for evaluating the safety against liquefaction. There is a great need to develop predictive procedures for these types of soils.
- Use of undisturbed sampling and laboratory cyclic load testing is not recommended as the sole means of assessing liquefaction resistance, except for some soils (e.g., silty or clayey soils, calcareous soils, etc.) for which there is either no or a limited amount of experience. (Obtaining samples for visual inspection and routine classification is, of course, always essential.) When the gathering and testing of soil samples are to be done, it is important to use extreme care and special techniques.
- Problems in which analysis of pore pressure buildup is essential must be approached with great care. These include, for example, cases where reliance is placed on partial dissipation of pore pressure to provide safety against flow failures or excessive deformation. While great advances have been made in the development of suitable techniques of analysis, more verification is required before they can be considered reliable tools for use in design. Special problems to be resolved include evaluating parameters required for analysis in ways that are not influenced greatly by sample disturbance, and accounting for dilation as significant permanent strains begin to develop.
- Centrifuge tests (and sometimes other small-scale tests) can provide valuable insights in understanding the behavior of foundations and earth structures and in formulating and testing mathematical models to predict performance. However, it is seldom possible to construct a truly scaled model for a specific prototype situation.
- Probabilistic analyses can provide approximate quantitative estimates for the probability of liquefaction, indicating the relative importance of uncertainty in the frequency and intensity of ground shaking and of uncertainty in the occurrence of liquefaction as a result of ground shaking.

5
Improving Seismic Stability To Resist Liquefaction

Classes of Projects Affected

Liquefaction of underlying soil deposits has the potential to cause damage to all classes of overlying or buried structures. Eyewitness examples of liquefaction are ample testimony to the catastrophic effects that occur when earthquakes induce large excess pore water pressures causing the soil to lose most or all of its strength and to liquefy. Structures that are particularly sensitive to liquefaction of underlying or retained soils are: buildings with shallow foundations, railway lines, highways and bridges, buried structures, dams, canals, retaining walls, port structures, utility poles, and towers.

The types of structural instability and structures most adversely affected are given in Table 5-1. It is clear that buried and surface structures will be affected by a loss of foundation bearing capacity if the underlying soils liquefy. Similarly, landslides induced by liquefaction affect all structures built on, at the base of, or downstream from unstable slopes. Liquefied soils underlying very flat slopes (on the order of less than 1 degree) or underlying horizontal soil surfaces have the potential for lateral spreading and disruption of surface and subsurface structures. Such lateral spreading can pull buildings apart and destroy highway pavements, railway alignments, and utility lines.

Furthermore, excess pore pressures in subsurface soils can produce buoyant forces that can push buried tanks and utility poles out of the ground. The ejection of liquefied sand from sand boils and resulting sink holes can destroy pavements and floor slabs. The liquefaction of backfill behind retaining walls and port structures also can cause complete collapse of such structures.

Minimizing Liquefaction Instability

There is now a general understanding of the types of soils that are most susceptible to liquefaction and the level of earthquake shaking

TABLE 5-1 Classes of Liquefaction-Induced Structural Instability

Types of Structural Instability	Structures Most Often Affected
Loss of foundation bearing capacity	Buried and surface structures
Slope instability slides	Structures built on or at the base of the slope Dam embankments and foundations
Movement of liquefied soil adjacent to topographic depressions	Bridge piers Railway lines Highways Utility lines
Lateral spreading on horizontal ground	Structures, especially those with slabs on grade Utility lines Highways Railways
Excess structural buoyancy caused by high subsurface pore pressure	Buried tanks Utility poles
Formation of sink holes from sand blows	Structures built on grade
Increase of lateral stress in liquefied soil	Retaining walls Port structures

that can cause these soils to liquefy. Therefore, new projects can be located at sites where there is little or no liquefaction potential, or if such a potential is recognized, treatment of the soils can be undertaken. Furthermore, remedial measures can be implemented to safeguard lifelines (either existing or planned) such as highways, railways, or pipelines that must traverse areas of liquefiable soil. The determination of what can be done to reduce the risk of failure of an existing structure's foundation is a more complicated problem—work must be done around or under the existing structure without adversely affecting it.

The following sections describe actions that may be taken if liquefaction is a concern. These actions include moving the project, accepting the risk of liquefaction, or performing remedial measures at the project site to reduce the potential for liquefaction.

Technical and nontechnical considerations in selecting remedial measures are discussed. These factors include:

- Feasibility
- Secondary effects (such as effects on static stability)
- Economics

A number of potential remedial measures are reviewed in detail, considering such factors as:

- Technical adequacy
- Field verifiability
- Costs
- Maintenance
- Long-term performance
- Public perception
- Environmental impact

Table 5-2 summarizes the technical and nontechnical considerations of each method.

Alternative Actions if Liquefaction Is a Concern

General

Several alternative approaches can be taken if earthquake-induced liquefaction is a threat to existing or proposed structures. For an existing structure the choices are: (1) retrofitting the structure and/or site to reduce potential failure, (2) abandoning the structure if the retrofit costs exceed the potential benefits derived from maintaining the structure, or (3) accepting the risk and maintaining the existing use. Additional options would be to continue use of the structure but to change the operation, or to alter the use of the structure such that the hazard becomes tolerable even if failure occurs.

For new construction, moving the project assumes that there are alternative sites where liquefaction is not a concern but that are equally appropriate for the proposed project. The costs of necessary mitigation actions may, in such cases, make selection of an alternative site a more cost-effective alternative than use of the primary site.

In an ideal case, site selection criteria for a proposed project would include the evaluation of mitigation costs of several alternative locations. However, for many critical facilities such as dams, ports, and other transportation facilities, there may be no alternative site. In such cases, a choice must be made between the two remaining alternatives: mitigating the risk through the selection of various techniques (described later), or choosing not to undertake mitigation and accepting the risk of liquefaction and possible structural dysfunction or failure.

The choice of accepting the risk of liquefaction, and the potential loss of life, social disruption, economic loss, and political ramifications that might result from structural failure, must be based upon the engineering evaluation of the site. However, the choice is not made only as a result of that evaluation. It must be addressed in a public policy and political context where input can be based on the determination of what is an "acceptable cost" or "level of risk." As this alternative is beyond the scope of this report, it will not be addressed

TABLE 5-2 Improvement of Liquefiable Soil Foundation Conditions

Method	Principle	Most Suitable Soil Conditions/Types	Maximum Effective Treatment Depth	Economic Size of Treated Area	Ideal Properties of Treated Material[a]	Applications[b]	Case[c]	Relative Costs[d]
			IN-SITU DEEP COMPACTION					
(1) Blasting	Shock waves and vibrations cause limited liquefaction, displacement, remolding, and settlement to higher density.	Saturated, clean sands; partly saturated sands and silts after flooding.	>40 m	Any size	Can obtain relative densities to 70–80%; may get variable density; time-dependent strength gain.	Induce liquefaction in controlled and limited stages and increase relative density to potentially nonliquefiable range.	2 3	Low ($2.00–$4.00/m³)
(2) Vibratory probe (a) Terraprobe (b) Vibrorods (c) Vibrowing	Densification by vibration; liquefaction-induced settlement and settlement in dry soil under overburden to produce a higher density.	Saturated or dry clean sand; sand.	20 m routinely (ineffective above 3–4 m depth); >30 m sometimes; Vibrowing, 40 m	>1,000 m²	Can obtain relative densities of 80% or more. Ineffective in some sands.	Induce liquefaction in controlled and limited stages and increase relative density to potentially nonliquefiable range. Has been shown effective in preventing liquefaction.	2 3	Moderate ($6.00–$13.00/m³)
(3) Vibrocompaction (a) Vibroflot (b) Vibro-Composer system (c) Soil Vibratory stabilizing	Densification by vibration and compaction of backfill material of sand or gravel.	Cohesionless soils with less than 20% fines.	>30 m	>1,000 m²	Can obtain high relative densities (over 85%), good uniformity.	Induce liquefaction in controlled and limited stages and increase relative densities to nonliquefiable condition. Is used extensively to prevent liquefaction. The dense column of backfill provides (a) vertical support, (b) drains to relieve pore water pressure, and (c) shear resistance in horizontal and inclined directions. Used to stabilize slopes and strengthen potential failure surfaces or slip circles.	1 2 △[e]	Low to moderate ($6.00–$9.00/m³)

(4) Compaction piles	Densification by displacement of pile volume and by vibration during driving, increase in lateral effective earth pressure.	Loose sandy soils; partly saturated clayey soils; loess.	>20 m	>1,000 m^2	Can obtain high densities, good uniformity. Relative densities of more than 80%.	Useful in soils with fines. Increases relative densities to nonliquefiable range. Is used to prevent liquefaction. Provides shear resistance in horizontal and inclined directions. Useful to stabilize slopes and strengthen potential failure surfaces or slip circles.	1 2 3	Moderate to high
(5) Heavy tamping (dynamic compaction)	Repeated application of high-intensity impacts at surface.	Cohesionless soils best, other types can also be improved.	30 m (possibly deeper)	>3,300 m^2	Can obtain high relative densities, reasonable uniformity. Relative densities of 80% or more.	Suitable for some soils with fines; usable above and below water. In cohesionless soils, induces liquefaction in controlled and limited stages and increases relative density to potentially nonliquefiable range. Is used to prevent liquefaction.	2 3	Low ($0.40–$6.00/m^3)
(6) Displacement/ compaction grout	Highly viscous grout acts as radial hydraulic jack when pumped in under high pressure.	All soils.	Unlimited	Small	Grout bulbs within compressed soil matrix. Soil mass as a whole is strengthened.	Increase in soil relative density and horizontal effective stress. Reduce liquefaction potential. Stabilize the ground against movement.	1 2 3	Low to moderate ($3.00-$15.00/m^3)

[a]SP, SW, or SM soils that have average relative density equal to or greater than 85 percent and the minimum relative density not less than 80 percent are in general not susceptible to liquefaction (TM 5-818-1). D'Appolonia (1970) stated that for soil within the zone of influence and confinement of the structure foundation, the relative density should not be less than 70 percent. Therefore, a criteria may be used that relative density increase into the 70–90 percent range is in general considered to prevent liquefaction. These properties of treated materials and applications occur *only under ideal conditions* of soil, moisture, and method application. The methods and properties achieved are not applicable and will not occur in all soils.

[b]Applications and results of the improvement methods are dependent on: (a) soil profiles, types, and conditions, (b) site conditions, (c) earthquake loading, (d) structure type and condition, and (e) material and equipment availability. Combinations of the methods will most likely provide the best and most stable solution.

[c]Site conditions have been classified into three cases. Case 1 is for beneath structures, Case 2 is for the not-underwater free field adjacent to a structure, and Case 3 is for the underwater free field adjacent to a structure.

[d]The costs will vary depending on: (a) site working conditions, location, and environment, (b) the location, area, depth, and volume of soil involved, (c) soil type and properties, (d) materials (sand, gravel, admixtures, etc.), equipment, and skills available, and (e) environmental impact factors. The costs are average values based on: (a) verbal communication from companies providing the service, (b) current literature, and (c) literature reported costs updated for inflation.

[e]△ means the method has potential use for Case 3 with special techniques required that would increase the cost.

TABLE 5-2 *Continued*

Method	Principle	Most Suitable Soil Conditions/Types	Maximum Effective Treatment Depth	Economic Size of Treated Area	Ideal Properties of Treated Material[a]	Applications[b]	Case[c]	Relative Costs[d]
			COMPRESSION					
(7) Surcharge/buttress	The weight of a surcharge/buttress increases the liquefaction resistance by increasing the effective confining pressures in the foundation.	Can be placed on any soil surface.	—	>1,000 m^2	Increase strength and reduce compressibility.	Increase the effective confining pressure in a liquefiable layer. Can be used in conjunction with vertical and horizontal drains to relieve pore water pressure. Reduce liquefaction potential. Useful to prevent movements of a structure and for slope stability.	2 3	Moderate if vertical drains used
			PORE WATER PRESSURE RELIEF					
(8) Drains (a) Gravel (b) Sand (c) Wick (d) Wells (for permanent dewatering)	Relief of excess pore water pressure to prevent liquefaction. (Wick drains have comparable permeability to sand drains.) Primarily gravel drains; sand/wick may supplement gravel drain or relieve existing excess pore water pressure. Permanent dewatering with pumps.	Sand, silt, clay.	Gravel and sand >30 m; depth limited by vibratory equipment; wick, >45 m	>1,500 m^2, any size for wick	Pore water pressure relief will prevent liquefaction.	Prevent liquefaction by gravel drains. Sand and gravel drains are installed vertically; however, wick drains can be installed at any angle. Dewatering will prevent liquefaction but not seismically induced settlements.	Gravel and sand 2 Δ^e Wick 1 2 3	Sand and gravel 0.3 m dia. ($11.50–$21.50/m^3); wick ($2.00–$4.00/m^3); dewatering very expensive
			INJECTION AND GROUTING					
(9) Particulate grouting	Penetration grouting—fill soil pores with soil, cement, and/or clay.	Medium to coarse sand and gravel.	Unlimited	Small	Impervious, high strength with cement grout. Voids filled so they cannot collapse under cyclic loading.	Eliminate liquefaction danger. Slope stabilization. Could potentially be used to confine an area of liquefiable soil so that liquefied soil could not flow out of the area.	1 2 3	Lowest of grout methods ($3.00–$30.00/m^3)

(10) Chemical grouting	Solutions of two or more chemicals react in soil pores to form a gel or a solid precipitate.	Medium silts and coarser.	Unlimited	Small	Impervious, low to high strength. Voids filled so they cannot collapse under cyclic loading.	Eliminate liquefaction danger. Slope stabilization. Could potentially be used to confine an area of liquefiable soil so that liquefied soil could not flow out of the area. Good water shutoff.	1 2 3	High ($75.00–$250.00/m³)
(11) Pressure-injected lime	Penetration grouting—fill soil pores with lime.	Medium to coarse sand and gravel.	Unlimited	Small	Impervious to some degree. No significant strength increase. Collapse of voids under cyclic loading reduced.	Reduce liquefaction potential.	1 2 3	Low ($10.00/m³)
(12)Electrokinetic injection	Stabilizing chemicals moved into and fills soil pores by electro-osmosis or colloids into pores by electro-phoresis.	Saturated sands, silts, silty clays.	Unknown	Small	Increased strength, reduced compressibility, voids filled so they cannot collapse under cyclic loading.	Reduce liquefaction potential.	1 2 3	Expensive
(13) Jet grouting	High-speed jets at depth excavate, inject, and mix a stabilizer with soil to form columns or panels.	Sands, silts, clays.	Unknown	Small	Solidified columns and walls.	Slope stabilization by providing shear resistance in horizontal and inclined directions, which strengthens potential failure surfaces or slip circles. A wall could be used to confine an area of liquefiable soil so that liquefied soil could not flow out of the area.	1 2 3	High $250.00–$650.00/m³

[a]SP, SW, or SM soils that have average relative density equal to or greater than 85 percent and the minimum relative density not less than 80 percent are in general not susceptible to liquefaction (TM 5-818-1). D'Appolonia (1970) stated that for soil within the zone of influence and confinement of the structure foundation, the relative density should not be less than 70 percent. Therefore, a criteria may be used that relative density increase into the 70–90 percent range is in general considered to prevent liquefaction. These properties of treated materials and applications occur *only under ideal conditions* of soil, moisture, and method application. The methods and properties achieved are not applicable and will not occur in all soils.

[b]Applications and results of the improvement methods are dependent on: (a) soil profiles, types, and conditions, (b) site conditions, (c) earthquake loading, (d) structure type and condition, and (e) material and equipment availability. Combinations of the methods will most likely provide the best and most stable solution.

[c]Site conditions have been classified into three cases. Case 1 is for beneath structures, Case 2 is for the not-underwater free field adjacent to a structure, and Case 3 is for the underwater free field adjacent to a structure.

[d]The costs will vary depending on: (a) site working conditions, location, and environment, (b) the location, area, depth, and volume of soil involved, (c) soil type and properties, (d) materials (sand, gravel, admixtures, etc.), equipment, and skills available, and (e) environmental impact factors. The costs are average values based on: (a) verbal communication from companies providing the service, (b) current literature, and (c) literature reported costs updated for inflation.

[e]△ means the method has potential use for Case 3 with special techniques required that would increase the cost.

TABLE 5-2 *Continued*

Method	Principle	Most Suitable Soil Conditions/Types	Maximum Effective Treatment Depth	Economic Size of Treated Area	Ideal Properties of Treated Material[a]	Applications[b]	Case[c]	Relative Costs[d]
			ADMIXTURE STABILIZATION					
(14) Mix-in-place piles and walls	Lime, cement, or asphalt introduced through rotating auger or special in-place mixer.	Sand, silts, clays, all soft or loose inorganic soils.	>20 m (60 m obtained in Japan)	Small	Solidified soil piles or walls of relatively high strength.	Slope stabilization by providing shear resistance in horizontal and inclined directions, which strengthens potential failure surfaces or slip circles. A wall could be used to confine an area of liquefiable soil so that liquefied soil could not flow out of the area.	1 2 3	High ($250.00–$650.00/m^3)
			THERMAL STABILIZATION					
(15) In-situ vitrification	Melts soil in place to create an obsidian-like vitreous material.	All soils and rock.	>30 m	Unknown	Solidified soil piles or walls of high strength. Impervious; more durable than granite or marble; compressive strength, 9–11 ksi; splitting tensile strength, 1–2 ksi.	Slope stabilization by providing shear resistance in horizontal and inclined directions, which strengthens potential failure surfaces or slip circles. A wall could be used to confine an area of liquefiable soil so that liquefied soil could not flow out of the area.	1 2 3	Moderate ($53.00–$70.00/m^3)

SOIL REINFORCEMENT								
(16) Vibro-replacement stone and sand columns (a) Grouted (b) Not grouted	Hole jetted into fine-grained soil and backfilled with densely compacted gravel or sand hole formed in cohesionless soils by vibro techniques and compaction of backfilled gravel or sand. For grouted columns, voids filled with a grout.	Sands, silts, clays.	>30 m (limited by vibratory equipment)	>1500 m^2; fine-grained soils, >1000 m^2	Increased vertical and horizontal load carrying capacity. Density increase in cohesionless soils. Shorter drainage paths.	Provides (a) vertical support, (b) drains to relieve pore water pressure, and (c) shear resistance in horizontal and inclined directions. Used to stabilize slopes and strengthen potential failure surfaces or slip circles. For grouted columns, no drainage provided but increased shear resistance. In cohesionless soil, density increase reduces liquefaction potential	1 2 Δ[e]	Moderate ($11.00–$70.00/m^3)
(17) Root piles, soil nailing	Small-diameter inclusions used to carry tension, shear, compression.	All soils.	Unknown	Unknown	Reinforced zone of soil behaves as a coherent mass.	Slope stability by providing shear resistance in horizontal and inclined directions to strengthen potential failure surfaces or slip circles. Both vertical and angled placement of the piles and nails.	1 2 3	Moderate to high

[a]SP, SW, or SM soils that have average relative density equal to or greater than 85 percent and the minimum relative density not less than 80 percent are in general not susceptible to liquefaction (TM 5-818-1). D'Appolonia (1970) stated that for soil within the zone of influence and confinement of the structure foundation, the relative density should not be less than 70 percent. Therefore, a criteria may be used that relative density increase into the 70–90 percent range is in general considered to prevent liquefaction. These properties of treated materials and applications occur *only under ideal conditions* of soil, moisture, and method application. The methods and properties achieved are not applicable and will not occur in all soils.

[b]Applications and results of the improvement methods are dependent on: (a) soil profiles, types, and conditions, (b) site conditions, (c) earthquake loading, (d) structure type and condition, and (e) material and equipment availability. Combinations of the methods will most likely provide the best and most stable solution.

[c]Site conditions have been classified into three cases. Case 1 is for beneath structures, Case 2 is for the not-underwater free field adjacent to a structure, and Case 3 is for the underwater free field adjacent to a structure.

[d]The costs will vary depending on: (a) site working conditions, location, and environment, (b) the location, area, depth, and volume of soil involved, (c) soil type and properties, (d) materials (sand, gravel, admixtures, etc.), equipment, and skills available, and (e) environmental impact factors. The costs are average values based on: (a) verbal communication from companies providing the service, (b) current literature, and (c) literature reported costs updated for inflation.

[e]Δ means the method has potential use for Case 3 with special techniques required that would increase the cost.

further in this section. Instead this chapter will examine the alternative remedial measures that are appropriate at the project site.

Actions to Mitigate Liquefaction

There are four general classes of mitigation measures available to the geotechnical engineer to ensure the desired functionality and safety of engineered projects subject to liquefaction. These classes are (Silver, 1985):

1. Changing operational procedures for the project (nonstructural solutions)
2. In-situ improvement
3. Changes to the project structure (structural solutions)
4. Control of undesirable pore water pressures (drainage solutions)

Operational procedures are decision options available to the owner or responsible operator of a project. After the likelihood of liquefaction failures and their consequences have been identified by appropriate investigations and analyses, the responsible entity, fully cognizant of the consequences of a project failure, may decide to:

- Take no action
- Control, relocate, or warn potentially affected parties to reduce loss of life or property
- Abandon the proposed or existing project

Although the most feasible operational option must be determined on a case-by-case basis, examples of the second option could include restricting access to potential hazard areas, early warning systems established through local law enforcement officials, and lowering of reservoirs to reduce inundation areas.

Methods for *improving in-situ foundation conditions* to reduce liquefaction susceptibility should consider the following techniques:

- Removal and replacement of unsatisfactory material
- Densification and increase of the lateral in-situ stress
- In-situ improvement by alteration of material
- Grouting or chemical stabilization

Removal and replacement of unsuitable material may be accomplished by:

- Excavation and engineered compaction of the existing soil
- Excavation and engineered compaction of materials improved with additives
- Excavation of existing soils and replacement with properly compacted nonliquefiable soils

Densification of in-situ material may be accomplished by:

- Compaction piles
- Vibratory probes
- Vibroflotation
- Compaction grouting
- Dynamic compaction (or consolidation)

Improved or altered in-situ material may be obtained by:

- Mixing in-place material with additives
- Removing in-place material by jetting and replacement with suitable material

Grouting operations may be carried out by pressure injection of chemicals, resins, or particulate matter into the voids of the potentially liquefiable foundation material. Figure 5-1 schematically illustrates the application of in-situ techniques to earth dams.

Structural solutions to mitigate the effects of liquefied soils in foundations or embankments can take several forms, but they are basically additions to the project to either stabilize or replace an unacceptable structure or foundation. For example, a berm may be added to the downstream slope of an embankment to increase its resistance to excessive deformation (slumping). A stable embankment may be similarly used to retain potentially liquefiable soils and prevent their flow or lateral spreading. A dam's freeboard could be increased to accommodate slumping yet retain a full reservoir. Where necessary, an additional independent structure may replace the function of the unacceptable structure; this would occur, for example, when a new downstream dam creates a larger reservoir that contains the original reservoir.

The questionable foundation support offered by liquefiable soils may be corrected by the use of end bearing piles, caissons, or fully compensated mat foundations designed for the predicted liquefaction phenomena. Complete removal and replacement of liquefiable soils have been necessary at some sites because of constraints and demands beyond the control of foundation engineers. The feasibility of freezing soils permanently to avert liquefaction may be considered in those cases that demand the use of in-situ soil. Examples of the use of structural measures for an earth dam are illustrated schematically in Figure 5-2.

Drainage solutions for control of undesirable pore pressures can lead to the acceptable performance of an otherwise liquefiable soil deposit. Control may be attained through the use of:

- Relief wells (stone columns)
- Dewatering systems

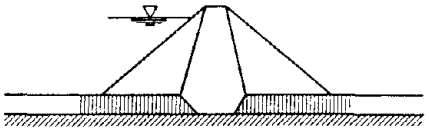

DENSIFICATION AND INCREASE OF LATERAL STRESS
- COMPACTION PILES
- VIBRATORY PROBE
- VIBROFLOTATION
- COMPACTION GROUTING

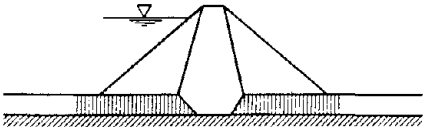

MATERIAL IMPROVEMENT
- INPLACE MIXING WITH ADDITIVES
- INPLACE JETTING AND REPLACEMENT

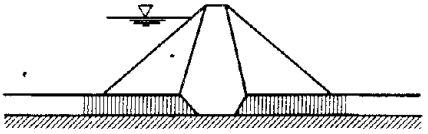

GROUTING (CEMENTATION)
- CHEMICAL GROUTING
- PARTICULATE GROUTING

FIGURE 5-1 Schematic illustration of some in-situ improvement techniques to reduce the liquefaction hazard for earth dams. Source: Silver (1985).

- Air injection into pore water
- Drains (e.g., chimney, blanket, and toe)
- Groundwater controls (e.g., ditches, upstream blankets, and plastic liners)

Control of pore pressures by means of pressure relief wells requires that the precise nature and extent of liquefiable deposits be well defined. Also, the likely mechanism of undesirable foundation performance resulting from excessive pore pressures must be identified to provide adequate drainage at critical locations.

Active dewatering systems involve the use of pumps and appropriate groundwater collection arrangements. In most cases, instrumentation

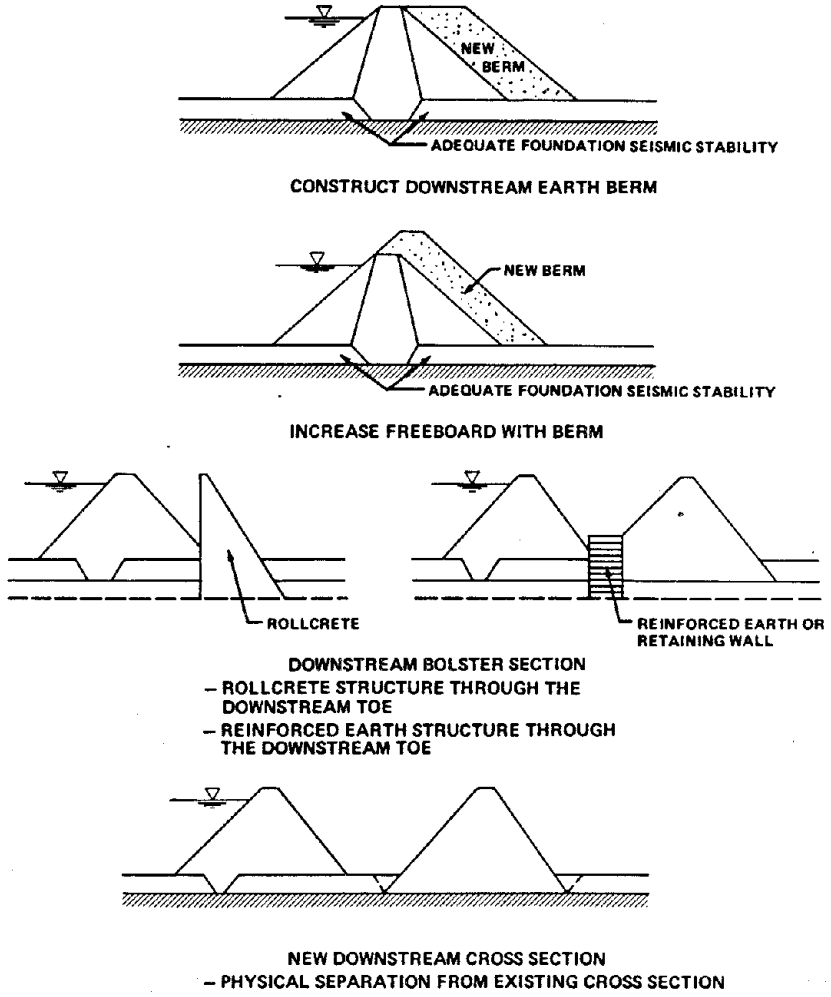

FIGURE 5-2 Schematic illustration of the use of structural measures to reduce the liquefaction hazard for earth dams. Source: Silver (1985).

for performance verification, such as piezometers, and an early warning method to detect rising groundwater levels are necessary. Precautions to prevent piping of fines from the foundation material during the lifetime of the project are necessary for this mitigation option.

Air injection into the pore water of potentially liquefiable soils has been discussed as a possible method of averting liquefaction. Liquefaction could be averted because the pores of the soil are partially filled with air so that compaction of the soil skeleton during seismic

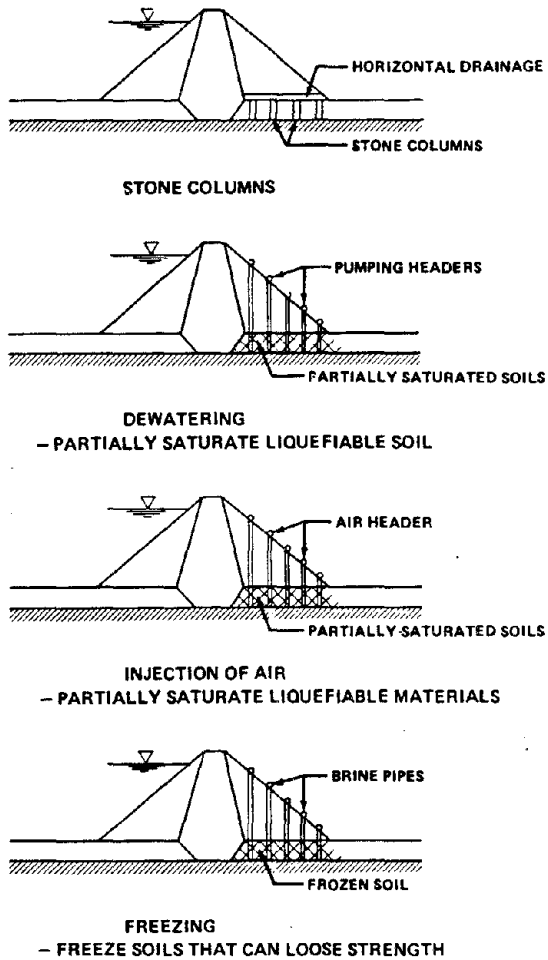

FIGURE 5-3 Schematic illustration of the use of groundwater control measures to reduce the liquefaction hazard for earth dams. Source: Silver (1985).

shaking does not appreciably increase the pore pressure. To date, however, there are no known applications of this technique.

Drains are an important class of method to reduce pore pressures in either liquefiable or nonliquefiable soils. Drains are most often incorporated into the design and construction of new facilities; in dams these may take the form of chimney drains, blanket drains, toe drains, and collector systems.

Areal groundwater controls are used to maintain known groundwater levels beneath the project. Plastic liners for ponds, upstream blankets

for reservoir projects, perimeter ditches to intercept groundwater flows, and slurry walls to serve as barriers to groundwater flow are all typical installations to accomplish areal groundwater control.

Figure 5-3 illustrates the application of groundwater control measures for earth dams.

General Considerations in the Selection of Remedial Measures

Feasibility

If remedial measures are required at an existing site, the potential methods most applicable for the site need to be identified and then studied for feasibility. For new sites, only in-situ improvement and drainage-type solutions would generally be considered.

For existing sites, nonstructural/operational solutions and structural solutions involve leaving the suspect material in place. Such solutions require that either satisfactory analyses of all potential failure modes be completed or that the potential consequences are acceptable. In general, the feasibility of in-situ improvement or drainage methods requires pilot studies at the site to verify that the effects of the proposed treatment will be accomplished. Field (and some laboratory) testing or monitoring will be required during the pilot program and can serve to establish the quality control measures for the treatment.

In-situ treatment methods generally remove the primary failure mode from consideration so that analysis is not required. However, some methods of in-situ improvement have been suggested that involve improvement or construction of columns or zones of treated ground while leaving the remainder untreated. Although such a support system can be analyzed by making an assumption that the stronger zones remain intact and stable, such a response is not certain. The use of such "islands" of improvement requires site-specific study before it can be offered as a recommended practice.

Effects of Remedial Measures Outside the Treatment Zone

Treatment is usually directed toward elimination of a specific failure mode. Care must be exercised to ensure that the treatment does not inadvertently produce an adverse response mechanism under a static or dynamic loading. Although specific cases of treatment producing an adverse secondary effect are not known and must be examined on a site-specific basis, several general scenarios can be postulated:

- In-situ densification of a foundation could produce settlement and resultant cracking of the existing structure.

- Drainage by relief wells or other means could increase hydraulic gradient and thereby increase the piping potential; thus, any drainage system should be designed with an adequate filter.
- Local densification of an area of the foundation or dam and foundation may result in differential settlement, resulting in cracking between portions of the structure overlying the treated and untreated foundation.
- Removal and replacement of potentially liquefiable material downstream of a dam may create an unstable seepage condition during the construction process.

Although the conditions cited may be remote, they serve as reminders to use common sense and good engineering judgment in correcting a problem. Correction protects against a hazard that is recognized but not easily analyzed. Treatment must not only correct the obvious problem but also guard against localized excessive strains and provide defense against potential secondary effects of cracking and piping.

Cost Versus Treatment Certainty

Remedial measures for liquefaction protection provide different levels of engineering confidence. Removal and replacement of material would be a virtually certain solution, while in-situ densification methods provide an estimated degree of improvement that may be considerably less certain and difficult to verify. Thus, in addition to direct construction costs, the value of the engineering confidence in the solution needs to be weighed.

Evaluation of a Specific Course of Action

Once a seismic stability problem has been identified and a decision for treatment has been made, the owner and the engineer are faced with a decision on the specific remedial measures to be taken. Any remedial work is bound to be expensive, and the profession has little experience for guidance. Among the difficulties confronting the engineer is verification that the work will positively improve stability. Thus, verifiability will be an important consideration in determining the best course of action in a particular case.

For some sites and structures, state-of-the-art techniques cannot guarantee the seismic stability. In that case, a decision must be made on what remedial measures or other courses of action are required. This obviously will be a very difficult decision and one that will be made at the policy levels within an organization, although it will require much technical assistance and advice from the engineer.

Because each structure and each site is unique, there will never be

a routine or "cookbook" approach to seismic stabilization treatment, but preliminary study of the problem suggests that there is a limited number of approaches from which to choose. The one that is most appropriate for a particular case will depend on the nature of the threat to stability, the consequences of failure, and the costs and benefits of remedial measures.

In the following paragraphs, specific courses of action are discussed that are identified as being potentially feasible, depending on the specific case or site conditions. The text (Marcuson and Franklin, 1983) and Table 5-2 (Ledbetter, 1985) provide information on some remedial improvements that can be made to the site and structure. Included are comments on the technical feasibility and adequacy of the mitigation measures, the possibility of verifying that the desired results have in fact been obtained, and data on cost to the extent that they are available. Implicit in the descriptions of methods are the long-term performance and maintenance requirements related to each remedial measure; these latter points must be fully evaluated. Community support for cost-effective seismic safety measures is often critical; therefore, positive public perception of the impact of these remedial measures must be promoted.

In-Situ Improvements

The efficacy of various forms of in-situ treatment is related to the grain size of the soil. Figure 5-4 summarizes this information, showing for comparison the grain size distributions most susceptible to liquefaction.

Grouting

The use of chemical and/or cement grout will increase the strength and stiffness of the foundation. Also, chemical and cement grouts are commonly used to reduce groundwater flow because they reduce average permeability. The increase in strengths in zones where the grout has penetrated can be verified by undisturbed sampling and testing. On the negative side, the decrease in permeability increases the drainage time and could increase the chance of postearthquake instability problems. Grouting is extremely expensive, and it is difficult to predict where the grout will go.

Grouts do not effectively penetrate silts and fine sands, so it cannot be guaranteed that continuous zones of liquefiable material will not remain even after a diligently executed grouting program. Additionally, there is a toxicity problem with some grouting chemicals; environmental considerations would preclude their use. If grouting is successful, it is a permanent solution that would require only infrequent verification.

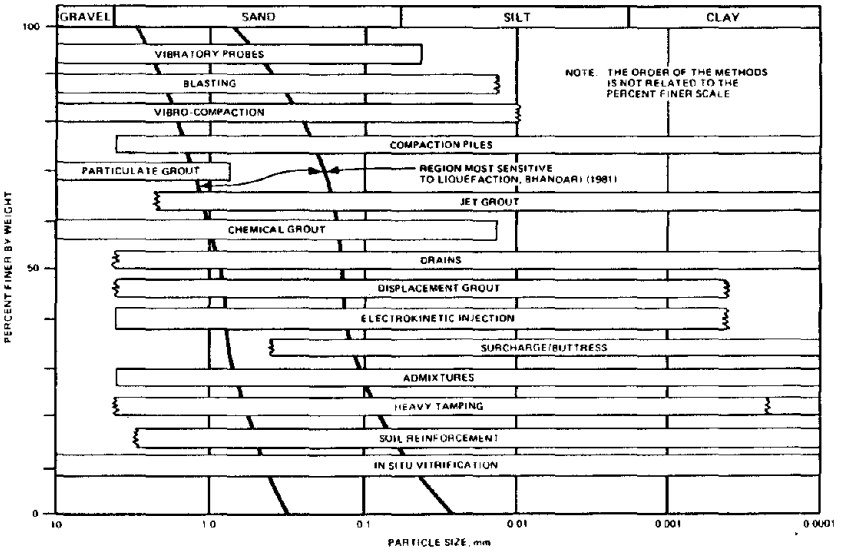

FIGURE 5-4 Applicable grain size ranges for soil improvement methods. Jagged lines at the ends of a bar indicate the uncertainty of applicability of the method. Source: Ledbetter (1985).

In-Situ Densification of the Foundation

Experience indicates that vibroflotation or the use of compaction piles with soil replacement can increase the relative density of foundation sands to about 70 percent. In most cases such an improvement would be adequate to preclude flow failures, but present knowledge suggests that large strains are still possible in the event of major earthquakes. Such techniques have been used to densify sands prior to construction, but they have not yet been used under an existing dam.

Under favorable conditions, such an approach would have the advantage of moderate cost as compared to some other methods, and the increase of density can be verified approximately using CPT, SPT, fixed-piston undisturbed samples, and measurements of surface heave and displacement. On the other hand, problems of differential settlements result. In fact, differential settlements are unavoidable and the potential for cracking and piping would be relatively high. Also, remolding of the sands by the densification process would mean that the gain in strength because of densification would be partially offset by the loss of the beneficial effects of age (and perhaps cementation) on the sand structure. Densification is a permanent solution and requires no maintenance.

Several in-situ densification techniques have been successfully used or are under development. These include compaction piles, dynamic

consolidation, vibratory probes, jet grouting, and compaction. Selections among these alternatives must include depth of treatment required, character of soils to be treated, and other factors.

Structural Solutions

The design of a new structure can, to some extent, incorporate features that would enhance its ability to resist damage in the event that liquefaction occurs on all or part of the site. It also may be possible to modify existing structures to reduce the consequences of liquefaction. It may be possible to reconstruct an existing structure incrementally, thereby permitting continued partial use. Features that enhance a structure's ability to withstand liquefaction damage include:

- Ductility
- Ability to accommodate large deformations
- Redundancy in foundation and superstructures
- Capacity for adjustment of supports to correct differential settlement (leveling)
- A foundation design that can span soft spots, such as a unified, stiff foundation mat
- Partial buoyancy (limited feasibility)

The foregoing solutions may lessen the possibility of serious damage, but probably will not completely solve the problem. They are most likely to be attractive for structures where some damage is acceptable and when other mitigations are too costly.

Structural approaches that would mitigate the effect of liquefaction include:

- Surcharge
- Replacement of structure
- Increased freeboard (for a dam)
- Decreases in shear stresses applied by the structure to the soil in question, as by constructing berms

Surcharge

In many instances stability can be improved by a surcharge that will result in higher effective confining stresses. This increase in initial effective stress increases the cyclic strength and the shear modulus of cohesionless soils. For dams, a surcharge may take the form of a berm. Verification of such action is straightforward since it relies only on measurements of geometry. On the other hand, preliminary analyses of the increase in liquefaction resistance show that modest surcharges will produce modest improvements in cyclic strength. Verification of the ultimate safety requires reliance on the definition of the design

earthquake, on the accurate measurement of liquefaction resistance from SPT or laboratory tests, and on the accurate prediction of cyclic stresses from a dynamic analysis. A temporary surcharge in combination with drainage wicks or devices may sometimes be used to increase in-situ density.

Replacement in a New Location

An extreme solution to the problem of a potentially unstable structure would be to build a replacement structure. Such a solution can be made almost totally safe except in the epicentral region of earthquakes with magnitudes greater than 8.0. For example, with the new structure all doubtful materials could be removed from the foundation and dense rolled-filled earth could be used for backfill. Such a solution presents the problems of high expense and the possible requirement of a new environmental impact statement. In some cases an acceptable site for the replacement structure may not exist.

Drainage Solutions

Dewatering

A potential solution is the permanent dewatering of saturated liquefiable zones. This would increase the effective stress, strength, and moduli, all of which would benefit stability. Also, partially saturated materials generally are not susceptible to seismically induced liquefaction. Positive factors include the facts that the liquefaction threat is eliminated even if the dewatering system does not survive the earthquake, and that if dewatering is successful it is completely effective, which can be easily verified by piezometers and geophysical techniques.

Dewatering a foundation sand below the water table is easier said than done. It might require continuous pumping as well as upstream and downstream slurry trenches, and even then there is no guarantee at the outset that an alluvial foundation can be dewatered. Positive seepage cutoff can be used in conjunction with a dewatering system to provide the required treatment.

Reduction in Drainage Paths

Stone columns or relief wells could be installed to reduce the lengths of drainage paths, thus allowing drainage and pore pressure dissipation to occur during the earthquake. Limited drainage greatly reduces pore pressure buildup during cyclic loading. (Stone columns were installed at the Jensen Filtration Plant following the San Fernando earthquake.) The effectiveness of the stone columns or relief wells could be verified with field pumping tests and piezometers. On the negative side, there is no proven way to install graded filters around stone columns, and

consequently there is no way to eliminate the possibility of piping. There is also no guarantee that these drains will not clog with time. Furthermore, there is no available field testing method to verify the performance of this action short of the actual earthquake occurrence.

Operational Solutions for Dams

Several nonstructural measures are particularly applicable to dams and may be worth considering for other structures in special situations. These measures are:

- Limiting public access to areas that might be dangerous in a liquefaction situation (e.g., downstream areas for dams).
- Lowering the maximum water level in the reservoir.

No Remedial Action

In some cases it may be concluded that the probability and consequences of failure are sufficiently small that the risk is a tolerable one and requires no remedial action. The reasoning behind such a course of action follows from the fact that major earthquakes are, in general, rare events. Maximum earthquakes have return periods of hundreds to tens of thousands of years. If the structure can be shown to be safe for lesser earthquakes with shorter return periods, then the risk might be acceptable, especially if only economic loss is involved. Certainly, some level of risk must be acceptable, since there is no such thing as "zero risk." In the case of dams the hydraulic design admits some probability of overtopping failure for floods larger than the "probable maximum flood." The estimated return periods of floods used for designing dams span 200 to 500 years.

It can be argued that the risk of failure due to an earthquake does not need to be smaller than the risk of overtopping failure, but the level of risk should be in balance with the public interest in the areas of safety, economics, and social impact. Ultimately, a decision on what constitutes an acceptable level of risk is one of public policy and is not a proper exercise of engineering judgment.

Negative factors in the "no action" option include the following:

- Engineers will have many problems in presenting the risk-based analysis and design to the public, primarily because of lack of experience.
- The present data base on return periods of earthquakes is weak.
- Presently, no more than a judgment can be made about the combined probability of experiencing the design earthquake and having the structure fail.

Summary

This chapter has discussed various ways of mitigating the potential for liquefaction. Technical and nontechnical considerations used in selecting the most appropriate alternatives have been examined. A shopping list of some of the alternatives has been provided and discussed in terms of technical adequacy, field verifiability, cost, long-term performance, environmental impact, and other factors. This discussion is not meant to be exhaustive but rather gives the owner or decision maker an idea of some of the issues involved.

Table 5-2 presents some considerations for 17 procedures to improve liquefiable soil foundation conditions. Careful consideration must be given to the technical feasibility and effectiveness of each procedure and its limitations. The short-term and long-term impacts on the public's needs and its perception of the effect of procedures on the environment must be carefully evaluated.

Research needs suggested in other parts of this report will largely satisfy the research required to improve understanding of how to lessen the potential for liquefaction. For example, research aimed at providing insight into the basic mechanism of how a dam fails when liquefied will also shed light on how best to stabilize the dam.

There is very little field experience to provide guidance in dealing with the treatment of sites and structures that have potential seismic liquefaction problems. Consequently, as owners and engineers start to deal with these problems in the late 1980s and 1990s, they must feel their way carefully and must be diligent in collecting and making full use of whatever relevant experience is available. This requires careful documentation of case histories.

6
Research Needs

The damaging effects of soil liquefaction were brought to the attention of engineers in 1964 by the disastrous earthquake in Niigata, Japan. Since then, impressive developments have been made in recognizing liquefaction hazards, understanding liquefaction phenomena, analyzing and evaluating the potential for liquefaction at a site, and developing the technology for mitigating liquefaction hazards. It is now known that liquefaction can occur in a variety of situations with soils of different properties and under stress conditions having different characteristics. Consequently, present methods require more expansion, especially through applied research to improve the assessment and mitigation of liquefaction hazard. To support applied research, there is a need for basic studies into the mechanisms of liquefaction under earthquake stresses. Such basic research can assist in extending and refining the practical methods.

All liquefaction problems have economic consequences that result in public and governmental involvement. Better public and governmental understanding of liquefaction and liquefaction engineering can provide needed support for research and for the development and implementation of remedial measures to improve structures and soil deposits to resist liquefaction. Societal issues concerning public awareness, zoning, and planning will continue to be important in liquefaction studies. The impact of these issues, however, requires more study than has been performed to date.

International cooperation on liquefaction research offers the possibility of significant benefits. Both Japan and China have frequently experienced liquefaction during earthquakes, sometimes with widespread costly damage. In some ways, particularly in field studies, research on liquefaction in these two countries is ahead of such research in the United States.

Specific research needs were identified by participants at the workshop. These needs have been categorized under two general headings: new initiatives and vital continuing studies.

New Initiatives

There are a number of research needs that have recently emerged as being important. Some of these initiatives are under way but are recent enough to be considered as new. The new initiatives identified by the committee involve: (1) instrumentation in highly seismic regions, (2) study of the liquefaction of soils other than clean sands, (3) methods of evaluating the magnitude of permanent soil deformations caused by earthquakes, (4) validation of the improved behavior of treated foundations and soils and procedures to predict the performance of at-risk building structures, (5) in-situ study of the state-of-stress effect, (6) centrifuged model tests on idealized soil structures, and (7) the use of explosive-generated stress waves.

1. Instrumentation of a limited number of selected sites is needed in highly seismic regions, where there is a high probability that liquefaction will soon occur, and at saturated cohesionless sites where pore pressure is expected to increase without liquefaction occurring. The installation of field instrumentation (e.g., pore pressure transducers and recorders, strong-motion accelerometers) at both types of site should proceed as expeditiously as possible.

The areas of anticipated liquefaction should include level and sloping ground so that differences in effects under these conditions can be identified and recorded. In addition, the characteristics of the sites should be determined before the anticipated earthquake to provide a knowledge of preearthquake conditions. (Sites where liquefaction will not occur in the near future are of lower priority in this regard since their characteristics are not likely to be significantly changed by the effects of the earthquake shaking; the soils' properties can be explored after an earthquake if necessary.) The requirements for the selection and instrumentation of one or more field sites are treated in more detail later in this chapter.

It has been observed that certain sites reliquefy during aftershocks, after liquefying during the main earthquake. Depending on the magnitude of the main shock, strong aftershocks occur after intervals of days to months. A substantial amount of information could be obtained by rapid deployment of equipment after a moderate to large earthquake, even if no pore pressure instrumentation were in place at the time of the main shock. Therefore short-term results can be obtained if portable installations are made ready for mobilization to record events associated with aftershocks. This arrangement avoids the maintenance and reliability problems that plague long-term installation of electrical gauges in saturated soil.

2. Study is needed of the liquefaction of soils other than clean sands. Recent field experience in China and in Idaho suggests that our

understanding of the dynamic strength of gravels and gravelly soils is not complete and that these soils can be susceptible to liquefaction. The study of gravels and gravelly soils is made difficult by sampling problems and by the large-scale equipment needed to test these materials in the laboratory. The potential use of these soils in remedial measures to improve safety against liquefaction emphasizes the need for a basic understanding of how such materials behave under dynamic loading.

On the other hand, understanding of those soil characteristics that preclude liquefaction is important to identify in-situ conditions where liquefaction may not be a concern. Experience shows that many soils with plasticity do not experience significant loss of strength in earthquakes. Substantial benefits will be derived from a better understanding of the limits (e.g., on grain size distribution, plasticity index, liquidity index, and permeability) outside which dynamic loss of soil strength and liquefaction instability need not be considered.

3. Methods of evaluating the magnitude of permanent soil deformations induced by earthquake shaking, while considered in the past, have emerged as a pressing need to understand the dynamic behavior of structures and soil deposits. Both triggering and dynamic soil strength must be considered in studying the effect of liquefaction or high pore pressures on deformations. Calculations based upon realistic constitutive models are needed to help comprehend the development of permanent deformations and progressive failure. The causes and development of delayed failure also require study. Understanding conditions under which unrestrained flow will develop is more advanced than understanding conditions when limited strain will take place. This difference in strain potential has important consequences when determining the safety of all classes of projects and requires immediate study.

4. Validation of the improved behavior of foundations and soil structures that have been treated to increase dynamic stability has become a major need. The number of case studies concerning the stability of natural deposits far exceeds field evidence of improved behavior of deposits that have been altered by drainage or in-situ soil improvement. Almost completely lacking are case histories involving sites or earth structures that have been improved and then subjected to earthquake shaking. This type of documentation should be developed wherever possible, and the relevant studies can be combined, in some cases, with fundamental investigations of pore pressure development in untreated adjacent regions of natural or fill soils.

It is necessary to develop procedures for analyzing and determining the probable performance of buildings constructed on soil deposits

vulnerable to liquefaction in the free field but for which the behavior under building loads may be significantly different. This is an especially important problem in built-up areas where liquefaction is likely, particularly for foundations that rely on deep piles that penetrate liquefiable soils and for wharf facilities built behind sheet piles or other types of bulkheads.

5. In-situ study of the effect of state of stress is also important for a better understanding of how remedial measures may be used to reduce the potential for soil liquefaction. It is known that in-situ densification and increase in lateral stress act together to improve dynamic soil strength. The ability to measure the in-situ state of stress (K_o) in soils susceptible to liquefaction would be a powerful tool to help verify that a remedial measure has adequately reduced liquefaction susceptibility.

6. Centrifuge model tests on idealized soil structures are needed to provide insights into mechanisms of failure associated with soil liquefaction. Such tests also may provide data for checking the applicability of analytical methods related to soil liquefaction. Model tests at normal gravity on very large shaking tables, permitting use of earth masses a meter or more in thickness, also have potential value.

7. The use of explosion-generated stress waves for studying liquefaction should be pursued. This offers the possibility of making detailed measurements on the process of liquefaction at prepared and instrumented sites. Although explosion-generated stress waves differ in characteristics from earthquake-generated stress waves, they do provide the possibility of examining the mechanism of liquefaction under controlled conditions.

Vital Continuing Studies

Although work in the following topic areas has been under way for some time, it is essential that research along these lines continue. Work of this type forms the vital backbone of liquefaction studies.

1. Continued investigations are needed of recent earthquake sites where liquefaction has occurred, or where unexpectedly it did not occur. The object here is to provide well-documented case histories that will yield insights into the liquefaction potential of soils, and data that can be used to explore the validity of analyses of experimental concepts and to refine and develop empirical correlations.

2. Continuing research is needed into new methods of measuring in-situ properties that reflect the liquefaction characteristics of soils, providing a reliable basis for identifying potentially liquefiable and

nonliquefiable sites. Most work to date has related liquefaction conditions to penetration test data, but other in-situ techniques need to be developed, especially for conditions where standard types of penetration tests (e.g., SPT and CPT) cannot be used.

3. Continued attention should be given to the development of laboratory tests procedures that will provide improved methods of characterizing the liquefaction properties of soils. This subject has received much attention in the past, but there are still important aspects that need clarification or in which new and important contributions can be made.

4. At a basic level there is a need for imaginative, continued development of constitutive (stress-strain) relations for soils applicable to the special circumstances of liquefaction. Both field instrumentation projects and centrifuge tests to evaluate the applications of such theories should be made.

Establishment of an International Experimental Site

In view of the particular importance attached to observations during actual earthquakes, the possibility of establishing an experimental site should be explored. Its general purpose would be to obtain field measurements of such factors as accelerations, pore pressures, and deformations under structures or within earth structures during actual earthquakes. Use of the site and data should be open to any researcher for testing field, laboratory, and theoretical techniques.

Obviously the site must be established at a location where strong ground motions can be expected within 5 to 10 years. For example, the success of the SMART ground motion array in Taiwan would make it a strong candidate for site selection, and a significant earthquake at Parkfield, California, has been predicted for the time period 1985-1992.* Earthquakes are expected in the southern California region during the next decade. Other locations, possibly in Japan, may also be available.

It will be necessary to establish an organization to develop, operate, and manage such a site. One essential step is a thorough exploration of the site to establish the basic characteristics of the soils (and rocks) present. Any structures such as embankments must be constructed, and all recording equipment must be installed, maintained, and oper-

*Since the workshop, the U.S. Geological Survey and Brigham Young University have proceeded with plans to place instruments at a free-field level ground site in Cholame Valley near Parkfield. This is an important step, but it falls short of the objectives of the proposed experimental site. Furthermore, being on private land, the Cholame Valley site might not be available as an international test site.

ated. Possibly the organization would be responsible for at least some degree of processing of recorded data.

Researchers using the site, or data from the site, would be funded separately from the funding for the development and operation of the site. A somewhat analogous situation is the large-scale structural testing under the U.S.-Japan program, where participation of the U.S. researchers in prediction of behavior and analysis of results was encouraged via a Request for Proposals.

It is recommended that consideration be given to forming a group to develop such a plan in more detail—identifying the best site, defining specific plans for construction of structures and concerning instrumentation, and preparing cost estimates for the development and operation of the site.

References

American Society for Testing and Materials (ASTM) (1984) "Standard Method for Deep, Quasi-Static, Cone and Friction-Cone Penetration Tests of Soil," pp. 533-540 in *Annual Book of Standards, Volume 4.08*, D3441-1979, American Society for Testing and Materials, Philadelphia, Pennsylvania.

Anagnos, T., and A. S. Kiremidjian (1984) "Stochastic Time-Predictable Model for Earthquake Occurrences," *Bulletin of the Seismological Society of America* 74(6):2593-2611.

Andersen, K. H. (1976) "Behavior of Clay Subjected to Undrained Cyclic Loading," pp. 392-403 in *Proceedings of the First International Conference on Behavior of Offshore Structures, Volume 1*, Norwegian Geotechnical Institute, Oslo, Norway.

Andersen, K. H. (1983) *Report, Foundation Analyses for Gravity Platforms—Stability, Soil Stiffness and Settlements*, Lecture, presented at the NIF-Course "Fundamentberegninger for Gravitasjonsplattformer," Fagernes 5.-7.12.1983, December 1983, Norwegian Geotechnical Institute, Oslo, Norway.

Andersen, K. H., O. E. Hansteen, K. Hoeg, and J. H. Prevost (1978) *Soil Deformations Due to Cyclic Loads on Offshore Structures*, Pub. No. 120, Norwegian Geotechnical Institute, Oslo, Norway.

Andersen, K. H., J. H. Pool, S. F. Brown, and W. F. Rosenbrand (1980) "Cyclic and Static Laboratory Tests on Drammen Clay," *Journal of the Geotechnical Engineering Division, ASCE* 106(GT5):499-529.

Anderson, L. R., J. R. Keaton, K. Aubry, and S. J. Ellis (1982) *Liquefaction Potential Map for Davis County, Utah*, Department of Civil and Environmental Engineering, Utah State University, Logan, Utah.

Andreson, A., and L. Bjerrum (1967) "Slides in Subaqueous Slopes in Loose Sand and Silt," pp. 221-239 in *Marine Geotechnique*, A. F. Richards, ed., University of Illinois Press, Urbana, Illinois.

Annaki, M., and K. L. Lee (1977) "Equivalent Uniform Cycle Concept for Soil Dynamics," *Journal of the Geotechnical Engineering Division, ASCE* 103(GT6):549-564.

Arulanandan, K. (1977) "Method and Apparatus for Measuring In-Situ Density and Fabric Soils," patent application, Regents of the University of California, Berkeley, California.

Arulanandan, K., A. Anandaraj, and A. Abghari (1983) "Centrifuge Modelling of Soil Liquefaction Susceptibility," *Journal of Geotechnical Engineering, ASCE* 109(103):281-300.

Arulmoli, K., K. Arulanandan, and H. B. Seed (1985) "New Method for Evaluating Liquefaction Potential," *Journal of Geotechnical Engineering, ASCE* 111(1):95-114.

Atkinson, G. M., and W. D. L. Finn (in press) (1985) "PROLIQ-2, A Computer Program for Estimating the Probability of Liquefaction including Areal and Fault Sources," *Soil Mechanics Report*, Department of Civil Engineering, University of British Columbia, Vancouver, B.C., Canada.

Atkinson, G. M., W. D. L. Finn, and R. G. Charlwood (1984) "Simple Computation of Liquefaction Probability for Seismic Hazard Applications," *Earthquake Spectra* 1(1):107-123.

Baladi, G. Y., and B. Rohani (1979) "Elastic-Plastic Model for Saturated Sand," *Journal of the Geotechnical Engineering Division, ASCE* 105(GT4):465-480.

Baldi, G., R. Bellotti, V. Ghionna, M. Jamiolkowsi, and E. Pasqualini (in press) (1985) "Penetration Resistance and Liquefaction of Sands," *Proceedings of the Eleventh International Conference on Soil Mechanics and Foundation Engineering*, A. A. Balkema Publishers, Rotterdam, Netherlands.

Bea, R. G., and J. M. E. Audibert (1980) "Offshore Platforms and Pipelines in Mississippi River Delta," *Journal of the Geotechnical Engineering Division, ASCE* 106(GT8):353-369.

Bea, R. G., S. G. Wright, P. Sircar, and A. W. Niedoroda (1980) "Wave-Induced Slides in South Pass Block 70, Mississippi Delta," Preprint 80-506, ASCE Convention and Exposition, Miami, Florida, October 1980, New York, New York.

Been, K., J. H. A. Crooks, D. E. Becker, and M. G. Jefferies (1985) "State Parameter Interpretation of the Cone Penetration Test in Sands," submitted for publication in *Geotechnique*, March 1985.

Bennett, M. J., T. L. Youd, E. L. Harp, and G. F. Wieczorek (1981) *Subsurface Investigation of Liquefaction, Imperial Valley Earthquake, California, October 15, 1979*, Open-File Report 81-502, U.S. Geological Survey, Menlo Park, California.

Bennett, M. J., McLaughlin, J. S. Sarmiento, and T. L. Youd (1984) *Geotechnical Investigation of Liquefaction Sites*, Open-File Report 84-252, U.S. Geological Survey, Menlo Park, California.

Bhandari, R. K. M. (1981) "Dynamic Consolidation of Liquefiable Sands," pp. 857-860 in *Proceedings of the International Conference on Recent Advances in Geotechnical Earthquake Engineering and Soil Dynamics, Volume 2*, University of Missouri, Rolla, Missouri.

Bierschwale, J. G., and Stokoe, K. H., II (1984) *Analytical Evaluation of Liquefaction Potential of Sands Subjected to the 1981 Westmorland Earthquake*, Geotechnical Engineering Report GR-84-15, Civil Engineering Department, University of Texas, Austin, Texas.

Birkeland, P. W. (1984) *Soils and Geomorphology*, Oxford University Press, New York, New York.

Blouin, S. E., and J. D. Shinn II (1983) *Explosion Induced Liquefaction*, Report to the U.S. Air Force Office of Scientific Research, Applied Research Associates, Inc., South Royalton, Vermont.

Booker, J. R., M. S. Rahman, and H. B. Seed (1976) *GADFLEA—A Computer Program for the Analysis of Pore Pressure Generation and Dissipation During Cyclic or Earthquake Loading*, Report No. EERC 76-24, Earthquake Engineering Research Center, University of California, Berkeley, California.

Bouckovalas G., R. V. Whitman, and W. A. Marr (1984) "Permanent Displacement of Sand with Cyclic Loading," *Journal of Geotechnical Engineering, ASCE* 110(11):1606-1623.

Campanella, R. G., and P. K. Robertson (1984) "A Seismic Cone Penetrometer to Measure Engineering Properties of Soil," *Proceedings of the Fifty-fourth Annual Meeting of the Society of Exploration Geophysicists*, Atlanta, Georgia.

Carson, S. E., and J. C. Matti (1982) *Contour Map Showing Minimum Depth to Groundwater, Upper Santa Ana River Valley Area, California, 1973-1979*, Open-File Report 82-1128, U.S. Geological Survey, Menlo Park, California.

Casagrande, A. (1936) "Characteristics of Cohesionless Soils Affecting the Stability of Slopes and Earth Fills," *Journal of the Boston Society of Civil Engineers*, reprinted in *Contributions to Soil Mechanics, 1925 to 1940*, Boston Society of Civil Engineers, Oct. 1940, pp. 257-276.

Casagrande, A. (1938) "The Shearing Resistance of Soils and its Relation to the Stability of Earth Dams," *Proceedings of the Soils and Foundation Conference of the U.S. Engineer Department.*

Casagrande, A. (1965) "Role of the 'Calculated Risk' in Earthquake and Foundation Engineering," *Journal of the Soil Mechanics and Foundations Division, ASCE* 91(SM4):1-40.

Casagrande, A. (1975) "Liquefaction and Cyclic Deformation of Sands—A Critical Review," *Proceedings of the Fifth Pan American Conference on Soil Mechanics and Foundation Engineering*, Buenos Aires, Argentina; also published as Harvard Soil Mechanics Series No. 88, January 1976, Harvard University, Cambridge, Massachusetts.

Casagrande, A., and F. Rendon (1978) *Gyratory Shear Apparatus Design, Testing Procedures, and Test Results on Undrained Sand*, Technical Report S-78-15, U.S. Army Corps of Engineers, Waterways Experiment Station, Vicksburg, Mississippi; also published as Harvard Soil Mechanics Series No. 89, Harvard University, Cambridge, Massachusetts.

Castro, G. (1969) *Liquefaction of Sands*, thesis presented to Harvard University in fulfillment of the requirements for the degree of Doctor of Philosophy.

Castro, G. (1975) "Liquefaction and Cyclic Mobility of Saturated Sands," *Journal of the Geotechnical Engineering Division, ASCE* 101(GT6):551-569.

Castro, G. (1976) "Comments on Seismic Stability Evaluation of Embankment Dams," *Proceedings of the Conference on Evaluation of Dam Safety.*

Castro, G., and S. J. Poulos (1977) "Factors Affecting Liquefaction and Cyclic Mobility," *Journal of the Geotechnical Engineering Division, ASCE* 103(GT6):501-506.

Castro, G., S. J. Poulos, J. W. France, and J. L. Enos (1982) *Liquefaction Induced by Cyclic Loading*, Report to National Science Foundation, Geotechnical Engineers, Inc., Winchester, Massachusetts.

Castro, G., S. J. Poulos, and F. D. Leathers (1985) "A Re-examination of the Slide of the Lower San Fernando Dam," *Journal of Geotechnical Engineering, ASCE* 111(GT9).

Chameau, J. L., and G. W. Clough (1983) "Probabilistic Pore Pressure Analysis for Seismic Loading," *Journal of Geotechnical Engineering, ASCE* 109(4):507-524.

Chameau, J. L., and J. L. Gunaratne (1984) "Performance Evaluation in Geotechnical Engineering Using Fuzzy Sets," pp. 264-267 in *Proceedings of the Fourth ASCE Specialty Conference on Probabilistic Mechanics and Structural Reliability*, ASCE, New York, New York.

Chang, C. S. (1981) "Residual Pore Pressure and Deformation Behavior of Soil Samples Under Variable Cyclic Loading," pp. 107-110 in *Proceedings of the International Conference on Recent Advances in Geotechnical*

Earthquake Engineering and Soil Dynamics, Volume 1, University of Missouri, Rolla, Missouri.

Chang, C. S., C. L. Kuo, and E. T. Selig (1983) "Pore Pressure Development during Cyclic Loading," *Journal of Geotechnical Engineering, ASCE* 109(1):103-107.

Charlie, W. A., G. E. Veyera, S. R. Abt, and H. D. Patrone (1983) "Blast-Induced Liquefaction—State-of-the-Art," pp. 62-68 in *Proceedings of the Symposium on the Interaction of Non-Nuclear Munitions with Structures, Part 2*, U.S. Air Force Academy, Colorado Springs, Colorado.

Charlie, W. A., G. E. Veyera, and S. R. Abt (1985) "Predicting Blast Induced Porewater Pressure Increases in Soils," *Journal of Civil Engineering for Practicing and Design Engineers* 4(3).

Cheney, J. A., et al. (1983) "Workshop for Development of Specifications for a Ground Motion Simulator for Centrifuge Modelling in Geotechnical Engineering," Department of Civil Engineering, University of California, Davis, California.

Christian, J. T., and J. M. E. Audibert (1976) "Analysis of Offshore Concrete Caisson Dikes Under Cyclic Loading," pp. 979-990 in *Proceedings of the Second International Conference on Numerical Methods in Geomechanics, Volume 2*, Virginia Polytechnic Institute, Blacksburg, Virginia, June 1976, published by ASCE, New York, New York.

Christian, J. T., and W. F. Swiger (1975) "Statistics of Liquefaction and SPT Results," *Journal of the Geotechnical Engineering Division, ASCE* 101(GT33):1135-1150.

Christian, J. T., P. K. Taylor, J. K. C. Yen, and D. C. Erali (1974) "Large Diameter Underwater Pipeline for Nuclear Power Plant Designed against Soil Liquefaction," pp. 597-606 in *Proceedings of the Offshore Technology Conference, Volume 2*, Paper OTC 2094, Offshore Technology Conference, Dallas, Texas.

Christian, J. T., R. W. Borjeson, and P. T. Tringale (1978) "Probabilistic Evaluation of OBE for Nuclear Plant," *Journal of the Geotechnical Engineering Division, ASCE* 104(GT7):907-919.

Chugh, A. K., and J. L. Von Thun (1985a) "Pore Pressure Response Analysis for Earthquakes," pp. 1367-1378 in *Proceedings of the Fifth International Conference on Numerical Methods in Geomechanics, Volume 3*, ASCE, New York, New York.

Chugh, A. K., and J. L. Von Thun (1985b) "Pore Pressure Response Analysis for Earthquakes," submitted for publication in *Canadian Geotechnical Journal*.

Cornell, C. A. (1968) "Engineering Seismic Risk Analysis," *Bulletin of The Seismological Society of America* 58(5):1583-1606.

Cornell, C. A. (1971) "Probabilistic Analysis of Damage to Structures Under Seismic Loads," *Dynamic Waves in Civil Engineering*, D. A. Howells, I. D. Haigh, and C. Taylor, eds., Wiley-Interscience, London.

Cox, D. R. (1970) *The Analysis of Binary Data*, Methuen, London, Great Britain.

D'Appolonia, E. (1970) "Dynamic Loading," *Journal of the Soil Mechanics and Foundations Division, ASCE* 96(SM1):49-72.

Davis, R. O., and J. B. Berrill (1981) "Assessment of Liquefaction Potential Based on Seismic Energy Dissipation," pp. 187-190 in *Proceedings of the*

International Conference on Recent Advances in Geotechnical Earthquake Engineering and Soil Dynamics, Volume 1, University of Missouri, Rolla, Missouri.

Davis, R. O., and J. B. Berrill (1982) "Energy Dissipation and Seismic Liquefaction in Sands," in *Earthquake Engineering and Structural Dynamics* 10:59-68.

De Alba, P. (1982) *A Model Study of Pile Settlement in Liquefying Sand Deposits Under Earthquake Loading*, Civil Engineering Report No. 82-1, University of New Hampshire, Durham, New Hampshire.

De Alba, P. (1983a) "Pile Settlement in a Liquefying Sand Deposit," *Journal of Geotechnical Engineering, ASCE* 109(9):1165-1180.

De Alba, P. (1983b) "Group Effect on Piles in a Liquefying Sand Deposit," pp. 300-314 in *Proceedings of the Conference on Geotechnical Practice in Offshore Engineering*, ASCE, New York, New York.

De Alba, P., H. B. Seed, and C. K. Chan (1976) "Sand Liquefaction in Large-Scale Simple Shear Tests," *Journal of the Geotechnical Engineering Division, ASCE* 102(GT9):909-927.

Dean, E. T. R., and A. N. Schofield (1983) "Two Centrifuge Model Tests: Earthquakes on Submerged Embankments," pp. 115-129 in *Atti del XV Convegno Nazionale di Geotecnica Spoleto, Volume 1.*

DeMello, V. F. B. (1971) "The Standard Penetration Test," pp. 1-86 in *Proceedings of the Fourth Pan American Conference on Soil Mechanics and Foundation Engineering, Volume 1.*

Der Kiureghian, A., and A. H-S. Ang (1977) "Fault Rupture Model for Seismic Risk Analysis," *Bulletin of The Seismological Society of America* 67(4):1173-1194.

Dikmen, S. U., and J. Ghaboussi (1984) "Effective Stress of Seismic Response and Liquefaction: Theory," *Journal of Geotechnical Engineering, ASCE* 110(5):628-644.

Dobry, R. (1985) unpublished data, personal files of R. Dobry, Rensselaer Polytechnic Institute, Troy, New York.

Dobry, R., K. H. Stokoe II, R. S. Ladd, and T. L. Youd (1981a) "Liquefaction Susceptibility from S-Wave Velocity," Preprint 81-544, ASCE National Convention, St. Louis, Missouri, October 1981, ASCE, New York, New York.

Dobry, R., F. Y. Yokel, and R. S. Ladd (1981b) "Liquefaction Potential of Overconsolidated Sands in Areas with Moderate Seismicity," pp. 643-664 in *Earthquakes and Earthquake Engineering: The Eastern United States*, J. E. Beavers, ed., Ann Arbor Science Publishers, Ann Arbor, Michigan.

Dobry, R., R. S. Ladd, F. Y. Yokel, R. M. Chung, and D. Powell (1982) "Prediction of Pore Water Pressure Buildup and Liquefaction of Sands During Earthquakes by the Cyclic Strain Methods," *Building Science Series 138*, National Bureau of Standards, U.S. Department of Commerce, U.S. Government Printing Office, Washington, D.C.

Dobry, R., R. Mohamad, P. Dakoulas, and G. Gazetas (1984) "Liquefaction Evaluation of Earth Dams—A New Approach," pp. 333-348 in *Proceedings of the Eighth World Conference on Earthquake Engineering, Volume 3*, Prentice-Hall, Inc., Englewood Cliffs, New Jersey.

Donovan, N. C. (1971) "A Stochastic Approach to the Seismic Liquefaction

Problem," pp. 513-535 in *Proceedings of the International Conference on Applications of Statistics and Probability to Soil and Structural Engineering*.

Donovan, N. C., and A. E. Bornstein (1978) "Uncertainties in Seismic Risk Procedures," *Journal of the Geotechnical Engineering Division, ASCE* 104(GT7):869-887.

Douglas, B. J., R. S. Olsen, and G. R. Martin (1981) "Evaluation of the Cone Penetrometer Test for SPT-Liquefaction Assessment," *In situ Testing to Evaluate Liquefaction Susceptibility*, Preprint 81-544, ASCE National Convention, St. Louis, Missouri, 1981, ASCE, New York, New York.

Drnevich, V. P., and F. E. Richart, Jr. (1970) "Dynamic Prestraining of Dry Sand," *Journal of the Soil Mechanics and Foundations Division, ASCE* 96(SM2):453-469.

Dyvik, R., R. Dobry, G. E. Thomas, and W. G. Pierce (1984) *Influence of Consolidation Shear Stresses and Relative Density on Threshold Strain and Pore Pressure During Cyclic Straining of Saturated Sands*, Miscellaneous Paper GL-84-15, Department of the Army, U.S. Army Corps of Engineers, Washington, D.C.

Easterling, R. G., and L. W. Heller (1976) "Discussion—Statistics of Liquefaction and SPT Results," *Journal of the Geotechnical Engineering Division, ASCE* 102(GT10):1126-1128.

Eide, O., and K. H. Andersen (1984) *Foundation Engineering for Gravity Structures in the North Sea*, Publication No. 154, Norwegian Geotechnical Institute, Oslo, Norway.

Fardis, M. N., and D. Veneziano (1982) "Probabilistic Analysis of Deposit Liquefaction," *Journal of the Geotechnical Engineering Division, ASCE* 108(GT3):395-417.

Finn, W. D. L. (1980) *Seismic Deformations in an Underwater Slope, Mediterranean Location*, Report to Earth Technology Corporation.

Finn, W. D. L. (1981) "Liquefaction Potential: Developments Since 1976," pp. 655-681 in *Proceedings of the International Conference on Recent Advances in Geotechnical Earthquake Engineering and Soil Dynamics*, University of Missouri, Rolla, Missouri.

Finn, W. D. L. (1982) "Computation of Seismically Induced Settlements in Sands," preliminary report to U.S. Army Corps of Engineers, Waterways Experiment Station, Vicksburg, Mississippi.

Finn, W. D. L. (1984) *Progress Reports*, U.S. Army Corps of Engineers, Office of Standardization, London.

Finn, W. D. L. (1985a) *Dynamic Analysis of EPR Gravity Platform*, Report to Exxon Production Research Company.

Finn, W. D. L. (1985b) *Permanent Deformations in Lornex Tailings Dam, Preliminary Feasibility Study*, Report to Klohn Leonoff Consultants Ltd.

Finn, W. D. L., and S. K. Bhatia (1981) "Prediction of Seismic Pore-water Pressures," pp. 201-206 in *Proceedings in the Tenth International Conference on Soil Mechanics and Foundation Engineering, Volume 3*, A. A. Balkema Publishers, Rotterdam, Netherlands.

Finn, W. D. L., and P. M. Byrne (1976) "Liquefaction Potential of Mine Tailing Dams," pp. 153-178 in *Proceedings of the Twelfth International Congress on Large Dams, Volume 1*, United States Committee on Large Dams, Boston, Massachusetts.

Finn, W. D. L., and G. R. Martin (1979a) "Analysis of Piled Foundations for Offshore Structures under Wave and Earthquake Loading," pp. 497-502 in *Proceedings of the Behavior of Offshore Structures (BOSS) Conference, Volume 1*, McGraw Hill/Hemisphere Publishing Company, New York, New York.

Finn, W. D. L., and G. R. Martin (1979b) "Aspects of Seismic Design of Pile-Supported Offshore Platforms in Sand," pp. 1-36 in *Proceedings of the Specialty Session, Soil Dynamics in the Marine Environment*, ASCE National Convention and Exposition, Boston, April 1979, ASCE, New York, New York.

Finn, W. D. L., P. L. Bransby, and D. J. Pickering (1970) "Effect of Strain History on Liquefaction of Sands," *Journal of the Soil Mechanics and Foundations Division, ASCE* 96(SM6):1917-1934.

Finn, W. D. L., J. J. Emery, and Y. P. Gupta (1971) "Liquefaction of Large Samples of Saturated Sand on a Shaking Table," pp. 97-110 in *Proceedings of the First Canadian Conference on Earthquake Engineering.*

Finn, W. D. L., K. W. Lee, and G. R. Martin (1977) "An Effective Stress Model for Liquefaction," *Journal of the Geotechnical Engineering Division, ASCE* 103(GT6):517-533.

Finn, W. D. L., K. W. Lee, Maartman, and R. Lo (1978) "Cyclic Pore Pressures Under Anisotropic Conditions," pp. 457-491 in *Proceedings of the ASCE Specialty Conference on Earthquake Engineering and Soil Dynamics, Volume 1*, ASCE, New York, New York.

Finn, W. D. L., G. R. Martin, and M. K. W. Lee (1978b) "Comparison of Dynamic Analyses for Saturated Sands," pp. 472-491 in *Proceedings of the ASCE Specialty Conference on Earthquake Engineering and Soil Dynamics, Volume 1*, ASCE, New York, New York.

Finn, W. D. L., S. Iai, and K. Ishihara (1982) "Performance of Artificial Offshore Islands under Wave and Earthquake Loading: Field Data Analyses," pp. 661-672 in *Proceedings of the Fourteenth Annual Offshore Technology Conference*, OTC 4220, Offshore Technology Conference, Dallas, Texas.

Finn, W. D. L., R. Siddharthan, F. Lee, and A. N. Schofield (1984) "Seismic Response of Offshore Drilling Islands in a Centrifuge Including Soil-Structure Interaction," pp. 399-406 in *Proceedings of the Sixteenth Offshore Technology Conference, Volume 1* Offshore Technology Conference, Dallas, Texas.

Fragaszy, R. J. (1985) personal communication, Department of Civil Engineering, Washington State University, Pullman, Washington.

Fragaszy, R. J., M. E. Voss, R. M. Schmidt, and K. A. Holsapple (1983) "Laboratory and Centrifuge Modeling of Blast-Induced Liquefaction," pp. III.5.1-20 in *Proceedings of the Eighth International Symposium on Military Applications of Blast Simulation, Volume 2.*

Franklin, A. G., and F. K. Chang (1977) *Permanent Displacements of Earth Embankments by Newmark Sliding Block Analysis*, Miscellaneous Paper S-71-17, U.S. Army Corps of Engineers, Waterways Experiment Station, Vicksburg, Mississippi.

Fuller, M. L. (1912) "The New Madrid Earthquake," Bulletin 494, U.S. Geological Survey, Menlo Park, California.

Ghaboussi, J., and S. U. Dikmen (1978) "Liquefaction Analysis of Horizontally

Layered Sands," *Journal of the Geotechnical Engineering Division, ASCE* 104(GT3):341-356.

Ghaboussi, J., and S. U. Dikmen (1981) "Liquefaction Analysis for Multi-Directional Shaking," *Journal of the Geotechnical Engineering Division, ASCE* 107(GT5):605-627.

Ghaboussi, J., and S. U. Dikmen (1984) "Effective Stress Analysis of Seismic Response and Liquefaction: Case Studies," *Journal of Geotechnical Engineering, ASCE* 110(5):645-658.

Gilbert, P. A. (1984) *Investigation of Density Variation in Triaxial Test Specimens of Cohesionless Soil Subjected to Cyclic and Monotonic Loading*, Technical Report GL84-10, Department of the Army, U.S. Army Corps of Engineers, Washington, D.C.

Goodman, R. E., and H. B. Seed (1966) "Earthquake-Induced Displacements in Sand Embankments," *Journal of the Soil Mechanics and Foundations Division, ASCE* 92(SM2):125-146.

Goulois, A., R. V. Whitman, and K. Hoeg (in press) (1985) "Effect of Sustained Shear Stress on the Cyclic Degradation of Clay," paper for publication in the ASTM *Geotechnical Testing Journal.*

Grantz, A., G. Plafker, and R. Kachadoorian (1964) *Alaska's Good Friday Earthquake, March 27, 1964*, Geological Survey Circular 491, Department of the Interior, Washington, D.C.

Gu, W., and Y. Wang (1984) "An Approach to the Quadratic Nonlinear Formulae for Predicting Earthquake Liquefaction Potential by Stepwise Discriminant Analysis," pp. 119-126 in *Proceedings of the Eighth World Conference on Earthquake Engineering, Volume 3*, Prentice-Hall, Inc., Englewood Cliffs, New Jersey.

Haldar, A., and W. H. Tang (1979) "Probabilistic Evaluation of Liquefaction Potential," *Journal of the Geotechnical Engineering Division, ASCE* 105(GT2):145-163.

Haldar, A., and W. H. Tang (1981) "Statistical Study of Uniform Cycles in Earthquakes," *Journal of the Geotechnical Engineering Division, ASCE* 107(GT5):577-589.

Harp, E. L., J. Sarmiento, and E. Cranswick (1984) "Seismic-Induced Pore-Water Pressure Records from the Mammoth Lakes, California, Earthquake Sequence of 25 to 27 May 1980," *Bulletin of the Seismological Society of America* 74(4):1381-1393.

Hedberg, J. (1977) "Cyclic Stress-Strain Behavior of Sand in Offshore Environment," Ph.D. thesis, Department of Civil Engineering, Massachusetts Institute of Technology, Cambridge, Massachusetts.

Heidari, M. (1981) "Centrifugal Modelling of Earthquake Induced Liquefaction in Saturated Sand," M. Phil. thesis, Cambridge University, England.

Heidari, M., and R. G. James (1982) "Centrifuge Modelling of Earthquake Induced Liquefaction in a Column of Sand," pp. 271-281 in *Proceedings of the Conference on Soil Dynamics and Earthquake Engineering, Volume 1*, A. A. Balkema, Rotterdam, Netherlands.

Henkel, D. J. (1982) "Geology, Geomorphology and Geotechnics," *Geotechnique* 32(3):175-194.

Horne, M. R. (1965) "The Behavior of An Assembly of Rotund, Rigid, Cohesionless Particles," pp. 62-97 in *Proceedings of the Royal Society, Part A, Volume 286*, Royal Society of London, United Kingdom.

Housner, G. W. (1958) "The Mechanism of Sand Blows," *Bulletin of the Seismological Society of America* 58:155-161.

Idriss, I. M. (1985) "Evaluating Seismic Risk in Engineering Practice," *Proceedings of the Eleventh International Conference on Soil Mechanics and Foundation Engineering*, A. A. Balkema Publishers, Rotterdam, Netherlands.

Idriss, I. M., A. W. Dawson, and M. S. Power (1982) *Evaluation of Liquefaction Opportunity and Liquefaction Potential in the San Diego, California, Urban Area*, Final Technical Report to the U.S. Geological Survey, Woodward-Clyde Consultants, San Diego, California.

Ikehara, T. (1970) "Damage to Railway Embankments Due to the Tokachioki Earthquake," *Soils and Foundations, Japanese Society of Soil Mechanics and Foundation Engineering* 10(2):52-71.

Ishihara, K. (1984) "Post-Earthquake Failure of a Tailings Dam Due to Liquefaction of the Pond Deposit," pp. 1129-1143 in *Proceedings of the International Conference on Case Histories in Geotechnical Engineering, Volume 3*, University of Missouri, Rolla, Missouri.

Ishihara, K. (1985) "Stability of Natural Deposits During Earthquakes," *Proceedings of the Eleventh International Conference on Soil Mechanics and Foundation Engineering*, A. A. Balkema Publishers, Rotterdam, Netherlands.

Ishihara, K., and I. Towhata (1980) "One-Dimensional Soil Response Analysis During Earthquakes Based on Effective Stress Method," *Journal of the Faculty of Engineering, University of Tokyo* 35(4).

Ishihara, K., and F. Yamazaki (1980) "Cyclic Simple Shear Tests on Saturated Sand in Multi-Directional Loading," *Soils and Foundations, Japanese Society of Soil Mechanics and Foundation Engineering* 20(1):45-59.

Ishihara, K., and S. Yasuda (1975) "Sand Liquefaction in Hollow Cylinder Torsion Under Irregular Excitation," *Soils and Foundations* 15(1):45-59.

Ishihara, K., F. Tatsuoka, and S. Yasuda (1975) "Undrained Deformation and Liquefaction of Sand Under Cyclic Stresses," *Soils and Foundations* 15(1):29-44.

Ishihara, K., K. Shimizu, and Y. Yamada (1981) "Pore Water Pressures Measured in Sand Deposits During an Earthquake," *Soils and Foundations* 21(4):85-100.

Jaime, A., L. Montanez, and M. P. Romo (1981) "Liquefaction of Enmedio Island Soil Deposits," pp. 529-534 in *Proceedings of the International Conference on Recent Advances in Geotechnical Earthquake Engineering and Soil Dynamics, Volume 1*, Prentice-Hall, Inc., Englewood Cliffs, New Jersey.

Johnson, R. A., and D. W. Wichern (1982) *Applied Multivariate Statistical Analysis*, Prentice-Hall, Inc., Englewood Cliffs, New Jersey.

Kavazanjian, E., R. A. Roth, and H. Echezuria (1985) "Liquefaction Potential Mapping for San Francisco," *Journal of Geotechnical Engineering, ASCE* 111(1):54-76.

Kawasumi, H. (ed.) (1968) *General Report on the Niigata Earthquake of 1964*, Electrical Engineering College Press, University of Tokyo, Tokyo, Japan.

Kim, K. J., and S. E. Blouin (1984) *Response of Saturated Porous Nonlinear Materials to Dynamic Loadings*, Report prepared for U.S. Air Force

Office of Scientific Research, Applied Research Associates, Inc., South Royalton, Vermont.

Kiremidjian, A. S., and T. Anagnos (1984) "Stochastic Slip-Predictable Model for Earthquake Occurrences," *Bulletin of the Seismological Society of America* 74(2):739-755.

Kok, L. (1981) "Settlements Due to Contained Explosions in Water-Saturated Sands," pp. 4.3-1 to 4.3-8 in *Proceedings of the Seventh International Symposium on Military Applications of Blast Simulation.*

Kokusho, T., Y. Yoshida, and Y. Esashi (1983) *Evaluation of Seismic Stability of Dense Sand Layer (Part 2)—Evaluation Method by Standard Penetration Test*, Report 383026, Central Research Institute for Electric Power Industry, Tokyo, Japan (in Japanese).

Kovacs, W. D., and L. A. Salomone (1982) "SPT Hammer Energy Measurement," *Journal of the Geotechnical Engineering Division, ASCE* 108(GT4):599-620.

Kovacs, W. D., L. A. Salomone, and F. Y. Yokel (1983) "Comparison of Energy Measurements in the Standard Penetration Test Using the Cathead and Rope Method," NUREG CR-3545, U.S. Regulatory Commission, Washington, D.C.

Kovacs, W. D., F. Y. Yokel, L. A. Salomone, and R. D. Holtz (1984) "Liquefaction Potential and the International SPT," pp. 263-268 in *Proceedings of the Eighth World Conference on Earthquake Engineering, Volume 3*, Prentice-Hall, Inc., Englewood Cliffs, New Jersey.

Kuo, C. L. (1983) "Modeling of Dynamic Deformation Mechanisms for Granular Material," Ph.D. dissertation, Department of Civil Engineering, University of Massachusetts, Amherst, Massachusetts.

Ladd, R. S. (1977) "Specimen Preparation and Cyclic Stability of Sands," *Journal of the Geotechnical Engineering Division, ASCE* 103(GT6):535-547.

Lambe, P. C., and R. V. Whitman (1985) "Dynamic Centrifugal Modeling of a Horizontal Dry Sand Layer," *Journal of Geotechnical Engineering, ASCE* 111(3):265-287.

Ledbetter, R. H. (1985) *Improvement of Liquefiable Foundation Conditions Beneath Existing Structures*, Technical Report REMR-GT-2, U.S. Army Corps of Engineers, Waterways Experiment Station, Vicksburg, Mississippi.

Lee, K. L., and A. Albeisa (1974) "Earthquake Induced Settlement in Saturated Sands," *Journal of the Soil Mechanics and Foundations Division, ASCE* 100(GT4):387-406.

Lee, M. K. W., and W. D. L. Finn (1975) "DESRA-1, Program for the Dynamic Effective Stress Response Analysis of Soil Deposits Including Liquefaction Evaluation," *Soil Mechanics Series No. 36*, Department of Civil Engineering, University of British Columbia, Vancouver, B.C., Canada.

Lee, M. K. W., and W. D. L. Finn (1978) "DESRA-2 Dynamic Effective Stress Response Analysis of Soil Deposits with Energy Transmitting Boundary Including Assessment of Liquefaction Potential," *Soil Mechanics Series, No. 38*, Department of Civil Engineering, University of British Columbia, Vancouver, B.C., Canada.

Lee, K. L., and J. A. Focht (1975) "Liquefaction Potential at Ekofisk Tank

in North Sea," *Journal of the Geotechnical Engineering Division, ASCE* 101(GT1):1-18.

Lee, F. H., and A. N. Schofield (1984) "Centrifuge Modeling of Artificial Sand Islands in Earthquakes," pp. 198-234 in *Proceedings of the Symposium on Recent Advances in Geotechnical Centrifuge Modelling*, University of California, Davis, California.

Liao, S. (1985) "Statistical Analysis of Liquefaction Data," Ph.D. thesis in progress at Massachusetts Institute of Technology, Cambridge, Massachusetts.

Liao, S., and R. V. Whitman (in press) (1985) "Overburden Correction Factors for SPT in Sand," technical note submitted to the *ASCE Journal of Geotechnical Engineering* for publication.

Liou, C. P., V. L. Streeter, and F. E. Richart (1977) "Numerical Model for Liquefaction," *Journal of the Geotechnical Engineering Division, ASCE* 103(GT6):589-606.

Luong, L. P., and J. F. Sidaner (1981) "Comportement Cyclique et Transitoire des Sols Sableux," pp. 257-260 in *Proceedings of the Tenth International Conference on Soil Mechanics and Foundation Engineering, Volume 3*, A. A. Balkema Publishers, Rotterdam, Netherlands.

Makdisi, F. I., and H. B. Seed (1978) "Simplified Procedure for Estimating Dam and Embankment Earthquake-Induced Deformations," *Journal of the Geotechnical Engineering Division, ASCE* 104(GT7):849-867.

Marcuson, W. F., III, and W. A. Bieganousky (1977) "SPT and Relative Density in Coarse Sands," *Journal of the Geotechnical Engineering Division, ASCE* 103(GT11):1295-1309.

Marcuson, W. F., III, and A. G. Franklin (1983) "Seismic Design Analysis and Remedial Measures to Improve Stability of Existing Earth Dams—Corps of Engineers Approach," pp. 65-78 in *Seismic Design of Embankments and Caverns*, Terry R. Howard, ed., ASCE, New York, New York.

Marr, W. A., and J. T. Christian (1981) "Permanent Displacements Due to Cyclic Wave Loading," *Journal of the Geotechnical Engineering Division, ASCE* 107(GT8):1129-1149.

Marr, W. A., A. Urzua, and G. Bouckovalas (1982) "A Numerical Model to Predict Permanent Displacement From Cyclic Loading of Foundations," pp. 297-312 in *Proceedings of the Third International Conference on the Behavior of Offshore Structures (BOSS), Volume 1*, McGraw Hill/Hemisphere Publishing Company, New York, New York.

Martin, G. R., W. D. L. Finn, and H. B. Seed (1975) "Fundamentals of Liquefaction Under Cyclic Loading," *Journal of the Geotechnical Engineering Division, ASCE* 104(GT5):423-438.

Martin, P. P. (1975) "Non-Linear Methods for Dynamic Analysis of Ground Response," Ph.D. dissertation, Department of Civil Engineering, University of California, Berkeley, California.

Martin, P. P., and H. B. Seed (1979) "Simplified Procedure for Effective Stress Analysis of Ground Response," *Journal of the Geotechnical Engineering Division, ASCE* 105(GT6):739-758.

Mavko, G. M., and E. Harp (1984) "Analysis of Wave-Induced Pore Pressure Changes Recorded During the 1980 Mammoth Lakes, California, Earth-

quake Sequence," *Bulletin of the Seismological Society of America* 74(4):1395-1407.

McFadden, D. (1974) "Conditional Logit Analysis of Qualitative Choice Behavior," pp. 105-142 in *Frontiers in Econometrics*, P. Zarembka, ed., Academic Press, New York, New York.

McFadden, D. (1982) "The Impacts of Temporal and Spatial Climatic Changes on Alluvial Soils Genesis in Southern California," Ph.D. dissertation, University of Arizona, Tucson, Arizona.

McFadden, L. D., and J. C. Tinsley (1982) "Soil Profile Development in Xeric Climates," pp. 15-19 in *Later Quaternary Pedogenesis and Alluvial Chronologies of the Los Angeles and San Gabriel Mountains Areas, Southern California, and Holocene Faulting and Alluvial Stratigraphy within the Cucamonga Fault Zone: A Preliminary View*, J.C. Tinsley, J.C. Matti, and L.D. McFadden, eds., Geological Society of America Guidebook, Field Trip 12, Geological Society of America, Anaheim, California.

McGarr, A. (1984) "Scaling of Ground Motion Parameters, State of Stress and Focal Depth," *Journal of Geophysical Research* 89(B8):6969-6979.

McGuire, R. K., F. Tatsuoka, F. Iwasaki, and K. Tokida (1978) "Probabilistic Procedures for Assessing Soil Liquefaction Potential," *Journal of Research*, Public Works Research Institute, Tokyo, Japan, 19:1-38.

McGuire, R. K., F. Tatsuoka, T. Iwasaki, and K. Tokida (1979) "Assessment of Probability of Liquefaction of Water Saturated Reclaimed Land," pp. 786-801 in *Proceedings of the Third International Conference Applications of Statistics and Probability in Soil and Structural Engineering*.

Melzer, L. S. (1978) *Blast-Induced Liquefaction of Materials*, AFWL-TR-78-110, Air Force Weapons Laboratory, Kirkland Air Force Base, New Mexico.

Mitchell, J. K. (1981) "Soil Improvement: State-of-the-Art," pp. 509-565 in *Proceedings of the Tenth International Conference on Soil Mechanics and Foundation Engineering, Volume 4*, A. A. Balkema Publishers, Rotterdam, Netherlands.

Mohamad, R., and R. Dobry (1983) Discussion of "Effect of Static Shear on Resistance to Liquefaction" by Vaid and Chern, *Soils and Foundations* 23(4):139-143.

Mroz, A., V. A. Norris, and O. C. Zienkiewicz (1978) "An Anisotropic Hardening Model for Soils and Its Application to Cyclic Loading," *International Journal of Numerical and Analytical Methods in Geomechanics* 2:203-221.

Mulilis, J. P., C. K. Chan, and H. B. Seed (1975) *The Effects of Method of Sample Preparation on the Cyclic Stress-Strain Behavior of Sands*, Report No. EERC 75-18, Earthquake Engineering Research Center, University of California, Berkeley, California.

Mulilis, J. P., H. B. Seed, C. K. Chan, J. K. Mitchell, and K. Arulanandan (1977) "Effects of Sample Preparation on Sand Liquefaction," *Journal of the Geotechnical Engineering Division, ASCE* 103(GT2):91-108.

Nemat-Nasser, S. (1980) "On Behavior of Granular Materials in Simple Shear," *Soils and Foundations* 20(3):59-73.

Nemat-Nasser, S. (1982) "Liquefaction and Densification of Cohesionless Granular Masses in Cyclic Shearing," keynote lecture presented at the

International Symposium on Numerical Methods in Geomechanics, A. A. Balkema Publishers, Rotterdam, Netherlands.

Nemat-Nasser, S., and A. Shokooh (1979) "A Unified Approach to Densification and Liquefaction of Cohesionless Sand in Cyclic Shearing," *Canadian Geotechnical Journal* 16(4):659-678.

Nemet-Nasser, S., and K. Takahashi (1984) "Liquefaction and Fabric of Sand," *Journal of Geotechnical Engineering, ASCE* 110(9):1291-1306.

Newmark, N. M. (1965) "Effects of Earthquakes on Dams and Embankments," *Geotechnique* 15(2):139-160.

Obermeier, S. F., G. S. Gohn, R. E. Weems, R. L. Gelinas, and M. Rubin (1985) "Geologic Evidence for Recurrent Moderate to Large Earthquakes near Charleston, South Carolina," *Science* 227:408-411.

Oda, M. (1972) "The Mechanism of Fabric Changes During Compressional Behavior of Sand," *Soils and Foundations* 12(2):1-18.

Oda, M., and J. Konishi (1974) "Microscopic Deformation Mechanism Granular Material in Simple Shear," *Soils and Foundations* 14(4):25-38.

Oda, M., J. Konishi, and S. Nemat-Nasser (1980) "Some Experimentally Based Fundamental Results on the Mechanical Behavior of Granular Materials," *Geotechnique* 30(4):479-495.

Okusa, S., S. Anma, and H. Maikuma (1980) "Liquefaction of Mine Tailings in the 1978 Izu-Ohshima-Kinkai Earthquake, Central Japan," pp. 89-96 in *Proceedings of the Seventh World Conference on Earthquake Engineering, Volume 3*, Prentice-Hall, Inc., Englewood Cliffs, New Jersey.

Park, T., and M. L. Silver (1975) *Dynamic Soil Properties Required to Predict the Dynamic Behavior of Elevated Transportation Structures*, Report DOT-TST-75-44, U.S. Department of Transportation, Washington, D.C.

Patwardan, A. S., R. B. Kulkarni, and D. Tocher (1980) "A Semi-Markov Model for Characterizing Recurrence of Great Earthquakes," *Bulletin of the Seismological Society of America* 70:323-347.

Peacock, W. H., and H. B. Seed (1968) "Sand Liquefaction Under Cyclic Loading Simple Shear Conditions," *Journal of the Soil Mechanics and Foundations Division, ASCE* 94(SM3):689-708.

Peck, R. B. (1979) "Liquefaction Potential: Science Versus Practice," *Journal of the Geotechnical Engineering Division, ASCE* 105(GT3):393-398.

Poulos, S. J. (1971) "The Stress-Strain Curves of Soils," unpublished paper, available from Geotechnical Engineers, Inc., Winchester, Massachusetts.

Poulos, S. J. (1981) "The Steady State of Deformation," *Journal of the Geotechnical Engineering Division, ASCE* 107(GT5):553-562.

Poulos, S. J., G. Castro, and J. W. France (1985) "Liquefaction Evaluation Procedure," *Journal of Geotechnical Engineering, ASCE* 111(6):772-791.

Power, M. S., A. W. Dawson, D. W. Strieff, R. C. Perman, and V. Berger (1982) *Evaluation of Liquefaction Susceptibility in the San Diego, California, Urban Area*, Final Technical Report to the U.S. Geological Survey, Woodward-Clyde Consultants, San Diego, California.

Prevost, J. H. (1978) "Anisotropic Undrained Stress-Strain Behavior of Clays," *Journal of the Geotechnical Engineering Division, ASCE* 104(GT8):1075-1090.

Prevost, J. H. (1981) *DYNA-FLOW: A Nonlinear Transient Finite Element*

Analysis Program, Report 81-SM-1, Princeton University, Department of Civil Engineering, Princeton, New Jersey.

Pyke, R., H. B. Seed, and C. K. Chan (1975) "Settlement of Sands Under Multi-directional Shaking," *Journal of the Geotechnical Engineering Division, ASCE* 101(GT4):379-398.

Rahman, M. S., H. B. Seed, and J. R. Booker (1977) "Pore Pressure Development Under Offshore Gravity Structures," *Journal of the Geotechnical Engineering Division, ASCE* 103(GT12):1419-1436.

Robertson, P. K. (1985) personal communication, Civil Engineering Department, University of British Columbia, Vancouver, B.C., Canada.

Robertson, P. K., and R. G. Campanella (1985) "Liquefaction Potential of Sands Using the CPT," *Journal of Geotechnical Engineering, ASCE* 111(GT3):384-403.

Robertson, P. K., R. G. Campanella, and A. Wightman (1983) "SPT-CPT Correlations," *Journal of Geotechnical Engineering, ASCE* 109(11):1449-1459.

Roth, R. A., and E. Kavazanjian (1984) "Liquefaction Susceptibility Mapping for San Francisco, California," *Bulletin of the Association of Engineering Geologists* 21(4):459-478.

Rowe, P. W. (1962) "The Stress-Dilantancy Relation for Static Equilibrium of an Assembly of Particles in Contact," pp. 500-527 in *Proceedings of the Royal Society of London, Series A, Volume 269*, Royal Society of London, United Kingdom.

Sarma, S. K. (1979) "Response and Stability of Earth Dams During Strong Earthquakes," Miscellaneous Paper GL-79-13, U.S. Army Corps of Engineers, Waterways Experiment Station, Vicksburg, Mississippi.

Sharma, S., and W. D. Kovacs (1982) "Preliminary Microzonation of the Memphis, Tennessee, Area," *Bulletin of the Seismological Society of America* 72(3):1011-1024.

Schmertmann, J. S., and A. Palacios (1979) "Energy Dynamics of SPT," *Journal of the Soil Mechanics and Foundation Division, ASCE* 105(GT8):909-926.

Schnabel, P. B., J. Lysmer, and H. B. Seed (1972) *SHAKE: A Computer Program for Earthquake Response Analysis of Horizontally Layered Sites*, Report No. EERC 72-12, Earthquake Engineering Research Center, University of California, Berkeley, California.

Schofield, A. N. (1980) "Cambridge Geotechnical Centrifuge Operations," *Geotechnique* 30(3):227-268.

Schofield, A. N. (1981) "Dynamic and Earthquake Geotechnical Centrifuge Modelling," pp. 1081-1100 in *Proceedings of the International Conference on Recent Advances in Geotechnical Earthquake Engineering and Soil Dynamics, Volume 3*, University of Missouri, Rolla, Missouri.

Schofield, A. N., and K. Venter (1984) "Earthquake Induced Pore Pressure in the Foundation of a Sea Dyke," pp. 157-163 in *Proceedings of the International Symposium on Geotechnical Centrifuge Model Testing*, Japanese Society of Soil Mechanics and Foundation Engineering, Tokyo, Japan.

Schofield, A. N., and C. P. Wroth (1968) *Critical State Soil Mechanics*, McGraw-Hill Book Company, New York, New York.

Schwartz, D. P., and K. J. Coppersmith (1984) "Fault Behavior and Char-

acteristic Earthquakes: Examples from the Wasatch and San Andreas Faults," *Journal of Geophysical Research* 89(87):5681-5698.

Scott, R. F. (1963) *Principles of Soil Mechanics*, Addison-Wesley, Reading, Massachusetts.

Scott, R. F., and K. A. Zuckerman (1973) "Sand Blows and Liquefaction," pp. 179-189 in *The Great Alaskan Earthquake of 1964—Engineering Volume*, Committee on the Alaska Earthquake, Division of Earth Sciences, National Research Council, National Academy of Sciences, Washington, D.C.

Seed, H. B. (1968) "Landslides During Earthquakes Due to Soil Liquefaction," *Journal of the Soil Mechanics and Foundations Division, ASCE* 94(SM5):1055-1122.

Seed, H. B. (1970) "Soil Problems and Soil Behavior," pp. 227-251 in *Earthquake Engineering*, R. L. Wiegel, ed., Prentice-Hall, Inc., Englewood Cliffs, New Jersey.

Seed, H. B. (1976) "Evaluation of Soil Liquefaction Effects on Level Ground During Earthquakes," pp. 1-104 in *Liquefaction Problems in Geotechnical Engineering*, ASCE Preprint 2752, presented at the ASCE National Convention, Philadelphia, Pennsylvania, ASCE, New York, New York.

Seed, H. B. (1979a) "Soil Liquefaction and Cyclic Mobility Evaluation for Level Ground During Earthquakes," *Journal of the Geotechnical Engineering Division, ASCE* 105(GT2):201-255.

Seed, H. B. (1979b) "Considerations in the Earthquake-Resistant Design of Earth and Rockfill Dams," *Geotechnique* 29(3):213-263.

Seed, H. B. (1984) unpublished data, personal files of H. B. Seed, University of California, Berkeley, California.

Seed, H. B., and I. M. Idriss (1967) "Analysis of Soil Liquefaction: Niigata Earthquake," *Journal of the Soil Mechanics and Foundations Division, ASCE* 93(SM3):83-108.

Seed, H. B., and I. M. Idriss (1971) "Simplified Procedure for Evaluating Soil Liquefaction Potential," *Journal of the Soil Mechanics and Foundations Division, ASCE* 97(SM9):1249-1273.

Seed, H. B., and I. M. Idriss (1982) *Ground Motions and Soil Liquefaction during Earthquakes*, monograph series, Earthquake Engineering Research Institute, Berkeley, California.

Seed, H. B., and K. L. Lee (1966) "Liquefaction of Saturated Sands During Cyclic Loading," *Journal of the Soil Mechanics and Foundations Division, ASCE* 92(SM6):105-134.

Seed, H. B., and W. H. Peacock (1971) "Test Procedures for Measuring Soil Liquefaction Characteristics," *Journal of the Soil Mechanics and Foundations Division, ASCE* 97(SM8):1099-1119.

Seed, H. B., I. Arango, and C. K. Chan (1975a) *Evaluation of Soil Liquefaction Potential During Earthquakes*, Report No. EERC 75-28, Earthquake Engineering Research Center, University of California, Berkeley, California.

Seed, H. B., I. M. Idriss, K. L. Lee, and F. I. Makdisi (1975b) "Dynamic Analysis of the Slide in the Lower San Fernando Dam During the Earthquake of February 9, 1971," *Journal of the Geotechnical Engineering Division, ASCE* 101(GT9):889-911.

Seed, H. B., I. M. Idriss, F. Makdisi, and N. Banerjee (1975c) *Representation*

of Irregular Stress Time Histories by Equivalent Uniform Stress Series in Liquefaction Analyses, Report No. EERC 75-29, Earthquake Engineering Research Center, University of California, Berkeley, California.

Seed, H. B., K. L. Lee, I. M. Idriss, and F. I. Makdisi (1975d) "The Slides in the San Fernando Dams During the Earthquake of February 9, 1971," *Journal of the Geotechnical Engineering Division, ASCE* 101(GT7):651-688.

Seed, H. B., R. Pyke, and G. R. Martin (1975e) *Analysis of the Effect of Multi-Directional Shaking on the Liquefaction Characteristics of Sands*, Report No. EERC 75-41, Earthquake Engineering Research Center, University of California, Berkeley, California.

Seed, H. B., P. P. Martin, and J. Lysmer (1976) "Pore Pressure Changes During Soil Liquefaction," *Journal of the Geotechnical Engineering Division, ASCE* 102(GT4):323-346.

Seed, H. B., K. Mori, and C. K. Chan (1977) "Influence of Seismic History on Liquefaction of Sands," *Journal of the Geotechnical Engineering Division, ASCE* 102(GT4):246-270.

Seed, H. B., I. M. Idriss, and I. Arango (1983) "Evaluation of Liquefaction Potential Using Field Performance Data," *Journal of Geotechnical Engineering, ASCE* 109(3):458-482.

Seed, H. B., K. Tokimatsu, L. F. Harder, and R. M. Chung (1984) *The Influence of SPT Procedures in Soil Liquefaction Resistance Evaluations*, Report No. UBC/EERC-84/15, Earthquake Engineering Research Center, University of California, Berkeley, California.

Shibata, T. (1981) "Relations Between N-value and Liquefaction Potential of Sand Deposits," pp. 621-624 in *Proceedings of the Sixteenth Annual Convention of Japanese Society of Soil Mechanics and Foundation Engineering* (in Japanese).

Siddharthan, R., and W. D. L. Finn (1982) *TARA-2, Two-Dimensional Nonlinear Static and Dynamic Response Analysis*, Soil Dynamics Group, University of British Columbia, Vancouver, B.C., Canada.

Sieh, K. (1978) "Prehistoric Large Earthquakes produced by Slip on the San Andreas Fault near Pallett Creek, California," *Journal of Geophysical Research* 83:3907-3939.

Sieh, K. E. (1984) "Lateral Offsets and Revised Dates of Large Prehistoric Earthquakes at Pallett Creek, Southern California," *Journal of Geophysical Research* 89(B9):7641-7670.

Silver, M. L. (1985) *Remedial Measures to Improve the Seismic Strength of Embankment Dams*, Report No. 85-10, Department of Civil Engineering, University of Illinois, Chicago, Illinois.

Silver, M. L., and H. B. Seed (1971) "Volume Changes in Sands During Cyclic Load," *Journal of the Soil Mechanics and Foundations Division, ASCE* 97(SM9):1171-1182.

Singh, S., H. B. Seed, and C. K. Chan (1982) "Undisturbed Sampling of Saturated Sands by Freezing," *Journal of the Geotechnical Engineering Division, ASCE* 108(GT2):247-264.

Stokoe, K. H., II, and R. J. Hoar (1978) "Variables Affecting In Situ Seismic Measurements," pp. 919-939 in *Proceedings of the ASCE Geotechnical Engineering Division Specialty Conference on Earthquake Engineering and Soil Dynamics, Volume 2*, ASCE, New York, New York.

Stokoe, K. H., II, and S. Nazarian (1985) "Use of Rayleight Waves in Liquefaction Studies," pp. 1-14 in *Proceedings, Measurement and Use of Shear Wave Velocity for Evaluating Dynamic Soil Properties*, sponsored by the Geotechnical Engineering Division, ASCE, New York, New York.

Sykes, L. R., and S. Nishenko (1984) "Probabilities of Occurrence of Large Plate Rupturing Earthquakes for the San Andreas, Jacinto, and Imperial Faults, California," *Journal of Geophysical Research* 89:5905-5927.

TM 5-818-1 (1983) *Soils and Geology Procedures for Foundation Design of Buildings and Other Structures (Except Hydraulic Structures)*, Technical Manual TM 5-818-1/AFM 88-3, Headquarters, Departments of the Army and Air Force.

Taniguchi, E., R. V. Whitman, and W. A. Marr (1983) "Prediction of Earthquake Induced Deformation of Earth Dams," *Soils and Foundations* 23(4):126-132.

Tanimoto, K. (1977) "Evaluation of Liquefaction of Sandy Deposits by a Statistical Method," pp. 2201-2206 in *Proceedings of the Sixth World Conference on Earthquake Engineering, Volume 3*, Prentice-Hall, Inc., Englewood Cliffs, New Jersey.

Tanimoto, K., and T. Noda (1976) "Prediction of Liquefaction Occurrence of Sandy Deposits During Earthquake by a Statistical Method," No. 256 in *Proceedings of the Japan Society of Civil Engineers*, Japanese Society of Civil Engineers, Tokyo, Japan.

Tepel, R. E., R. L. Volpe, and G. Bureau (1984) "Performance of Anderson and Coyote Dams during the Morgan Hill Earthquake of 24 April 1984," pp. 53-70 in *The 1984 Morgan Hill, California Earthquake*, Special Publication 68, California Department of Conservation, Division of Mines, Sacramento, California.

Thurston, C. W., and H. Deresiewicz (1959) "Analysis of a Compression Test of a Model of A Granular Medium," *Journal of Applied Mechanics, ASME* 26:251-258.

Tinsley, J. C., T. L. Youd, D. M. Perkins, and A. T. F. Chen (in press) (1985) "Evaluating Liquefaction Potential," *Evaluating Earthquake Hazards in the Los Angeles Region, an Earth Science Perspective*, Professional Paper 1360, J. I. Ziony, ed., U.S. Geological Survey.

Tokimatsu, K., and Y. Yoshimi (1983) "Empirical Correlation of Soil Liquefaction Based on SPT N-Value and Fines Content," *Soils and Foundations, Japanese Society of Soil Mechanics and Foundation Engineering* 23(4):56-74.

Trifunac, J. D., and A. G. Brady (1975) "On the Correlation of Seismic Intensity Scales with the Peaks of Recorded Strong Ground Motion," *Bulletin of the Seismological Society of America* 65(1):139-162.

Tsuchida, H. (1970) "Prediction and Countermeasure Against the Liquefaction in Sand Deposits," pp. 3.1-3.33 in *Abstract of the Seminar in the Port and Harbor Research Institute* (in Japanese).

Vaid, Y. P., and J. C. Chern (1983) "Effect of Static Shear on Resistance to Liquefaction," *Soils and Foundations* 23(1):47-60.

Valera, J. E., and N. C. Donovan (1977) "Soil Liquefaction Procedures—A Review," *Journal of the Geotechnical Engineering Division, ASCE* 103(GT6):607-625.

Veneziano, D., and S. Liao (1984) "Statistical Analysis of Liquefaction Data,"

pp. 206-209 in *Proceedings of the Fourth ASCE Specialty Conference on Probabilistic Mechanics and Structural Reliability*, ASCE, New York, New York.

Wang, J. N., and E. Kavazanjian, Jr. (1985) *Pore Water Pressure Development in Non-uniform Cyclic Triaxial Tests*, Report No. 73, The John A. Blume Earthquake Engineering Center, Stanford University, Stanford, California.

Wang, Y., F. Luan, Q. Han, and G. Li (1980) "Formulae for Predicting Liquefaction Potential of Clayey Silt as Derived from a Statistical Method," pp. 227-234 in *Proceedings of the Seventh World Conference on Earthquake Engineering, Volume 3*, Prentice-Hall, Inc., Englewood Cliffs, New Jersey.

Whitman, R. V. (1971) "Resistance of Soil to Liquefaction and Settlement," *Soils and Foundations* 11(4):59-68.

Whitman, R. V. (1984) "Evaluating Calculated Risk in Geotechnical Engineering," *Journal of Geotechnical Engineerng, ASCE* 110(2):145-188.

Whitman, R. V. (in press) (1985) "On Liquefaction," *Proceedings of the Eleventh International Conference on Soil Mechanics and Foundation Engineering*.

Whitman, R. V., and P. C. Lambe (1985a) "Effect of Boundary Conditions Upon Centrifuge Experiments," paper submitted for publication to the *Geotechnical Testing Journal, ASTM*.

Whitman, R. V., and P. C. Lambe (1985b) unpublished data, personal files of R. V. Whitman, Massachusetts Institute of Technology, Cambridge, Massachusetts.

Whitman, R. V., and S. Liao (1985) *Seismic Design of Gravity Retaining Walls*, Miscellaneous Paper GL-85-1, U.S. Army Corps of Engineers, Waterways Experiment Station, Vicksburg, Mississippi.

Whitman, R. V., P. C. Lambe, and J. Akiyama (1982) "Consolidation During Dynamic Tests on a Centrifuge," Preprint 82-063, ASCE National Convention, Las Vegas, Nevada, April, 1982, ASCE, New York, New York.

Wood, H. O., and F. Neumann (1931) "Modified Mercalli Intensity Scale of 1931," *Bulletin of the Seismological Society of America* 21(4):277-283.

Woods, R. D. (1978) "Measurement of Dynamic Soil Properties," pp. 91-178 in *Proceedings of the ASCE Geotechnical Engineering Division Specialty Conference on Earthquake Engineering and Soil Dynamics, Volume 1*, ASCE, New York, New York.

Xie, J. (1979) "Empirical Criteria of Sand Liquefaction," *The 1976 Tangshan China Earthquake*—Papers Presented at the Second U.S. National Conference on Earthquake Engineering, Stanford University, 1979, published by Earthquake Engineering Research Institute, Berkeley, California, March 1980.

Yegian, M. K. (1976) "Risk Analysis for Earthquake-Induced Ground Failure by Liquefaction," Ph.D. thesis, Department of Civil Engineering, Massachusetts Institute of Technology, Cambridge, Massachusetts.

Yegian, M. K., and B. M. Vitelli (1981a) *Probabilistic Analysis for Liquefaction*, Report No. CE-81-1, Department of Civil Engineering, Northeastern University, Boston, Massachusetts.

Yegian, M. K., and B. M. Vitelli (1981b) "Analysis for Liquefaction: Empirical Approach," pp. 173-177 in *Proceedings of the International Conference*

on Recent Advances in Geotechnical Earthquake Engineering and Soil Dynamics, Volume 1, University of Missouri, Rolla, Missouri.

Yegian, M., and R. V. Whitman (1978) "Risk Analysis for Ground Failure by Liquefaction," *Journal of the Geotechnical Engineering Division, ASCE* 104(GT7):921-938.

Yoshimi, Y., and K. Tokimatsu (1977) "Settlement of Buildings on Saturated Sand During Earthquakes," *Soils and Foundations, Japanese Society of Soil Mechanics and Foundation Engineering* 17(1):23-38.

Yoshimi, Y., and K. Tokimatsu (1978) "Two-Dimensional Pore Pressure Changes in Sand Deposits During Earthquakes," pp. 853-863 in *Proceedings of the Second International Conference on Microzonation for Safer Construction—Research and Applications, Volume 2*, National Science Foundation, Washington, D.C.

Yoshimi, Y., F. E. Richart, Jr., S. Prakash, D. D. Barkan, and V. A. Ilyichev (1977) "Soil Dynamics and Its Application to Foundation Engineering," pp. 605-650 in *State of the Art Report, Ninth International Conference Soil Mechanics and Foundation Engineering, Volume 2*, A. A. Balkema Publishers, Rotterdam, Netherlands.

Yoshimi, Y., M. Hatanaka, and H. Oh-oka (1978) "Undisturbed Sampling of Saturated Sands by Freezing," *Soils and Foundations, Japanese Society of Soil Mechanics, and Foundation Engineering* 18(3):59-73.

Yoshimi, Y., K. Tokimatsu, O. Kaneko, and Y. Makihara (1984) "Undrained Cyclic Shear Strength of a Dense Niigata Sand," *Soils and Foundations, Japanese Society of Soil Mechanics and Foundation Engineering* 24(4):131-145.

Youd, T. L. (1972) "Compaction of Sands by Repeated Straining", *Journal of the Soil Mechanics and Foundations Division, ASCE* 98(SM7):709-725.

Youd, T. L. (1984a) "Recurrence of Liquefaction at the Same Site," pp. 231-238 in *Proceedings of the Eighth World Conference on Earthquake Engineering, Volume 3*, Prentice-Hall, Inc., Englewood Cliffs, N.J.

Youd, T. L. (1984b) "Geologic Effects—Liquefaction and Associated Ground Failure," pp. 210-232 in *Proceedings of the Geologic and Hydrologic Hazards Training Program*, Open-File Report 84-760, U.S. Geological Survey, Menlo Park, California.

Youd, T. L., and M. J. Bennett (1983) "Liquefaction Sites, Imperial Valley, California," *Journal of Geotechnical Engineering, ASCE* 109(3):440-457.

Youd, T. L., and S. N. Hoose (1976) "Liquefaction During 1906 San Francisco Earthquake," *Journal of the Geotechnical Engineering Division, ASCE* 102(GT5):425-439.

Youd, T. L., and S. N. Hoose (1977) "Liquefaction Susceptibility and Geologic Setting," pp. 2189-2194 in *Proceedings of the Sixth World Conference on Earthquake Engineering, Volume 3*, Prentice-Hall, Inc., Englewood, Cliffs, New Jersey.

Youd, T. L., and M. Perkins (1978) "Mapping Liquefaction-Induced Ground Failure Potential," *Journal of the Geotechnical Engineering Division, ASCE* 104(GT4):433-446.

Youd, T. L., and J. B. Perkins (in press) (1985) "Map Showing Liquefaction Susceptibility in San Mateo County, California," *Miscellaneous Investigations Series Map I-1257-G*, U.S. Geological Survey, Menlo Park, California.

Youd, T. L., and G. F. Wieczorek (1984) *Liquefaction During the 1981 and Previous Earthquakes Near Westmorland, California*, Open-File Report 84-680, U.S. Geological Survey, Menlo Park, California.

Youd, T. L, J. C. Tinsley, D. M. Perkins, E. J. King, and R. F. Preston (1978) "Liquefaction Potential Map of San Fernando Valley, California," pp. 268-278 in *Proceedings of the Second International Conference on Microzonation for Safety Construction—Research and Applications, Volume 1*, National Science Foundation, Washington, D.C.